Swansea University
Prifysgol Abertawe

Cronfa
Setting Research Free

Swansea University E-Theses

Metallic and organic coating development for high performance pre-finished steels.

Taylor, Christopher James

How to cite:

Taylor, Christopher James (2009) *Metallic and organic coating development for high performance pre-finished steels..* thesis, Swansea University.
http://cronfa.swan.ac.uk/Record/cronfa42304

Use policy:

This item is brought to you by Swansea University. Any person downloading material is agreeing to abide by the terms of the repository licence: copies of full text items may be used or reproduced in any format or medium, without prior permission for personal research or study, educational or non-commercial purposes only. The copyright for any work remains with the original author unless otherwise specified. The full-text must not be sold in any format or medium without the formal permission of the copyright holder. Permission for multiple reproductions should be obtained from the original author.

Authors are personally responsible for adhering to copyright and publisher restrictions when uploading content to the repository.

Please link to the metadata record in the Swansea University repository, Cronfa (link given in the citation reference above.)

http://www.swansea.ac.uk/library/researchsupport/ris-support/

Metallic and Organic Coating Development for High Performance Pre-finished steels

Christopher James Taylor

Submitted to the University of Swansea in fulfilment of the requirements

for the Degree of Doctor of Engineering

UNIVERSITY OF WALES SWANSEA LIBRARY

ProQuest Number: 10798012

All rights reserved

INFORMATION TO ALL USERS
The quality of this reproduction is dependent upon the quality of the copy submitted.

In the unlikely event that the author did not send a complete manuscript
and there are missing pages, these will be noted. Also, if material had to be removed,
a note will indicate the deletion.

ProQuest 10798012

Published by ProQuest LLC (2018). Copyright of the Dissertation is held by the Author.

All rights reserved.
This work is protected against unauthorized copying under Title 17, United States Code
Microform Edition © ProQuest LLC.

ProQuest LLC.
789 East Eisenhower Parkway
P.O. Box 1346
Ann Arbor, MI 48106 – 1346

Acknowledgements

I would like to take this opportunity to express my gratitude to the Engineering Physical Sciences Research Council and Corus Group Plc for their funding and support throughout the duration of this project.

Great thanks must be bestowed upon my supervisors throughout the project. Firstly, I would like to thank Professor Dave Worsley for guiding me through the technical and sometimes bewildering elements of the project. Dave has been constant source of ideas, suggestions and patience that have helped keep motivation, direction and enjoyment throughout the last four years. Thank-you also to Paul Jones and Jon Elvins for all the help they have given from an industrial point of view. I hope the time and input received in discussion and review along the course of the project is reflected in the finished article, as it is a testament to the willingness and accessibility of both Paul and Jon and their contribution to the direction and relevance of the work.

Thanks to all the Guys and Girls in the world famous 'Corrosion Group'. It has been a pleasure to work alongside you for the last few years and has provided an endless resource of both help and amusement. Thanks also to Rich, Mike, Jim and Dai, who have each at one time or another fulfilled the roles of housemate, workmate and drinking partner.

I would like to thank my parents Julie and Steve and the rest of my family for their unerring love and encouragement in everything that I have done and continue to do. Finally thank-you to Katie who has had to suffer endless hours of motorway miles for the past four years, your love, support and patience have been greatly appreciated.

Summary

Organic coated steels are extremely popular in the construction industry due to their flexibility, cost, ease of construction and aesthetic nature. However the fact that they can be produced in many colours and finishes in large volumes slightly belies the complexity of the system itself. Many of the components have a degree of environmental sensitivity and therefore with the introduction and implementation of strict environmental legislation constant improvement is needed to keep in line or ahead of such directives. Improvement of the coating system from the substrate up is presented in this thesis.

Initial work was undertaken to understand the species that would be released from an organic coating. To this end PVC based model coatings were produced and subjected to natural weathering for one year, the coatings were designed to degrade by addition of a U grade TiO_2 to ensure that results were obtained during the period. The leachate species were monitored on a monthly basis and identified using inductively coupled plasma mass spectrometry (ICPMS). From this work it was found that pigmentation has an effect on the degradation of coatings. It was shown that monitoring of metallic run off is important as it provides details on species type, while some species can be identified as markers to photo-degradation of the coating.

The comparison of stabilisers historic, present and novel using the same natural weathering method and testing period. Hydrotalcite was identified as a potential novel stabiliser for PVC based coatings. When compared to organotin based stabilisers as used in the past or Barium/Zinc based stabilisers that are currently used Hydrotalcite performed favourably both from a chemical and physical point of view.

With regard to improving the coating system as a whole the next phase of work involved the identification of an optimum galvanised coating weight. Samples of Zn/Al galvanised steels with increasing coating weight were subjected to natural weathering for one year and the amount of zinc monitored monthly. Conventional hot dipped galvanised steel and Zalutite coatings were included in the sample field to provide further comparison points. A coating weight of 255 gm^{-2} was found to be the optimum with respect to the natural weathering, while Zalutite which contains a high aluminium addition performed best overall.

This gave rise to the next section of work that involved used of the Scanning Vibrating Electrode Technique (SVET) to characterise the corrosion performance of galvanised coatings with aluminium additions greater than 4.8%. It was found that increasing the aluminium content improved both surface and cut edge corrosion. Under the parameters under which the samples were produced a wholly eutectic structure was achieved at a target addition of 6.1%.

The final phase of work was a study on reducing the coating thickness of the high aluminium coatings to see if the improvement in corrosion performance attributed to increased aluminium addition carried across to thinner coatings. The samples were again tested using the SVET. The results suggest that there is some scope for reducing the coating thickness at certain aluminium levels.

DECLARATION

This work has not previously been accepted in substance for any degree and is not being concurrently submitted in candidature for any degree.

Signed .... (candidate)

Date .....2/10/09.....

STATEMENT 1

This thesis is the result of my own investigations, except where otherwise stated. Where correction services have been used, the extent and nature of the correction is clearly marked in a footnote(s).

Other sources are acknowledged by footnotes giving explicit references. A bibliography is appended.

Signed .... (candidate)

Date .....2/10/09.....

STATEMENT 2

I hereby give consent for my thesis, if accepted, to be available for photocopying and for inter-library loans **after expiry of a bar on access approved by the Swansea University.**

Signed ..... (candidate)

Date .....2/10/09.....

Table of Contents

Chapter 1

Introduction and literature review

Research Aims and Objectives

The main aim of this research is to go some way towards improving the performance of coated strip steel products. The constant pressure of ever tightening environmental legislation coupled with the drive for improvement of coated products has given rise to a need for close monitoring of the components that make up an Organically Coated Steel (OCS) for use in the construction industry. It is therefore important to consider the stability of the coating and how additives to the system may affect the coatings performance in the natural environment. Natural weathering of model coatings is used as a method of assessing the performance of different pigments, while the leachate provides a medium to monitor the species that are released during a testing period of one year. Similarly this also provides the opportunity to test novel stabilising compounds and compare them to both current and historical compounds. This will serve to identify any species that are environmentally sensitive and also provide useful information to the development of the next generation of organic coatings for strip steels.

It is also the aim of this thesis to address the whole system of coated steel products. This includes the metallic coating applied to the strip steel substrate. Firstly, via natural weathering, the impact of coating thickness will be considered by comparing the zinc levels released in the leachate from Galvalloy® coated sample panels and comparing this to other commercial galvanised coatings. This will serve to help identify the optimum coating thickness to be applied to strip steel.

Further to this, investigations into the corrosion performance of Zn/Al galvanised coatings with additions of aluminium higher than 4.8% will provide information on the development of superior performing galvanised coatings. Accelerated electrochemical techniques will be used on sample panels with increasing aluminium content to provide a comparison of corrosion performance. Coupled with this the influence of coating weight and aluminium content will be addressed. The aim of this is two fold, to try and develop a galvanised coating with superior corrosion performance and also assess the impact of higher aluminium content on samples with lower coating weight. This may give rise to a cost saving related to the production of galvanised steels, which could provide significant benefit to producers given the recent fluctuating prices in the metal markets.

1.0.0 Aqueous Corrosion

Scientists and engineers have been battling against the forces of corrosion since the first structural use of metals such as iron. Corrosion is defined as a process that occurs via a physicochemical reaction between the material and its environment, which leads to a change in the properties of the material concerned[1]. Although the mechanism of corrosion can be beneficial to the material, for example through forming a passive layer, more often than not it is the inherent change in the material's properties that has a detrimental effect to the performance of the material in question and can then ultimately lead to failure.

Corrosion therefore has both environmental and sociological consequences. A 2001 study funded by the Federal Highway Administration and undertaken by CC Technologies Inc of Dublin, Ohio and NACE International in Houston, Texas calculated that the direct cost of corrosion on the United States economy was $276 billion a year[2], of which partial break up is shown in Figure 1.1. It is therefore imperative to prevent or at least minimise corrosion wherever possible.

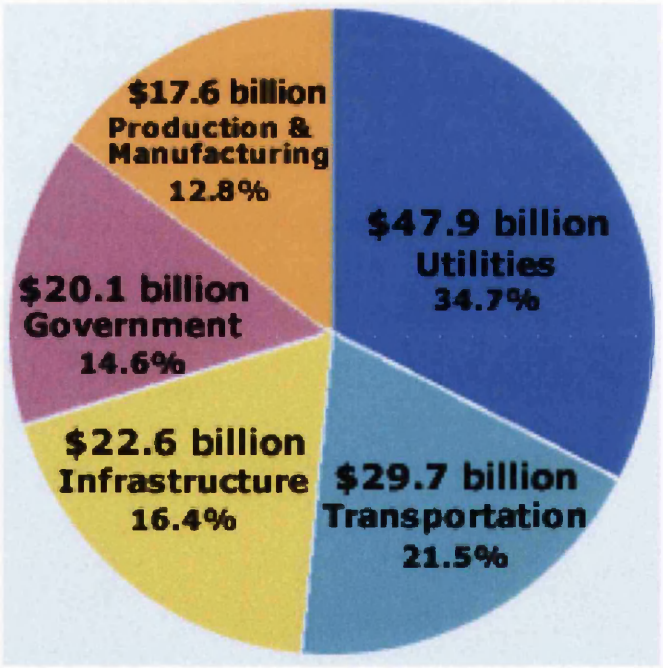

Figure 1.1. The annual cost of corrosion in the United States[2]

Metals are among the most widely used materials. They are also very susceptible to corrosion. The corrosion of a metal is most frequently electrochemical in nature and ordinarily begins at the surface[3]. The corrosion of a metal, M, occurs because there is a thermodynamic driving force for uncombined metals to return to an entropically lower energy state via interactions with the environment to form compounds similar to that of the metals natural ore state[4]. Equation 1.1 represents the corrosion of a metal, M, by oxidation[3].

$$M \rightarrow M^{n+} + ne^{-} \qquad \text{(Equation 1.1)}$$

Most metals are found in nature in a combined state or ore. It is in this state that thermodynamic stability is achieved. The energy change which is the thermodynamic force driving chemical change from metal to metal oxide is usually negative and therefore is inevitable. This energy change is known as the Gibbs Free Energy Change or ΔG, with ΔG^* representing the small activation energy to be overcome before oxidation can occur[5]. The change of a metal ore, to its metal and back again can be seen in Figure 1.2[6].

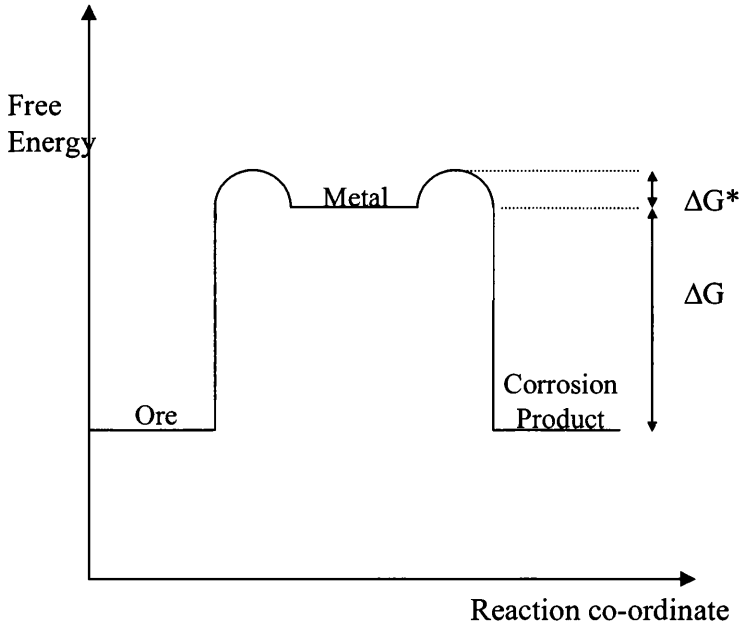

Figure 1.2. Thermodynamic energy profile for metals and their compounds[6]

For corrosion of a metal to occur in an aqueous solution anodic and cathodic sites must be present on the surface of the metal, with an electrolyte present so that current can flow between them[7]. The occurrence of anodic and cathodic sites on the surface of a corroding metal can be due to one or more of things such as; local differences in metal composition, local differences in oxygen concentration, local differences in pH or local differences in the permeability of a passive layer[8]. The anode is the site where oxidation occurs and reduction occurs at the cathode. Typical half equations are shown below, Equation 1.2 shows the oxidation of zinc, Zn, and Equation 1.3 shows the reduction of oxygen, O_2[3]. Eliminate one or more of these factors and corrosion cannot occur.

$$Zn \rightarrow Zn^{2+} + 2e^- \qquad \text{(Equation 1.2)}$$

$$\tfrac{1}{2}O_2 + H_2O + 2e^- \rightarrow 2OH^- \qquad \text{(Equation 1.3)}$$

When oxidation occurs at the anodic site a potential is set up with the electrolyte in which it is immersed. This single potential can be quantified with use of a reference electrode to which all others can be related[7]. This then enables the potentials of all metals to be compared and their thermodynamic performance, with regard to corrosion predicted. From these experiments series of electrode potentials can be set up for experimental reference. The most commonly used electrode potential series gives reference to the Standard Hydrogen Electrode (SHE), in which a platinum electrode is immersed in a 1 molar solution of H^+ ions and bathed in hydrogen at 1 atm pressure at 298 K. By convention the SHE is given the value 0V[1]. The Electrochemical Series as related to SHE is shown in Table 1.1.

Metals with positive potentials such as gold (Au) +1.42 V are less likely to oxidise. These are known as noble metals. Metals with negative potentials such as lithium (Li) -3.05 V are more likely to oxidise. It must be stated however that these values are only valid under the conditions stated above. In practice and under normal environmental conditions the values may differ from those in Table 1.1.

Electrode Reaction	Standard Electrode Potential
$Au^{3+} + 3e^- \leftrightarrow Au$	+ 1.42
$Ag^+ + e^- \leftrightarrow Ag$	+ 0.80
$Cu^{2+} + 2e^- \leftrightarrow Cu$	+ 0.34
$H^+ + e^- \leftrightarrow ½ H_2$	0
$Pb^{2+} + 2e^- \leftrightarrow Pb$	- 0.13
$Fe^{2+} + 2e^- \leftrightarrow Fe$	- 0.41
$Zn^{2+} + 2e^- \leftrightarrow Zn$	- 0.76
$Al^{3+} + 3e^- \leftrightarrow Al$	- 1.71
$Mg^{2+} + 2e^- \leftrightarrow Mg$	- 2.38
$Na^+ + e^- \leftrightarrow Na$	- 2.71
$Ca^{2+} + 2e^- \leftrightarrow Ca$	- 2.76
$K^+ + e^- \leftrightarrow K$	- 2.92
$Li^+ + e^- \leftrightarrow Li$	- 3.05

Table 1.1. The Electrochemical Series[7].

It is perhaps more useful to consider the free corrosion potential of metals as in the Galvanic Series, which shows free corrosion potentials (E_{corr}) instead of standard electrode potentials. The data relates to specific conditions, usually in sea water, and therefore gives a more accurate representation of the likely behaviour of the metal under those conditions. The Galvanic Series also incorporates various alloys of the tested metals, for example aluminium alloys. This gives a known range of potentials that the metal will adopt in different conditions. The various alloying elements may in themselves improve the corrosion performance of the metal. This occurs in the Galvanic Series with zinc (Zn) and aluminium (Al). When considering SHE potentials Zn has a more positive

potential than that of Al and therefore is less likely to corrode. However, in the Galvanic Series it is shown that Zn has the more negative potential and therefore it is this which is more likely to corrode. Hence zinc is used as a sacrificial anode for many Al applications. This is shown in Figure 1.3.

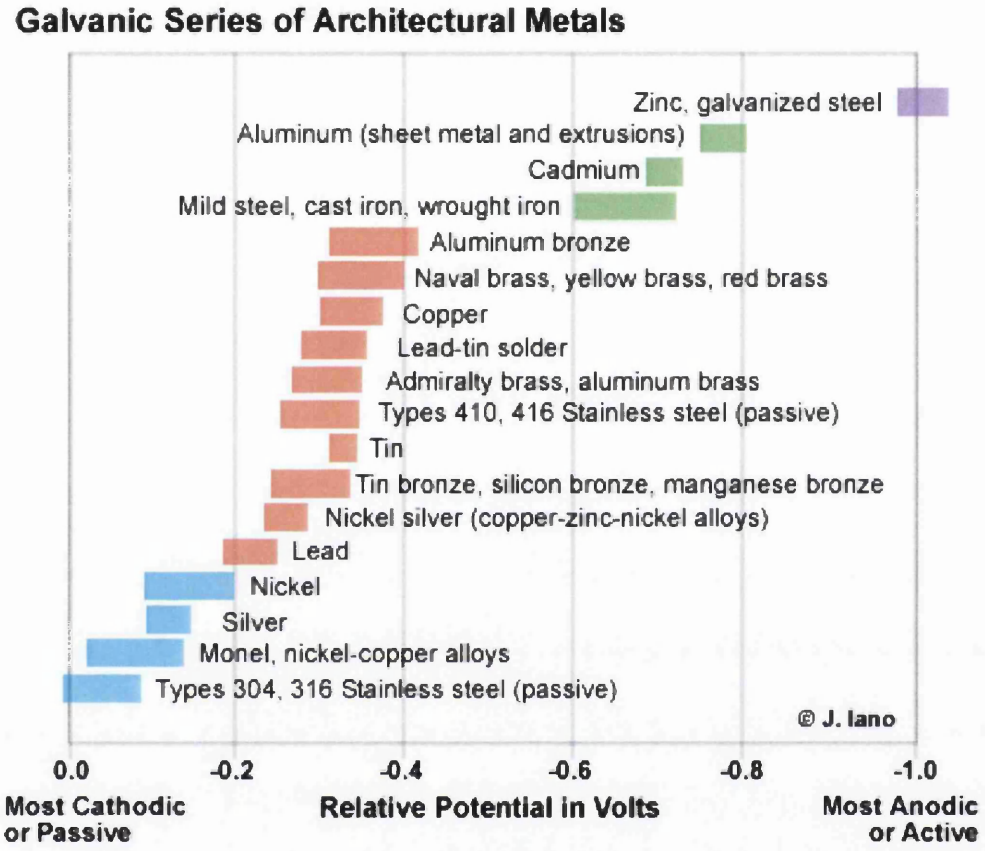

Figure 1.3. A schematic of the Galvanic Series of architectural metals[9], showing typical free corrosion potential values.

The addivity principle[10] states that the corresponding anodic and cathodic activity that occurs on the surface of a corroding metal act independently of each other. Furthermore any current flowing from the metal surface to an external circuit will be equal to the sum of the current flowing between the anodic and cathodic sites on the metal surface. Therefore under free corrosion conditions the sum of the current can be written as shown Equation 1.4[8].

$\sum i_{anodic} = -\sum i_{cathodic} = i_{corr}$ (Equation 1.4)

This i_{corr} value represents the corrosion current and represents the rate of corrosion. This can be shown easily on a Tafel plot. A Tafel plot for a corroding metal subjected to an electrolyte gives a linear representation of anodic and cathodic processes that are occurring on the surface of the metal[11].

This data can then further be represented using an Evans diagram which combines all the Tafel data for the individual electrode reactions in a single diagram, as shown in Figure 1.4. Evans diagrams can therefore be used not only to determine the rate of corrosion, i_{corr} but also E_{corr} the potential which the system will adopt when corrosion occurs under free corrosion conditions.

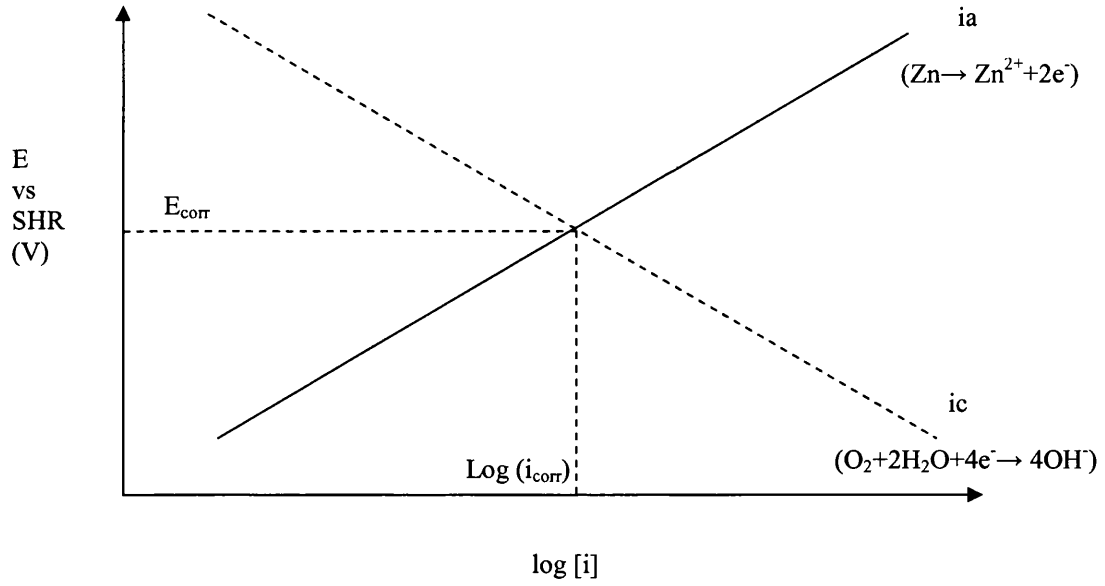

Figure 1.4. The Evans Diagram for Zn

The thermodynamic stability of metals in corrosive environments can be represented in Pourbaix diagrams. These diagrams consider the stability of a metal when there are changes in pH and potential. The Pourbaix diagrams also consider the products formed from the corrosion process at different pH and potential.

According to Pourbaix, metal is said to be corroding when the concentrations of its ions is $\geq 10^{-6}$ Mol dm^{-3}. If the concentration is less than this the metal is said to be immune and therefore no corrosion occurs. If the corrosion product is insoluble and is protecting the metal from corrosion then the metal is said to be passive and again no corrosion occurs.

The diagrams show the regions of immunity, passivity and where corrosion occurs. A simple example of the Pourbaix diagram for zinc can be seen in Figure 1.5. This shows that zinc is passive (in water) between pH 8.2 and 11, but corrodes in lower and higher pH. This arises since the hydr(oxide) is amphoteric.

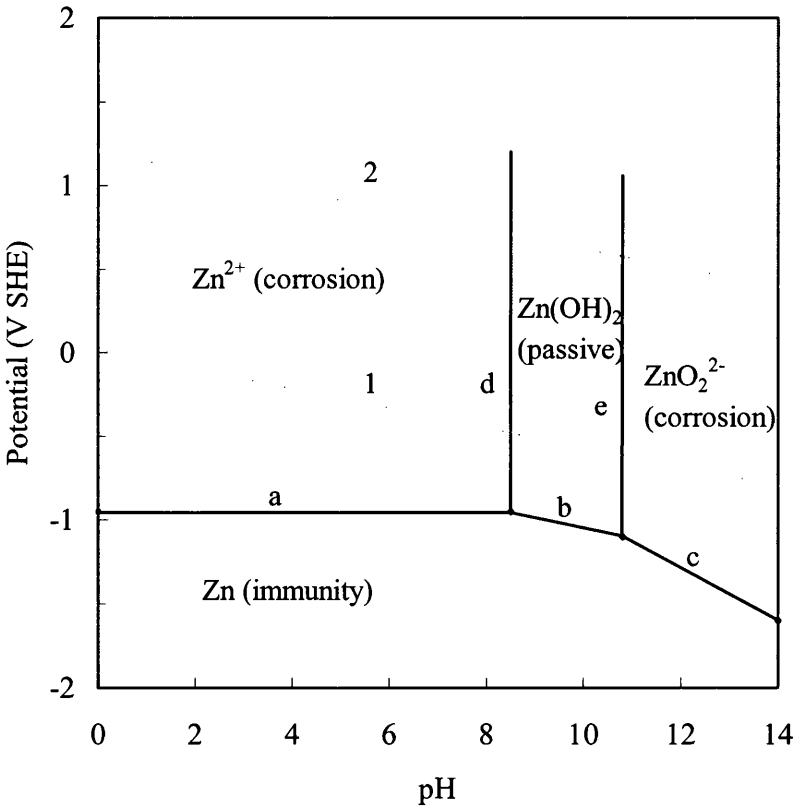

Figure 1.5. The Pourbaix Diagram for Zinc in Water[6].

1.0.1 The Mechanisms of Corrosion

Corrosion of metals as a whole can be separated under two broad headings, generalised corrosion and localised corrosion. It can occur in many different ways and under a variety of conditions. It is the circumstance and the conditions under which the corrosion occurs which characterises the corrosion mechanism.

Generalised corrosion occurs with equal intensity on the exposed metal surface. It usually occurs over a long period of time. This type of corrosion has deleterious effects on the properties and the function of the material and usually ends in failure of the component. However, failure of the material can be easily predicted as data can be easily extrapolated.

Localised corrosion can have a more immediate effect on a metals properties and performance. This is because many forms of localised corrosion occur under restrictive conditions which work to increase the corrosiveness of the local environment. Localised corrosion can take many forms some of which are discussed below.

1.0.2 Dissimilar Metals Corrosion

Dissimilar metals corrosion occurs when two different metals form a corrosion cell with each other. Each of the metals will have a different free corrosion potential as discussed earlier. The metal with the most negative potential will form the anode and will be corroded. Conversely the metal with the most positive potential will become the cathode. The further apart the two metals are in the Galvanic series the quicker corrosion will occur. Corrosion will only occur in this way if the two metals are in contact, electrically, with either an electrolyte or another conducting material. This form of corrosion is fairly common and results and can result in catastrophic failure of the component in question. However, as well as dissimilar metals being potentially disastrous, it is also widely used to as the basis of protection in many applications. Perhaps the most common and most popular example of this is how zinc is used to protect steel. As discussed earlier this is due to the free corrosion potential of zinc being more negative that the iron in the steel, the zinc will be corroded first if a corrosion cell were to be set up between the two, with cathodic activity focussed on any exposed steel.

This situation is frequently used in industry. Large zinc blocks are placed on the hull of ships as sacrificial anodes. As the zinc corrodes the ships structure is kept intact. Once these anodes are used up, they are replaced at significantly lower cost compared to that if the whole ship had to be repaired. Similarly sheet steel is galvanised with zinc as added protection against corrosion. Figure 1.6 shows the Pourbaix diagram for iron (idealised).

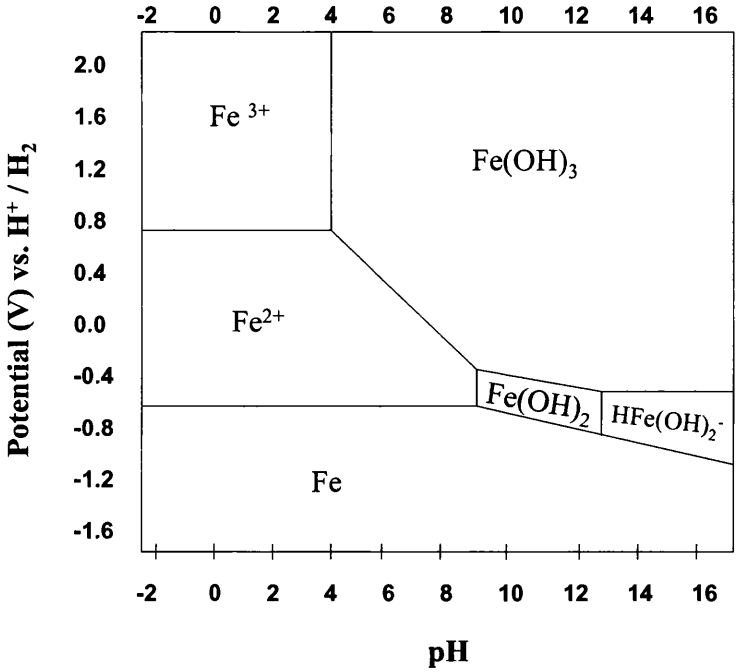

Figure 1.6. The Pourbaix Diagram for Iron

The E_{corr} value is directly in an area where corrosion occurs (ca -0.7 at neutral pH). Two choices exist for protection of iron. Firstly anodic polarisation rendering the iron passive and secondly cathodic polarisation rendering the iron immune. Galvanising is an example of the latter as the potential adapted (ca -1.05) is similar to that of pure zinc. There are many ways to prevent dissimilar metals corrosion including:

- Elimination of one or more of the corrosion cell components.
- Use of an additional metal which will act as a sacrificial anode to the other metals in the component.
- Making the cathode small compared to the anode so the effect is minimised.

- Use of inhibitors to prevent or slow the effects of corrosion.

1.0.3 Crevice Corrosion

Crevice corrosion is another form of aqueous corrosion that occurs when the electrolyte is in a restricted environment. It is often associated with complex geometries. Where the electrolyte has passed into the crevice the pH can change and this can lead to enhanced corrosion, due to increased levels of chloride ions.

The Fontana-Greene mechanism of corrosion control[12] principally refers to crevice corrosion in stainless steels; however it can be applied in this way to most metals. There are four main stages to the Fontana-Greene mechanism.

1. In the initial stages of corrosion there is enough oxygen available within the restricted site that both anodic and cathodic processes cancel each other out.
2. However this can only last a limited period of time. Once the oxygen is used up within the crevice, more oxygen diffuses from elsewhere. Subsequently the rate of oxygen reduction slows and therefore the cathodic rate slows. However metal dissolution still continues and the anodic rate is unaffected and is the dominant process. Therefore an anodic site is set up within the crevice. Therefore the overall charge of the site becomes more positive. This then leads to negative ions from the surrounding solution flowing in to address the balance of the system.
3. These ions can frequently be chloride. On their own they increase the corrosion rate but they also combine with metal ions to form complexes which in turn react with water to produce acid.
4. The production of acid and continued flow of chloride ions into the crevice lead to aggressive corrosion taking place. Once the process has started it becomes autocatalytic in nature. This means that it is self sustaining and will continue to become more aggressive.

Figure 1.7 and 1.8 show possible mechanisms of crevice corrosion. Figure 1.7 shows the mechanism of anodic delamination which occurs when thick paint layers are present. It is easier for oxygen to pass through the electrolyte layer rather than the paint

layer therefore an anodic area is formed at the nose of the crevice. On the other hand, as shown in Figure 1.8, when thinner paint layers are present cathodic delamination takes precedent as it is easier for the oxygen to pass through the paint layer rather than the electrolyte. Therefore a cathodic site is set up at the nose of the crevice.

Crevice corrosion can be controlled by following a few simple measures.

- Consideration should be give to the geometry of the components. So that electrolyte is less likely to become stagnant.
- Sealing and/or filling of joints so as to prevent electrolyte from entering any potential crevices.
- Application of barrier coatings so as to eliminate the possibility of a corrosion cell forming.
- Application of cathodic protection electrically.

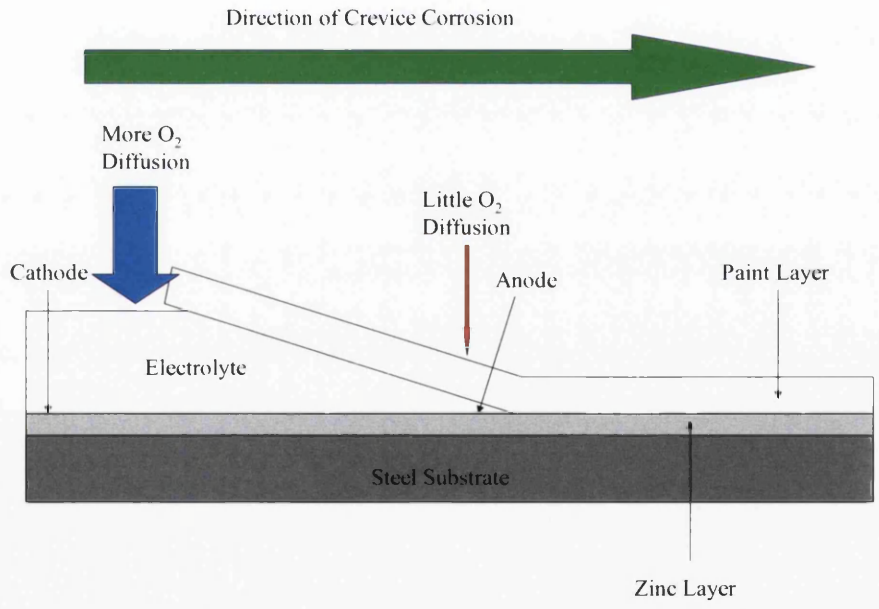

Figure 1.7. The Mechanism of Anodic Delamination

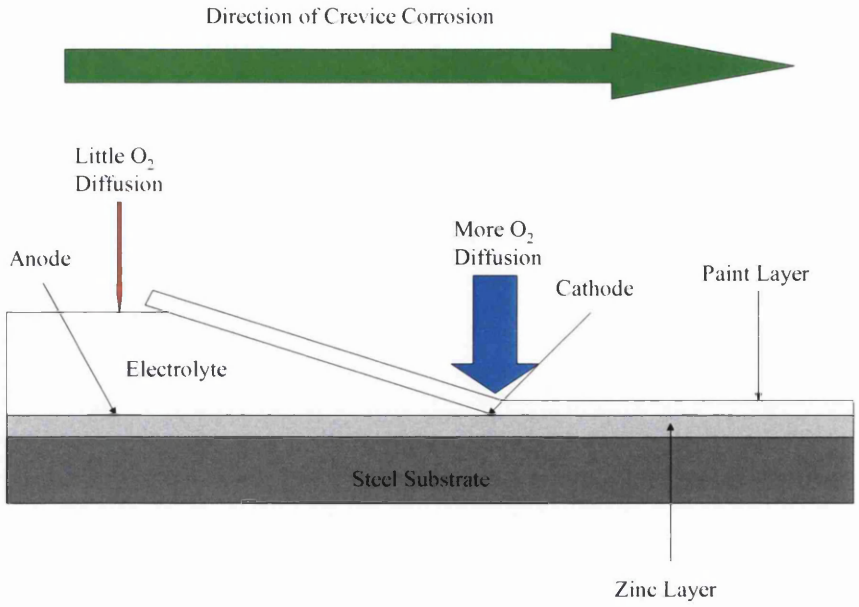

Figure 1.8. The Mechanism of Cathodic Delamination

1.0.4 Pitting Corrosion

Pitting corrosion is a significant form of aqueous corrosion when considering the surfaces of metals. This type of corrosion often occurs at a defect of imperfection on the surface if the metal either in the coating or protective oxide layer. As these defects are usually very small the effect is highly localised. The anode site is formed where the defect is located and the result is a highly positive compared to the surrounding area. Therefore corrosion occurs. The formation of a film of corrosion product over the pit balances the system as it prevents oxygen getting to the site and therefore stabilises it. If the pit becomes sealed it is unable to propagate and is terminated. However, if a film of corrosion product is unable to form and the system is still able to receive oxygen the pit therefore propagates. This can lead to premature failure as is found in intergranular corrosion.

There are measures that can be taken to prevent pitting corrosion. These are as follows.

- Preparation of the metal surface with various chemical pre-treatments to grow a passive layer.
- In the case of stainless steel the metal can be polarised with an alternating current to improve pitting corrosion resistance.

1.0.5 Differential Aeration Corrosion

Differential aeration corrosion occurs when a metal is exposed to an electrolyte and there are different levels of oxygen concentration. At points where the oxygen levels are lower, then anodic behaviour will be dominant. Conversely at points where the oxygen concentration is higher cathodic behaviour will be the most prevalent. The mechanism of differential aeration corrosion can be represented using the Evans water droplet. Under the water droplet anodic and cathodic activity initially occur overs the surface. As time passes, the oxygen in the electrolyte is used up. Therefore more is drawn in from the external atmosphere. The oxygen takes the shortest path. This is at the edge of the droplet. The cathodic site is therefore set up at the edge of the droplet corresponding to the site where oxygen diffusion is at a maximum. Therefore the anodic site is set up at the point of the longest path i.e. at the centre of the droplet. Metal ions diffuse towards the edge of the droplet as hydroxide ions diffuse towards the edge of the droplet. Where they meet, a ring of corrosion product forms, giving a ring like appearance from above. This can be represented schematically as in Figure 1.9[13].

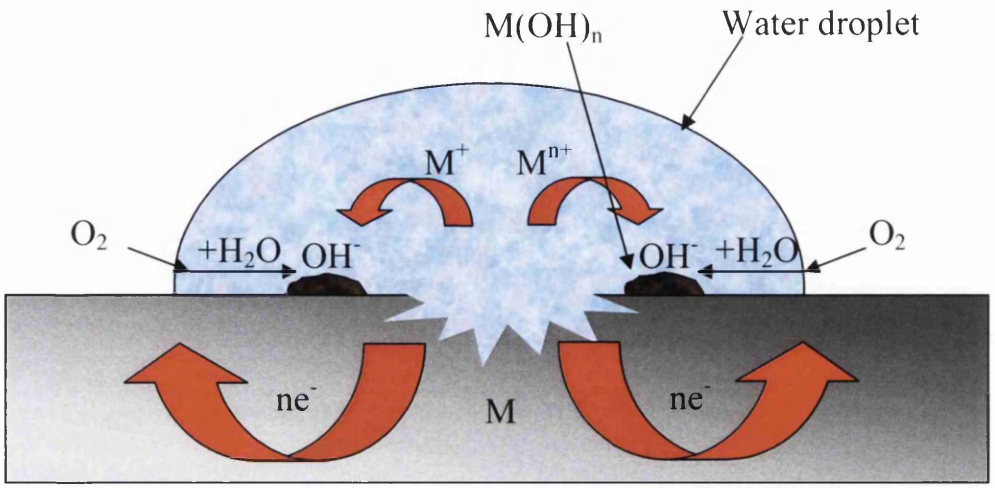

Cathodic Oxygen Reduction	Anodic metal dissolution	Cathodic Oxygen Reduction
$O_2 + 2H_2O + 4e^- \rightarrow 4OH^-$	$M \rightarrow M^{n+} + ne^-$	$O_2 + 2H_2O + 4e^- \rightarrow 4OH^-$

Figure 1.9. A schematic of an Evans water droplet, showing the mechanism of differential aeration corrosion[13].

Prevention methods include.

- Avoiding water absorbance, this may result in a differential aeration cell being created.
- Allow for sufficient drainage and ventilation to prevent formation of electrolyte pools on the surface of metal.

In coated steel products such corrosion can occur when organic coatings of widely different symmetries are used. For example, as illustrated in Figure 1.10, oxygen access to the galvanised layer on the thin coated side is greater and therefore becomes cathodic, conversely, anodic behaviour is focussed beneath the thicker paint layer on the other side of the product.

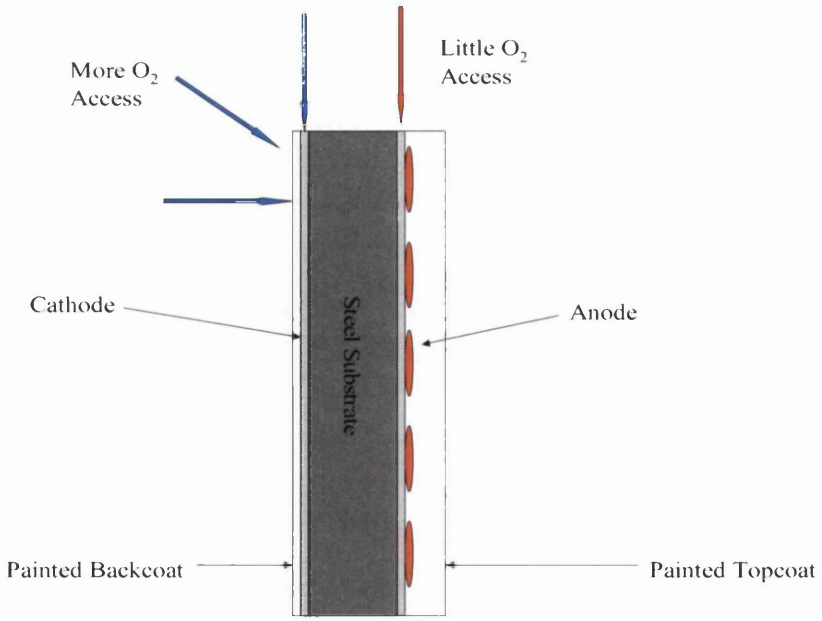

Figure 1.10. A Representation of Differential Aeration Corrosion on a Coated Steel Product

1.1.0 Organic Coated Steels

Steel is one of the most widely used materials in modern everyday life. It is also one of the most widely used materials in industry. It finds use in such things as construction, domestic, packaging and automotive applications. However in order to prevent corrosion of the steel it has become increasingly popular to pre-coat the steel to increase the lifespan in the desired application. Due to the improved solvent and other contaminating emissions, Organic Coated Steels (OCS) have emerged as the major material used in many of these applications, as shown in Figure 1.11[16, 17].

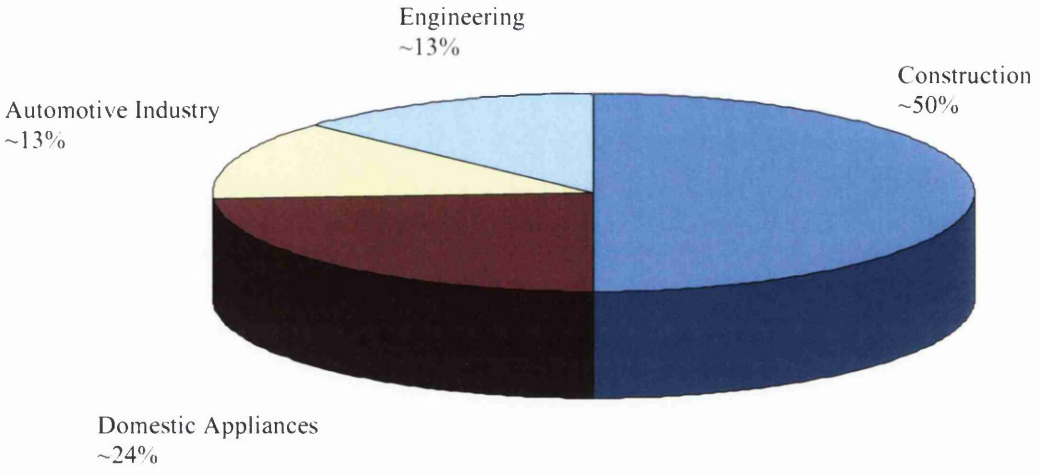

Figure 1.11. An Outline of the Major Uses of OCS[16, 17]

As seen the construction industry accounts for 50% of the major markets for OCS. However in Europe the construction industry accounts for an estimated 70% of the total consumption of OCS[14]. This is also aided by the modern trend for buildings to aesthetically pleasing finishes. This therefore increases the market further for pigmented coatings which improve the properties of the sheet steel. It is also increasingly necessary in the modern era for cladding used in the construction industry to have a long lifespan. This is because regular replacement of the cladding sheet is not only a bad reflection on the supplier but is also uneconomical and undesirable for the customer. Therefore it is not untypical for "a single guarantee of 30 years to be applied to the whole building envelope"[15].

For the purposes of architectural cladding or roofing, mild steel strip is used. The gauges of such steel vary from 0.55mm to 0.7mm for cladding and roofing respectively[16]. Having rolled the mild steel strip substrate to the desired thickness, it is then coated, usually via a hot dip galvanising route although electroplating or vapour deposition can be used to achieve thinner coatings.

1.1.1 Sacrificial Protection: The Galvanising of Steel

Sacrificial protection of steel has long been an accepted method of corrosion prevention in industry, especially with regard to organic coated steels. Most of the sacrificial protection for OCS used in the construction industry is provided by Zinc or zinc alloys. As well as providing barrier protection and self healing qualities to the steel, Zinc coating provide sacrificial protection to cut edges due to the fact it is less noble than steel and therefore corrodes preferentially to the steel maintaining the integrity of the substrate.

In the hot-dipping process, simplified schematically in Figure 1.12, the metal

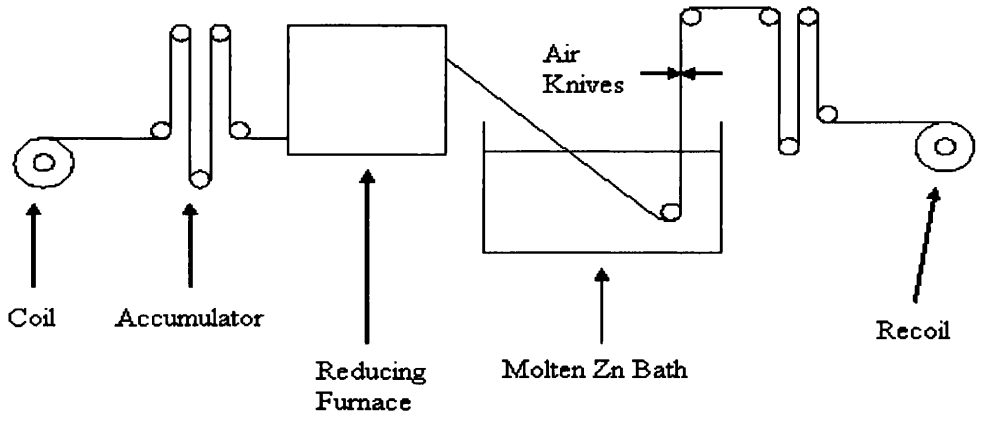

Figure 1.12. A Schematic of a Continuous Hot Dip Gavanising Line

substrate is immersed a molten metal bath. Zinc lends itself particularly well to this process as it has a lower melting point in comparison to steel and also gives sacrificial protection to the steel strip once coated. The speed at which the substrate moves through the molten metal bath determines the thickness of the coating. The rapid reaction between the molten metal and the substrate causes the formation of Fe/Zn intermetallics and hence a strongly bonded metal coating. However these intermetallics are brittle in nature and

therefore in conventional dipping, additions of Aluminium to the bath in the region on 0.12% allows for a thin layer of Fe_2Al_5 to form in preference to the Fe-Zn intermetallics[18].

Coating thickness is controlled after the dipping process is complete via a set of gas knives. This provides a surface free of marks and a constant thickness of coating. Thicknesses of the zinc coating on hot-dipped samples can range from 4-50μm [19].

There has been much research into the Zinc based coatings used for galvanising some of the more common galvanised steel systems are explained below.

1.1.2 Galvanneal

Galvanneal is obtained by annealing conventional hot dipped galvanised steel (HDG). After the dipping process, the sheet is rapidly heated to 550°C by use of an induction heater or in a direct fired furnace. The heating promotes the diffusion of the iron from the steel leading to the formation of Fe-Zn delta intermetallics in the coating[13]. Gavanneal can be readily formed, welded or painted, due to the presence of these columnar grains growing normal to the substrate. The intermetallics appear to improve the resistance of the coating to flaking during forming. The surface finish of the coating is such that it provides a good key to any further finishing such as painting[20] and as such Galvanneal is widely in the automotive industry.

1.1.3 Galfan

Galfan was first investigated at the Centre de Recherches Metallurgiques, Belgium in 1980 in conjunction with the ILZRO. Galfan is a Zinc based coating with the addition of 4.6-5% Al.(typically 5%) and 0.1% misch metal and is produced via the hot dipping process at temperatures between 420-440°C. Under equilibrium conditions the eutectic point in the Zn-Al binary system is at an Al addition of 5%wt, at a temperature of 381°C, the liquid will solidify producing a wholly eutectic structure. The conditions on a continuous hot dipping line are never equilibrium however and therefore the resulting microstructure of a typical Galfan coating consists of fine dendrites of proeutectic zinc

which are first to solidify, surrounded by a Zn-Al eutectic in which all the aluminium content is present[13].

Galfan has many advantages over conventional hot dipped galvanised steel. It has improved corrosion resistance due to the presence of aluminium oxide which prevents corrosion. Galfan also shows more formability than conventional hot dipped galvanised steel in that there are no intermetallics present within the system. The presence of aluminium at the levels seen in Galfan coatings also leads to a brighter more textured surface than that of HDG. However the Aluminium level does affect the surface texture of the coating around the boundaries of the eutectic cells[21] at points where the eutectic cells meet. This was shown to result from a degree of solidification shrinkage in the coating[22, 23].

Cooling rates[24] and microstructure have been seen to have a great influence on the corrosion performance of Galfan type coatings. Alloying elements can be added to act as grain refiners to produce a fine microstructure without changing the characteristic two phase microstructure.

Corus currently use a zinc/aluminium coating of similar composition to Galfan. It is known commercially as Galvalloy.

1.1.4 Zalutite / Galvalume

Zalutite / Galvalume is a Zn-Al alloy metallic coating consisting of 55% Al and 43.5% Zn. The microstructure is controlled by a further addition of 1.5% Silicon. This helps restrict and refine the growth of the microstructure. This results in primary aluminium dendrites surrounded by zinc rich phase.

Due to the increased aluminium content there is increased corrosion performance due to the formation of Al_2O_3 which helps to passivate the system against attack. However Zalutite shows poor paint adhesion and is therefore mainly used uncoated in dry arid environments.

The microstructures of all the metallic coatings discussed can be seen below in Figures 1.13-1.16, courtesy of J. H. Sullivan, Materials Research Centre, Swansea University.

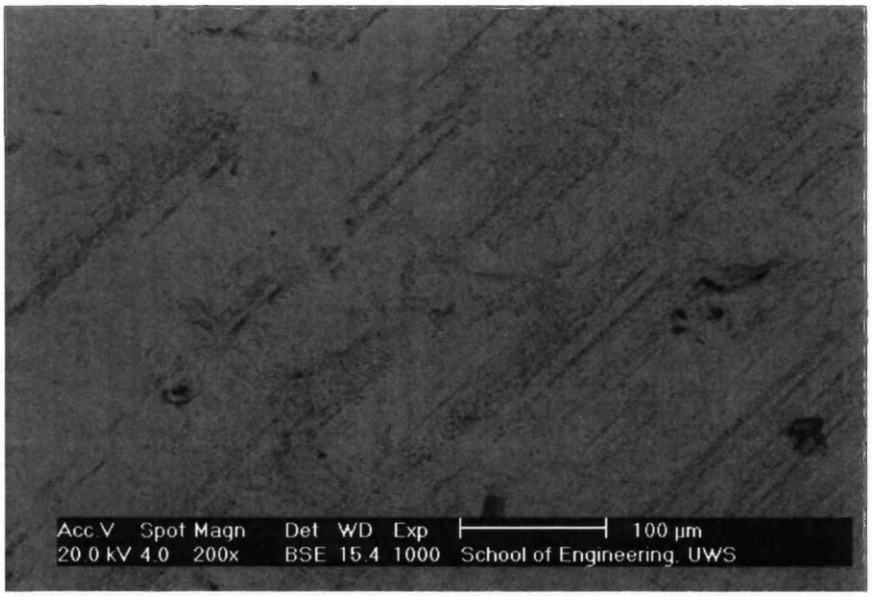

Surface

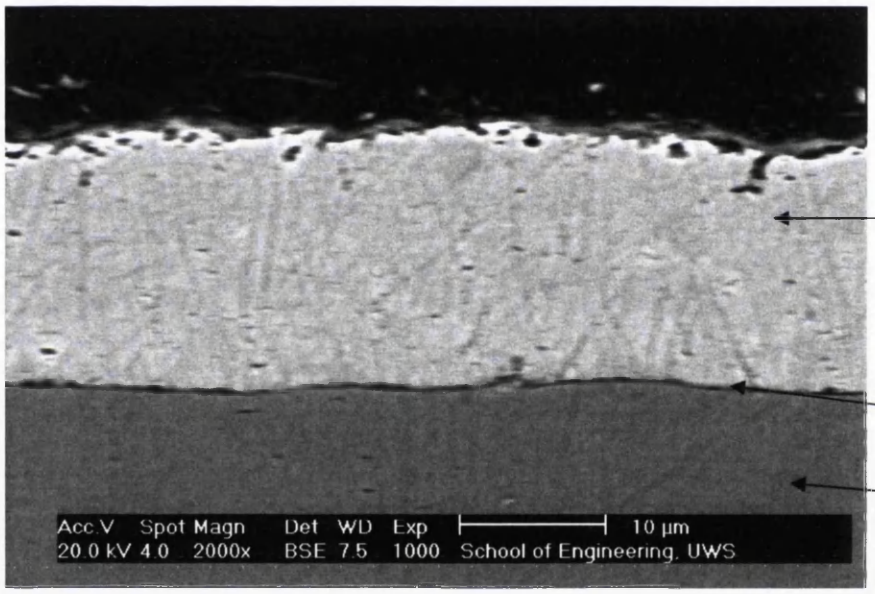

HDG coating

Thin intermetallic layer

Steel

Cut-edge

Figure 1.13. Surface and cut-edge micrographs of HDG coating on steel substrate.

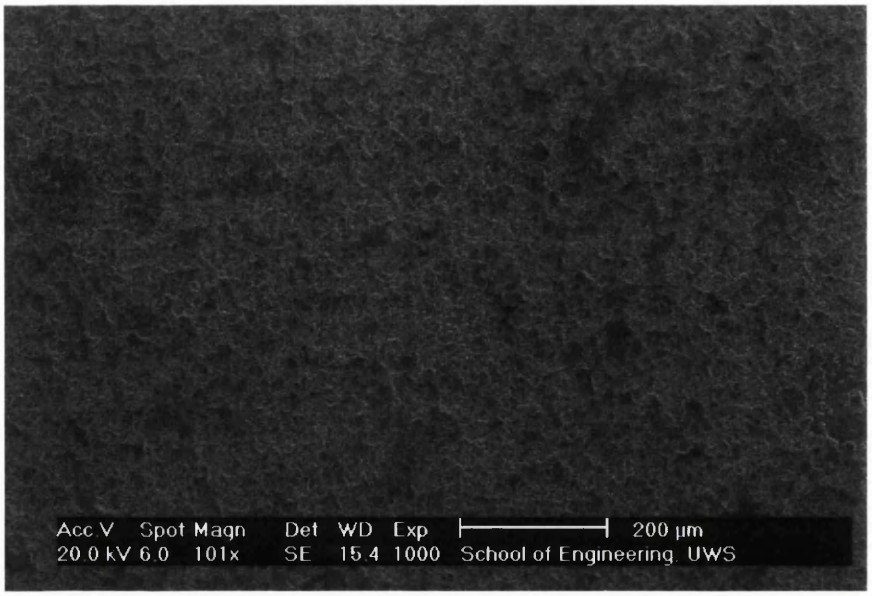

Surface

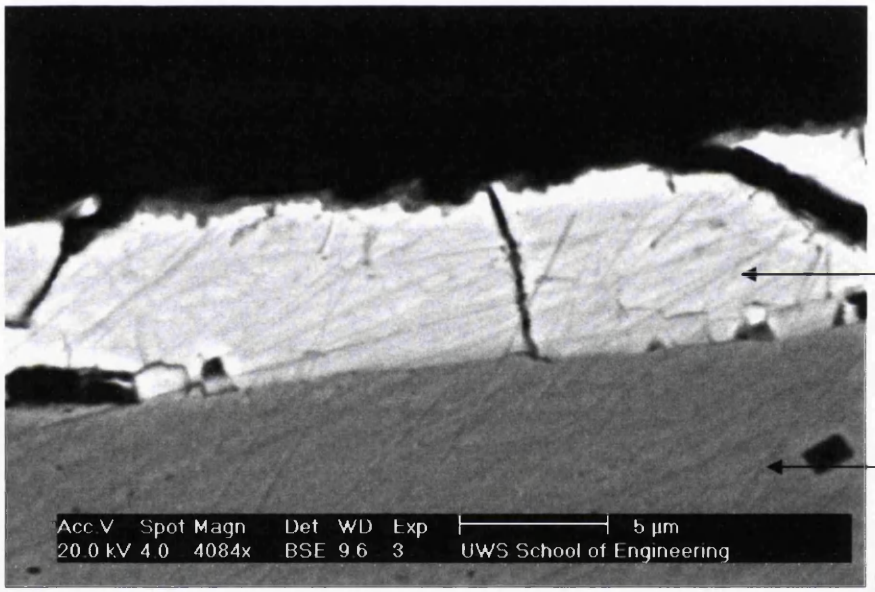

Cut-edge

Figure 1.14. Surface and cut-edge micrographs of Galvanneal (IZ) coating on steel substrate.

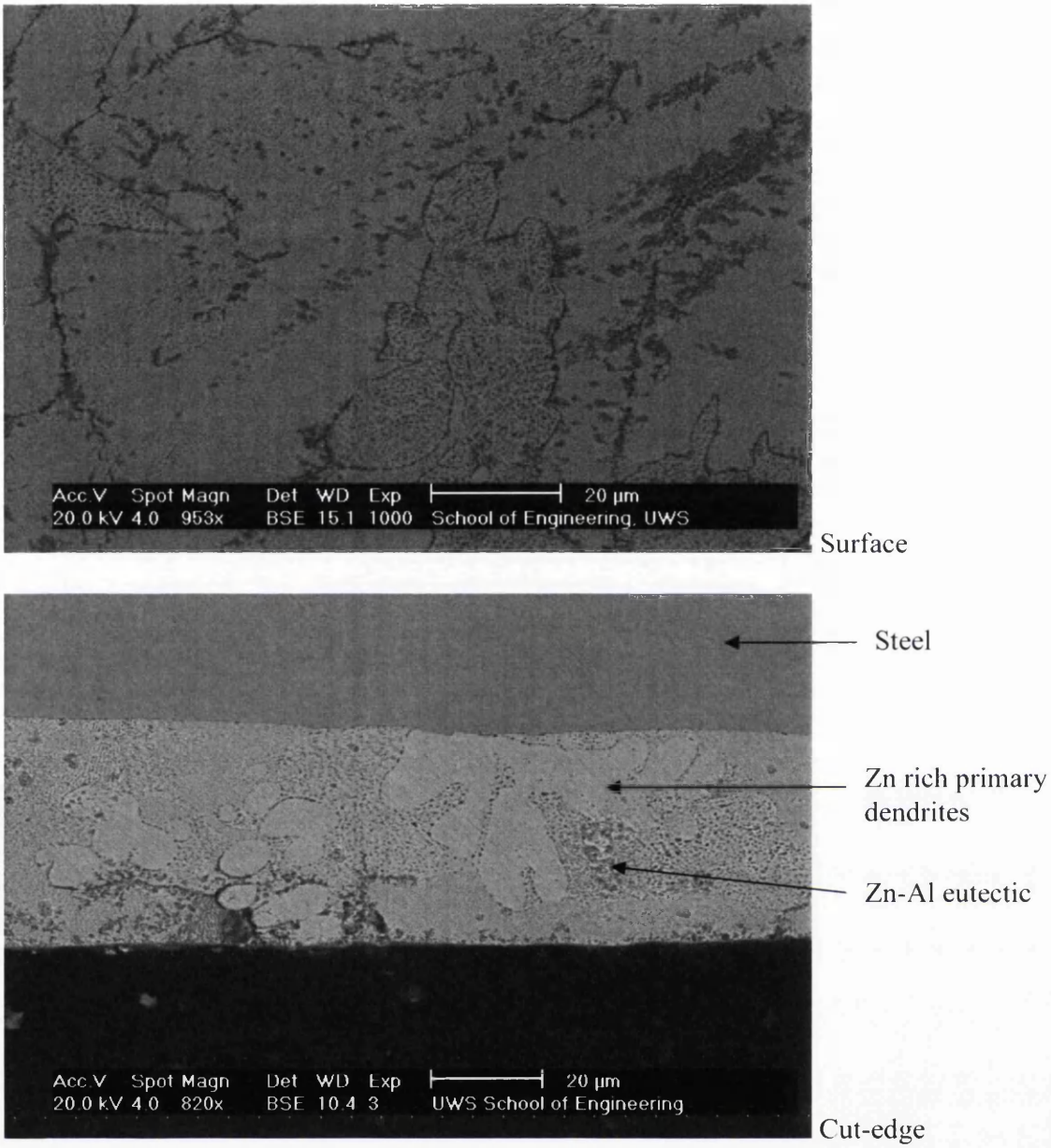

Figure 1.15. Surface and cut-edge micrographs of Galfan coating on steel substrate.

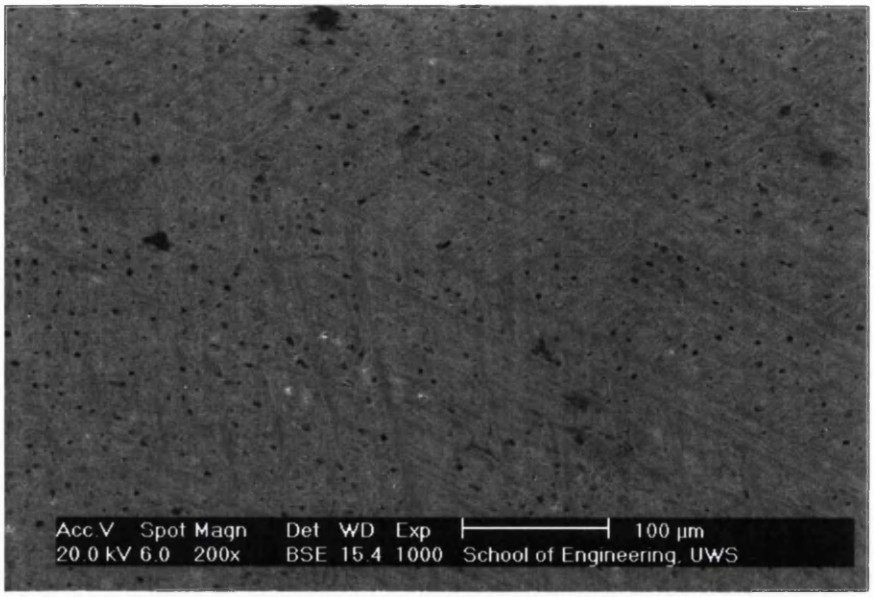

Surface

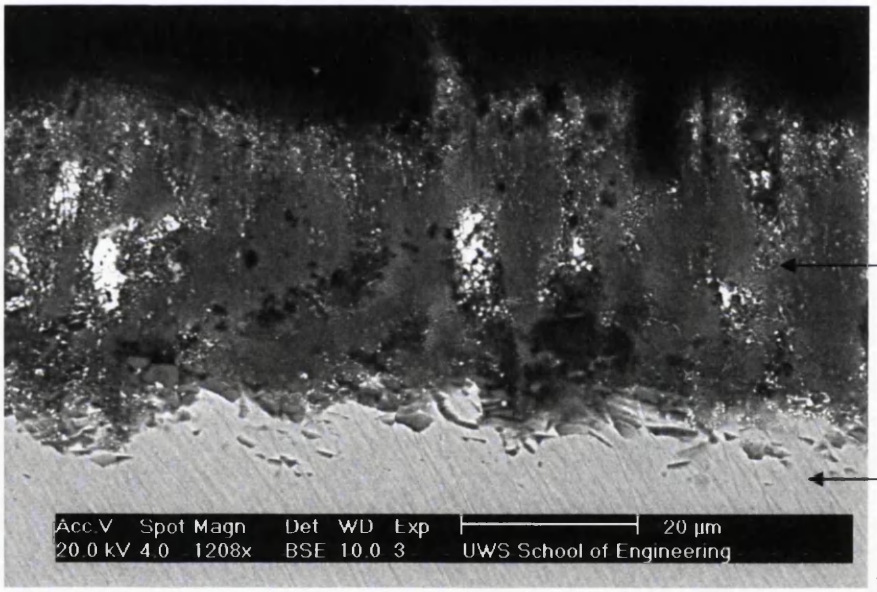

Zalutite coating

Steel

Cut-edge

Figure 1.16. Surface and cut-edge micrographs of Zalutite coating on steel substrate.

1.1.5 PVC Plastisol Coated Steel

Having acquired the galvanised steel substrate, the surface must be prepared for final painting. This is achieved with the use of pre-treatments and primers. The pre-treatment of the substrate has two functions it etches the surface of the substrate which allows the primer layer to adhere to it more easily, it also has corrosion resistant properties. Until very recently both the pre-treatments and the primers had chemistry that is based around chromium and hexavalent chromates[25]. The topcoat is then applied to the steel via a coating line, shown schematically in Figure 1.17. PVC Plastisol coated steel is one of Corus' most popular products. The term plastisol refers to a dispersion of PVC in plasticizer. However there are a number of constituents necessary to form a stable and useful coating system. These include PVC, plasticizer, pigments and stabilisers to protect the coating from the effects of harsh environments. The make up of an OCS is shown schematically in Figure 1.18.

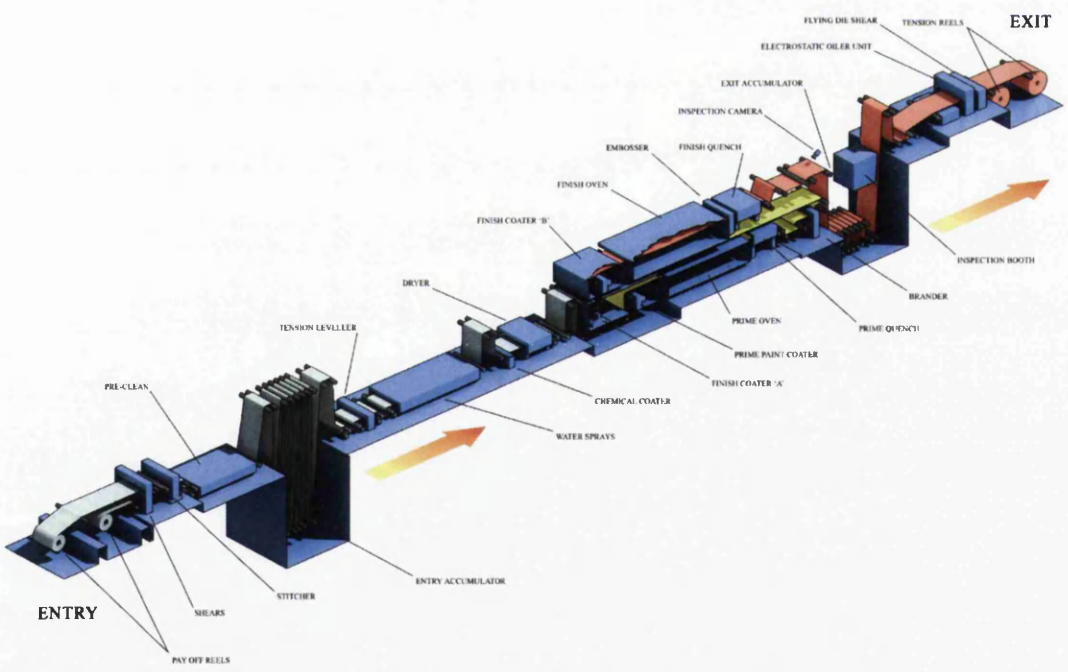

Figure 1.17. A Schematic of a Modern Coating Line

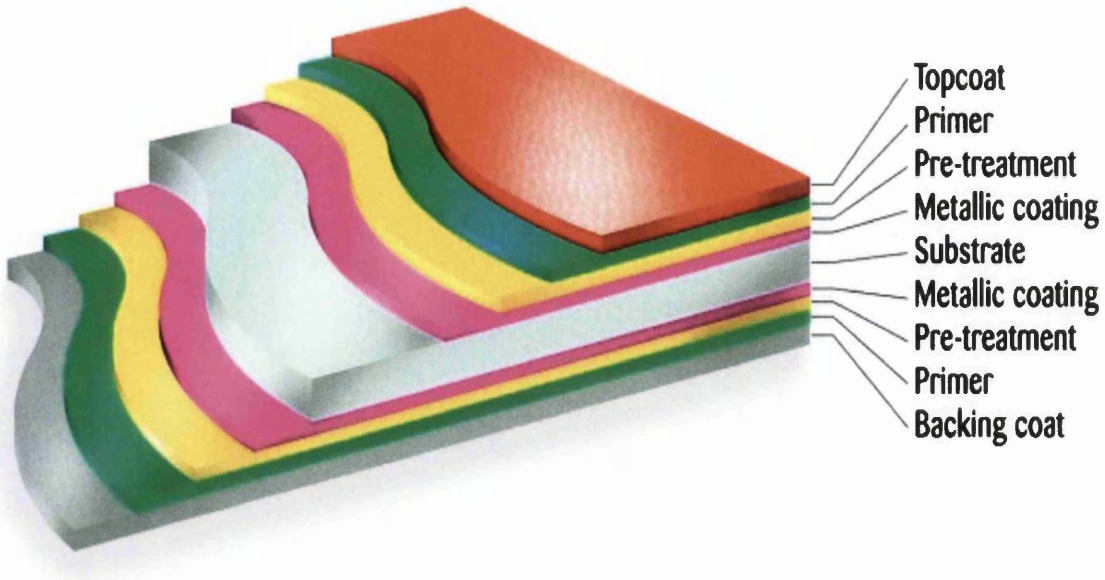

Figure 1.18. A Schematic of an Organic Coated Steel[14]

1.1.6 The Production of PVC

The PVC provides the bulk of the coating formulation. PVC is formed from polymerisation of vinyl chloride. CH_2==$CHCl$. This monomer can be produced by two routes. The most common route is known as the ethylene route or balanced process. Dichloroethane is produced by direct catalytic chlorination of ethylene. This is then purified and pyrolysed directly to vinyl chloride[26]. This process is outlined below.

$$CH_2{=}{=}CH_2 \xrightarrow[\substack{\text{High T}\\ O_2\ \text{Catalyst} + HCl}]{\text{Cl Catalyst}} CH_2Cl{-}CH_2Cl \xrightarrow{\text{Pyrolysis}} CH_2{=}{=}CHCl + HCl$$

The second way of obtaining the vinyl chloride monomer is the acetylene route. This was heavily favoured until the 1960s with particular prominence in Europe[26]. Acetylene is generally more expensive to obtain and therefore in recent times the ethylene route is the more popular, as mentioned earlier. The acetylene route to producing the vinyl chloride monomer is a one stage process and can be seen below.

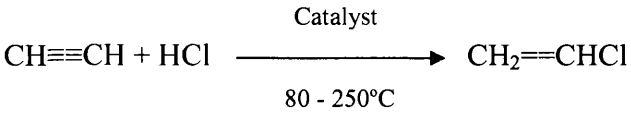

There are three main ways of producing PVC from the vinyl chloride monomer, these are, suspension polymerisation, emulsion polymerisation and bulk polymerisation. In suspension polymerisation, monomer droplets (50-150μm) are suspended in water via agitation in a pressurised vessel, which contain a monomer soluble free-radical initiator. The polymerisation takes place at a slightly elevated temperature. The method of suspension polymerisation accounts for ~ 80% of commercial polymer production.

In emulsion polymerisation there are still the water and monomer present, as well as emulsifiers and a water soluble free-radical initiator. Agitation can result in extremely fine droplets of monomer down to ~ 0.1μm. Free-radicals are formed in the aqueous phase and initiation occurs at the interface between the monomer and the aqueous phase. Emulsion polymerisation accounts for ~ 10-15% of commercial polymer production.

Bulk polymerisation is the simplest system of the three. It only comprises of a free-radical initiator and the monomer and is performed under pressure. There are two stages to the process. In the first stage the system is highly agitated, polymer grains then form uniformly. Once the grains have grown to sufficient size and strength, they are transferred to a second stage reactor. Here more monomer and initiator are added and growth occurs until completion. Bulk polymerisation is difficult to operate and therefore despite high quality products and favourable properties, it only accounts for less than 10% of commercial polymer production[26].

1.2.0 The Theory of Plasticisers

The definition of a plasticiser states that: "A plasticiser is a material incorporated in a plastic to increase its workability and flexibility or distensibility."[27] Plasticisers are typically organic in nature.

On polymerisation PVC forms a rigid structure and therefore a rigid product. There are many theories on the action of plasticizers on PVC.

1.2.1 Types of Plasticiser

As mentioned before, plasticisers are usually organic in nature and can come from a variety of substances. Many plasticisers have different properties and therefore can be chosen specifically for these to enhance performance of the product in the desired application.

Sulphonic acid esters are now replacing phthalates. This family of plasticizers has very good colour retention properties and therefore they find use in applications where aesthetics are important. The general structure of a sulphonic acid ester is shown below[25].

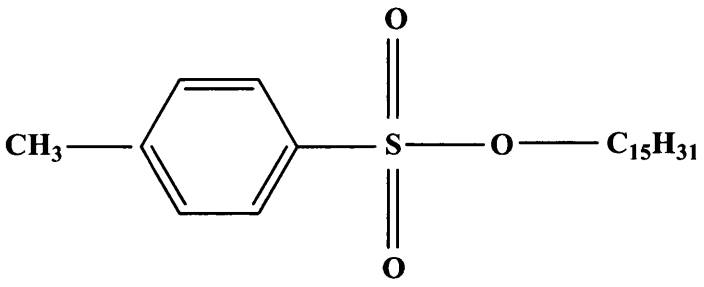

This type of phthalate free plasticiser is now used in most plastisol products; under the trade name Mesamoll.

1.3.0 Additives to Plastisol Systems

Many substances are added to a plastisol system to improve its properties and performance. These substances are not necessarily incorporated within the resin but can be included within the build up of layers that contribute to the final plastisol coating[27].

1.3.1 Heat and Light Stabilisers

These additives are used to scavenge the HCl that is formed on degradation. They also act to deactivate spots on the chain where the initial chlorine atoms have come from to stop the catalytic effect of HCl formation. The most common stabilizers of this kind

are metallic salts from organic acids or phenols, the most common of which include combinations of barium, zinc and calcium salts[28]. Such salts are usually acetates which remove HCl releasing an acetic acid which does not cause degradation.

1.3.2 Ultraviolet Absorbers

These stabilisers are used when the PVC product is exposed to either fluorescent light or sunlight for extended periods of time. The use of 2-hydroxybenzophenones increases the weathering performance of plasticized PVC markedly. It works by dissipating the energy of UV light. It is a reversible reaction and therefore the stabiliser is left unaffected and can continue to perform the task a number of times[24]. The hydroxybenzophenone undergoes a restructuring mechanism during the energy dissipation reaction this is shown in Figure 1.19[17].

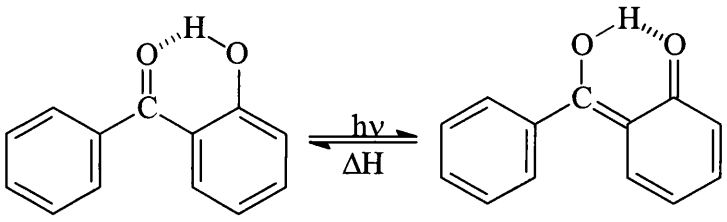

Keto Enol

Figure 1.19. The Restructuring of Hydroxybenzophenone[17]

1.3.3 Pigments and Dyes

In a general PVC formulation insoluble solid pigments are more frequently used over dyes. This is due to the fact that dyes, by their nature, are more prone to degradation and leaching. This may lead to migration and possible colour transfer from the product. Pigments on the other hand can be either organic or inorganic in nature and are insoluble. The primary reason for addition of a pigment is to provide an aesthetically pleasing product. However some pigments also aid the performance of the coating such as carbon black, which is both an efficient UV absorber and can also act as an antioxidant. It is also true to say however that a pigment should be carefully chosen as the pigment usually

resides in the topcoat of the system and therefore in outdoor applications, it is the first line of defence against weathering and degradation[28].

1.3.4 Flame Retardants

Flame resistance is of high importance in plastisol products due to the high amount of usage in the construction industry. Many flame retardants act so as to slow down the chain reaction of the combustion process[25]. In recent times antimony oxide and trioxide have been popular in their use as flame retardants.

1.3.5 Fragrance and Colour Masks

Plasticised PVC can occasionally have an undesirable odour. Therefore it is not unusual to add an industrial fragrance to mask this and make the product more desirable to the customer. In this vain, fragrances that give aromas associated to cleanliness or luxury can be added to the PVC compound[28, 29].

1.3.6 Optical Brighteners

Optical brighteners are used to enhance the appearance of the product. They are compounds which absorb near UV radiation and re-emit the energy by fluorescence as a blue-white light. They are usually used in white goods where brightness is a selling point. They do, however have a limited lifespan in the sunshine and can contribute to UV degradation[27].

1.4.0 Degradation of PVC

Where there is a coating there is always the potential for that coating to become degraded or fail. There are many causes of degradation. These include; UV light, heat, oxygen and mechanical stress. Therefore there is a need for stabilisers to be added to the coating make up as mentioned previously. Below there is a description of typical types of degradation with regard to PVC.

1.4.1 Photodegradation

Photodegradation occurs when polymers are exposed to UV light. This leads to the physical or chemical changes that could be detrimental to the polymers performance. These changes can change the structure of the polymer chain, additions to the polymer during the processing route can act as impurities promoting degradation. Different types of polymers absorb different frequencies of UV light. Table 1.2[17] shows typical frequencies that are absorbed by certain polymers.

Polymer	Bonds present	Absorption (max.)
Polyolefins	C-C, C-H	140nm ($\sigma=\sigma^*$)
Poly(vinylhalides)	C-Halogen, C-C, C-H	190nm ($n=\sigma^*$)
Poly(vinylalcohol)	C-C, C-H, C-O, O-H	200nm ($n=\sigma^*$
Polybutadiene	C-C, C-H, C=C	220nm ($\pi=\pi^*$)
Polystyrene	C-C, C-H, C=C	230-280nm ($\pi=\pi^*$)
Aliphatic polyamides	C-C, C-H, N-H, C=O, C-N	220nm ($n=\pi^*$)

Table 1.2. Absorption Frequencies of Certain Polymers[17].

The frequencies shown are at the high end of the sunlight frequencies. Polymers with additions throughout the processing route are particularly susceptible to photodegradation. There are a number of mechanisms by which photodegradation can occur.

1.4.2 Photo-oxidation

This is a common mechanism and occurs on exposure to radiation in the presence of oxygen. This would occur on exterior weathering of the polymer.

1.4.3 Photo-thermal Degradation

This is degradation that occurs at temperatures between standard temperature and the temperature where thermal degradation becomes the most dominant mechanism to occur.

1.4.4 Photolysis

This is the case where the main chain of the polymer is responsible for absorption of radiation rather than the branches and functional groups.

1.4.5 Photohydrolysis

This is the case when the polymer is exposed to radiation under conditions of high humidity[17].

There are three major steps involved in degradation. These are initiation, propagation and termination. This however relies on the formation of free radicals. This is shown in Figure 1.20.

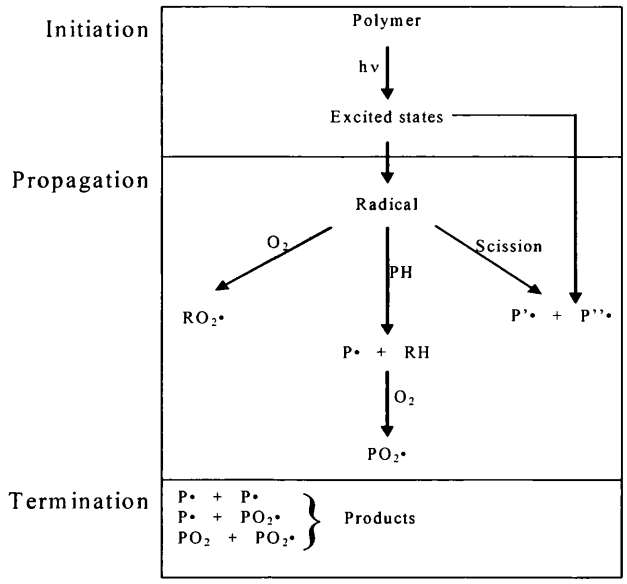

Figure 1.20. An Outline of a Free Radical Reaction [17]

1.4.6 Initiation

During the initiation stage the polymer is induced into an excited state in some cases causing a photo-cleavage, and due to the aromatic nature of some of the additions that are introduced into to the polymer systems that will absorb UV light readily. This leads to the formation of a highly reactive free radical. It is this free radical that begins the degradation sequence[17].

1.4.7 Propagation

Although harboured by the solid state of the polymers, these free radicals can easily form alkyl radicals by scavenging a hydrogen atom, which form peroxy radicals and polymer radicals.

The formation of radicals and the continuation of the reaction will occur until two radicals collide and no further radicals form. Other pathways include alkoxy or hydroxy abstraction of hydrogen. This is known as chain branching and is responsible for the auto-accelerated kinetics that is common in the photodegradation of polymers. This chain

branching can be seen in Figure 1.21. As seen, alkoxy and hydroxy pairings are formed via the POOH photolysis. This is due to the polymer matrix restricting diffusion and therefore the reduction in the chain branching effect[17].

1.4.8 Termination

Termination is the process whereby discrete degradation reactions within the system can no longer continue automatically. It is most likely to occur between two peroxy radicals ($PO_2\cdot$). They have a high affinity for each other and therefore the chances of collision are higher. On collision the peroxy radicals form an unstable tetra-oxide. The subsequent loss of the oxygen results in increase in cross linking and stiffness in the polymer. Other than this there is also the possibility of the formation of alcohol and ketone groups on the polymer. These reactions are shown in Figures 1.22 and 1.23 respectively[30].

.

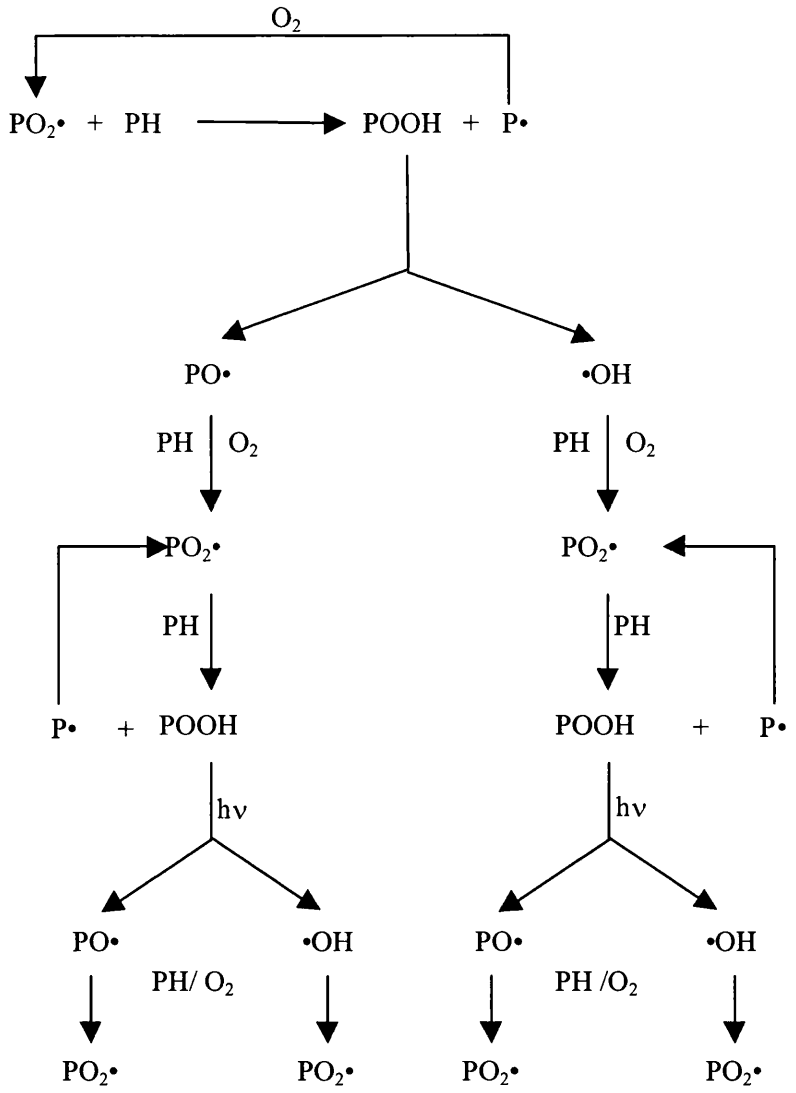

Figure 1.21. A Schematic of Chain Branching

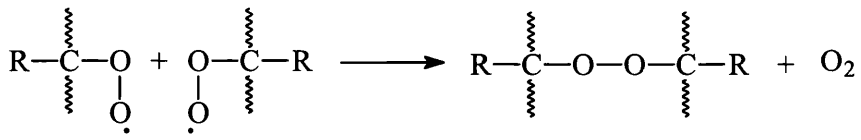

Figure 1.22. An Example of Cross linking within the Polymer

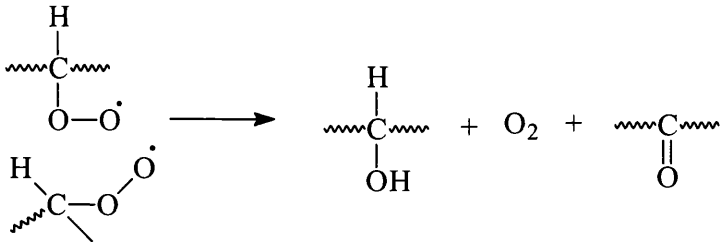

Figure 1.23. The Formation of Alcohol and Ketone Groups During Termination

1.4.9 Thermal Degradation

It is possible, that all polymers may be susceptible to a type of thermal degradation. The thermal degradation of PVC can lead to phenomena such as discolouration, evolution of hydrogen chloride and depreciation of physical and chemical properties.

One of the most recognised degradation pathways are the elimination reactions that give rise to totally distinct compounds such as the dehydrochlorination of PVC which will be discussed later. There are also pathways such as depolymerisation and substitution reactions. In the former, the main polymer chain is split into smaller polymers. In the latter functional groups are changed, due to the elimination or radical reaction of the original groups.

In general, the stability of the polymer is dependant on the form and strength of the main backbone of the polymer. This is due to the differing strengths and lengths of the chemicals bonds present. The stronger the bonds, the more resistant the polymer will be to degradation[17].

1.4.10 Dehydrochlorination of PVC

Dehydrochlorination of PVC can occur both thermally and photochemically. It is caused by the progressive elimination of adjacent hydrogen and chlorine atoms in the polymer chain. This leads to a double bond bring formed between the carbons from which the hydrogen and chlorine originally came. This produce two free radicals, one

hydrogen and one chlorine. The mechanism of dehydrochlorination is shown in Figure 1.24 below[17].

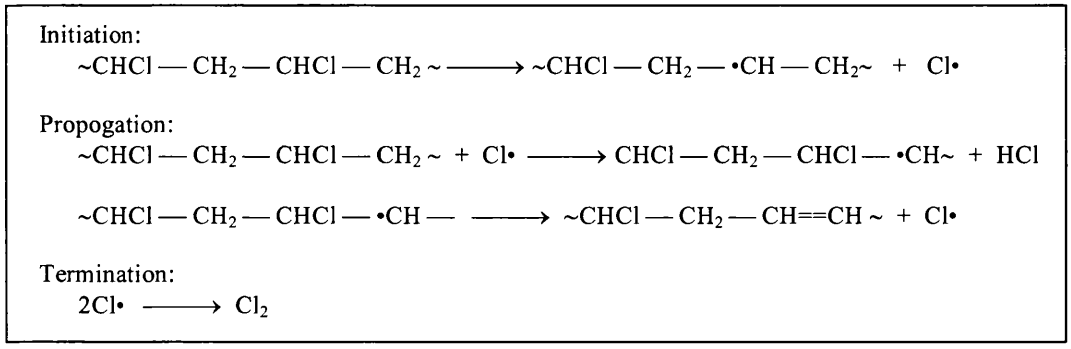

Figure 1.24. The Dehydrochlorination of PVC.

1.5.0 Analytical Techniques

1.5.1 Mass Spectrometry

Mass Spectrometry (MS) is an excellent quantitative analytical tool. It can be use to both quantify and identify compounds. As a technique it offers extremely high sensitivity which means that it can detect to very low levels of abundance within a sample typically one part in ten [31].

MS sorts ions according to their mass/charge ratio (m/z). The sample is ionised in a vacuum chamber. The ions then proceed into the analyser where they are subjected to a magnetic force. This force bends the paths of the ions, the larger the trajectory the larger the m/z and it therefore follows that the heavier the element. By changing the magnetic field strength, particular ions can be sought. This allows calibration of the apparatus for detection specific elements. Once the elements present have been detected, a mass spectrum is drawn up relating to what is present in the sample. This spectrum is represented as an arrangement of peaks and troughs. From this, identification of the species can be achieved.

It is generally accepted that mass spectrometers with quadrupole analysers are easier to use than magnetic sector analysers[32]. The quadrupole design was proposed in 1953[33]. Potential is applied to the rods; this sets up a total field to which the ions are

exposed as they travel through the sample chamber. The quadropole analyser offers many advantages, such that it is small, easy to use and little maintenance is needed. A schematic of a quadrupole analyser can be seen in Figure 1.25 [34].

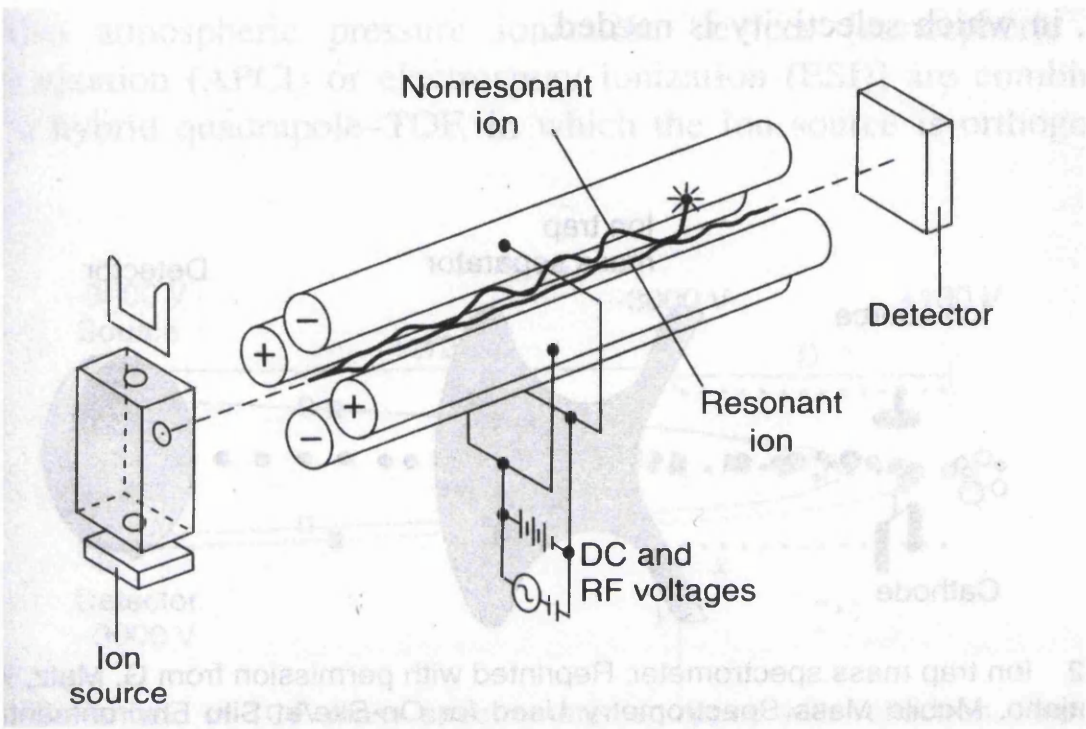

Figure 1.25. A Schematic of a Quadrupole Mass Spectrometer[34]

1.5.2 Chromatography

Chromatography is a very useful technique in a broad sense. This is due to the fact that it works on the basis of separation of similar compounds. The compounds are separated via selective adsorbtion onto a medium so that each different compound present forms a characteristic zone, from which the compound can be identified. In general, chromatographic techniques entail the sample that is to be analysed to be mobile, usually in solution, and passed over a stationary phase where separation will occur. The order of separation depends on the partition coefficient of the compounds in the sample with the stationary phase[34].

1.5.3 Inductively Coupled Plasma Mass Spectrometry(ICPMS)

Inductively coupled plasma is a very high temperature source. It is used to ionise atoms for mass spectrometry and is very efficient at doing so. Samples are converted into an aerosol and then shrouded with high temperature (10,000°C) argon[35]. This forms the plasma. Thus plasma is then introduced into the mass spectrometer, where the identity and concentration of species present can be confirmed[35].

In order for the sample to be introduced to the machine it must be of an acceptable form. For ICPMS the sample is introduced in the form of a spray. Only spray droplets of the right size and velocity are allowed to be introduced into the plasma. This is achieved via a spray chamber. The plasma is generated by the coupling of the energy from a radio frequency generator into a suitable gas via magnetic field. In order for the plasma to be linked effectively with the mass spectrometer, there is an interface in place which enables the ions to pass from the plasma to the mass spectrometer through a lens system. This lens system is used to focus the ions and stop them diverging during their passage from the plasma. The mass spectrometer is a quadrupole unit as described earlier and is used as a mass filter, elements can be distinguished at the detector by their mass-charge ratio[36].

1.5.4 Scanning Vibrating Electrode Technique

In recent years electrochemical scanning techniques have become well established accelerated testing methods for the measurement and long term prediction of corrosion. Many reviews have been published outlining the various scanning methods available[37]. One particular method, the scanning vibrating electrode technique (SVET) has become an important asset in the investigation of localised corrosion mechanisms in organically coated steels[38, 39, 40, 41] as well as pitting corrosion. The SVET operates by measurement of the potential difference above corroding metals immersed in solution. This potential difference is generated by the flow of ionic current through the electrolyte. The flow of current causes potential gradients to be set up where corrosion is occurring on the surface of the metal[4].

Anodic and cathodic reactions are occurring on a corroding surface can be assumed to occur as point sources. Using the Laplace equation, shown in Equation 1.5,

$$\nabla^2 E = 0 \qquad \text{(Equation 1.5)}$$

the distribution of potential and ionic current can be determined, where E is the electrical potential, used in conjunction with Ohm's law, shown in Equation 1.6,

$$i = -k \,.\, \nabla E \qquad \text{(Equation 1.6)}$$

where i is the current and k is the conductivity of the solution, it can be assumed that current i originates from a single point source in space at z = 0 on an insulated x y plane the potential at any point in solution would be inversely proportional to the distance from the source, giving Equation 1.7 as,

$$E = \frac{i}{2\pi\kappa\sqrt{(x^2 + y^2 + z^2)}} \qquad \text{(Equation 1.7)}$$

The SVET measures the vertical component of current flux in solution at known heights by way of a movable microtip vibrating electrode[43]. This is achieved by a glass encased platinum microtip (diameter 125μm) scanning across the surface in a predefined matrix. The tip is vibrated at a constant frequency (140Hz), amplitude (25μm) and scan height (100μm). The frequency and drive voltage are controlled by a lock-in amplifier (EG & G) and the tip is maneuvered into place step-wise controlled by a micro manipulator (Time and Precision). An alternating potential is registered at the frequency of vibration of the tip. This is due to the tip being vibrated within a potential field occurring above the point source.

As the SVET measures the normal component of current flux, Equation 1.7 can be differentiated with respect to distance to give the potential field above a point current source at a known height z, where k is again represents the conductivity of the solution to give Equation 1.8:

$$F = \frac{dE}{dz} = \frac{iz}{2\pi\kappa\sqrt{(x^2 + y^2 + z^2)^{1.5}}} \qquad \text{(Equation 1.8)}$$

The maximum potential field strength will occur directly above the point source where x and $y = 0$ giving Equation 1.9 as,

$$F\max = \frac{i}{2\pi\kappa z^2} \qquad \text{(Equation 1.9)}$$

the presence of an inverse square relationship to distance z, means that the SVET is extremely sensitive to changes in scan height and therefore it is critical that said scan height is kept constant throughout testing if viable comparisons are to be drawn from the results.

Resolution of the SVET is an important factor as it is dependent on scan height and probe geometry. The resolution specific to this apparatus can be calculated theoretically by considering the signal peak width at half maximum potential (*whm*). Further to this, if a point source is considered on the x, y plane at a distance r as in Equation 1.10.

$$r = (x^2 + y^2)^{0.5} \qquad \text{(Equation 1.10)}$$

Equation 1.10 can then be substituted in to the equation for maximum field strength where F is equal to *whm* giving Equation 1.11 as:

$$0.5F_{\max} = \frac{iz}{2\pi\kappa(r^2 + z^2)^{1.5}} \qquad \text{(Equation 1.11)}$$

The ratio of the above equations is given in Equation 1.12 as,

$$r = z(2^{2/3} - 1)^{0.5} \qquad \text{(Equation 1.12)}$$

The peak generated by the SVET has a width twice the distance r therefore,

$$whm = 2r = 1.533z \qquad \text{(Equation 1.13)}$$

Given that z is typically 100μm the resolution of the SVET would be 153μm in theory. However in reality the resolution is around twice this value due to the constraint arising from the dimensions of the SVET probe itself.

1.6.0 Metal Run Off and Leaching

Metal run off could arise from a number of areas within an organic coating system. Previous work has focussed on the zinc run off caused by cut edge corrosion of organically coated galvanised steel whilst being exposed to different environmental conditions[42]. Both natural and accelerated methods have been used to enable quantification and qualification of run off species. However, it has also been shown that the levels of zinc in run off from OCS poses little threat to humans and organisms[43]. Another point of interest is how the complete coating system performs when exposed to similar testing procedures[44]. Accelerated testing is a proven method for the prediction of performance of coating and polymers in general[45,46] and there are established methodologies for the prediction of the service life of coatings[47, 48].

State of the art weathering techniques have provided some interesting results when considering the zinc run off from organically coated steels. Results have already been obtained for different types of galvanising and microstructure on steel substrate. The performance of these different types has been monitored over thirty months and a comparison drawn.

The leaching rate of coatings could also give an indication of the service life of the coating. It is critical for the coating to be able to perform satisfactorily and as such leaching or weathering of the system so that it becomes ineffective is undesirable. There is a concern as to what species are leaching and why. Particular interest has been focussed on Cr^{VI} used in certain pre treatments and primer system as a corrosion inhibitor. A model for the kinetics of chromate release from OCS has been proposed[49]. However it is thought that from a complete coating system that there may be more potential leachates than Zn and Cr^{VI}, some of which may be organic in nature rather than the heavy metals that are commonly targeted as sources of concern.

1.7.0 Environmental Issues

It is probable that anything that is exposed to the environment will have an impact on it. Obviously some have more of an effect than others, it all depends on the stability and make up of the article in question. When regarding OCS and more specifically Plastisol coated steel, there are a number of substances in the processing and production that hold potential risks to both the humans and the environment.

1.7.1 PVC

PVC has been used for years within industry and concerns about its safety and its effect on the environment have followed this use. There are many primary concerns associated with the use of PVC, right through from production to use to disposal. This has made PVC one of the most researched materials in industry.

Environmental groups have claimed that the manufacture of PVC releases toxic substances which are harmful to the environment such as dioxins. This is because of the use of chlorine in the manufacture process of PVC. PVC is 57% chlorine[50]. Up until the early 1990s chlorine was still being produced using the mercury cell process. In 1993, 76% of European chlorine production and 39% of global chlorine production was achieved via the mercury cell route. There is also evidence of one chlorine plant emitting 100kg/day of mercury discharge[51]. Exposure to mercury can cause plant to have decreased chlorophyll, root damage, hampered nutrient uptake and restricted growth. In humans and animals, mercury exposure can lead to interference with the central nervous system. This may lead to the development of tremors in the limbs, but also emotional and psychological disturbance. Links between mercury exposure and leukaemia and cancer have also been shown[52]. As well as the production of chlorine, the vinyl chloride monomer (VCM) which is polymerised to produce PVC is regarded as a health hazard as it was found to have carcinogenic properties in the 1970s and precautions must be in place for handling and processing to minimise direct human contact[26].

However, when using PVC in the production of Plastisol paints and indeed, in the coating process of strip steel, no dioxins are released. This is due to the fact that the production used solid PVC dispersed in liquid, with plasticisers being used to cause it to

swell and soften. Therefore it is seen as a physical process and so no chemical processes take place[50].

The disposal of PVC holds more concerns from an environmental point of view due to the amount of dioxins that could potentially be released. However a 1995 survey shows that the incineration of chemical waste, including PVC does not release as many dioxins as the incineration of domestic and clinical waste[53]. However it is true that the conditions under which chemical waste is disposed of are perhaps more stringent than other waste categories. Although incineration is expensive, the burning of waste such as PVC provides a source of energy which could be put to other uses. However the production of HCl during incineration would lead to degradation of the combustion equipment.

1.7.2 PVC Additives

1.7.3 Plasticisers

In recent times with regard to plasticized PVC it is the use of phthalate based plasticisers in flexible PVC that has caused considerable concern. Plasticisers can be emitted from a plasticized product at any stage during their life cycle[51]. Studies have been undertaken to investigate the migration of plasticiser and its affect on coating properties[54]. Also, given that phthalates have a reputation for being suspected carcinogens and endocrine disrupters this concern may not be unfounded. In the 1980s ingestion of phthalates by rats showed an increase in the likelihood of contracting liver cancer[55] but work carried out since both in Europe and the USA have shown no trend relating to species more representative of the human race[51]. With regard to phthalates being endocrine disrupters, there is conflicting evidence, studies have shown that phthalates have had a possible role in the reduction of semen levels in humans[53] and the affect of specific phthalates have been further investigated in rats[56]. These concerns led to a European Union risk assessment classification of five commercial phthalates (DBP, DEHP, DINP, DIDP, and BBP) in 2001. None were give any cancer warnings. DBP and BBP caused concern for humans with regard to fertility, and DEHP should be treated as if it causes effects in humans with regard to fertility[55]. The concern over phthalates acting

as oestrogen mimickers has been largely dismissed since 1995 and so far as to say "The vast majority of in-vitro screening tests and, more importantly, all in-vivo oestrogenicity and two-generation studies indicate none of the phthalates nor any other plasticisers possess oestrogenic activity"[53]. However, there are still concerns as to the affect of phthalates and derivatives on other species such as fish. As mentioned earlier a plasticiser can be emitted at any time during its life cycle and therefore there is a probability that levels in surrounding water supplies may fluctuate and for some phthalates the risk is low due to their low solubility in water. Dibutyl phthalate is known to be toxic to aquatic organisms and studies have commenced to show the effects of phthalates on fish[55]. Studies have shown that complex organic molecules found in effluent waste water including phthalates have contributed to the occurrence of intersex fish particularly in the UK[57].

With these concerns in mind it is no surprise that Corus are taking the initiative within the coatings industry and are moving away from the use of phthalates in its flagship PVC coating system, by using Mesamoll, a sulphonic acid ester plasticiser.

1.7.4 Stabilisers and Retardants

One of the main concerns when considering the stabilisers used within Plastisol systems, is that they tend to be compounds containing heavy metals. In the HPS200 system a variety of stabilisers are used. All of which contain heavy metals of varying degrees, although lead and cadmium stabilisers have been largely phased out and organotin and barium zinc combination stabilisers are used.

Organotin compounds have proved to be extremely versatile in their chemical and physical properties and industrial use has reflected this from a few tonnes in the 1950s to over 40,000 tonnes in the late 1990s. Organotin compounds show excellent heat stability and many have been passed safe for use in food contact PVC[52]. However certain organotins are not without concern. Triorganic tin compounds break down readily in the environment and therefore there is a probability of leaching into surrounding soils and groundwater. These triorganic tin compounds find usage as anti fouling agents in paints meant for both use on wood and in marine environments. These leach directly from the

paint into water to give dibutyl tin compounds that cannot be distinguished from those used in the coil coating industry[51].

Barium zinc stabilisers have taken over the void left by cadmium stabilisers due to their superior environmental performance compared to the cadmium stabiliser systems. It has been shown however that barium can affect the growth of plants by up to 50%[58].

Antimony trioxide is used in the Plastisol coating system as a fire retardant. Antimony is a heavy metal in the same fold as cadmium and lead. This tie leads to the suspicion of antimony being a carcinogen. Uptake of antimony is slow and is highly dependant on the chemical form to which the subject is exposed. Retention has been shown to occur in the major organs such as lungs, kidneys and liver[58]. In depth studies on the toxicology and carcinogenicity of various antimony compounds, including antimony trioxide have taken place[59,60]. Trivalent antimonials are more toxic than pentavalent compounds, causing fibrosis, bone marrow damage, carcinoma and cardio toxicology. Concern was drawn to antimony trioxide in the late eighties as having a role in Sudden Infant Death Syndrome[61]. As mentioned, antimony trioxide is a common fire retardant and was used as such in polyvinyl cot mattresses. However this hypothesis could not be verified in following studies[62].

1.7.5 Chromate Pre-treatment and Primers

Chromate pre-treatments and primers are used extensively in the coatings industry in order to prepare the system for the application of the topcoat. It also provides increased corrosion resistance. There are two main states to be considered when regarding the environment. These are trivalent chromate (Cr^{III}) and hexavalent chromate (Cr^{VI}). It is Cr^{VI} which causes most concern. It is a recognised carcinogen and therefore should be treated with caution. Cr^{III} the most stable state and shows lower or no toxicity, in fact Cr^{VI} is seen to be 100 to 1000 times more toxic than the trivalent species[63].

Cr^{VI} and Cr^{III} can be leached into the surrounding environment from various sources. It is possible for Cr^{VI} to be reduced to Cr^{III} in soil if there is an adequate amount of organic material present. However conversely it is also possible that Cr^{III} could be converted to Cr^{VI} if there are adequate amounts of oxidising compounds present. Furthermore it is the nature of the soil that will determine the subsequent movement of

chromium species from the area[52]. Cr^{VI} is present in waste from blast furnaces and is used in the manufacture of cement and can cause allergic contact dermatitis. It is thought that chromium contact accounts for 8.1% of the allergic contact dermatitis cases[64].

1.7.6 Zinc

As mentioned earlier, zinc is used to provide a sacrificially protecting barrier coating to the steel substrate. The leaching of which would be detrimental to these protective properties and some environmental concerns could arise if sufficient levels of zinc are leached. Drinking water usually contains ~ 0.2μg L^{-1} [65]; however levels can fluctuate depending on geographical location and the maximum permissible level is set at 5mg L^{-1} [66]. It is present naturally in most living things. Zinc is not highly toxic to plants, however in areas where high levels of zinc are present in soils the growth and development of plants can be affected and this could be passed up thorough the food chain due to the efficiency at which plants accumulate it[52].

Zinc itself is not regarded as having any carcinogenic effects. Zinc compounds can have adverse effects on humans; particularly zinc chloride and zinc oxide. Over exposure to these compounds may cause irritation to the respiratory tract[67] and metal fume fever[68] respectively. Recommendations and regulations are in place for reference with regard to limits of intake and exposure.

1.8.0 Legislation

In order for a product to be deemed safe it has to comply with various legislation right through from the manufacturing process to disposal.

With regard to organic coated steels, in particular Plastisol coated steel and its use in construction as cladding it is important for the product to last and also have aesthetic appeal to the customer. Conversely in meeting these requirements it is also important that the product has as little impact on the environment as possible. In its function as cladding on architectural structures, the Plastisol will be subjected to varying conditions and degradation; however it must remain stable and give consistent performance throughout

the expected life cycle. Therefore it is obvious that minimal or no leaching must occur to ensure this is the case, both from a performance and an environmental point of view.

Different customers will have different applications and needs from the product, such that Corus' Plastisol coating has been approved as a drinking water catchment system. This means that water that is collected and flows over this particular coating has been certified as safe to drink. This in itself implies that the Plastisol system produced by Corus would have little impact on the surrounding environment when used in situ.

In order to gain approval as a catchment system for drinking water, the Plastisol system has to comply with BS 6920.

1.8.1 BS 6920

BS 6920 is the accepted standard for the 'Suitability of Non-Metallic Materials for Use in Contact with Water Intended for Human Consumption with Regard to their Effect on the Quality of Water.'

There are 5 sets tests that within BS 6920. These are:

1.8.2 Odour and Flavour of the Water

This tests the ability of the product to impart a noticeable odour or flavour on the water and can take up to fifteen days to complete. The test uses samples of both chlorinated and non chlorinated water. Both samples must be without flavour and odour on completion of the set.

1.8.3 Appearance of the Water

This tests the ability of the product to impart the any noticeable colour or turbidity to the water. Again this may take up to fourteen days to complete. If any colour or turbidity has been gained, it must be >5 Hazen units and 0.5 FNU respectively.

1.8.4 Growth of Aquatic Micro-organisms

This tests the ability of aerobic micro-organisms to grow on the surface of the product when in contact with the water. This may take up to 8 weeks to complete, with the ability of the product to support the growth being reviewed after weeks 5 and 7. The levels after the test must not be more than 1.7mg L^{-1}.

1.8.5 Cytotoxicity Test

A screening and extraction process assessing the toxicity of the product. It takes 7 days to complete. The first extraction must show no toxicity and if there is a cytotoxic response in the final extraction then the test has been failed unless two further extraction so no cytotoxicity.

1.8.6 The Extraction of Metals

This test assesses the leaching of metals into the water from the product. Any metal present in the sample after the four week test must not exceed the levels outlined in the odour and flavour test.

1.8.7 Directives

In order to obtain continued success it is important that Corus and other industrial companies endeavour to offer competitive and new products to the market place. However, as well innovation there is a constant drive to make novel products 'greener' as both a selling point and also to minimise the environmental impact of the component over its lifetime. To this end, it is imperative that the product more than complies with existing environmental legislation. The following summary outlines many directives and acts that have to be considered and followed with regard to any product similar to those Corus offer.

1.8.8 ELVD – 'End of Life Vehicles Directive'.

This was devised with regard to the prevention of waste, re-use and recycling and recovery of old vehicle parts. The directive should have been implemented in 2002, the target was then placed for 2004, finally being in place in 2006. The directive places responsibility on manufacturers and producers. Lead and other trace elements will have tolerances upon them, while the directive also includes restrictions on Cadmium and Chromium.

1.8.9 WEEE – 'Waste Electrical and Electronic Equipment Directive'.

This directive outlines means for the prevention of waste, re-use and recycling and recovery of waste electrical and electronic equipment. It will apply to anything that draws and electric current or makes use of an electromagnetic field. The directive applies to maximum voltages of:

- 1000v AC.
- 1500v DC.

Some materials were to be phased out by 1 January 2004. In some cases there are exceptions under the RoHs regulations. The RoHs regulations themselves become enforceable on 1 July 2006 and are explained in more detail in a later section.

Any material containing Pb, Hg, Cd, Be, Cr (VI) has to be separated from the rest of the WEEE waste and processed accordingly (Article 4of Council Directive 75/442/EEC).

1.8.10 ROHS – 'Restriction of the use of Certain Hazardous Substances in Electrical and Electronic Equipment Regulations 2005'.

This is essentially an update of the WEEE directive and became enforceable from 1st July 2006. It concentrates on the levels of use of hazardous materials within electrical and electronic equipment. The following materials will be placed under scrutiny, having specific usage levels placed upon them:

- Lead
- Mercury
- Cadmium
- Chromium (VI)
- Polybrominated Biphenyls (PBB)
- Polybrominated Diphenyl Ethers (PBDE)

It is required that use of these materials should be fully outlined in comprehensive technical documentation. This documentation is to be made public to show total compliance with the directive. The directive will be regulated and enforced on behalf by the Department of Trade and Industry on behalf of the Secretary of Trade and Industry.

Failing to comply with the directive or failing to submit the correct technical documentation holds a maximum penalty of £5000.

1.8.11 Registration, Evaluation and Authorisation of Chemicals (REACH)

The framework was proposed in October 2003. The aim was to improve the protection of human health and the environment through earlier and more thorough identification and evaluation of properties and impact of chemical substances.

REACH aims to give responsibility of management and evaluation of chemicals to manufacturers and importers. They will be required to provide information on properties and risks associated to their substances. This information will then be submitted to a central database. Substances produced or imported in quantities higher than 1 tonne a year will have to be registered on the database.

All substances of very high concern will be subject to authorisation. Authorisation will only occur if use of the substance can be adequately controlled and that the socio-economic benefits of using the said substance are deemed to outweigh the risks involved. Some examples of the types of substance that will require authorisation are:

- CMRs (Carcinogenic, mutagenic or toxic to reproduction).

- PBTs (Persistent, bio-accumulative and toxic).

- vPvBs (Very persistent, very bio-accumulative and toxic).

- Substance identified as having irreversible effects on human health. (For example, hormone disrupters).

Although final adaptation of the proposal is expected by the end of 2006, it is thought that an eleven year plan will see the registration of high production volume chemicals and high risk chemicals initially through to low volume, low risk chemicals.

With regard to industry, REACH is substance based and therefore it is substances that need to be registered not preparation methods in which the chemicals are involved.

1.9.0 References

1. MATTSON, E. 'Basic Corrosion Technology for Scientists and Engineers' Ashgate Publishing, Second Edition, 1996.
2. www.corrosioncost.com
3. CALLISTER, W. D., 'Fundamentals of Materials Science and Engineering', Wiley and Sons, Fifth Edition, 2001.
4. BOUGHTON, J., 'Environmentally Controlled Scanning Vibrating Electrode Technique for Localised Pipeline Steel', MPhil Thesis, University of Wales, Swansea, 2001.
5. WORSLEY, D. A., 'Design Against Corrosion', Technical Notes University of Wales Swansea, 2004.
6. TRETHEWEY, K. R., CHAMBERLAIN, J., 'Corrosion for Science and Engineering' Longman Group, Second Edition, 1998.
7. SCULLY, J. C., 'The Fundamentals of Corrosion', Pergamon, Third Edition, 1990.
8. WILLIAMS, D., 'Mechanistic Corrosion Studies in Organically Coated Galvanised Steels', Eng D Thesis, University of Wales Swansea, 2003.
9. www.ianosbackfill.com
10. WAGNER, C., TRAUD, W., Z. Electrochem., 44, 1938, 391.
11. TAFEL, J., Zeit, Physik, Chem. 50A, p.641, 1905
12. FONTANA, M. G., GREENE, N. D., 'Corrosion Engineering', McGraw Hill Higher Education, Third Edition, 1986.
13. SULLIVAN, J., 'Metallic Run Off from Coated Steels', PhD Thesis, University of Wales Swansea, 2003.
14. CORUS, 'The Colorcoat Building', Corporate Technical Manual, 1995.
15. CORUS, 'The Colorcoat Building', Corporate Technical Manual, 2005.
16. SEARLE, J. R., 'Titanium Dioxide Pigment Photocatalysed Degradation of PVC and Plasticised PVC Coatings', Eng D Thesis, University of Wales Swansea, 2002.
17. ROBINSON, A. J., 'The Development of Organic Coatings for Strip Steels with Improved Resistance to Photo Degradation', Eng D Thesis, University of Wales Swansea, 2005.

18. PERROT, P., TISSIER, J.C., REUMONT, G., DAUPHIN J.Y and FOCT, J., 'Conditions of Dross Formation During Continuous Hot Dip Galvanising in Zinc-Aluminium Baths.' European General Galvanisers Association – Zinc Coated Steel Sheet (UK), 1994.
19. SUZUKI, I., 'Corrosion-resistant Coatings Technology', Marcel Dekker, 1989.
20. Galvanizers association, The engineers and architects guide to hot dip galvanising, Jan 1998.
21. ELVINS, J., SPITTLE J.A. and WORSLEY, D.A., 'Microstructural Changes in Zinc Aluminium Alloy Galvanising as a Function of Prcessing parameters and their Influence on Corrosion,' Corrosion Science, vol. 47, issue 11, p2740-2750 2005.
22. BLUNI, S. T., NOTIS, M. R. and MARDER, A. R., 'Nucleation Characteristics and Microstructure in Off Eutectic Al-Zn Alloys,' Acta Metallurgica Materialia, vol. 43, issue 5 1995.
23. PELERIN, J., SERVAIS, J. P., COUTSOURADIS, D., HERRSCHAFT, D.C. and RADKE, S.F., Proceedings. 13th Intl. Galvanising Conference, London, Zinc Development Association. 1982.
24. GOODWIN, F., SKERAZI, A. F., and LYNCH, R. Proceedings. 25th Annual Conference of Metallurgists, Toronto, Canada, Canadian institute of Mining and Metallurgy (1986)
25. COLLINS, E. V., 'Leaching Rates During the Weathering of Coated Steels', 2000.
26. TITOW, W. V., 'PVC Technology Fourth Edition', Elsevier Applied Science Publishers, 1984.
27. SEARS, J. K., DARBY, J. R., 'The Technology of Plasticisers', Wiley and Sons, 1982.
28. LASMAN, H. R., SCULLIN, J. P., 'Miscellaneous Modifying Additives', in 'The Technology of Plasticisers', Wiley and Sons, 1982.
29. 'Parfumers Handbook and Catalog', Frtzsche Brothers, Inc, 1944, in 'The Technology of Plasticisers', Wiley and Sons, 1982.
30. ALLEN, A. R., EDGE, M., 'Fundamentals of Polymer Degradation and Stabilisation', Elsivier Applied Science Publishers Ltd., London 1992.
31. The American Society of Mass Spectrometry

32. ASHCROFT, A. E., 'Ionisation Methods in Organic Mass Spectrometry', The Royal Society of Chemistry, 1997.
33. PAUL, W., STEINWEDEL, H. S., 'A New Mass Spectrometer Without Magnetic Field', Z. Naturforsch. 8a, 448, 1953.
34. DOWN, R. D., LEHR, J. H., 'Environmental Instrumentation and Analysis Handbook', John Wiley and Sons Inc, 2005.
35. STUEWER, D., JAKUBOWSKI, N., 'Elemental Analysis by Inductively Coupled Mass Spectrometry with Sector Field Instruments: a Progress Report', J. Mass Spectrom. 33, 579-590, 1998.
36. 'The Thirty Minute Giude to ICPMS', Perkin Elmer Ltd, 2000.
37. OLTRA, R., MAURICE, V., AKID, R. and MARCUS, P., (Eds) 'Local Probe Techniques for Corrosion Research'. IOM^3, Woodhead Publishing Ltd, Cambridge, 2007.
38. BOHM, S., CHALLIS, M., HEATLEY, T., WORSLEY D.A., 'An Investigation of the Effects of Magnesium Levels on the Kinetics and Mechanism of Cut Edge Corrosion in Organically Coated Zinc Aluminium Alloy Galvanised Steels', Trans IMF, 2001.
39. ELVINS, J., SPITTLE, J. A., WORSLEY, D. A., ' Relationship Between Microstructure and Corrosion Resistance in Zn-Al Alloy Coated Galvanised Steels', Corrosion Engineering Science and Technology, vol. 38, No.3, 2003.
40. WORSLEY, D. A., McMURRAY, H. N., BELGHAZI, A., 'Determination of Localised Corrosion Mechanisms using a Scanning Vibrating Reference Electrode Technique', Chem. Commun. 1997.
41. CHALLIS, M., WORSLEY, D. A., 'Cut Edge Corrosion Mechanisms in Organically Coated Zinc-Aluminium Alloy Galvanised Steels', British Corrosion Journal, vol. 36 No. 4, 2001.
42. BELGHAZI, A., BOHM, S., SULLIVAN, J. H., WORSLEY, D. A., 'Zinc Runoff From Organically Coated Galvanised Architectural Steel', Corrosion Science 44, 1639-1653, 2002.

43. SULLIVAN, J. H., WORSLEY, D. A., 'Zinc Runoff from Galvanised Steel Materials Exposed in Industrial/Marine Environment', British Corrosion Journal, vol. 37, No. 4, 2002.
44. BOHM, S., SULLIVAN, J. H., WORSLEY, D. A., 'A New Corrosion Test for Coated Galvanised Steel Products', Materials and Corrosion 52, 540-545, 2001.
45. REAL, L. P., ROCHA, A. P., GARDETTE, J-L., 'Artificial Accelerated Weathering of Poly(vinyl chloride) for Outdoor Applications: The Evolution of the Mechanical and Molecular Properties', Polymer Degradation and Stability 82, 235-243, 2003.
46. MEEKER, W. M., YANG, C., 'Using Accelerated Tests to Predict Service Life of Organic Materials Subjected to Outdoor Weathering', Department of Statistics, Iowa State University, Ames, IA 50011-1210, USA.
47. MARTIN, J. W., BAUER, D. R., 'Service Life Prediction Methodology and Metrologies', ACS Symposium Series; 805, American Chemical Society 2002.
48. BRUNNER, S., RICHNER, P., MÜLLER, U., GUSEVA, O., 'Accelerated Weathering Device for Service Life Prediction for Organic Coatings', Polymer Testing 24, 25-31, 2005.
49. PROSEK, T., THIERRY, D., 'A Model for the Release of Chromate from Organic Coatings', Progress in Organic Coatings 49, 209-217, 2004.
50. BROWN, N., 'PVC Based Coatings and Their Effect on the Environment', Steel Times, 1997.
51. CORUS TECHNICAL NOTES, 'Environmental Aspects of PVC Products – A Literature Review', Jan 1997.
52. ANKE, M., IHNAT, M., STOEPPLER, M., 'Elements and Their Compounds in the Environment', 2nd Ed, Wiley-VCH, 2004.
53. TAYLOR, S., 'How Green is the Precoating Process', Sheet Metal Industries, June 1997.
54. MONNEY, L., JAMOIS-TASSERIE, M., DUBOIS, C., LALLET, P., VILLA, F., RENAUD, C., 'Plasticiser Migration and Structural Changes in an Aged PVC Coating', Polymer Degradation and Stability, 72, 459-468, Elsevier Science Ltd. 2001.

55. CADOGAN, D., 'Health and Environmental Impact of Phthalates', Plastics Additives and Compounding, June 2002.
56. STROHEKER, T., CABATON, N., NOURDAIN, G., REGNIER, J., LHUGUENOT, J., CHAGNON, M., 'Evaluation of Anti-androgenic Activity of Di-(2-ethylhexyl)phthalate', Toxicology, 208, 115-121, Elsevier Ireland, 2004
57. HILL, E., TYLER, C., 'Endocrine Disruption and UK River Stocks', RSC, Environmental Chemistry Group Bulletin, Jan 2005.
58. WANG, W., 'Site Specific Barium Toxicity to Common Duckweed, Lemna Minor', Aquatic Toxicology, 12, 203-212, 1998.
59. Integrated Risk Information Sysytem, Antimony Trioxide CASRN-1309-64-4.
60. NAS USA, 'Toxicological Risks of Flame Retardant Chemicals', 229-261, The National Commission of Life Sciences, 2000.
61. RICHARDSON, B. A., 'Cot Mattress Biodeterioration and Sudden Infant Death Syndrome', Lancet 335, 610, 1990.
62. JENKINS, R. O., CRAIG, P. J., GOESSLER, W., IRGOLIC, K. J., 'Biovolatisation of Antimony and Sudden Infant Death Syndrome', Human and Experimental Toxicology 17, 231-238, 1998.
63. KATZ, S. A., SALEM, H., 'The Toxicology of Chromium with Respect to its Chemical Speciation: A Review', Journal Applied Toxicology. 13, 217-224, 1993.
64. MEYER, J. D. C. Y., HOLT, D. L., BECK, M. H., CHERRY, N. M., 'Occupational Contact Dermatitis in the UK: A Surveillance Report from EPIDERN and OPRA', Occupational Medicine 50, 265-273, 2000.
65. 'Exposure and Risk Assessment for Zinc', US Environmental Agency Office of Water Regulations, 1980.
66. 'Guidelines for Drinking Water Quality', Vol. 1 Recommendations, World Health Organisation, Geneva, 1983.
67. MATERESE, S. L., MATTHEWS J. L. 'Zinc Chloride (Smoke Bomb) Inhalation Lung Injury', Chest, 89, 208-209, 1986.
68. MUELLER, E. J., SEGER, D. L., 'Metal Fume Fever: A Review', Journal of Emergency Medicine 2, 271-274, 1985.

Chapter 2

Experimental Procedure

2.0 Experimental Procedure

2.1 External Weathering

2.1.1 Production of Near Commercial Painted Samples

A series of near commercial paints were formulated at Akzo-Nobel in Darwen. The paints were formulated so that they would produce some results over the limited period of exposure. The formulations were based on commercial PVC plastisol. It was decided that a range of colours should be chosen to represent the range as offered by Corus in their Colorcoat® portfolio and therefore a number of different pigments were used. For the purposes of the investigation there were also three different stabilisers used Ba/Zn, Sn1/Sn2 and Hydrotalcite. The general formulation of the coated samples was as follows:

- 14% TiO_2 (Kronos K1001)
- 1% Stabiliser
- 1% Colour Pigment

NB. The K1001 pigment is not suited to external exposure but was chosen in order to accelerate photodegradation. The pigments used in the coatings were:

- DPP Red (Diketo-pyrrolo-pyrrole).
- GLSM Blue (Pthalocyanine).
- GLN Green (Pthalocyanine).
- Printex Black (Carbon).
- Sicotan Yellow (Titanium-oxide-chromate).

Base PVC plastisol resin with most stabilising additives removed was combined with the TiO_2, stabiliser and colour pigment using a high shear mixer until completely dispersed. The paints were then placed in a vacuum so that no excess gas remained for

the coating process. After the vacuum degassing, the paints were coated onto commercially primed steel panels using a coating bar to a thickness of ~200μm. The coated panels were then cured. A full matrix of the coated panels can be seen in Table 2.1.

In keeping with the theory that every layer of an organic coated steel contributes to the performance of the coating as a whole, a series of pretreated, primed and uncoated Galvalloy coated steel panels were also obtained for testing.

COLOUR	PLASTICISER	COATING TYPE	PIGMENT	STABILISER
Base	Mesamoll	HPS 200	None	None
White 28	Mesamoll	HPS 200	K1001 TiO_2	None
White 16	Mesamoll	HPS 200	K1001 TiO_2	Ba/Zn 1%
White 13	Mesamoll	HPS 200	K1001 TiO_2	Sn1/Sn2 1%
White 14	Mesamoll	HPS 200	K1001 TiO_2	HT 5%
Red 15	Mesamoll	HPS 200	K1001 TiO_2 DPP 1%	Ba/Zn 1%
Blue 50	Mesamoll	HPS 200	K1001 TiO_2 GLSM 1%	Ba/Zn 1%
Green 49	Mesamoll	HPS 200	K1001 TiO_2 GLN 1%	Ba/Zn 1%
Black 47	Mesamoll	HPS 200	K1001 TiO_2 Carbon Black 1.5%	Ba/Zn 1%
Yellow 93	Mesamoll	HPS 200	K1001 TiO_2	Ba/Zn 1%

Table 2.1. Matrix of coated panels exposed externally.

2.1.2 Bare Galvanised Samples

In keeping with the theory that every layer of an organic coated steel contributes to the performance of the coating as a whole, a series of uncoated, galvanised steel panels were also obtained for testing. Samples of hot dipped galvanised steel (HDG), Galvalloy with varying coating weights and Zalutite were also obtained for testing. All of these samples were line produced. A full matrix of bare surface panels can be seen in Table 2.2.

COATING TYPE	COATING WEIGHT (gm^{-2})
HDG (Non Chromated)	200
GALVALLOY	120
GALVALLOY	150
GALVALLOY	200
GALVALLOY	255
GALVALLOY	300
GALVALLOY	325
ZALUTITE	180-200

Table 2.2. Matrix of uncoated panels exposed externally.

2.1.3 Sample Preparation

Both the coated panels and the bare panels are 10cm x 15cm. The bare panels have had the back surface taped and the edges sealed with epoxy resin. The coated samples have an area of coating that is restricted by the length of the coating bar. The coating area is consistent throughout, therefore as well as back surface being covered with tape, a maximum are of the coating is also exposed with the edges of the coating being taped so as not to induce any sort of crevice corrosion.

2.1.4 Run off Collection Vessel

The panels were subjected to natural weathering conditions at the Port Talbot weathering site. Figure 2.1 shows the apparatus used for exposure of the panels.

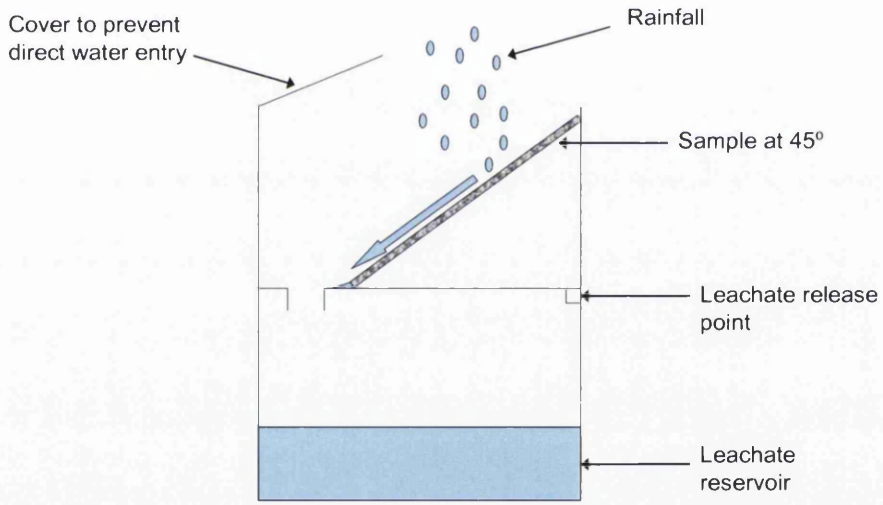

Figure 2.1. Apparatus for external exposure of panels.

The sample is placed at 45° in the apparatus in a south facing direction. This allows the rainfall to run across the sample and pass through to the leachate reservoir. Figure 2.2 shows the panels in situ. This run-off is then collected monthly and analysed via chemical techniques for the presence of metallic species (ICPMS).

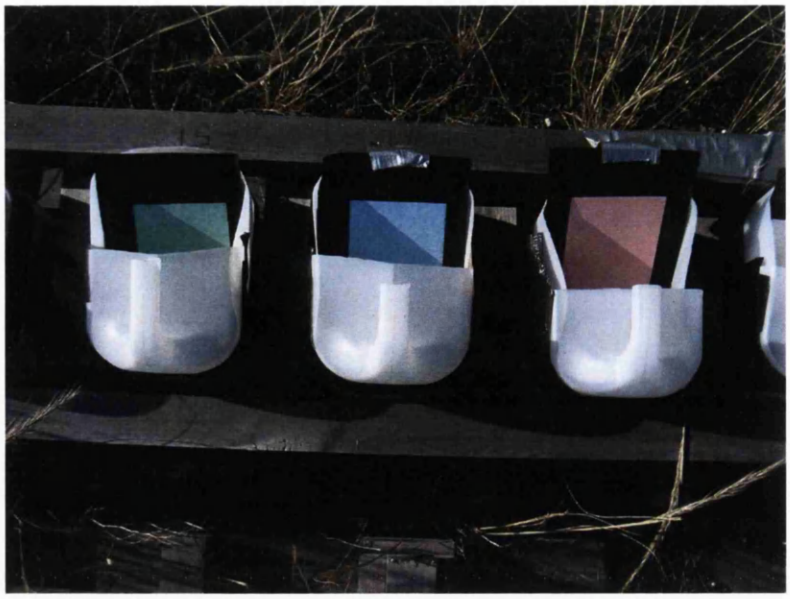

Figure 2.2. Coated panels in situ at Port Talbot.

2.1.5 Inductively Coupled Plasma Mass Spectrometry (ICPMS)

Inductively coupled plasma is a very high temperature source. It is used to ionise atoms for mass spectrometry and is a very efficient at doing so. Samples are converted into an aerosol and then shrouded with high temperature (10,000°C) argon[1]. This forms the plasma. Thus plasma is then introduced into the mass spectrometer, where the identity and concentration of species present can be confirmed[2].

In order for the sample to be introduced to the machine it must be of an acceptable form. For ICPMS the sample is introduced in the form of a spray. Only spray droplets of the right size and velocity are allowed to be introduced into the plasma. This is achieved via a spray chamber. The plasma is generated by the coupling of the energy from a radio frequency generator into a suitable gas via magnetic field. In order for the plasma to be linked effectively with the mass spectrometer, there is an interface in place which enables the ions to pass from the plasma to the mass spectrometer through a lens system. This lens system is used to focus the ions and stop them diverging during their passage from the plasma. The mass spectrometer is a quadrupole unit and is used as a mass filter,

elements can be distinguished at the detector by their mass-charge ratio[3]. Throughout the investigation the ICPMS apparatus used was a ..... manufactured by Perkin Elmer.

2.2 Accelerated Weathering

Accelerated weathering tests were performed on the model coated samples. Conventional accelerated weathering testing methodology includes Ultra Violet (UV) exposure. There are many types of UV testing techniques available on a laboratory scale. For the purposes of the model samples UV-A testing was identified as the most relevant. This is due to the fact that UV-A lamps simulate more closely the effect of exposure to sunlight[4]. Also as the coated model samples are partly pigmented with a photo-active grade of TiO_2 which will more suit the exposure to UV-A rather than the harsher UV-B as it is the effect of exposure to sunlight that is the primary criteria of the testing regime. UV-B light has a shorter wavelength and therefore the photons that are emitted harbour a greater energy. This, coupled with the photo-active TiO_2 would lead to a shorter more damaging test regime which would not be a true comparison of the coatings' performance in natural sunlight.

2.2.1 UV-A Accelerated Weathering

The coated samples were subjected to alternate cycles of UV-A radiation and condensation in a QUV-A Accelerated Weathering Tester supplied by Q-Panel. The alternate condensation - radiation cycles simulates the effect of rainfall followed by sunlight respectively. It has been observed that material resistant to either UV testing or condensation testing usually fail when a combination of the two is used[5]. The standard cycle for UV – condensation testing is 8 hours exposure to UV-A radiation followed by 4 hours condensation. This allows for 2 complete cycles to occur within a 24 hour period.

The samples were assessed at regular intervals to make sure they remained in condition to produce useful results.

2.3 Galvanised Coatings with Improved Performance

2.3.1 Production of Samples

The test samples were produced using galvanizing line conditions on an Iwatani-Rhesca Hot Dip Simulator (HDS). Polishing compounds and consumables were purchased from Buehler, while chemicals were sourced from Aldrich in their highest purity. All solutions were prepared in distilled de-ionized water.

2.3.2 HDS

The HDS has proved to be an excellent tool for producing near line quality galvanized samples on a small scale[6]. The HDS is computer controlled and as such many parameters such as line speeds, cooling rates and coating weight can be altered in the main program interface relatively simply. There is also scope for using the HDS for both continuous and batch galvanising. It also provides an excellent tool for experimenting with bath chemistry, eliminating the need for full scale line trials.

There are three main areas on the operational HDS equipment the upper chamber, where the sample is mounted and cooled, lower chamber, where the sample is heated and the melt, in to which the sample is dipped. Away from the main area of the equipment there is a gas management cabinet and the main computer from which the dip cycle is controlled.

Steel sections used in the simulator are guillotined into panels of dimensions 200 x 120 mm. The panels are then chemically cleaned using alkali cleaners and acetone to remove all rolling oil contamination. A thermocouple is then spot welded onto the panel which controls sample temperature though the dip cycle. During a dip cycle a sample is moved via a drive rod from the upper chamber to an infra-red furnace. This heats the panel to a temperature ca. 700°C for one minute, while in a reducing (hydrogen 4% nitrogen 96%) atmosphere to remove any surface oxide. The sample is the cooled to the relevant entry temperature, typically 460°C before being lowered into the melt (420-440°C). When the sample is withdrawn from the melt the air knives that are situated just above the melt are used to control the coating weight to ca. 255gm^{-2} (20μm). A schematic

of the HDS equipment is shown in Figure 2.3 schematically and Figure 2.4 photographically.

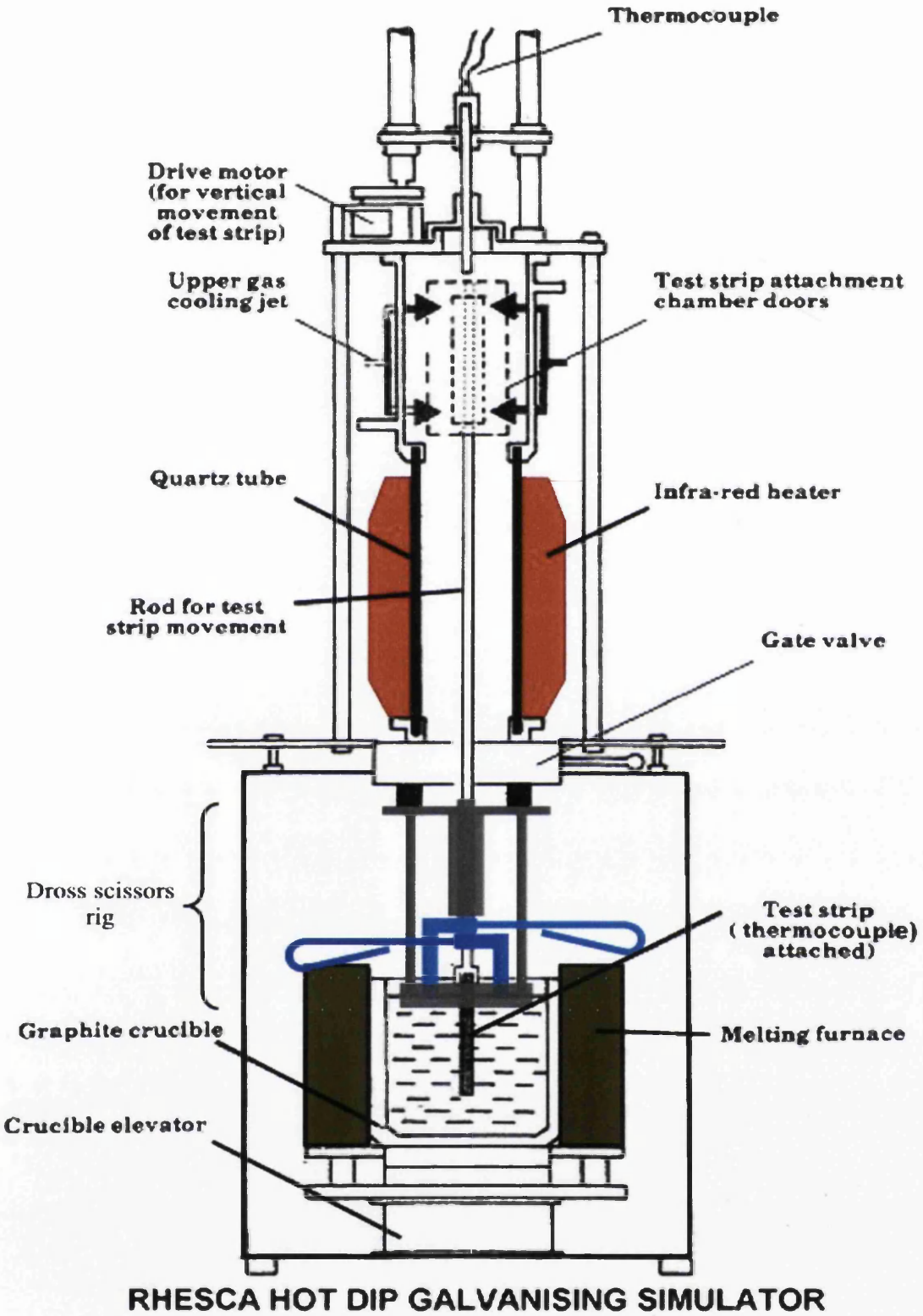

Figure 2.3 A schematic of the Iwatani-Rhesca Hot Dip Simulator

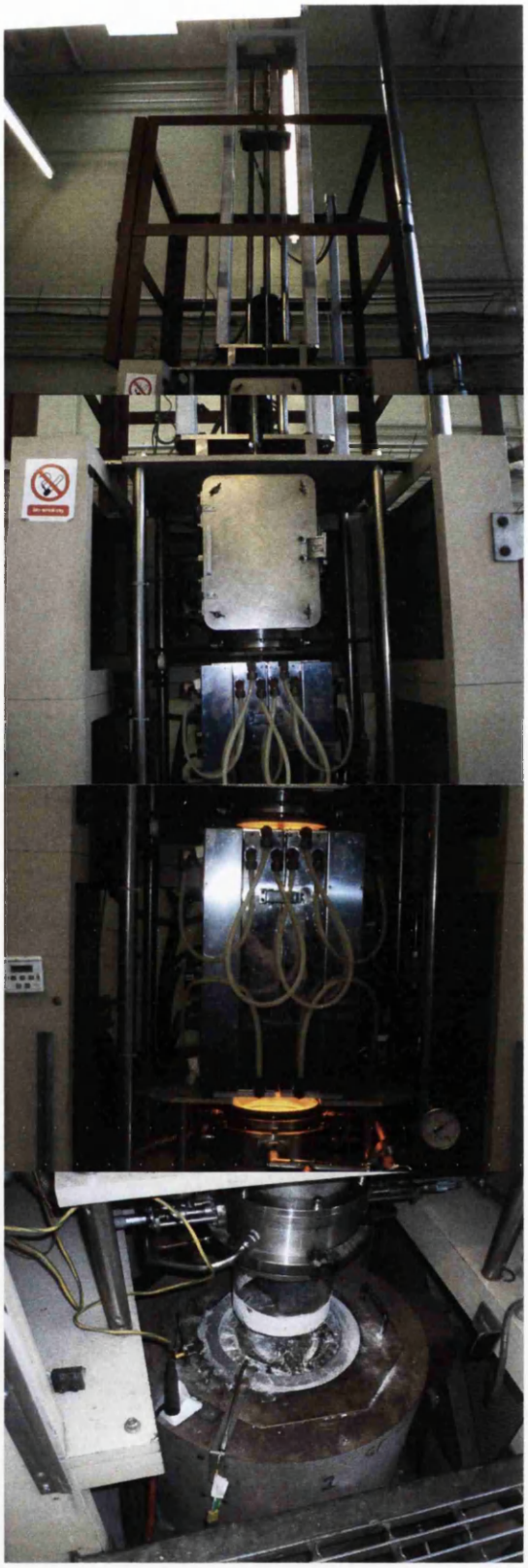

Figure 2.4 Photographic representation of the HDS equipment

2.4 Metallographic Investigation

2.4.1 Sample Preparation

Samples of dipped panels for each Al addition were guillotined into 20 x 20mm coupons and mounted flat in phenolic mounting compound.

2.4.2 Microscopic Observation of Sample Surface

A Vickers Hardness Tester was used to indent the sample at three reference points. The diameters of the indents were then measured and the sample was carefully polished in several stages using 1μm diamond slurry. After each stage the indent diameters were measured, the sample etched using 1% Nital and micrographs of the microstructure taken on a Reichert MEF3 optical microscope, building a solidification profile. As more and more of the surface coating was polished away the Vickers indent became smaller and smaller. This enabled each polish to be related as a function of depth through the coating via a simple trigonometric calculation. This calculation is shown in Figure 2.5.

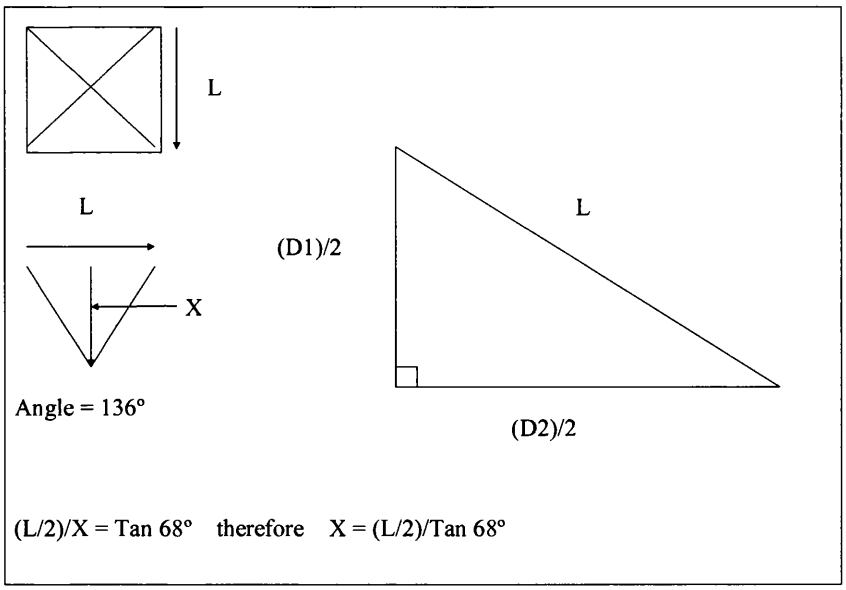

Figure 2.5 Trigonometric calculation for coating depth.

Where D represents the diagonal of the Vickers indent, L is the length of one side of the indent and X is the depth. As the indentation angle was known (136°) it was possible to work out, via trigonometry, the coating depth.

2.5 Corrosion testing using the SVET

It is possible to replicate the potential weathering conditions that galvanised strip steel for external use may experience using the scanning vibrating electrode technique (SVET) and recent work has shown a reasonable correlation between external weathering performance conducted over periods of years with SVET testing conducted in 0.1% NaCl in 24 hours[7]. During electrochemical corrosion, areas of corresponding anodic and cathodic activity occur on the surface in contact with the electrolyte. The SVET scans a vibrating platinum microtip in a pre-defined matrix over the corroding surface, picking up an alternating potential that is proportional to potential gradient in the direction of vibration. Therefore the signal picked up by the SVET is directly proportional to the component of ionic current density in the direction of vibration at the scan height[8, 9].

This is achieved by a glass encased platinum microtip (diameter 125μm) scanning across the surface in a predefined matrix. The tip is vibrated at a constant frequency (140Hz), amplitude (25μm) and scan height (100μm). The frequency and drive voltage are controlled by a lock-in amplifier (EG & G) and the tip is maneuvered into place step-wise controlled by a micro manipulator (Time and Precision). Figure 2.6 shows a schematic of the SVET head in more detail, while Figure 2.7 shows the SVET apparatus in situ.

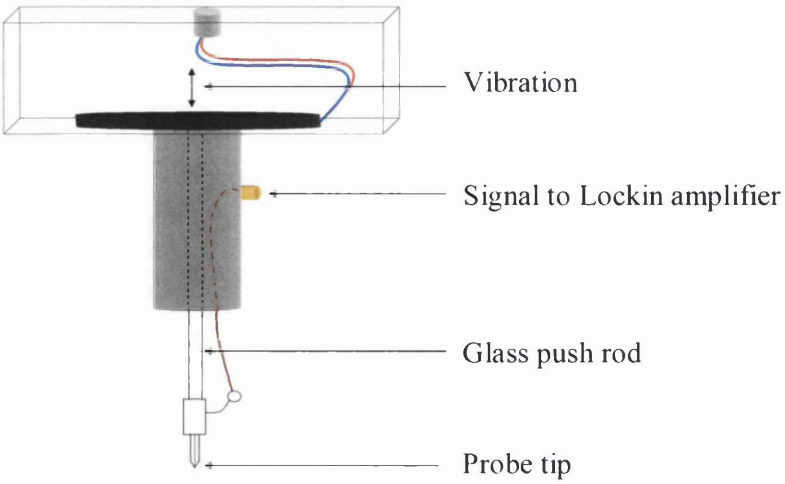

Figure 2.6 A schematic showing the detail of the SVET head.

Figure 2.7 The SVET apparatus in situ.

Both surface (10 x 10mm) and cut edge (22 x 2mm) samples for each Al addition were tested in 0.1% NaCl electrolyte. Each sample was scanned once an hour for 24 hours and the data logged in relevant software files.

2.5.1 Sample Preparation

The galvanised steel samples were cut into coupons to make them more suitable for testing on a laboratory scale.

2.5.2 Preparation of surface samples for SVET testing

The galvanised samples were cut into coupons of 50mm x 50mm. The sample was first degreased with acetone and then sealed with extruded Teflon tape to leave a scan area of 10mm x 10mm exposed for testing while the rest of the sample remained impervious to electrolyte. The size of the sample allowed more than one test to be undertaken on one sample and enabled more consistent comparison between samples. Once prepared the samples were taped to the stage in the SVET tank ready for testing.

2.5.3 Preparation of cut edge samples for SVET testing

For cut edge samples, the galvanised steel samples were cut into 20mm x 20mm coupons and mounted in styrene resin such that the cut edge was exposed at the surface of the sample. The sample was then polished to a one micron finish and fixed to the SVET stage with nylon screws ready for testing. A schematic of test ready surface and cut edge samples is shown in Figure 2.8.

2.5.4 Calibration of the SVET

Calibration of the SVET was achieved using a two compartment cell. Each part of the cell contains a platinum electrode and known currents were passed between them using a nano-galvanostat. The two parts of the cell are separated by a vertically oriented glass tube (ID 5mm). During calibration the SVET tip was lowered into the glass tube and vibrated. The purpose of the tube is to allow lines of current flux to flow over the tip in a planar fashion, such that the tip is vibrated in an area of uniform current density. The

normal current density (Am^{-2}) at each applied current is then plotted graphically versus the respective signal (V) received and the gradient of this plot provides a calibration factor for the instrument. The use of this calibration cell eliminates any height factor that may arise from other methods. Figure 2.9 shows a schematic diagram of the cell used to calibrate the SVET.

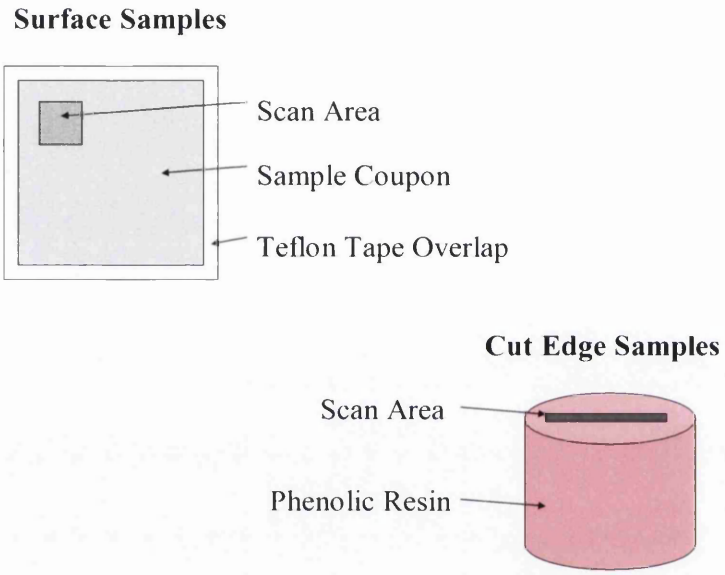

Figure 2.8 A schematic showing test ready surface and cut edge samples for SVET testing.

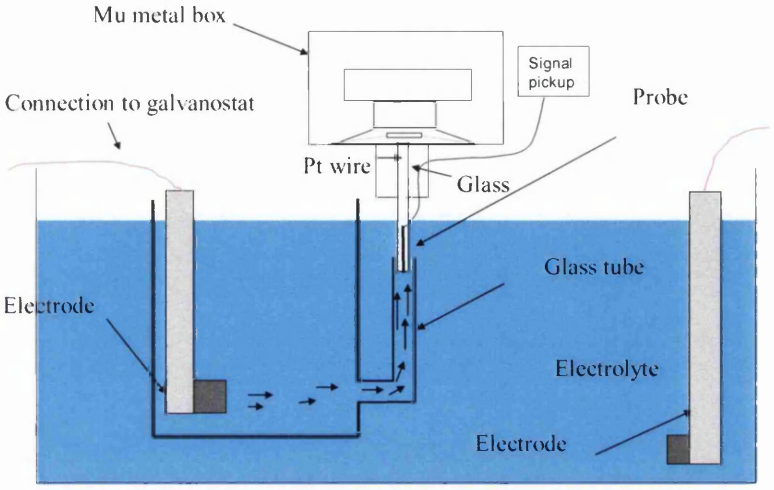

Figure 2.9 A schematic of the SVET calibration cell.

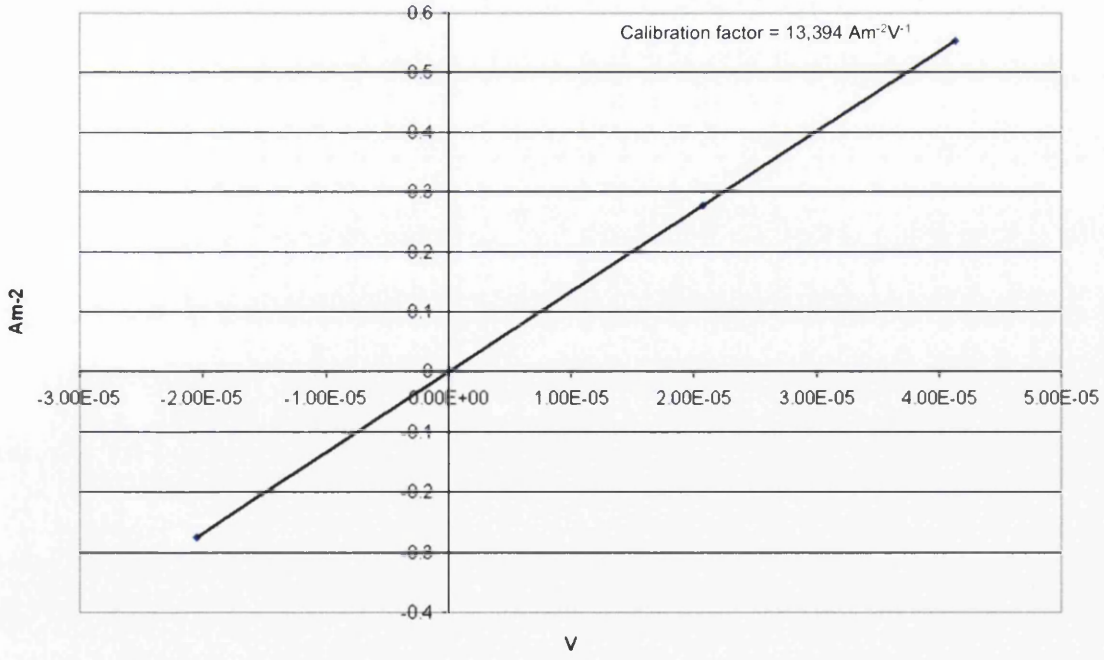

Figure 2.9a A calibration plot gained from using the SVET calibration cell

2.5.5 SVET mass loss calculations from first principles

Calibration of the SVET facilitates the calculation of metal loss associated with the corrosion activity across the sample during each test. The use of cartography software (Surfer v.8) allows for the interpretation of the raw data gained from the SVET. The following steps are undertaken to go from the raw data gained from the SVET to a value for metal loss for each hour from any given sample.

- Raw data from the SVET is given in nV.
- Integration of anodic events via cartography software returns a value in $nVmm^2$.
- Dividing by 10^9 returns a value in Vmm^2
- Dividing by a further 10^6 returns a value in Vm^2
- Multiplying by the Calibration factor (units $Am^{-2}V^{-1}$) returns a value for current (A).
- Multiplying by the time in seconds in an hour 3600 give a value for charge Q.
- Using Faraday's law it is possible to gain a value for mass loss per hour/scan such that:
    - Mass loss = $(Q/nF) \times A_w$
    - Q = Charge (C) (as above)
    - F = Faraday's constant (96485 C/mol)
    - n = Number of electrons (2 for Zn)
    - A_w= Atomic weight (65 for Zn)

The main assumptions in using this method are that it is assumed that the probe will travel in a planar fashion across the sample at a constant height of 100μm thus compromising between amplitude and scan height effects. It is also assumed that for the scan period (usually one hour) the current is constant across the sample. Resolving of the data in this way allows for only one type of metal loss to be calculated. For the purposes of this body of work the metal loss quoted will be zinc.

4.4.6 Limitations of the SVET

The SVET method is not without limitations. Scans are typically taken once every hour; as such corrosion activity occurring throughout the scan period is detected via the vibrating micro probe. Typically a scan will last for approximately ten minutes of every hour. SVET corrosion maps give an indication of corrosion activity at the instant of scanning. Metal loss values gained from the SVET will be lower than those actually occurring and provide general trends in corrosion performance rather than exact values.

2.6 References

1. DOWN, R. D., LEHR, J. H., 'Environmental Instrumentation and Analysis Handbook', John Wiley and Sons Inc, 2005.
2. STUEWER, D., JAKUBOWSKI, N., 'Elemental Analysis by Inductively Coupled Mass Spectrometry with Sector Field Instruments: a Progress Report', J. Mass Spectrom. 33, 579-590, 1998.
3. 'The Thirty Minute Guide to ICPMS', Perkin Elmer Ltd, 2000.
4. 'A choice of lamps for QU', Q-Panel Lab Products, Cleveland, 1994.
5. GROSSMAN, D. M., 'The weather and how to produce it in the laboratory', Q-Panel Lab Products, Cleveland, 1994.
6. HINTERBERGER, F., MASHECK, W., FADERL, J., in 'Zinc-Based Steel Coating Systems: Production and Performance', 281, GOODWIN, F. E., Editor, 1998.
7. SULLIVAN, J. H., WORSLEY, D. A., 'Zinc Runoff from Galvanised Steel Material Exposed in Industrial Marine Environment', British Corrosion Journal, Vol. 37, No. 4, 2002.
8. ISAACS, H. S., VYAS, B., in: 'Electrochemical Corrosion Testing', MANSFIELD, F. and BERTOCCI, U., Editors, ASTM STP 727, 3, 1981.
9. McMURRAY, H. N., WORSLEY, D. A., in: 'Advances in Chemical Kinetics', 4, 149, COMPTON, R.G., HANCOCK, G., Editors, 1997.

Chapter 3

Analysis of run off from organic coated steels

3.1 Introduction

In recent years the question of environmental impact has migrated from the board room of major industrial companies on to the debate floor of government chambers. This has given rise to many directives such as REACH, RoHS and WEEE that are now in force across Europe today; each will have a varying degree of impact on major industrial companies, whether it be process or product related.

Although the organic coating system may appear to be simple at face value, there are in fact many constituents that are needed to produce an OCS system. Fundamental to the system are the steel strip and galvanised layer both of which contain various metallic alloying additions, such as Mn in the steel and Al in the galvanising. The steel substrate is then overpainted with pre-treatment and primer layers that could contain metals such Cr and Sr, while the topcoat that is the final layer may hold metallic elements in additives such as pigments and stabilisers, many of which come under 'heavy metal' classification and as such have heightened environmental sensitivity. OCS are popular in the construction industry due to their formability, cost, ease of construction and aesthetic nature, however it is important to understand the stability of the top coat in it's use for external facades becomes the norm. Inevitably there are many square metres of OCS currently exposed and while long guarantees are in place assuring clients of performance, exposure to natural weathering will lead to degradation and eventual breakdown of the coating. It is during this exposure that many of the stabilisers and other additives will start leach out of the system as they try to protect the coating.

There is much work published on the failure of organic coated steel cladding[1]. Principal failure mechanisms have been associated with cut edge corrosion[2] leading to delamination of the coating or the coating itself can fail due to effects bought about by extensive photodegradation causing chalking or discolouration. This chapter concerns the stability of model plastisol coatings when exposed to an industrial marine environment over a period of one year. It is proposed that the level of metallic run off will provide a marker as to the coating stability and effect of pigmentation on coating performance. Identification of metallic species via ICPMS will give an indication of potential environmental impact of any particular coating under exposure.

3.1.0 Results and Discussion

A series of model near commercial coatings were prepared as outlined in Chapter 2. The coatings were pigmented with an active 'U' graded TiO_2 (Kronos 1001) for the purpose of ensuring degradation within the short timeframe and a selection of coloured pigments. A full matrix of the panels is shown in Table 2.1 on page 65.

3.1.1 Analysis of Metallic Run-off from Organic Coated Steels

The coated panels were exposed as outlined in section 2.1.4 (p.68). During the exposure period the following metals detected via ICPMS of the run off samples: Cr, Mn, Zn, Sr, Ti, Cu, Sb and Ba. From the results it was clear that Antimony (Sb) and Barium (Ba) stand out as the two most leached species in each panel. This is a concern as they are both classified as 'heavy' metals and Sb in particular is known as being poisonous. It is present in the PVC resin in the form Sb_2O_3 (Antimony trioxide), as a flame retardant. However when considering the levels at which it is being leached from the panel, the accepted level of Sb allowed in drinking water currently stands at 5ppb. The case is very similar when considering Ba which is used in salt form as a stabiliser. In this case the accepted level for Ba currently stands at 1000ppb.

Figure 3.1 below shows the Sb run off after the first month of exposure and it is shown that the levels present in run off in each case far exceed the permissible levels allowed in drinking water as shown by the red line the graph.

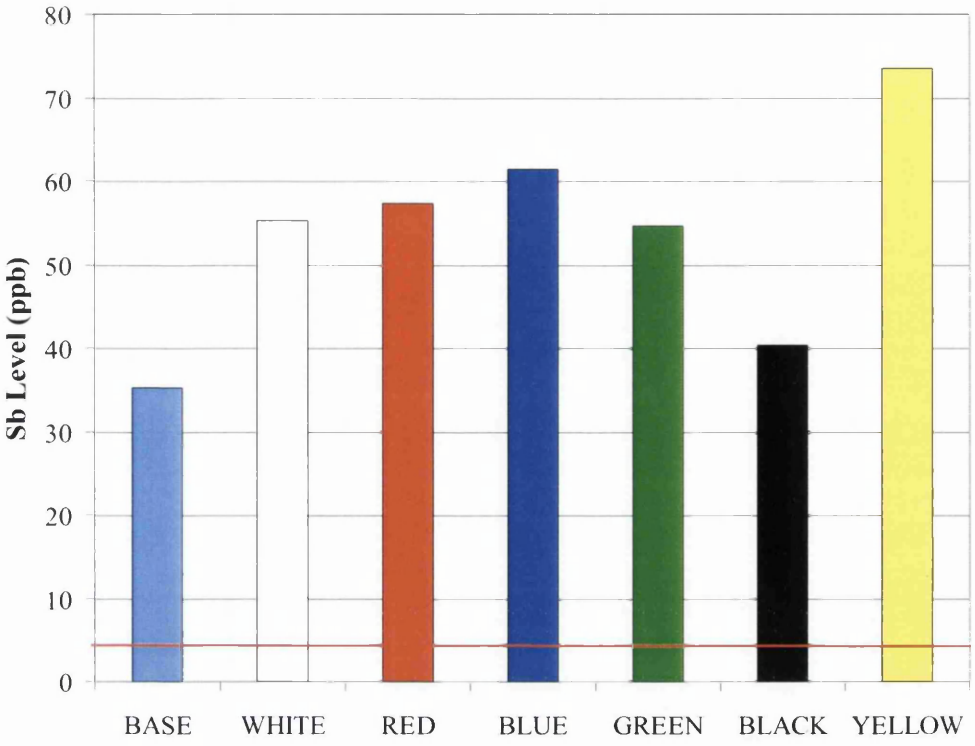

Figure 3.1 Sb Level (ppb) detected via ICPMS after 1 month external exposure.

It should be noted that the coatings exposed were designed to photodegrade and are not completely commercial. However the levels of Sb released by the coating are still surprising even when an initial flush of metallic species may be expected. Levels range from 35ppb from the unpigmented base to 73ppb from the yellow pigmented system. Continuous leaching at these levels will not only be damaging to the coating but also the surrounding environment due to cumulative uptake by plants and soil.

Ba shows a similar flush during the first month of exposure, however in this case not all of the samples exceeded the permissible level in drinking water. This is shown graphically in Figure 3.2 below.

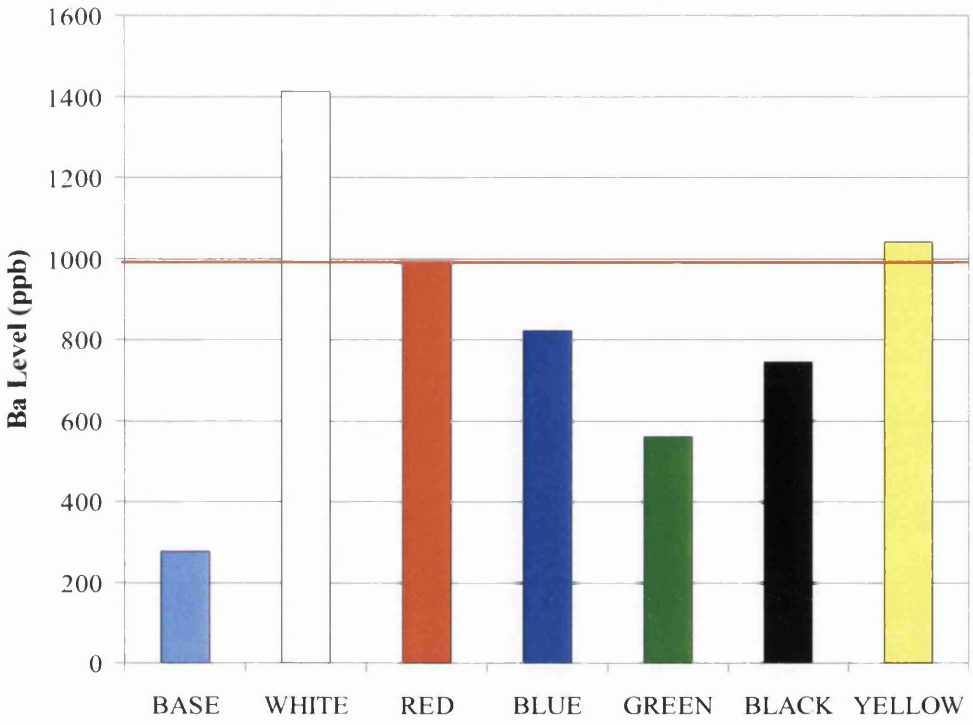

Figure 3.2 Ba Level (ppb) detected via ICPMS after 1 month external exposure.

It can be seen that only two of the samples leached Ba in excess of the permissible level for drinking water, with levels ranging from 1410ppb in the white sample and 1040ppb in the yellow sample, while the green sample leached least Ba with 560ppb. From the above graph it could be said that in the short term, adding pigment to the coating system as well as TiO_2 stabilises the coating against photodegradation.

Figure 3.3 shows the monthly ppb levels of Ba leached throughout the exposure period. It can be seen that after the initial flush seen above in Figure 3.2, the amount of barium leaching off the coatings tails off as it is being used to stabilise the highly active coating, raising slightly when the level of rainfall is at a higher level.

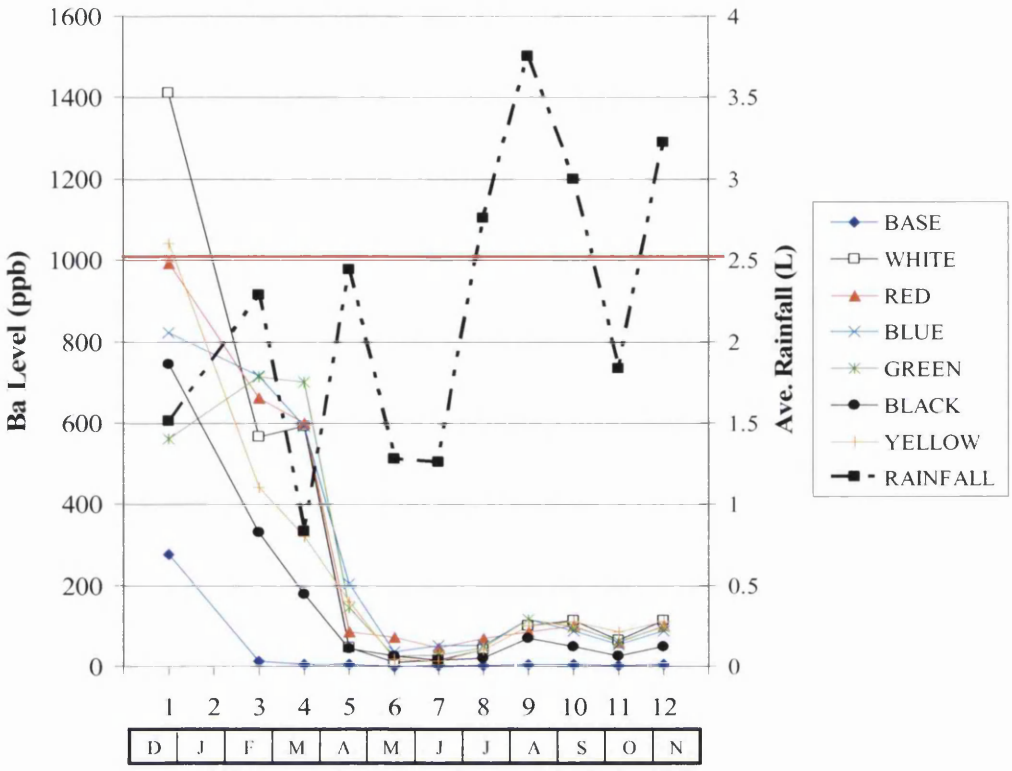

Figure 3.3 Monthly Ba levels (ppb) with permissible drinking level indicated by the red line.

It is also clear from the above graph that pigmentation of the paint system has an impact on photodegradation. This is highlighted by the fact that the base resin consistantly leaches less Ba than any of the other coatings. This behaviour continues when considering the data in the form of micrograms per panel, shown in Figure 3.4

The Sb release, shown in Figure 3.5, is much more related to the rainfall level. The reason for this is that Sb is added to the system primarily as a heat stabiliser and flame retardant for the curing process and is therefore not used to stabilise the coating from degradation. This leads to a much more consistent leaching profile. The levels shown in Figure 3.5 are ppb or µg/litre. If the data is considered in µg then the trend with rainfall is highlighted further. This is shown graphically in Figure 3.6. It should be noted again that the levels shown are given in micrograms per panel. The panel area was $0.015m^2$.

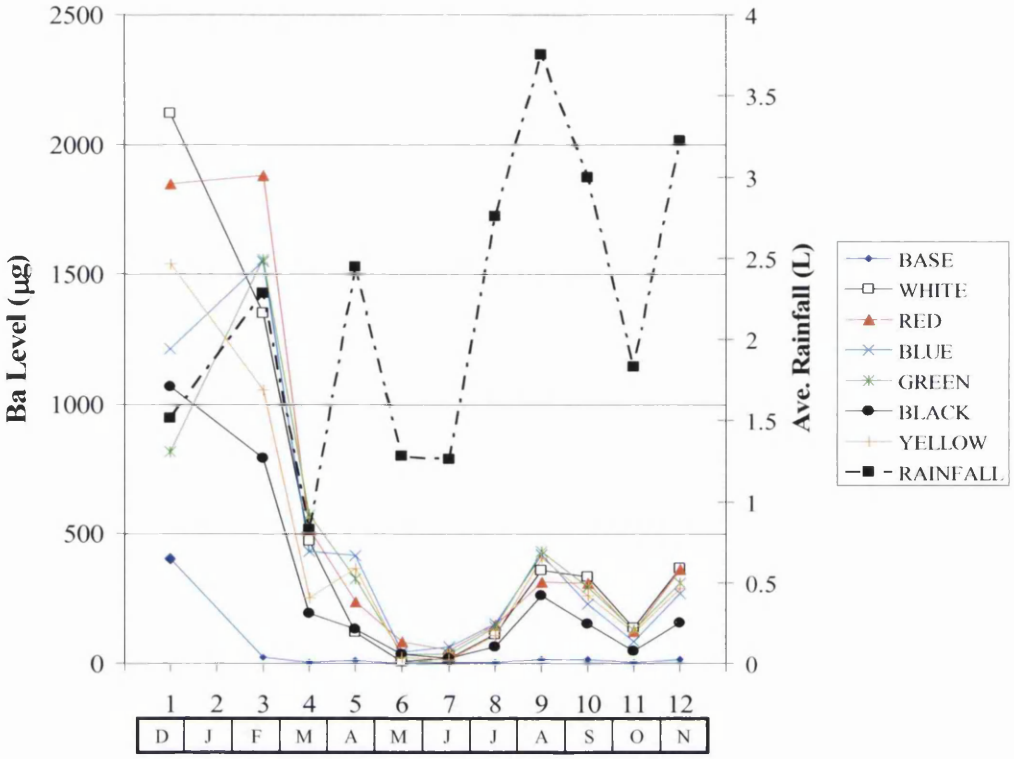

Figure 3.4 Monthly Ba levels (µg / panel) showing leachate trend with rainfall.

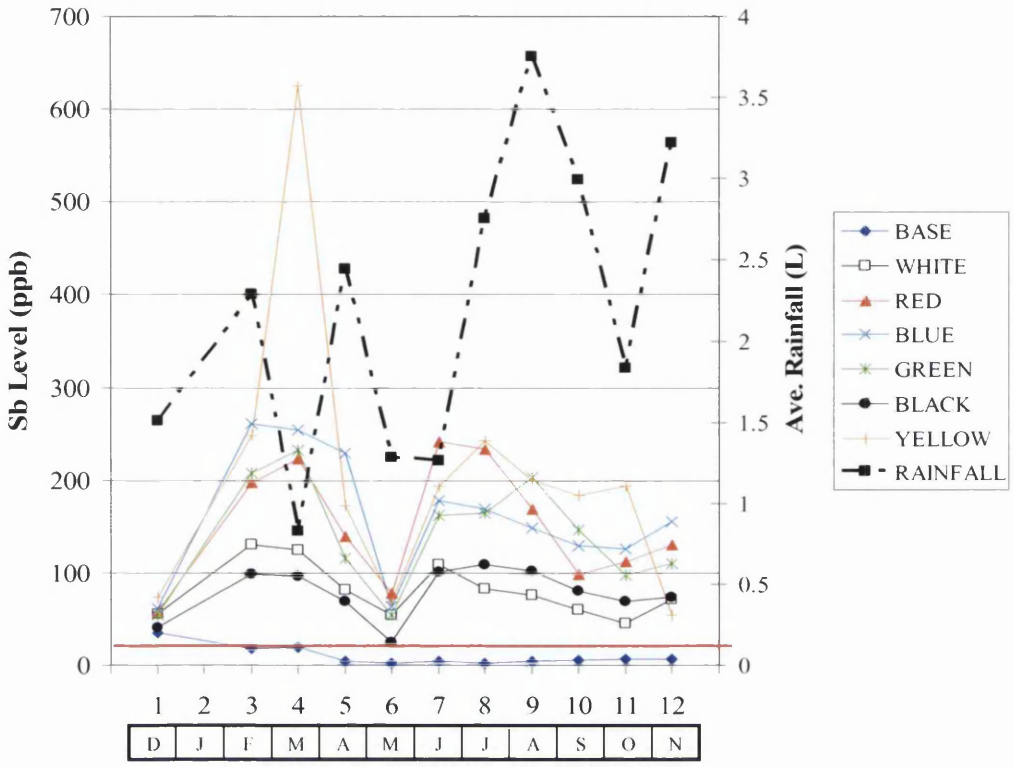

Figure 3.5 Monthly Sb levels (ppb) with permissible drinking level indicated by the red line.

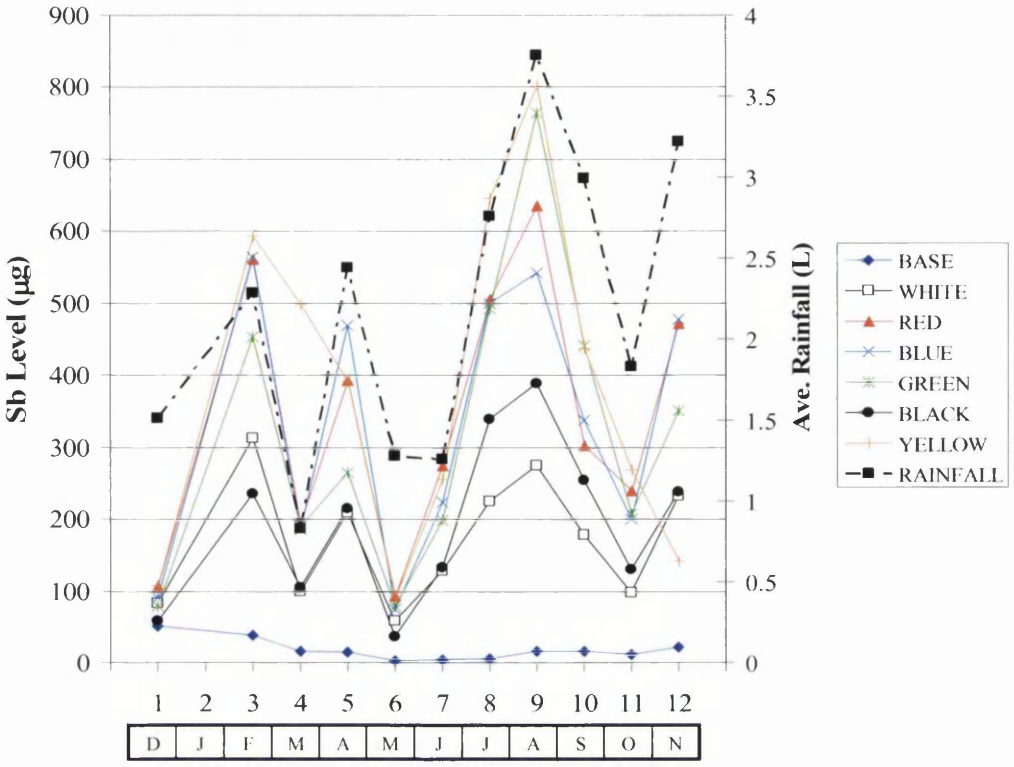

Figure 3.6 Monthly Sb levels (µg / panel) showing leachate trend with rainfall.

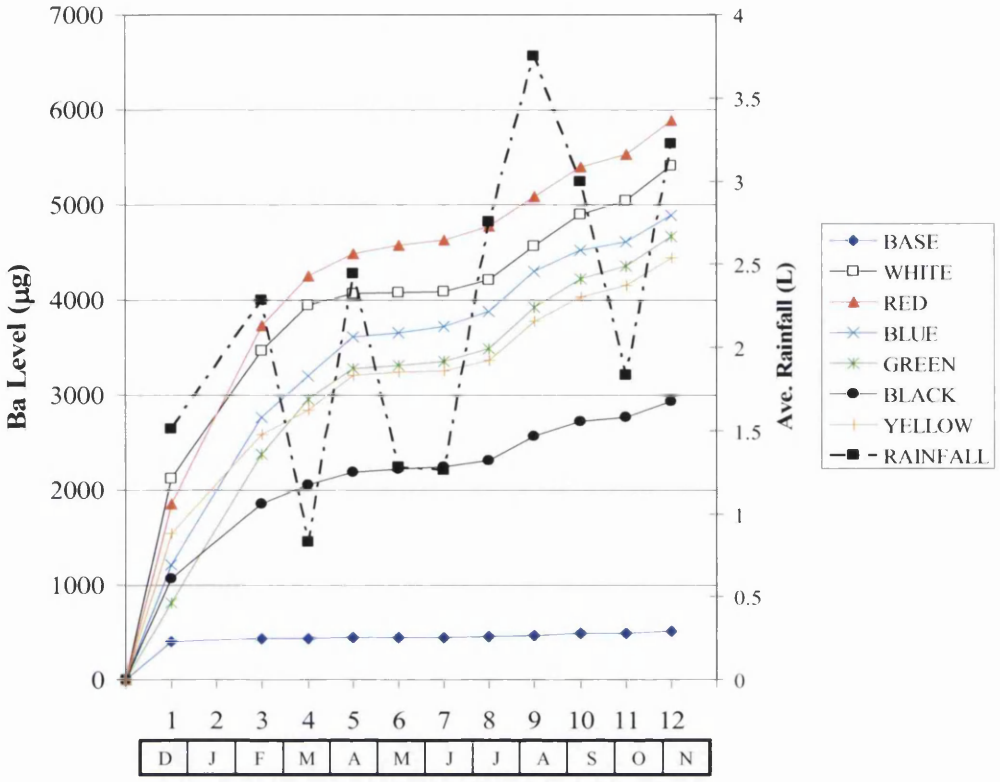

Figure 3.7 Cumulative Ba release (µg) throughout the exposure period.

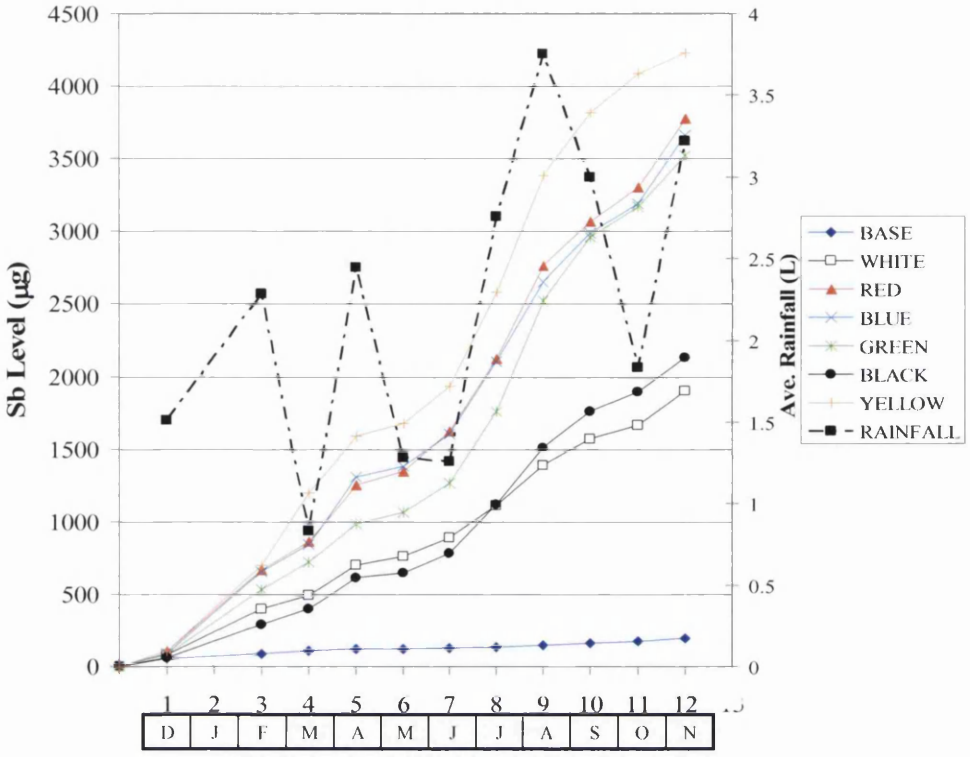

Figure 3.8 Cumulative Sb release (µg) throughout the exposure period.

Cumulative graphs for Ba and Sb (Figures 3.7 and 3.8 respectively) further show the pattern of release with rainfall. The pattern is again more apparent in the release of Sb shown in Figure 3.8. This suggests that Sb is more sensitive to leaching via transient rainfall than through photodegradation. Ba exhibits a steady release with the cumulative plot, Figure 3.7, showing less dependency on rainfall, however there is some response to rainfall levels particularly at month 3 and 12.

With regard to the effect of pigmentation on coating performance/stability it has been shown to affect the characteristics of organic coatings[3]. It is perhaps best to consider the total amount of each metallic species leached from each of the coatings exposed. For this the cumulative value for each significant metallic element was taken and given a rank from 1-7, with the lowest level achieving a rank of 1 and the highest level achieving a rank of seven. The rankings are then added up for each panel and element to give a final rank which is related to panel colour/ pigmentation and runoff level. Thus, the sample with the highest amount of ranking points is identified as the worst performer or least

stable coating. This ranking system can be seen in Table 3.1 with the final rank can be seen in Figure 3.9.

Total Leachate Level µg/panel (Rank)									
	Cr	**Mn**	**Zn**	**Sr**	**Ti**	**Cu**	**Sb**	**Ba**	**Ranking Points**
BASE	3.86 (5)	9.62 (1)	465.41 (6)	52.31 (1)	17.64 (1)	146.13 (7)	198.56 (1)	508.6 (1)	**23**
WHITE	1.37 (1)	94.01 (4)	294.06 (3)	99.89 (3)	58.07 (2)	72.50 (4)	1899.4 (2)	5411.7 (6)	**25**
RED	8.34 (7)	343.1 (6)	130.67 (1)	117.01 (4)	151.55 (7)	41.48 (2)	3777.9 (6)	5894.2 (7)	**40**
BLUE	2.54 (3)	125.8 (5)	367.33 (4)	126.71 (6)	126.21 (6)	30.56 (1)	3666.3 (5)	4883.4 (5)	**35**
GREEN	2.15 (2)	18.04 (2)	509.37 (7)	122.41 (5)	87.62 (4)	95.07 (5)	3522.1 (4)	4665.1 (4)	**33**
BLACK	7.91 (6)	56.21 (3)	229.52 (2)	70.48 (2)	77.70 (3)	57.79 (3)	2132.0 (3)	2928.5 (2)	**24**
YELLOW	3.45 (4)	11520.7 (7)	420.76 (5)	144.35 (7)	100.87 (5)	140.86 (6)	4233.1 (7)	4449.6 (3)	**44**

Table 3.1 Total runoff levels ranked against pigment/colour. Run off quantities reproducible within 10%.

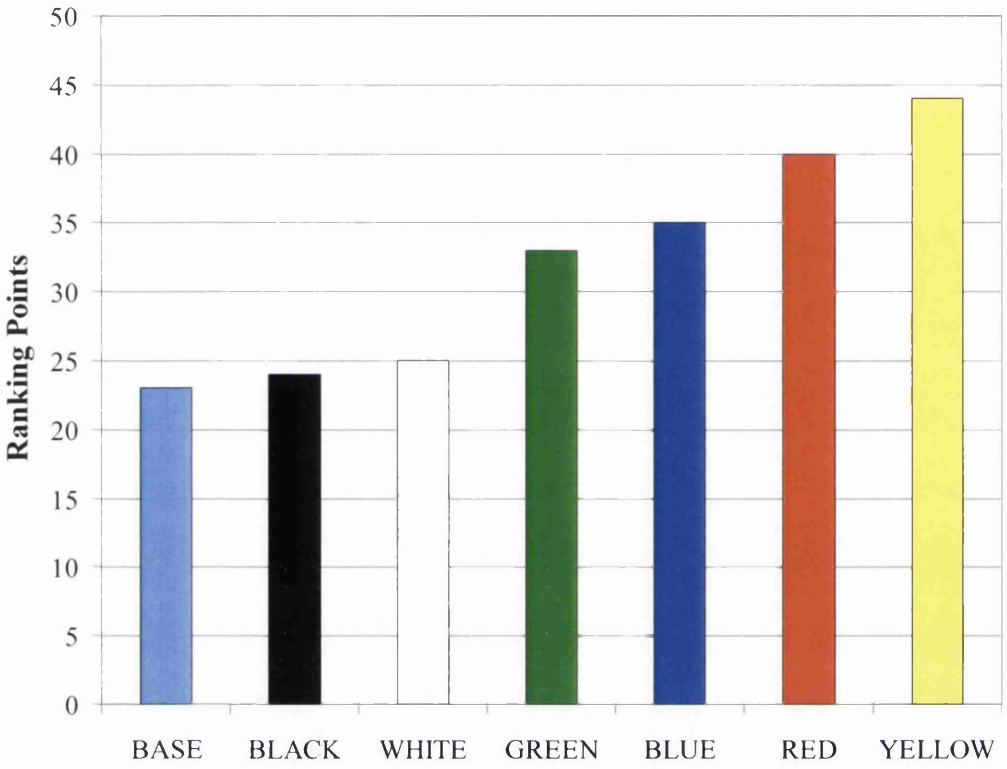

Figure 3.9 Coating pigmentation vs Leachate rank.

From the ranking process it can be seen that the worst performing coating is the Sicotan yellow pigmented coating. Ironically the best performing coating is the base resin. However, this result should be approached with caution. This is because it was used in the 'as received' condition without stabiliser or any other additives; therefore there are no metal ions present to be leached out. The lack of stabiliser and additive to the system may have given rise to the level of Zn runoff from the base resin as this could only have come about from the galvanised layer. This suggests that the base resin as a coating could have a higher level of porosity than the other stabilised and pigmented systems.

The yellow pigmented coating performs the worst out of the sample field. This is due to the fact that yellow pigmented systems will absorb only blue light, which lies at the end of the visible light spectrum with a shorter wavelength and higher frequency and as such, a higher energy. It is this energy that will contribute to the photodegradation of

the coating as the blue photon pass through the coating exciting the already active TiO_2. In addition, the yellow pigment is also a chrome titanate which may have its own photoactivity.

Red pigments absorb both blue and green light and therefore a larger frequency range of light will be passing through the coating with green and blue lying next to each other in the visible spectrum, although not at the highest energy levels as seen with photons of blue light.

Next in the ranking lies the green coating. Green pigments will absorb red and blue light. Red light has the lowest energy of the visible light spectrum and as such may be expected to do the least damage to a coating; however this coupled with the absorption of the high energy blue photons leads to more photodegradation. When comparing the green system performance to that of the blue, this may be seen as surprising due to the higher energy absorbance however green pigmentation of this sort has been seen to consistently out perform other pigments in polyurethane systems using photostable TiO_2[4].

The white system is pigmented wholly with a U-grade TiO_2, therefore there is no other pigment to inhibit or accelerate photodegradation. Excitement of the TiO_2 by UV light is the principal mechanism for degradation and metal release as all visible light is reflected by white pigments. This is why one of the metallic species to come off the sample in greater abundance was Ba which is used principally used as a UV stabiliser.

The black sample proves to be a slight anomaly. With black pigmentation it is expected that all light frequencies are absorbed leading to inferior performance. This is not the case however when considering the metal runoff. The black pigment is elemental by mature in the form of Carbon. This could lead to the take up of ions within the paint system rather than a flush over time. However, another possibility is that the black pigment absorbs all the photons giving rise to a screening effect for the TiO_2. It can be seen from Table 3.1 that the black system performs consistently throughout with regard to metal loss.

The nature of the pigment will have an influence on the degradation as a whole due to solubility levels of the pigment itself, distribution of the pigment within the paint and porosity of the final coating as the sample were produced on a laboratory scale.

To further understand the degradation of the sample it is necessary to try and comprehend the weathering data with respect to the change physical properties bought about by the weathering process.

Figures 3.10 to 3.16 represent the reflectance spectrums for the coloured panels before exposure, after exposure and after sonication of the weathered panel. Measurements were taken using handheld CieLab Colour Space apparatus. This measures the reflectance of light from 380-720nm.

Comparing the panel's appearance before and after exposure it was clear that chalking had occurred on all the panels apart from the base (no pigment). This was due to presence of photo-active TiO_2. This chalking effect can be seen in the refelectance data as a shift in the spectrum to higher values. This higher reflectance value corresponds to the white appearance of the chalking and therefore results in a greater reflectance of light.

The panels were sonicated to try and eliminate the reflecting effect of the 'chalked' TiO_2 on the surface and give true value of weathering with regard to reflectance. It can be seen that in most cases this resulted in a level being reached in between that of the unweathered and weathered states. There are a couple of exceptions; the white and yellow panels exhibited a further increase in reflectance.

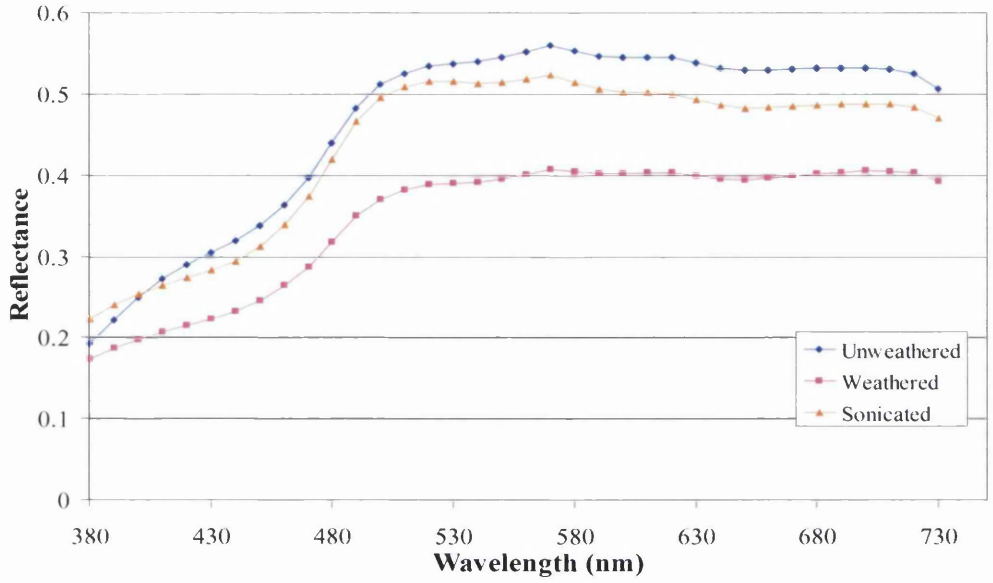

Base Resin

Figure 3.10 Reflectance spectrum for Base Resin in unweathered, weathered and sonicated condition.

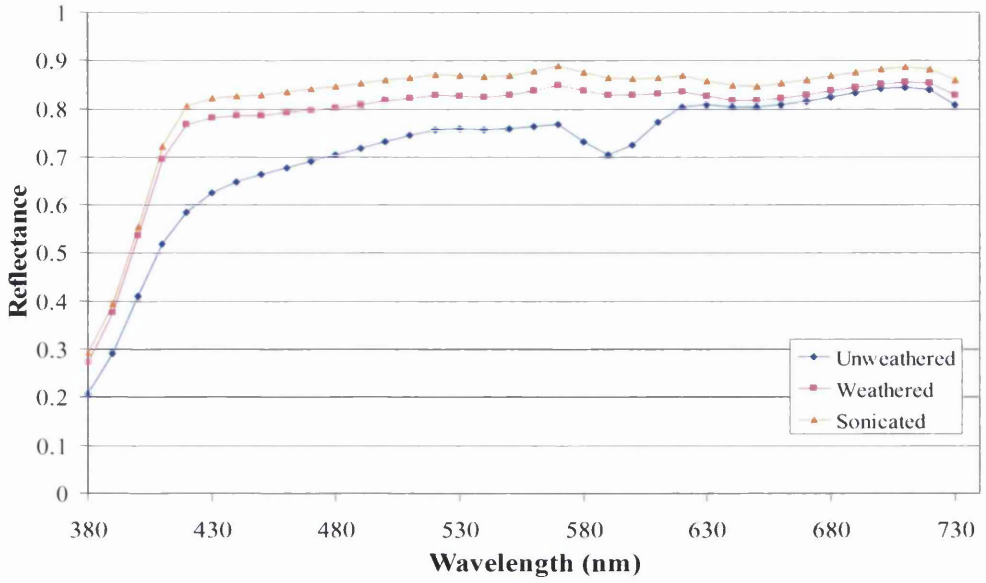

White

Figure 3.11 Reflectance spectrum for White in unweathered, weathered and sonicated condition.

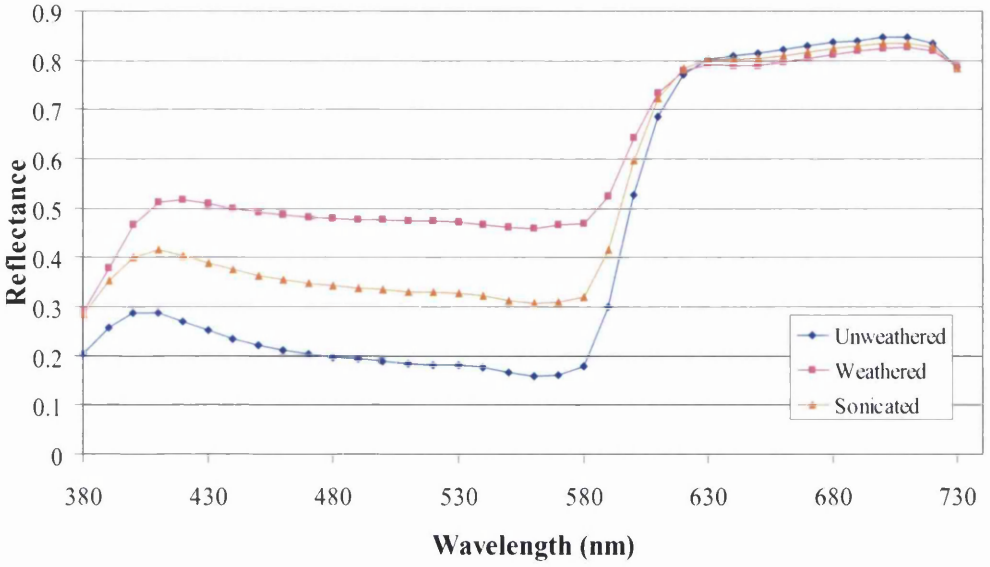

Red

Figure 3.12 Reflectance spectrum for Red in unweathered, weathered and sonicated condition.

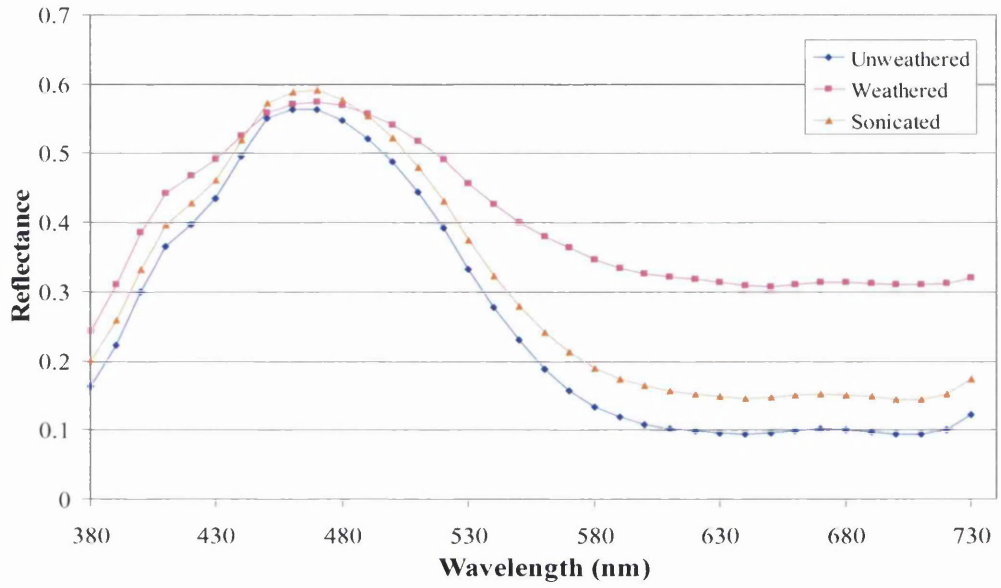

Blue

Figure 3.13 Reflectance spectrum for Blue in unweathered, weathered and sonicated condition.

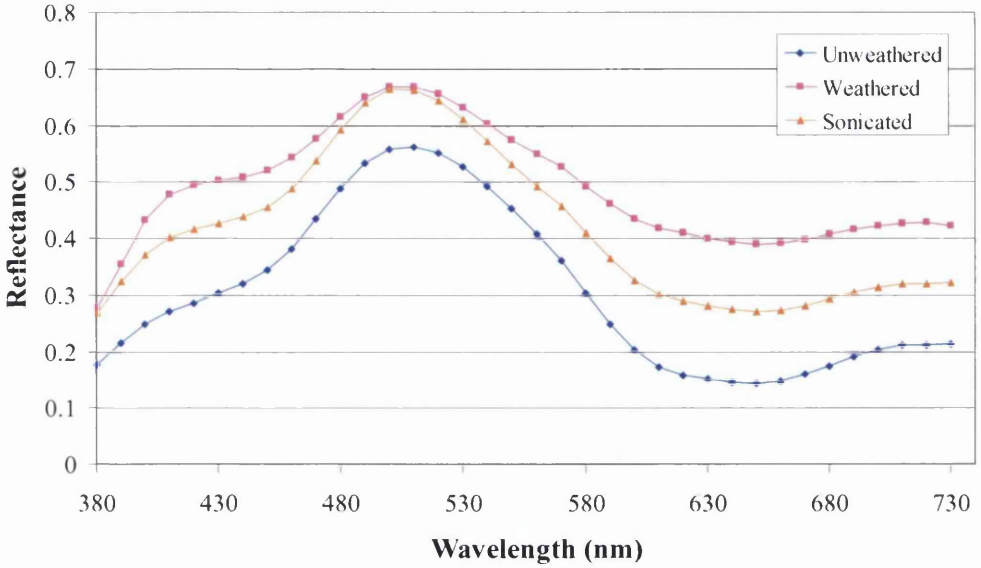

Green

Figure 3.14 Reflectance spectrum for Green in unweathered, weathered and sonicated condition.

UNIVERSITY OF WALES SWANSEA LIBRARY

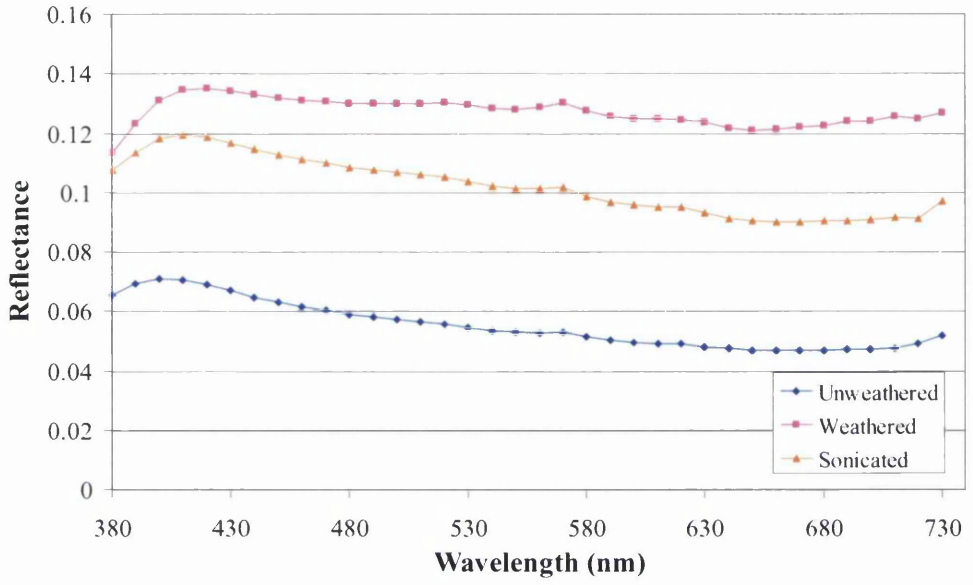

Black

Figure 3.15 Reflectance spectrum for Black in unweathered, weathered and sonicated condition.

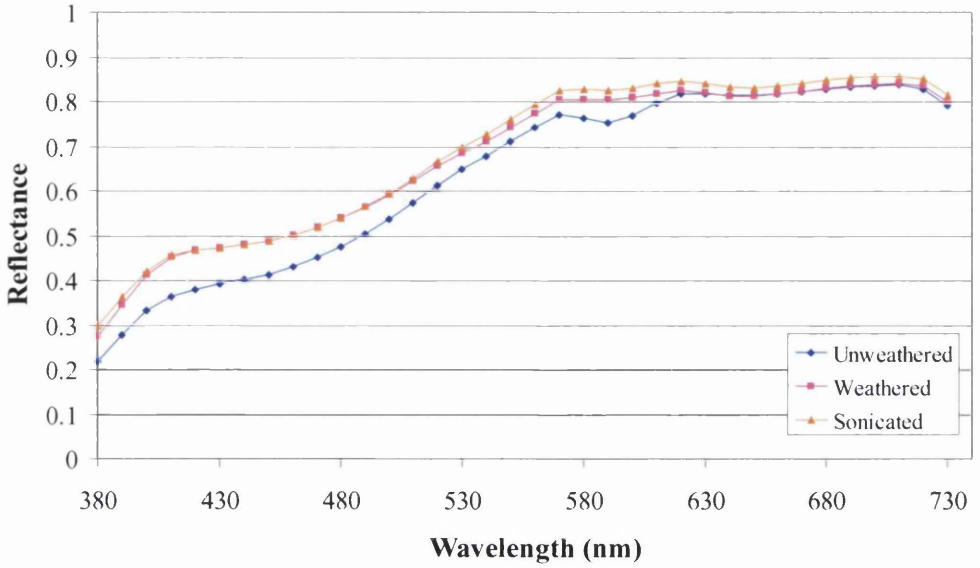

Yellow

Figure 3.16 Reflectance spectrum for Yellow in unweathered, weathered and sonicated condition.

This data has also been represented in Figure 3.17 as a measurement of average reflectance for each of the coloured panels at the unweathered, weathered and sonicated stages.

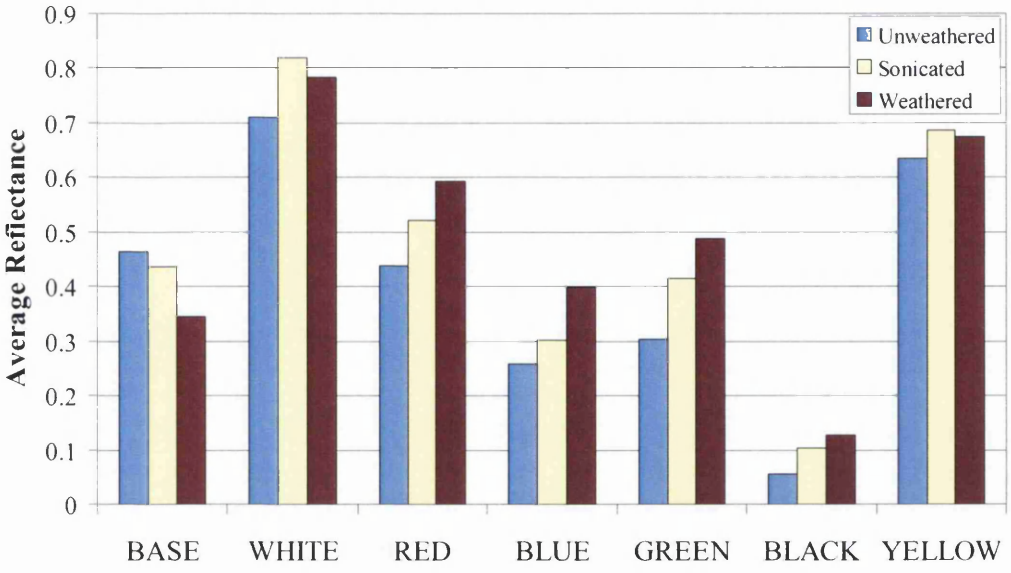

Figure 3.17 Average reflectance in unweathered, weathered and sonicated condition.

From this it is possible to calculate a value for ΔR, the change in reflectance. This value can then plotted against total Ba release (μgm^{-2}) as shown in Figure 3.18 and it can be seen from this that there is a general trend that is formed between the change in reflectance and total Ba release. In general it can be said that an increase in total Ba release relates to and increased change in reflectance (ΔR).

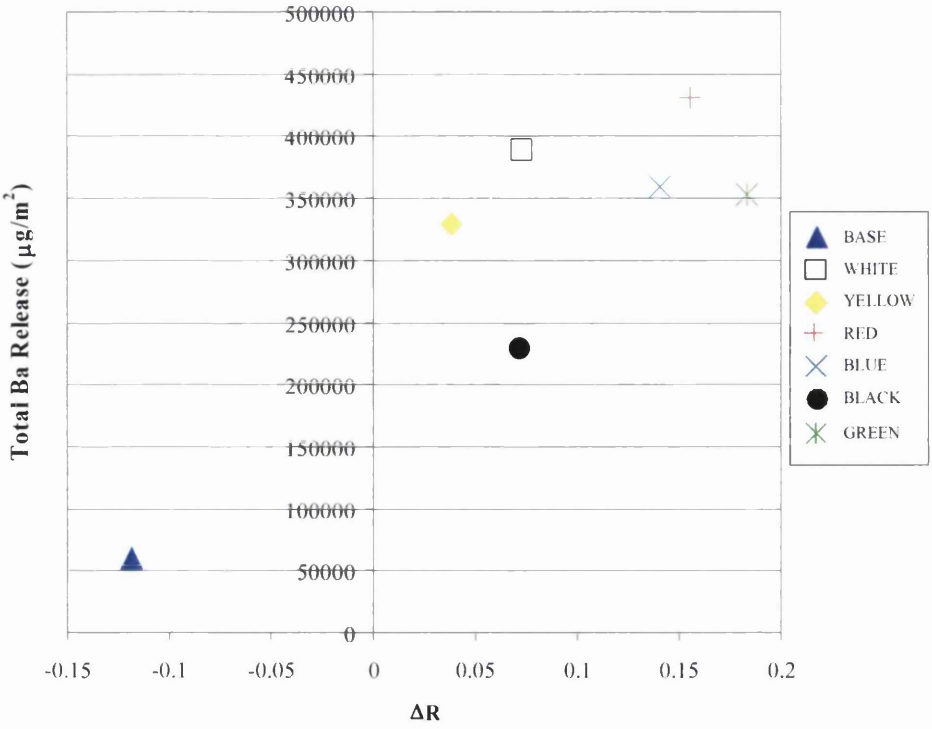

Figure 3.18 Total Ba release vs Change in reflectance (ΔR)

A similar conclusion can be drawn when relating the ΔE values for the coloured panels to the total Ba release. ΔE value gives a value for total colour change and is calculated by using Equation 3.1:

$$\Delta E = \sqrt{(L^2 + A^2 + B^2)} \qquad \text{Equation 3.1}$$

Where L corresponds to brightness from 0-100, A corresponds to red and green light and B corresponds to blue and yellow light. It can be seen in Figure 3.19 that an increase in total Ba release leads to an increase in colour change (ΔE).

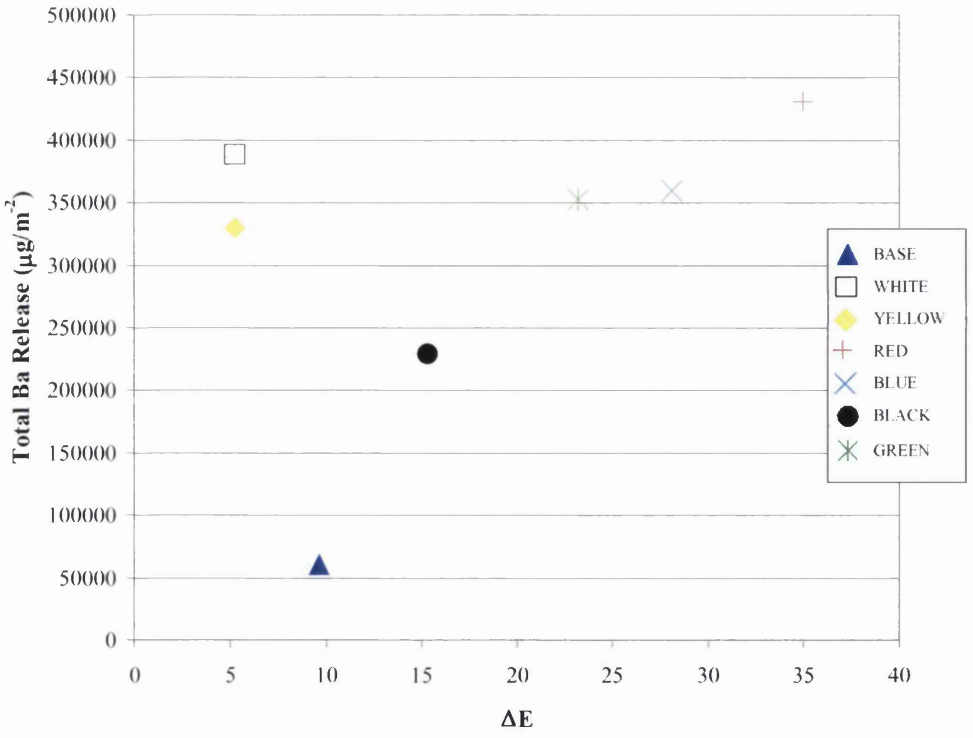

Figure 3.19. Total Ba release vs Total colour change (ΔE)

The Ba release values were chosen to be representative as Ba/Zn is currently used commercially as the principal UV stabiliser in this type of coating. Further to this, metallic runoff could provide a short term marker for stability of a coating. Much research has been published[5, 6] on accelerated UV degradation of PVC coatings as a function of CO_2 release. CO_2 is a by-product of photodegradation of PVC[5] and as such measurement of levels produced under accelerated conditions has become an accepted method for prediction of coating stability. Different pigment combinations produce different rates of CO_2 release and therefore alter the rate of degradation of the polymer coating[4].

On comparing the raw ppb Ba release data gathered from the first month of exposure in Figure 3.20 to the CO_2 release rates from previous work a good correlation was seen to exist between the levels of Ba released from the coating and the CO_2 release rate. The correlation with the CO_2 data is shown in Figure 3.21. It should be noted that

the blue and black systems have swapped places in terms of stability, however the rest of the results ring true with the published data.

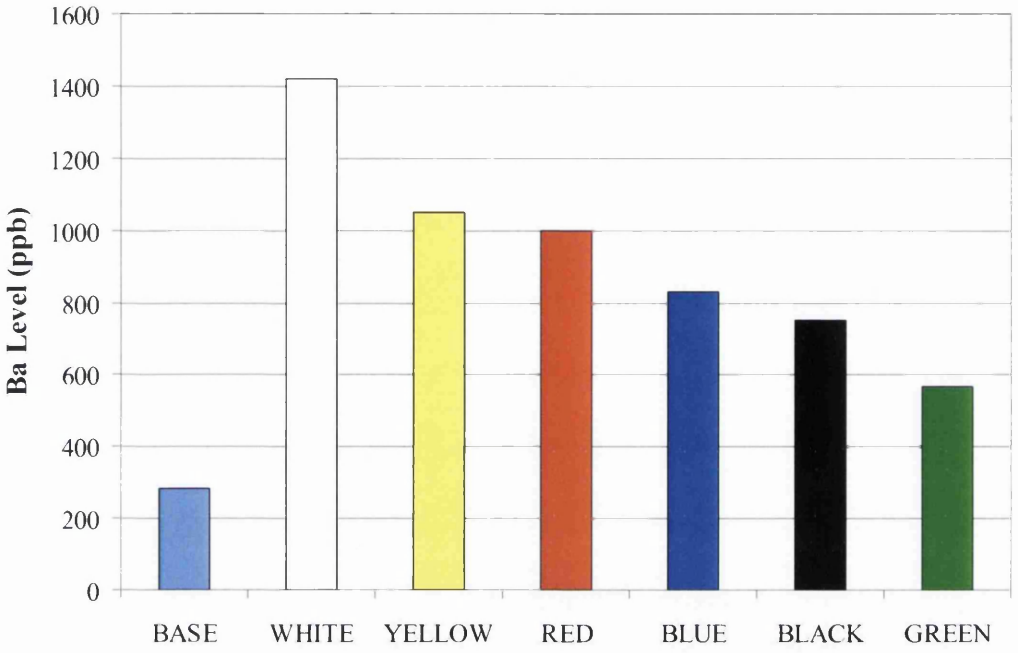

Figure 3.20 Ba levels (ppb) after one month natural weathering.

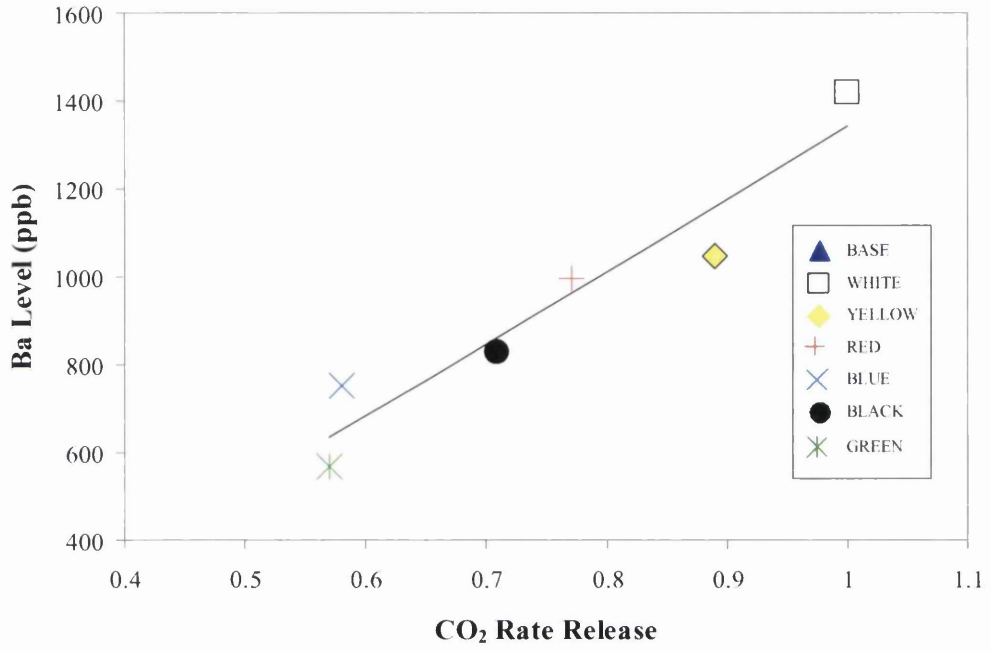

Figure 3.21 Ba levels (ppb) after one month natural weathering.vs 24hr CO_2 rate release ($\mu gm^{-2}min^{-1}$)

Overall this would suggest that the barium release from the series of coatings after one month of exposure could act as a good test to predict the long term stability of the coating. It should be noted that the published data was produced on UPVC films with additions of TiO_2 possessing greater photoactivity than that of the K1001 used for the external weathering program.

3.2 Conclusion

This chapter has shown that metallic runoff from external weathering provides a useful tool with regard to the prediction and ranking of pigmented PVC coatings. The effect of pigmentation on PVC based coatings has been addressed and related to metallic leachates, with yellow pigments seemingly the most detractive to coating performance.

Monitoring metallic runoff provides an insight into potential species that could come out of the coating during the products lifetime, in particular highlighting those metals of a 'heavy' nature that could offer serious environmental impact across the lifetime of a building or warehouse for example.

This work has also shown in the short term Ba levels that leach from coating stabilisers can provide a quick insight into the performance of the coating in the natural environment which holds with accelerated laboratory methods.

3.3 References

1. RYAN, P. A., WOLSTENHOLME, R. P., HOWELL, D. M., in: 'Durability of Cladding - A State of the Art Report', WS. Atkins, Thomas Telford, 1994.
2. CHALLIS, M., WORSLEY, D. A., 'Cut Edge Corrosion Mechanisms in Organically Coated Zinc-Aluminium Alloy Galvanised Steels', British Corrosion Journal, vol. 36 No. 4, 2001.
3. PERERA, D. Y., 'Effect of Pigmentation on Organic Coating Characteristics' Progress in Organic Coatings, 50, 247-262, 2004.
4. ROBINSON, A. J., WRAY, J., WORSLEY, D. A., 'Effect of Coloured Pigmentation on Titanium Dioxide Photo-catalysed PVC Degradation', Materials Science and Technology, vol. 22, No. 12, 2006.
5. CHRISTENSEN, P. A., DILKS, A., EGERTON, T. A., TEMPERLEY, J., 'Infrared Spectroscopic Evaluation of the Photodegradation of Paint: Part 1 The UV Degradation of Acrylic Films Pigmented with Titanium Dioxide.
6. ROBINSON, A. J., SEARLE, J. R., WORSLEY, D. A., 'Novel Flat Panel Reactor for Monitoring Photodegradation', Materials Science and Technology, vol. 20, 2004.

Chapter 4

The effect of stabiliser type on organic coated steels

4.0 Introduction

PVC Plastisol is widely used for high performance industrial coatings for external architectural cladding for walling and roofing. Long commercial guarantees coupled with ever tightening environmental legislation lead to constant research being undertaken to balance durability and environmental performance.

Due to their nature PVC coatings are susceptible to photo-degradation. This can be due to activation of TiO_2 (a common pigment in the PVC plastisol systems), which leads to de-hydrochlorination of the PVC itself causing discolouration[1] and the formation of hydrochloric acid. Stabilisation of PVC has been achieved in the past by using organo tin and barium zinc compounds. Increasing environmental sensitivity has lead to research into the use of non toxic stabilisers to inhibit corrosion in coated systems[2, 3, 4].

Hydrotalcite ($Mg_6Al_2(OH)_{16}CO_3 \cdot 4H_2O$) is one such pigment. It exists as a white Mg/Al hydroxycarbonate known for its ease and low cost of synthesis. Hydrotalcite is an anionic clay in nature and has a layered structure containing exchangeable anions[5]. Hydrotalcite (HT) has been identified as having the ability to perform a number of functions. Among these uses are as an ion exchanger, corrosion inhibitor[3], flame retardant, halogen scavenger and PVC stabiliser[5]. For the purposes of this investigation the latter two uses shall be utilised against the dehydrochlorination of the PVC based coatings. It has been proposed that HT will exchange the Cl^- ions with the CO_3^{2-} ions in its structure to produce a weaker less damaging carbonic acid compared to HCl, reducing the rate of degradation of the coating and therefore improving performance. HT has shown to be an effective addition to paint systems tested for degradation by measurement of CO_2 release, a byproduct of photo- degradation of UPVC films[2].

This chapter investigates the use of Hydrotalcite (HT) for the photo-stabilisation of PVC coatings. Part stabilised model coatings have been prepared for exposure to natural weathering and accelerated testing. The aims of the study are to compare the performance of HT against conventional stabilisers past and present and to establish any metallic ions that may serve as a marker for long term performance in service.

4.1 Effect of Stabiliser type on the Stability of Model PVC Plastisol Coatings

Model phthalate-free white pigmented coatings were produced as outlined in Chapter 2 and are shown in Table 4.1. These were then subjected to natural and accelerated weathering tests. Natural weathering was undertaken at the Port Talbot weathering site (industrial marine), with the run off monitored monthly for metallic species via ICP mass spectrometry. Accelerated weathering tests were undertaken using QUVA methods as detailed in Chapter 2.

Colour	Resin	Plasticiser	Pigment	Stabiliser
WHITE	PLASTISOL	MESAMOLL	14% TiO_2	NONE
WHITE	PLASTISOL	MESAMOLL	14% TiO_2	Ba/Zn 1%
WHITE	PLASTISOL	MESAMOLL	14% TiO_2	Sn1/Sn2 1%
WHITE	PLASTISOL	MESAMOLL	14% TiO_2	5% HT

Table 4.1 Samples with different stabilisers exposed to natural weathering for one year.

4.1.1 External Exposure

All the samples were exposed to natural weathering conditions for a period of one year. The run off was collected monthly and analysed via ICP mass spectrometry for metallic species. This gave regular data at the species in the leachate and also allowed cumulative levels to be assessed over time. Table 4.2 shows the cumulative levels of metallic species (normalised against a 'blank' sample) detected over the 12 month exposure period. It should be noted that no tin was seen to leach out of any sample, even that containing the tin stabiliser.

	Metal Ion Run off (cumulative over 12 months (mgm^{-2}))						
Stabiliser	**Mn**	**Zn**	**Sr**	**Ti**	**Cu**	**Sb**	**Ba**
HT	4.5	10.3	10.3	8.1	2.5	444	340
Tin	0.1	12.0	10.3	8.5	6.8	113	271
No Stab	13.5	15.1	10.4	11.7	4.8	287	411
Ba/Zn	5.61	18.4	6.0	0.5	0.4	127	361

Table 4.2 Cumulative metal ion release detected (normalised) detected by ICPMS over 12 months exposure. Run off quantities reproducible within 10%.

It is clear from the above table that the both Antimony (Sb) and Barium (Ba) leached out of the coatings in excessive levels from all stabiliser types. The presence of both these metals is associated to their addition as stabilisers to the as recieved PVC granules prior to their inclusion in the plastisol coatings, since Ba is present in all samples, even without Ba stabiliser addition and Sb is not added to the paint system in any format. As such there is a level of barium present that is unavoidable. Further to this there is no other pigmentation or any additional inhibition present to stabilise the coating.

Of the other metallic species seen, strontium (Sr) appears as a result of exposure of the primer layer. This could be due to pin-holing of the topcoat during the manufacture of the coatings on a lab scale. Titanium (Ti) can only come from some interaction with the active TiO_2 used as a pigment. This is quite surprising due to the insolubility of the compound and therefore could suggest dissolution mechanism bought about by photo-activation, by combination with choride or more oxygen ions. It is possible (and perhaps more likely) that during the weathering process, chalking occurs (as mentioned previously), this will lead to migration of TiO_2 to the surface of the coating. Subsequent

rainfall will wash the TiO_2 nano-particles off into the leachate reservoir, which when passed through the nebuliser of the ICPMS becomes vapourised and detected.

Copper (Cu) and Manganese (Mn) are surprising in that they appear at levels above the 'blank'. The steel substrate is a Mn bearing grade and during the galvanising process Mn is known to migrate to the surface[7, 8], however it is normally seen either from the cut edge or from the surface of bare uncoated galvanised samples. Cu must be present in some form as a plastisol ingredient, however it does not appear in any of the ingredients that are added by the paint makers, so at this stage remains a curiosity.

Corus' flagship building envelope HPS 200 currently holds BS 6920 which enables any recovered rain water to be collected for human consumption (test briefly outlined in Chapter 1 p53). With this in mind it is perhaps useful to assess the metallic runoff from the panels with regard to permissible drinking water for the various ions detected. Table 4.3 shows the average ppb (μg/l) of each ion detected for each month over the exposure period

	Average Metal Ion Run off (ppb) per month.						
Stabiliser	**Mn** **(50ppb)**	**Zn** **(5000ppb)**	**Sr** **No limit**	**Ti** **No Limit**	**Cu** **(2000ppb)**	**Sb** **(5ppb)**	**Ba** **(1000ppb)**
HT	4.38 (26.16)	7.06 (23.08)	9.50 (48.50)	6.00 (26.53)	4.90 (23.78)	310.03 (*870.81*)	283.28 (*1006.74*)
Tin	1.04 (3.74)	5.66 (22.00)	5.42 (34.29)	12.39 (120.82)	5.49 (15.78)	73.57 (*156.58*)	239.66 (*1105.56*)
No Stab	7.92 (27.22)	7.82 (27.91)	6.80 (33.00)	10.17 (84.71)	3.76 (9.31)	171.64 (*299.35*)	305.33 (*964.82*)
Ba/Zn	4.47 (18.03)	13.53 (51.55)	6.42 (42.32)	3.81 (26.91)	5.42 (37.55)	31.12 (*130.60*)	279.57 (*1410.75*)

Table 4.3 Average metal ion run off (ppb) per month. Max. levels in brackets, italics where level exceeded. Run off quantities reproducible within 10%.

From Table 4.3 it is possible to ascertain the permissible level in drinking water for the relative metal ion (bold), the average level seen each month, the maximum value over the exposure period (brackets) and finally where the level has exceeded the level allowed in drinking water (italics).

It is shown that Sb and Ba are again the most abundant species with levels consistently exceeding those allowed for drinking water. This reflects the findings for coloured paint systems, outlined in Chapter 3. A maximum level of Sb was seen to occur from the HT stabilised panel reaching 870ppb in month 3, 174 times the level allowed in drinking water. Ba reached a maximum level of 1410ppb, 1.4 times the allowed limit, which occurred from the Ba/Zn stabilised sample after just one month's exposure. Whilst the excess Ba can be related to the combination of the PVC granules, the Sb levels are something of a concern, especially to paint makers as many systems are marketed as Sb free as this may not be the case.

Although the latter of these results could be attributed to an initial flush of a new coating, the general discrepancy between the average and the maximum values shown across the board suggests that metal release is not necessarily predictable. It is perhaps useful to consider the influence of rainfall on Sb and Ba release. Figure 4.1 shows the Sb release in ppb across the exposure period while Figure 4.2 shows Sb release in terms of μg per panel.

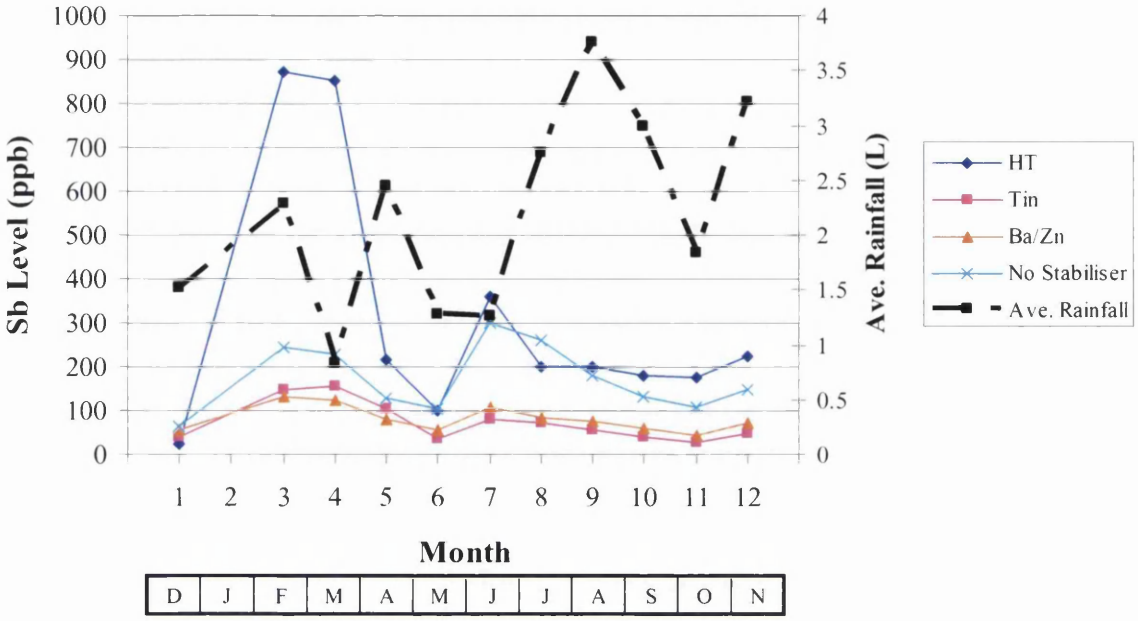

Figure 4.1. Sb release (ppb) vs. Stabiliser type over 12 month exposure period

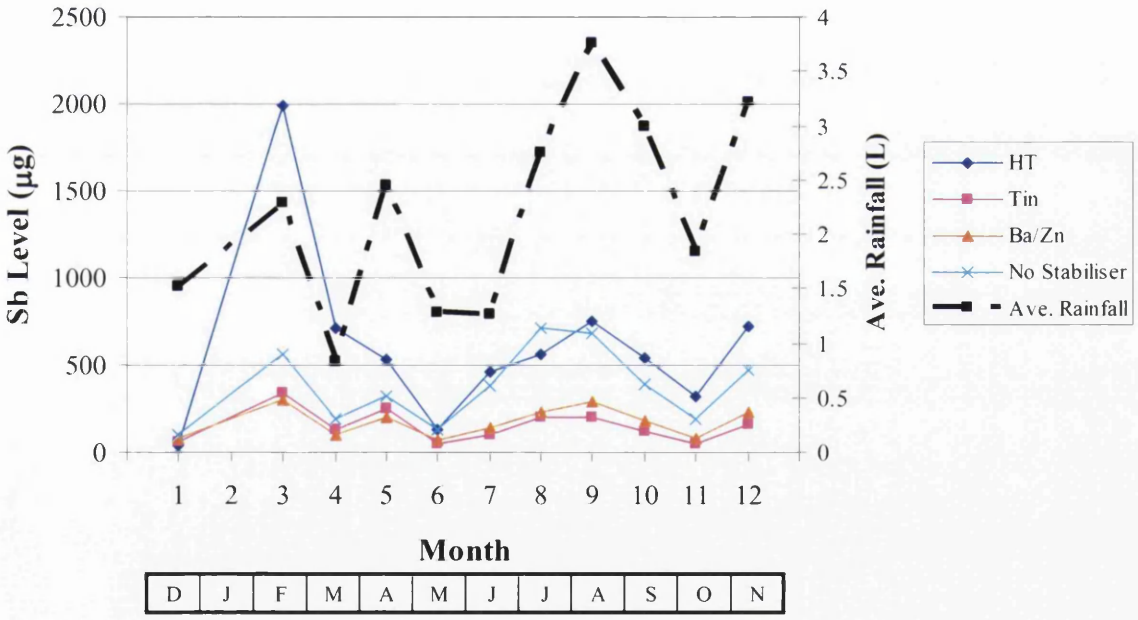

Figure 4.2. Sb release (µg) per panel vs. Stabiliser type over 12 month exposure period

From the previous figures it is shown that Sb release can be related to rainfall as a slight trend can be picked up across the profile of the detected ion levels. This suggests that although the stabilisers are present in the paint system, the coatings are still

susceptible to the effects of leaching via rainfall. Sb is present in the system as a stabiliser as mentioned previously but it is clear that it is not bound within the system by the other stabilising ingredients present.

Figures 4.3 and 4.4 show the monthly Ba release from each stabiliser type in ppb and µg per panel respectively. It is shown that the release of barium is much less dependent on the level of rainfall with both ppb and µg levels generally showing a tailing off effect as the stabiliser is being used up. This could be due to the nature of the stabiliser itself as it is added to the system to provide UV stabilisation and due to the nature of the test constant exposure to natural UV light results in the Barium leaching out of the coating. As discussed previously, barium stabilisation is added during the manufacture of the PVC used to make the base resin of the plastisol coating and therefore is present in each of the coatings at a background level while it is added to one panel as a stabiliser to allow comparison against the other stabilisers. With this considered the level at which Ba is leached off all the coatings is slightly surprising as the assumption may be that the sample containing the Ba/Zn stabiliser should leach the most Ba out of the coating on a monthly basis. However it is shown that this is not the case, with the Ba/Zn bearing sample leaching the most Ba on only three occasions throughout the exposure.

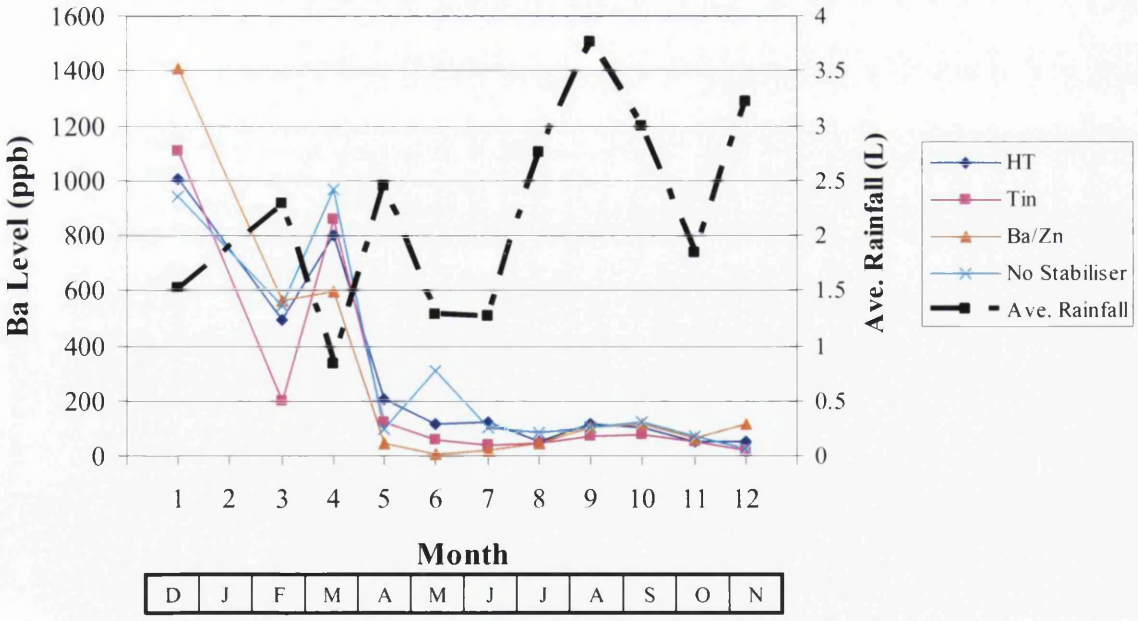

Figure 4.3 Ba release (ppb) vs. Stabiliser type over 12 month exposure period.

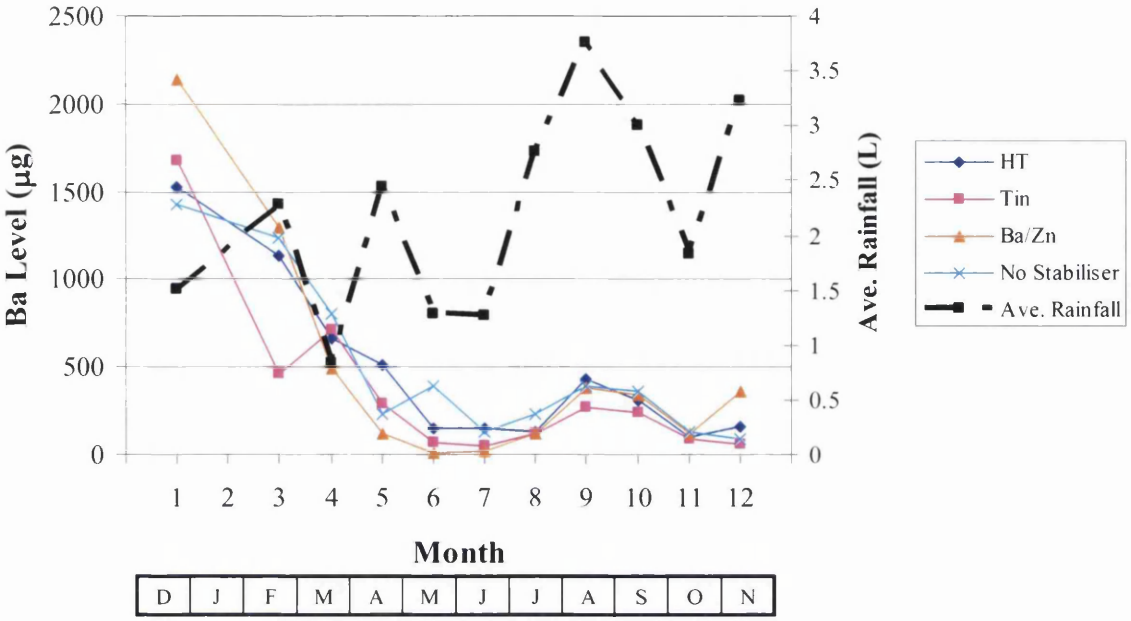

Figure 4.4 Ba release (µg) vs. Stabiliser type over 12 month exposure period.

Cumulative values of Ba and Sb show the progressive release over the period of exposure for each stabiliser type. From the cumulative values it is possible to identify which stabiliser type performs best with regard to heavy metal leaching. Figure 4.5 through 4.8 show the cumulative values of Sb and Ba release in ppb and µg respectively.

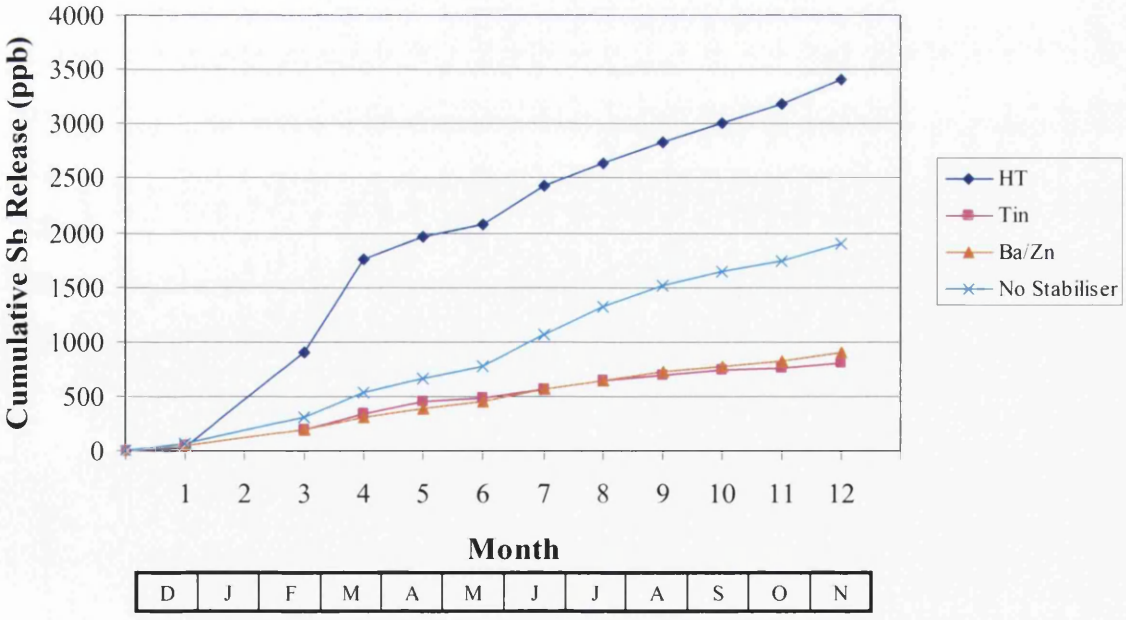

Figure 4.5 Cumulative Sb release (ppb) per panel vs Stabiliser type

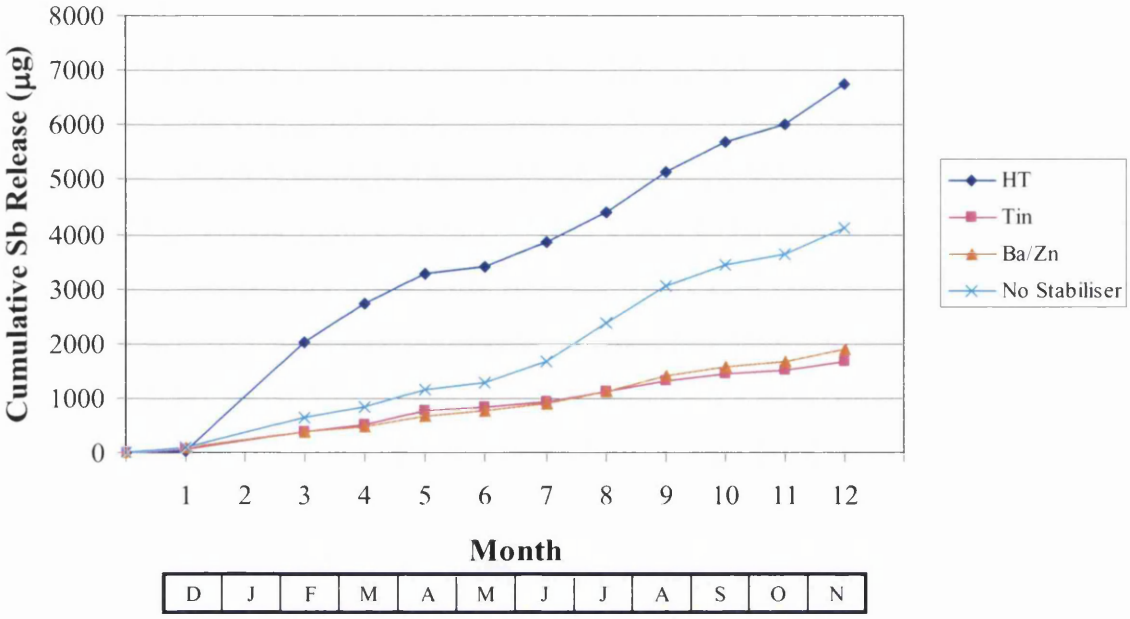

Figure 4.6 Cumulative Sb release (µg) per panel vs Stabiliser

The tin and barium stabilisers perform best with regard to Sb release however the levels at which it is leached out of the coating are consistently still way in excess of the allowed limit of 5ppb. Again the Sb is attributed to the PVC granules as none was added to the system during film preparation.

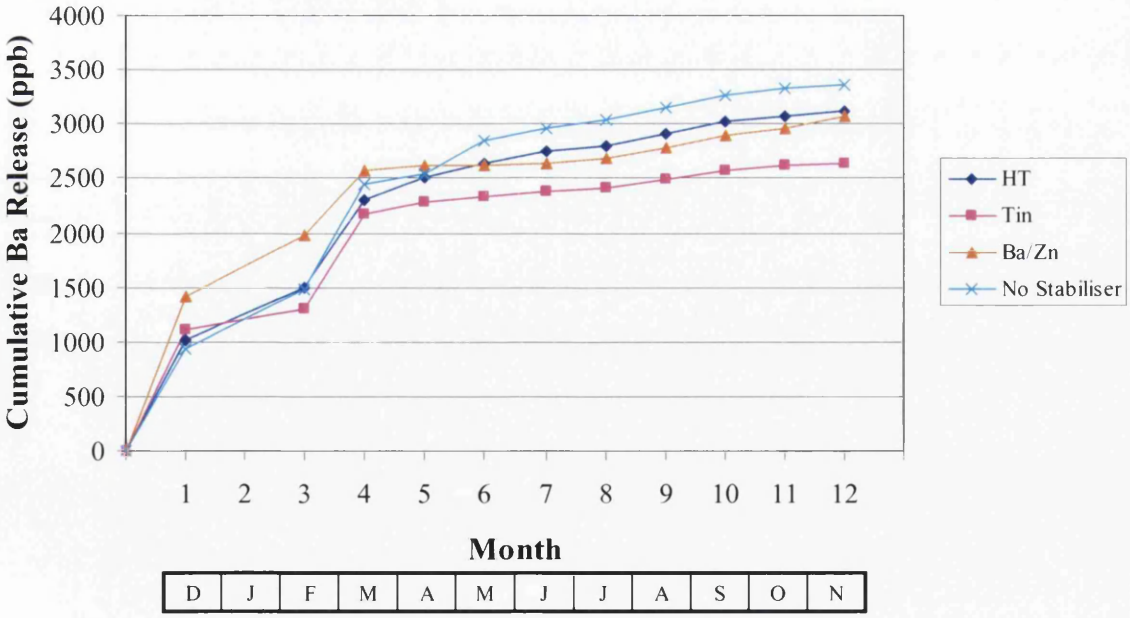

Figure 4.7 Cumulative Ba release (ppb) per panel vs Stabiliser type

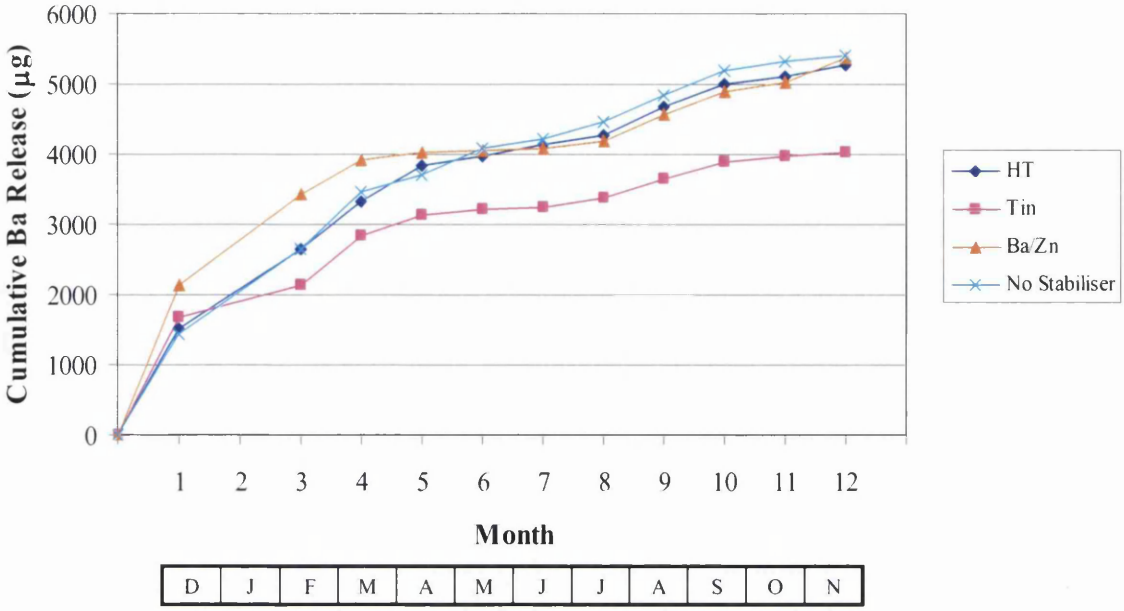

Figure 4.8 Cumulative Ba release (µg) per panel vs Stabiliser type.

When considering Ba release, Hydrotalcite and Ba/Zn perform fairly similarly with regard to total values released with 5257µg and 5383µg released respectively. This would suggest that HT stabilises the coating to a similar level of the Ba/Zn stabiliser. However similar to results shown for Sb release the tin stabiliser out performs all other stabilisers with regard to minimizing heavy metal release. This in itself is an issue as the tin based stabilisers were superceded by the barium/zinc due to environmental concern, however due to ever tightening environmental legislation barium based stabilisers are now under scrutiny and research is ongoing to find sufficient replacements. Hydrotalcite (HT) is one such replacement and from the results gained from natural exposure it is seen to show significant promise with regard to maintaining photo-stability when comparing it to current stabiliser chemistry. High Ba and Sb release from HT stabilised samples maybe attributed to a change in the surface properties of the system due to the addition of HT as a solid thereby increasing the solid content from 14 per hundred resin (PHR) to 19 PHR.

4.2 Effect of HT stabilisation on physical properties of organic coatings

Photo-degradation of PVC yields mineral oxidation products such as CO_2 [7,8] and potentially, HCl. Stabilisation against de-hydrochlorination is important, as the loss of HCl leads to the generation of poly-ene sequences that cause discolouration[8]. This is undesirable from both an aesthetic and performance point of view. Samples of the type investigated throughout this chapter were subjected to additional accelerated testing such as QUVA atmospheric testing for 750 hours using a cycle of 50% irradiation and 50% dark condensation under a standard test regime (8 light hours followed by 4 dark hours and condensation cycle). This testing method enables the gloss values taken before testing to be compared to those after the testing cycle as a value of gloss retention. The percentage gloss retention after 750hrs for each stabiliser type is shown in Figure 4.9. It is clear to see the different effect of each stabiliser type.

Hydrotalcite performs outstandingly in this instance, retaining 76% of it gloss after testing. The tin and barium stabilisers follow, retaining 22% and 6% respectively. Interestingly the sample with no additional stabilisation out performed the barium stabilised sample. This is more likely to be down to excess chalking of the TiO_2 which would reflect light more readily. The performance of the hydrotalcite could be attributed to a combination of stabilisation against degradation and the fact that it is the only stabiliser added to the system as a solid, therefore providing physical shield to UV light as well as chemical stabilisation.

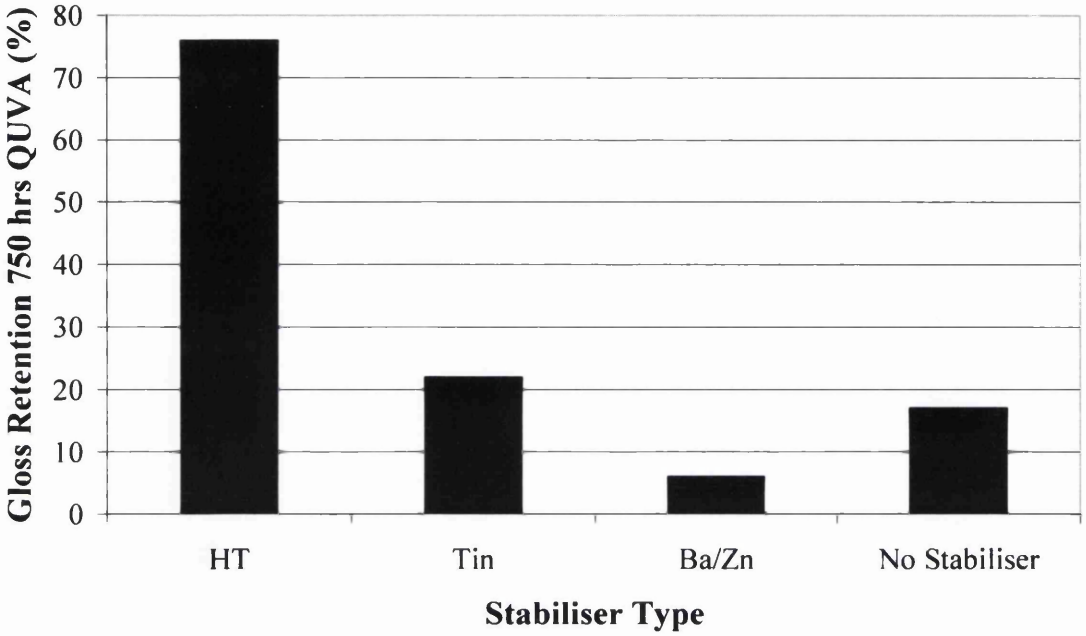

Figure 4.9 Gloss retention following QUVA testing for 750 hours for near commercial paints pigmented with photoactive titanium dioxide (K1001).

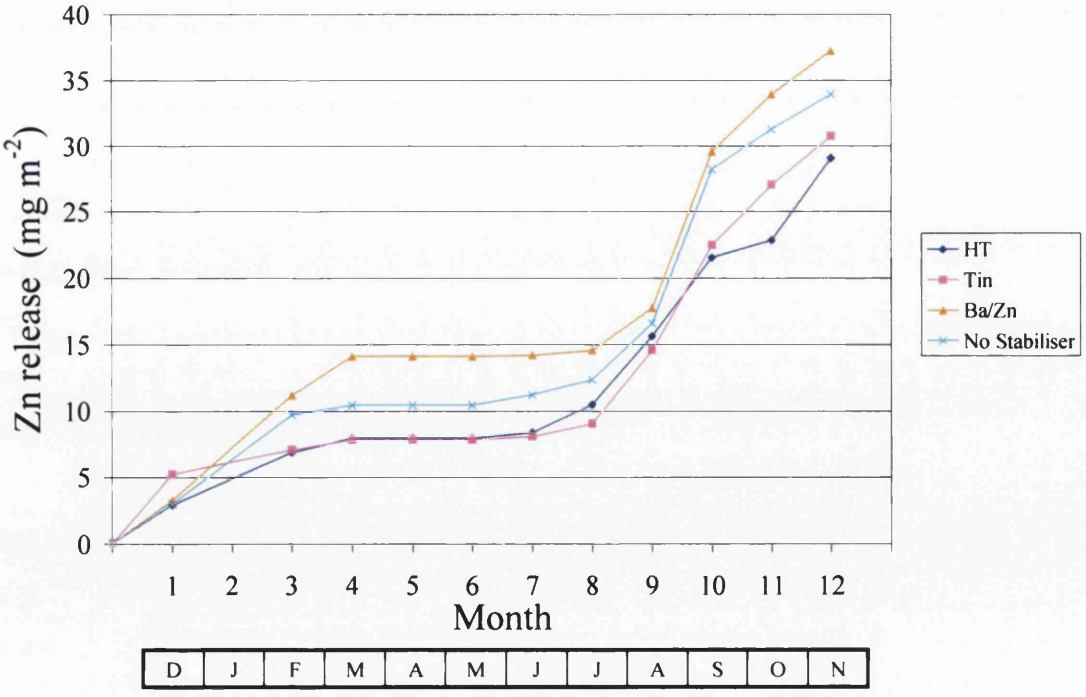

Figure 4.10 Cumulative zinc release from stabilised near commercial paints.

Figure 4.10 shows the cumulative zinc release from the panels throughout 12 months external exposure. It can be seen by looking at the final values of the zinc release that they follow the rank of the gloss retention results. This is shown below in Figure 4.11.

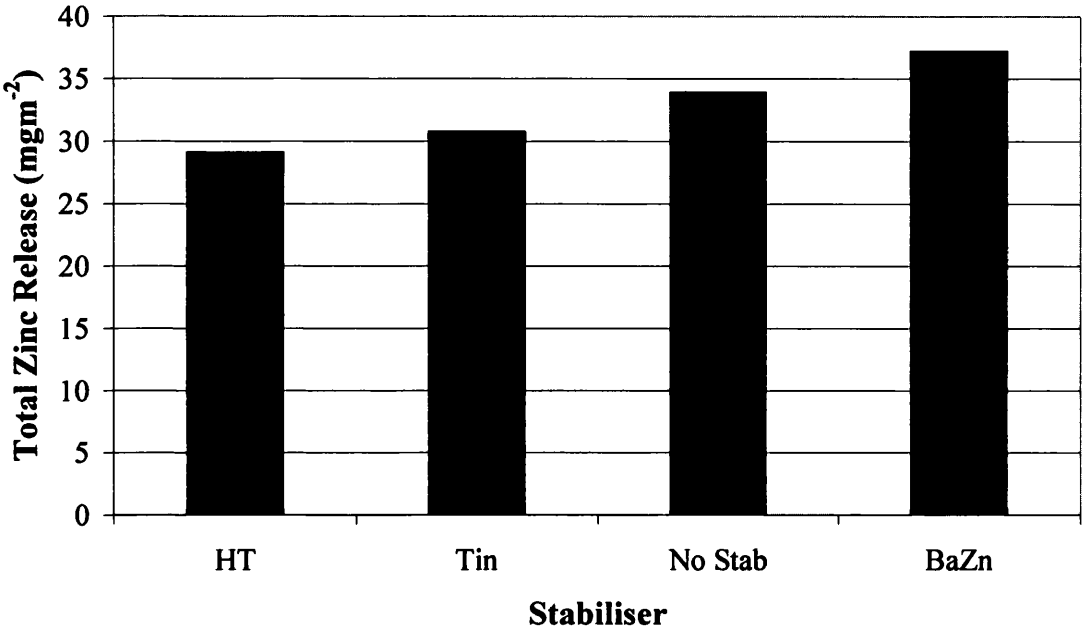

Figure 4.11 Total zinc release for each stabiliser type after 12 months natural weathering at the Port Talbot (Industrial Marine) site.

Hydrotalcite is again determined the best performer as it released the least total zinc over the exposure period. While the barium stabilised sample again performed least favourably. This correlation between gloss retention and total zinc release is shown graphically in Figure 4.12. It is this correlation between metal ion release and physical performance that suggests zinc release could lend itself as a reliable indicator for long term coating performance from accelerated testing.

Further to this, it is possible to assess coating stability in terms of actual colour change versus gloss retention. The actual colour change experienced by the coatings was determined after 1 year exposure following cleaning of the panels to remove chalking. Again, it should be emphasised that these coatings were made deliberately unstable by inclusion of an active grade of TiO_2. To this end we have used gloss retention values

inclusion of an active grade of TiO_2. To this end we have used gloss retention values gained from accelerated QUVA testing and have not quoted gloss retentions from natural weathering since these were all similarly reduced as a result of heavy chalking.

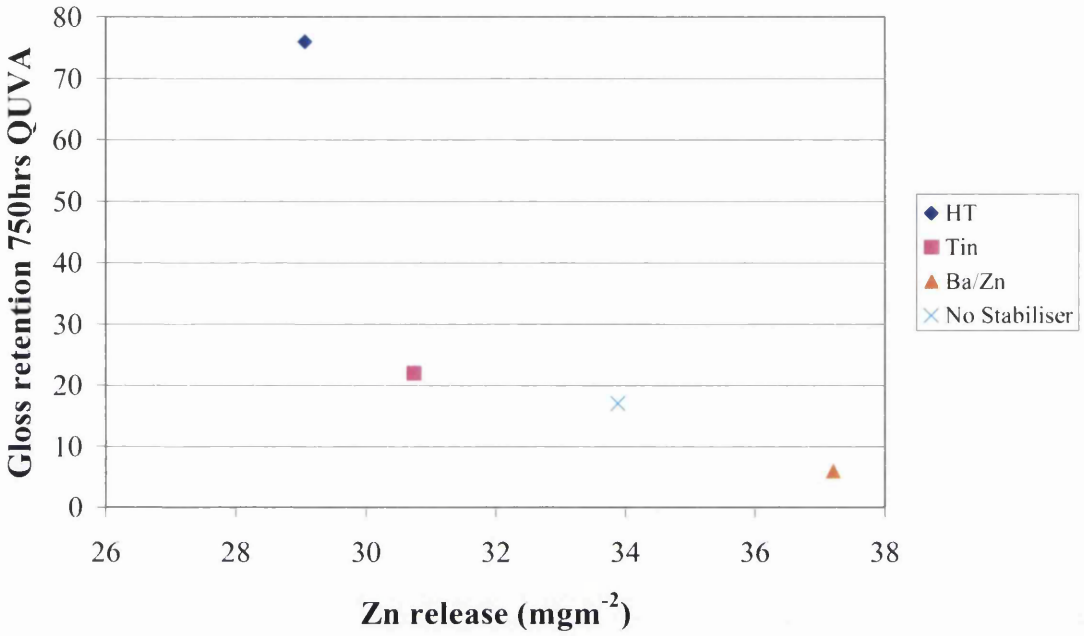

Figure 4.12 Gloss retention (750 hrs QUVA) vs Total Zinc release (12 months natural weathering at the Port Talbot (Industrial Marine) site).

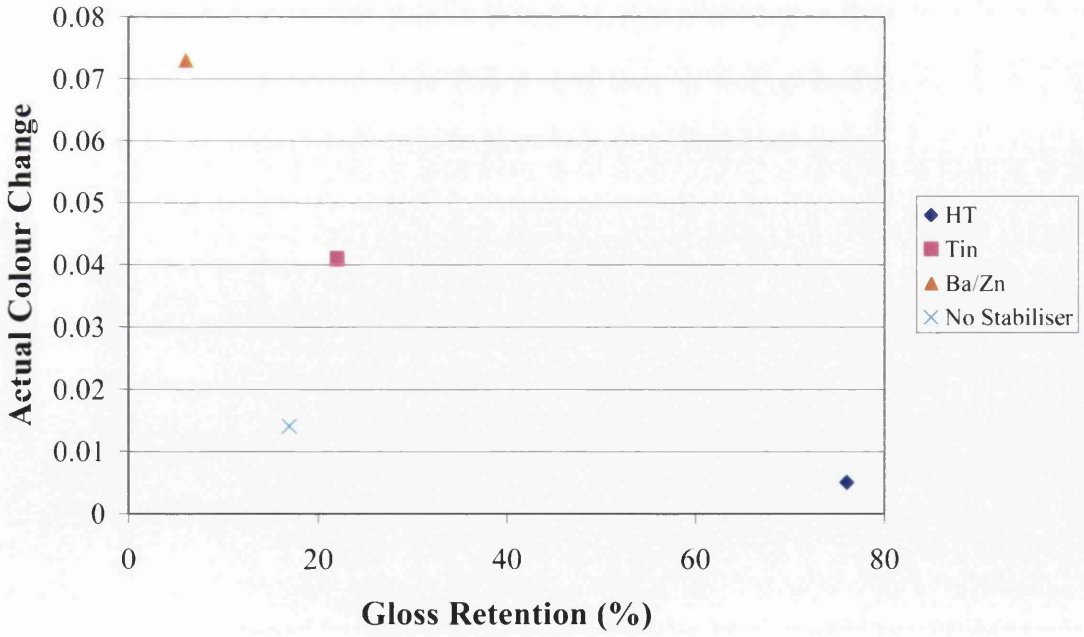

Figure 4.13 Relationship between actual colour change (12 months natural weathering at the Port Talbot (Industrial Marine) site) and Gloss retention (750 hrs QUVA).

Figure 4.13 shows reasonable continuity in the performance of stabiliser type with respect to colour change and gloss retention. Hydrotalcite is shown once again to perform the best, followed by the tin stabilised sample, while the Ba/Zn stabilised sample exhibits the worst performance, giving the highest colour change and lowest gloss retention. The sample with no stabiliser has proved yet again to be the anomaly of the set, giving a lower than anticipated colour change.

When comparing actual colour change to total zinc release from external exposure, as shown below in Figure 4.14, there is again a reasonable indication that the zinc runoff is an indicator of overall product stability.

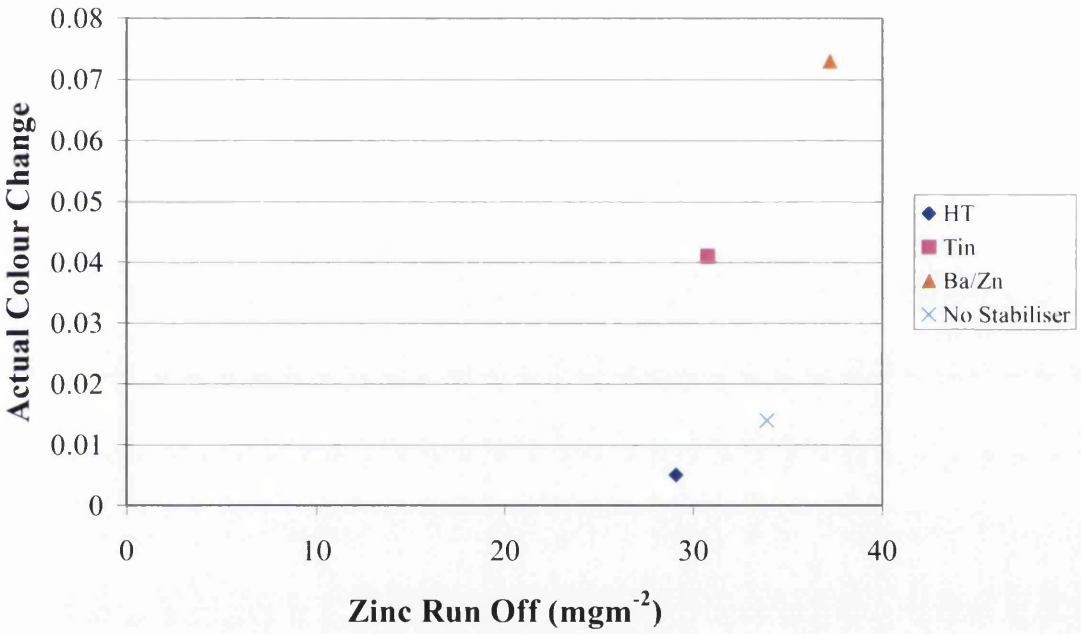

Figure 4.14 Relationship between the actual colour change (determined from the coating reflectance spectrum following 12 months natural weathering) and total zinc release (12 month external weathering at the Port Talbot (industrial marine) site).

The performance ranking of the tin, Ba/Zn and HT stabilisers are shown in Figure 4.15 for all of the tests on model systems performed and existing data concerning CO_2 release data from model unplasticised PVC coatings[2]. It is clear that the HT is the best performing pigment with the Ba/Zn system generally being the worst. The only metal ion

which relates to the photostability ranking is zinc with other metals appearing to be unrelated to the overall product photostability. The ranking from zinc release correspond to that of all the accelerated testing methods used.

Data from previous workers [2,8] using CO_2 release from PVC films is used below to illustrate the relationship between metal release and accelerated testing methods. The test, using a rapid flat panel reactor is an established way of predicting short term performance of unplasticised PVC films and the technique is covered in detail in the literature[8]. The test is usually over 24 hrs and as such provides a good reference point for comparison against longer term testing methods. Ranking of the sample for each test is represented by the value on the axis, 1 being the best performing and 3 the worst. Ultimately the smallest area around the origin corresponds the best performing stabilizer.

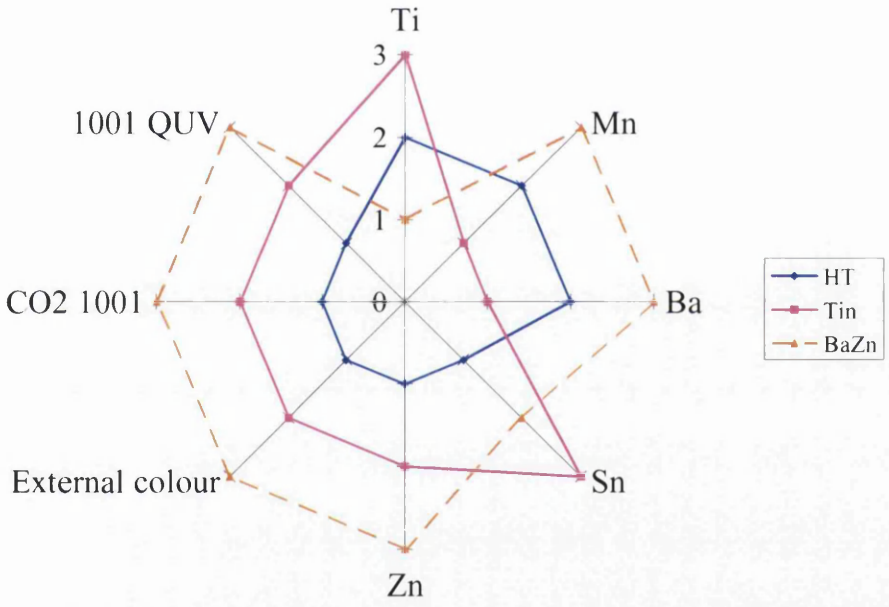

Figure 4.15 Performance ranking of the different stabiliser systems in the flat panel[9] reaction (CO2 1001), QUVA testing (1001 QUV), and external exposure (External colour) and in terms metal ion released into rainwater.

4.3 Conclusions

This work has demonstrated that in model PVC plastisol paints pigmented with active and stabilised TiO_2, Hydrotalcite is an excellent potential stabilising additive to

remove the damaging effects of dehydrochlorination. It is thought that Hydrotalcite stabilises the PVC matrix by removing hydrochloric acid (through chloride exchange) and replacing it with carbonic acid. In all testing of near commercial formulated paints with active TiO_2 Hydrotalcite provides a greater level of protection than the current commercial stabiliser systems for these white pigmented materials. This highlights the important role that the environmental production of hydrochloric acid in particular within the painted systems has on product stability. There are many metal ion species detected in the runoff from the painted products but the only one that seems to relate closely to photostability of the paint, and is thus an ionic marker, is zinc. Whether this zinc is of substrate or coating origin cannot be defined at this point, however the fact that Ba does not fit the same trend would indicate the former is perhaps more likely.

Hydrotalcite has produced impressive results when considering the stabilisation of physical or aesthetic properties; however the work in this chapter has highlighted the worth of monitoring the external run off from organic coated strip steel products, and the importance of knowledge of the ingredients. Increasingly strict environmental constraints are placing great pressure on the release of heavy metals into surrounding ecosystems. It appears that of all the stabiliser types investigated none produce predictable results with regard to the release of metallic species, excluding zinc. This is also important when considering the potential use of these systems for water recovery for human consumption. There are vast areas of organic coated strip steel products cladding anything from schools to warehouses in a variety of environments. It is not unreasonable to suggest that in these quantities; commercially stabilised systems have the potential to release significant amounts of metallic ions into the surrounding environment.

To this end it is advisable that along with constant monitoring of paint ingredients for heavy metals, external weathering continues to play an important part in the testing of novel or existing coating formulation.

4.4 References

1. POSPISIL, J., NESPUREK, S., 'Photostabilization of Coatings. Mechanisms and Performance', Progress in Polymer Science, vol. 25, 2000.

2. MARTIN, G., 'The Stabilisation of PVC Plastisiol Using Hydrotalcite (HT)', EngD Thesis, University of Wales, Swansea, 2007.
3. WATSON, T. M., 'Corrosion Mechanisms and Inhibition on Organic Coated Packaging Steel', EngD Thesis, University of Wales, Swansea, 2004.
4. LOVERIDGE, M., WORSLEY, D. A., McMURRAY, H. N., 'Chrome Free Pigments for Corrosion Protection in Coil Coated Galvanised Steels', Vol. 41, No. 3, Corrosion Engineering Science and Technology, 2006.
5. VACCARI, A., 'Clays and Catalysis: A Promising Future', Applied Clay Science, vol. 14, 1999.
6. PENNEY, D., 'The Study of Galvalloy® Coated Steels Using Metallographic and Scanning Electrochemical Techniques', EngD Thesis, University of Wales, Swansea, 2006.
7. ELVINS, J., 'The Relationship Between the Microstructure and Corrosion Resistance of Galfan Coated Steels', EngD Thesis, University of Wales, Swansea, 2005.
8. ROBINSON, A. J., SEARLE, J. R., WORSLEY, D. A., 'Novel Flat Panel Reactor for Monitoring Photodegradation', Materials Science and Technology, vol. 20, 2004.

Chapter 5

Analysis of run off from Zinc/Aluminium galvanised steels

5.0 Introduction

In order to improve the overall performance of organic coated strip steels (OCS) it is necessary to consider the metallic coated substrate as well as the topcoat. To this end a number of different galvanised samples have been obtained and subjected to natural weathering (as outlined in Chapter 2) for a period of 12 months.

Metallic coatings have long been used as a method of preventing corrosion. This is due to the fact that they protect the coating in two ways. Firstly as a physical barrier coating and secondly, in the case of Zinc coating on steel, as a sacrificial layer that corrodes preferentially keeping the substrate intact. There are numerous Zn based galvanised coatings available for a variety of different uses within industry. Presently Zn-Al coatings are the most important from a commercial point of view, superceding conventional hot dip galvanised steel (HDG) that was used previously. Of these Zn-Al alloys, Galfan/Galvalloy® (~5wt% Al) is the most important for the purposes of this study. Other Zn-Al coatings of significance include Galvalume/Zalutite (55wt% Al) along with conventional HDG. Each of these samples will perform differently with regard to weathering. The weathering performance of coated systems has been assessed previously and has proved to be a useful tool with regard to predicting coating performance.

The aim of this chapter is to assess the weathering performance of surface sections of bare galvanised strip steel. Coating weight and coating type will provide comparison points over a years testing period. ICPMS will be used to determine metal ion levels in rainfall run off water at the end of each month. The data will then be compared retrospectively to existing electrochemical performance data.

5.1 Results and Discussion

A series of Galvalloy® panels were obtained from a line trial at Corus' Shotton works at Deeside. The coating weights across the sample field have been varied and are outlined in Table 5.1 below. The coating weight is adjusted by changing the air knife pressure above the dipping pot whilst keeping the line speed constant. Additional samples of non chromated HDG and Zalutite were included in the scope of the experiment.

Sample Type	Coating Thickness (gm^{-2})	Sample ID
Galvalloy	120	120G
Galvalloy	150	150G
Galvalloy	200	200G
Galvalloy	255	255G
Galvalloy	300	300G
Galvalloy	325	325G
Non-Cr HDG	280	HDG
Zalutite	~ 250	ZAL

Table 5.1 Sample matrix for natural weathering at Port Talbot weathering site.

5.1.1 Effect of coating weight on the weathering performance of Galvalloy coated steels

Each of the panels outlined in Table 5.1 above were cut into sections and cut edges and back face were sealed as outlined previously in Chapter 2. This meant that a surface area of 0.015m^2 was achieved for exposure in the leachate collection vessel (LCV).

When considering the weathering performance of the samples it is perhaps favourable to consider the difference in coating weight as the first comparative variable. For this analysis only the Galvalloy coatings shall be considered. Figure 5.1 shows the monthly level (ppb) as analysed by ICPMS.

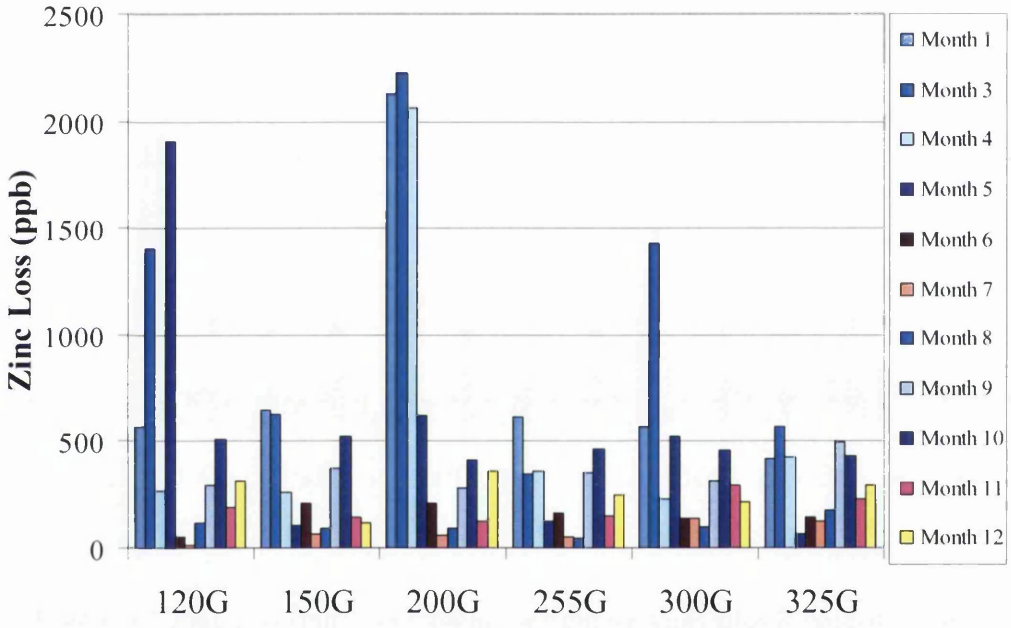

Figure 5.1 Monthly runoff level (ppb) vs Coating weight for Galvalloy® coated steels.

In Figure 5.1 it is seen that an initial burst of zinc release is seen during the first two months of exposure. This is followed across the sample field by a drop off in release through the middle period of the exposure. From a pure concentration value there are three coating weights that show comparable performance. These are 150G, 255G and

325G, with maximum levels of 647, 615, 569 ppb respectively. All other samples show inferior performance over the 12 month exposure period.

It may be difficult to differentiate between the overall performance of each of the coatings. This is because each sample has slightly different rainfall amounts and panel area, therefore, as monthly rainfall varies for the site a more realistic measure of corrosion each month is given by the metal runoff per square metre of panel exposed. This is shown in Figure 5.2.

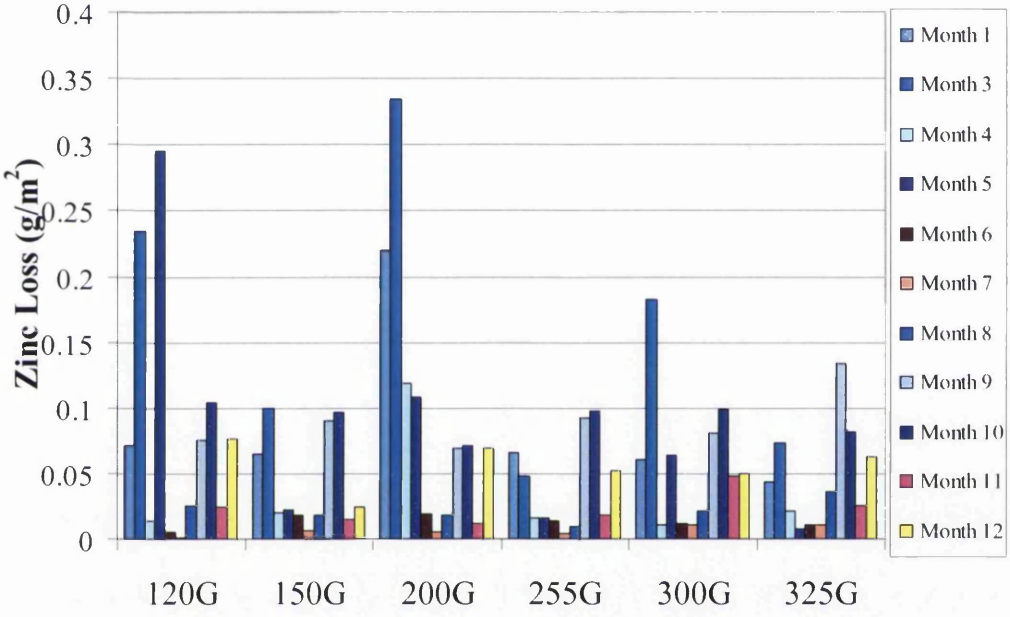

Figure 5.2 Zinc loss (gm^{-2}) vs Coating weight for Galvalloy® coated steels.

Figure 5.2 gives a more absolute comparison with regard to zinc release from the sample field. From this it is possible to identify 255G as the best performer. Sample 150G is close behind while 325G is shown to have the worst performance out of the samples identified as having close performance in the previous figure concerning ppb values. Of the other samples 120G and 200G look to have the worst performance. In the case of the thinner coating (120G) this could be attributed to the removal of aluminium

rich liquid as discussed later, thereby raising the primary zinc volume fraction and possibly exposing more at the surface.

The amount of rainfall will influence the amount of zinc that is released into the environment. Due to its sacrificial nature with regard to steel, zinc is bound to be released in a corrosive environment in varying levels. Large areas of bare galvanised steel such as roofs and safety fences at borders release zinc into the natural environment leading to contamination of the soil and therefore impacting the surrounding environment[1, 2]. The influence of rainfall on zinc release is shown in Figures 5.3.

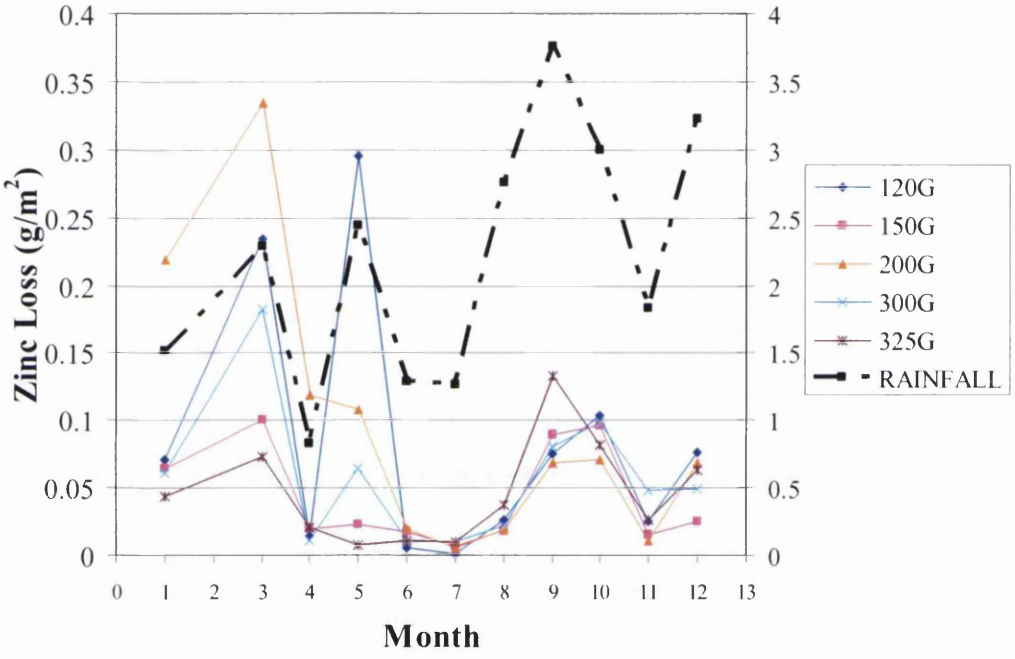

Figure 5.3. Monthly zinc loss levels Vs Average rainfall

It is clear that as with coated products, the level of rainfall does have a significant influence on metal release, in this case zinc. The peaks and troughs of the rainfall throughout the exposure period are generally reflected by the sample field.

In order to identify the best performing coating throughout the exposure period it is useful to consider the cumulative values finally giving a total value for zinc release from each of the coatings during the exposure period. Figures 5.4 to 5.6 show the

cumulative zinc release as a value of ppb, gm^{-2} and total zinc release gm^{-2}; while the overall coating rank is broken down in Table 5.2. This ranking will enable the identification of the coating that would potentially perform favourably if taken forward as a development for future consideration for use within the organic coated steels market.

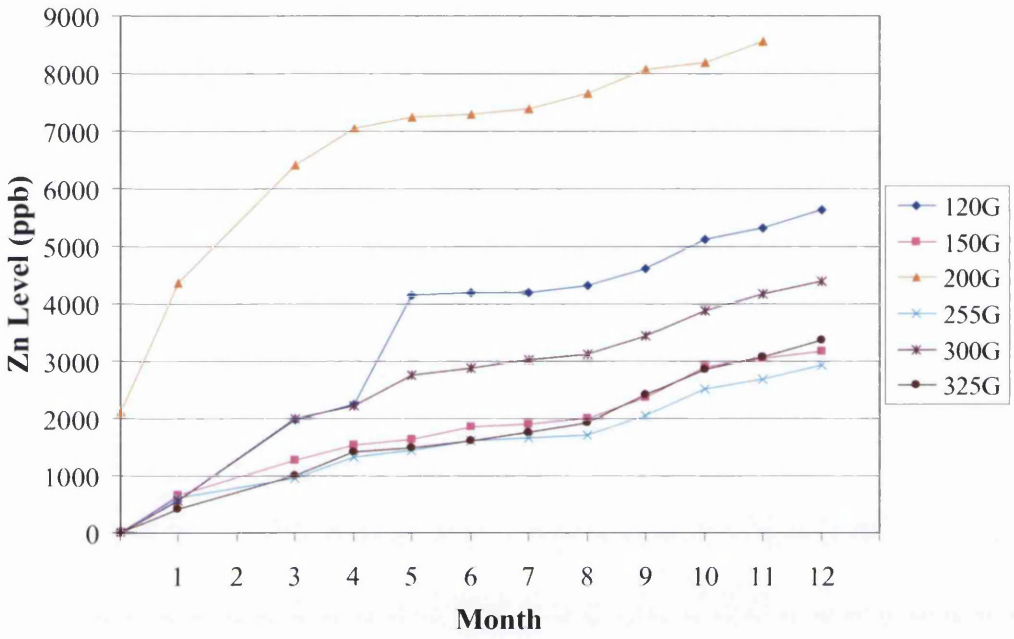

Figure 5.4 Cumulative zinc release (ppb) for each Galvalloy® coated steel.

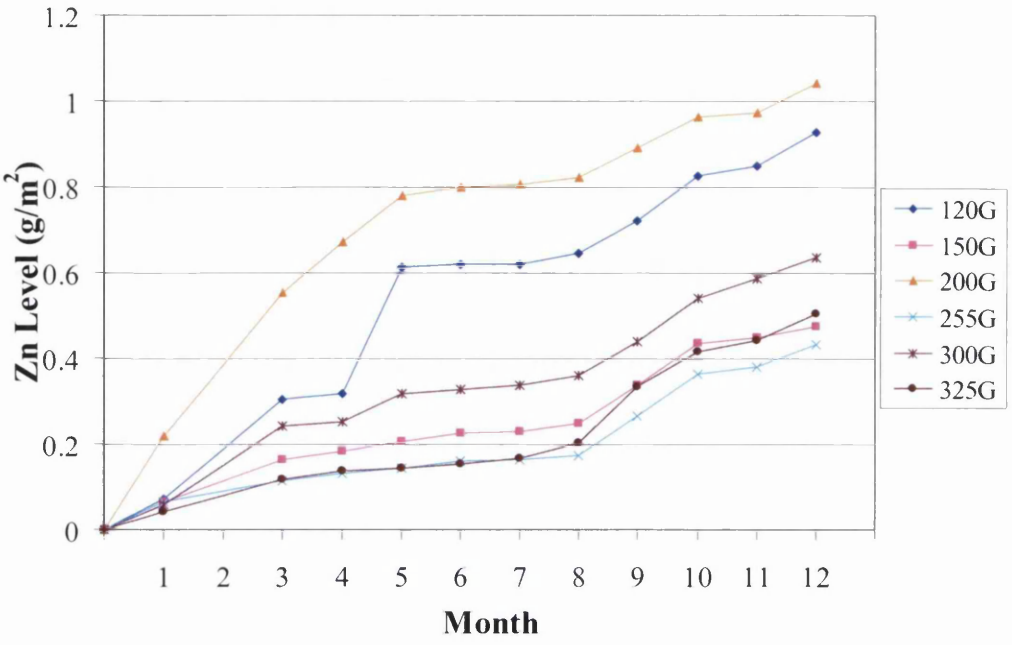

Figure 5.5 Cumulative zinc release (gm^{-2}) for each Galvalloy® coated steel

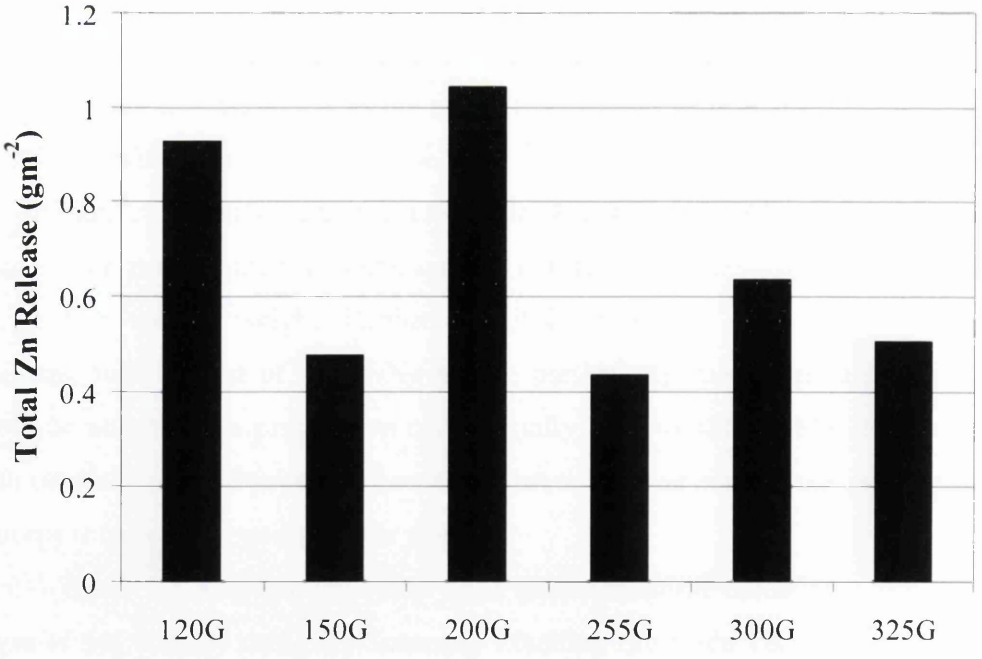

Figure 5.6 Total Zn release vs Galvalloy® coating weight.

Sample ID	Coating Weight (gm^{-2})	Total Zn Release (gm^{-2})	Cut Edge Zn Release (μg)	**Cut Edge Rank**	**Surface Rank**	**Overall Coating Rank**
120G	120	0.93	519	5	5	10
150G	150	0.47	469	4	2	6
200G	200	1.04	352	3	6	9
255G	255	0.43	332	2	1	3
300G	300	0.64	312	1	4	5
325G	325	0.51	N/A	N/A	3	N/A

Table 5.2 Coating rank with regard to total Zn release (gm^{-2})

From Table 5.2 it is possible to identify sample 255G as the best performing with regard to runoff. While 200G was the worst performing, releasing 1.04 gm^{-2} compared to the 0.43 gm^{-2}. Currently Corus run a Galvalloy® coating of ~265gm^{-2} and so these results suggest that performance in operation will not necessarily be adversely affected by this decrease in coating weight. Furthermore it is shown in Table 5.2 that even thinner coatings, such as that of the 150G sample particularly show similar performance this could be an attractive proposition commercially as it would provide economic relief in both raw material and processing cost without sacrificing commercial performance. This concept is to be discussed at a later stage.

Table 5.2 also contains data from electrochemical corrosion testing of the cut edges of the samples using the Scanning Vibrating Electrode Technique and a 5% NaCl solution. The testing method is in line with that explained in Chapter 2 (p75). Figure 5.2 shows the results of the cut edge corrosion testing[3].

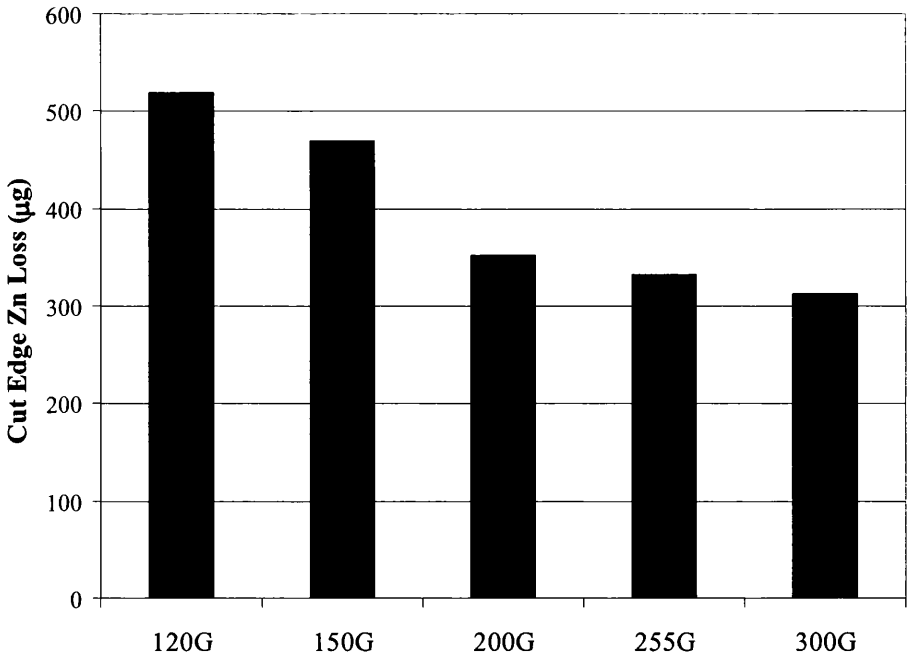

Figure 5.7 Cut edge Zn loss (SVET) vs Coating Weight[3]

The results shown in Figure 5.7 were obtained from accelerated testing using coated samples. It is seen that there is a significant increase in cut edge performance as the coating thickness increases. The sample with the thickest coating has the lowest corrosion rate and on referring back to Table 5.2, where the rankings are displayed, is shown that, while the 300G sample does perform favourably, it is the 255G sample that provides the best combined surface and edge protection against corrosion.

5.1.2 The effect of coating weight on the microstructure of Galvalloy® coated steels

Having identified that 255G is the best coating out of the sample field it is useful to try and understand the reasons for this. It is well documented[4] that adjusting the coating weight will affect the microstructure of the coating and since microstructure is shown to have significant influence on corrosion performance, it will have some bearing on the corrosion performance of the coatings.

Figure 5.8 shows the difference in microstructure of the thinnest coating (120G) against that of the 255G coating as obtained by D. Penney[3] from the same sample set.

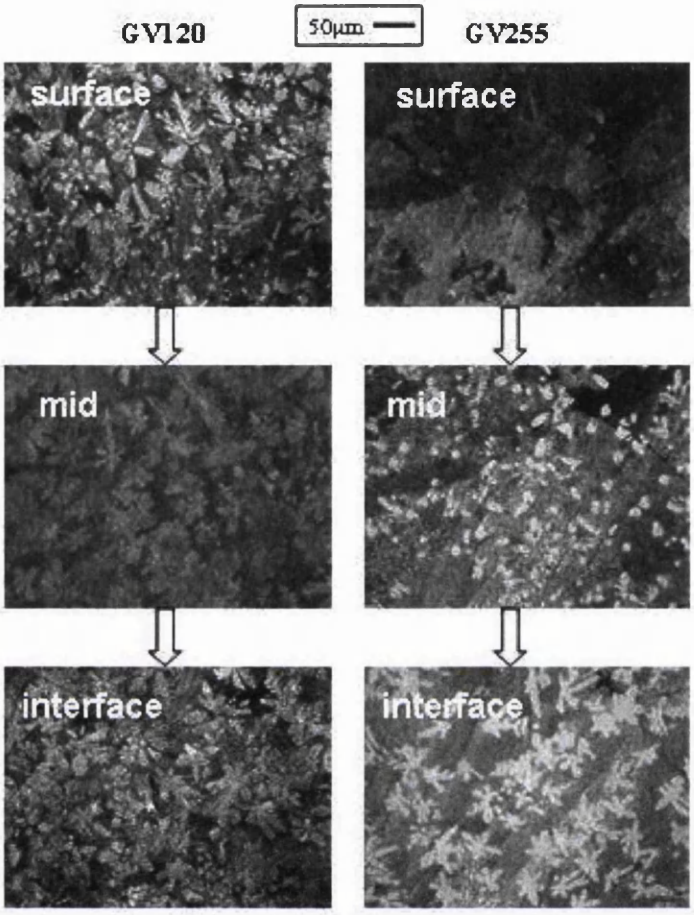

Figure 5.8. The difference in coating microstructure from surface to interface between thin (120G) and thicker (255G) Galvalloy® coatings.[4]

It can be seen from Figure 5.8 that there is a marked difference in the microstructure when comparing the thinnest coating (120G) and the thicker coating (255G). Perhaps the most obvious difference between the coatings occurs at the surface of the coating. A significant amount of primary zinc is seen visible at the surface compared to that of the thicker coating where there is none seen at all. Previous work[4] has postulated that this exposed primary zinc phase is due to the action of increased air

pressure of the air knives as the strip leaves the bath. This results in the removal of unsolidified liquid from the coating. This in turn leads to a quicker cooling time, and as all other processing conditions are kept constant this in turn will result in a higher nucleation rate[5] and ultimately a thinner coating. It has been observed[4] that the volume fraction of the primary phase increases during the production of thinner Zn/Al coatings. This is attributed to the fact that the liquid removed during passage through the air knives is aluminium rich as it is progressively rejected into the liquid. This leads to a change in coating composition by way of a decrease in aluminium content. The increase in nucleation rate is illustrated in Figure 5.8 as an increase in dendrite number through the coating, particularly at the interface.

5.1.3 Effect of galvanising type on the weathering performance of galvanised strip steel

The final stage is to compare the performance of the 255G sample that has a 255 g/m^2 coating weight to other commercial galvanised coatings that were tested such as HDG and Zalutite. Figures 5.9 and 5.10 show the cumulative values in ppb and gm^{-2} respectively for Zn release of 255G versus HDG and Zalutite.

In both cases it is shown that when compared to conventional HDG the 255G sample is far superior with regard to zinc release from the bare samples. Zalutite is shown to be the best performer. However the 255G sample shows comparable performance, especially when normalised against the rainfall level to give release in gm^{-2}. This is favourable as Zalutite is known to have excellent corrosion resistant properties, however with a view to use as part of a coated system, it is well documented that Zalutite does not lend itself favourably to over-coating so to find a sample that is shown to perform in a similar fashion is desirable.

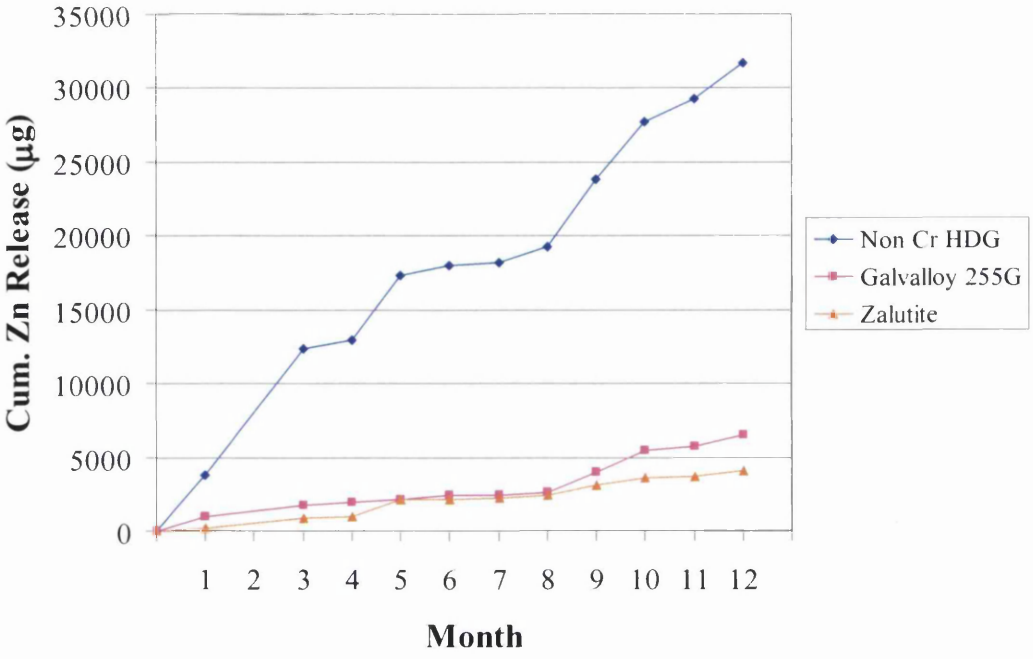

Figure 5.9 Cumulative Zn release (ppb) vs Substrate type.

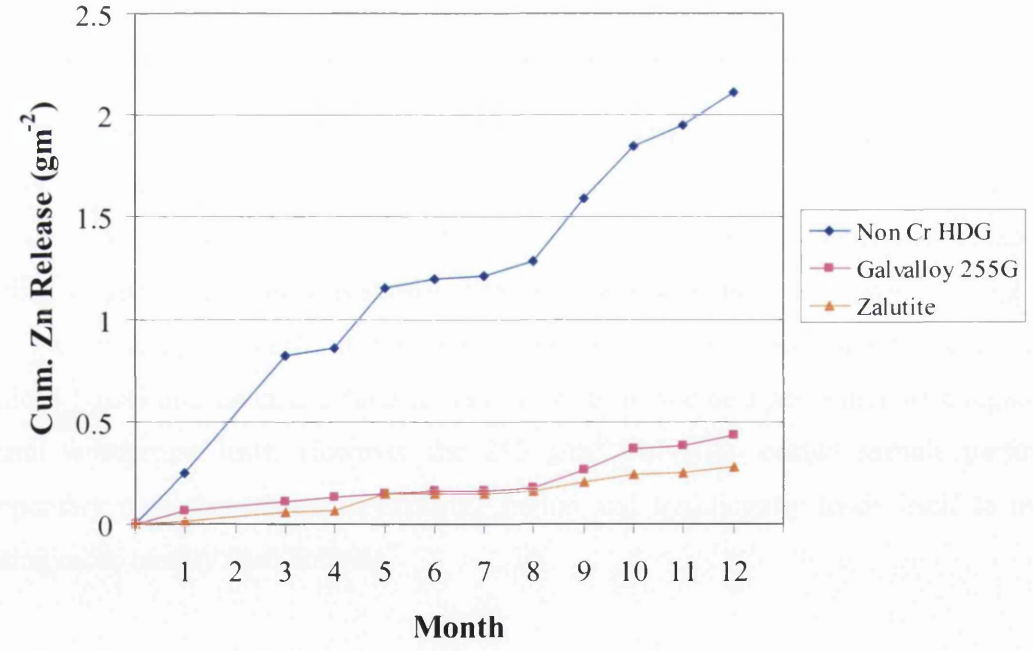

Figure 5.10 Cumulative Zn release (gm^{-2}) vs Substrate type.

5.2 Conclusion

The work in this chapter has shown that changing the thickness of a galvanised coating has a significant effect on both the microstructure and corrosion performance. All the samples were produced using the same parameters. The coating weight was controlled using variations in air knife power. This was shown to have two effects. Firstly, more dendrites of primary phase were present in the thinner coating suggesting a higher nucleation rate bought about by an increase in cooling rate. Secondly, primary zinc was seen to be present at the surface of the coating in the samples with thinner coatings.

This would suggest that the thinner coatings may have inferior corrosion performance than the thicker coatings. However weathering of surface samples of the coating showed that this was not clearly obvious. Thinner coatings (150G) marginally out performed thicker coatings (325G). While some thicker coatings (200G) performed worse than expected with regard to Zn release. It must be noted that these samples were exposed to a heavily industrial site and open to a natural environment. From these tests a coating weight of 255 g/m^2 was identified to provide optimum surface protection from corrosion.

On comparison with existing electrochemical test data for cut edge corrosion for the same sample field, it is clear that under the processing conditions specific to this trial, thinner coatings are poorer compared to the samples with thicker coatings. However after a ranking exercise it was shown that for combined surface and cut edge performance a coating weight of 255 g/m^2 was shown to exhibit the best result.

Comparing the performance of the 255 g/m^2 against other industrial galvanised coatings (HDG and Zalutite), Zalutite was shown to be the best performer with regard to natural weathering tests. However the 255 g/m^2 Galvalloy coated sample performs comparably over the 12 month exposure period and traditionally lends itself to over-coating more readily than Zalutite.

5.3 References

1. SCHRIEWER, A., HORN, H., HELMREICH, B., 'Timefocussed Measurements of Roof Runoff Quality', Corrosion Science, vol. 50, No. 2, 2008.
2. HE, W., ODNEVALL WALLINDER, I., VEIRBIEST, P., LEYGRAF, C., 'Effects of Exposure Direction and Inclination on the Runoff Rates on Zinc and Copper Roofs', Corrosion Science, vol. 42, 2000.
3. PENNEY, D., 'The Study of Galvalloy® Coated Steels Using Metallographic and Scanning Electrochemical Techniques', EngD Thesis, University of Wales, Swansea, 2006.
4. PENNEY, D., SULLIVAN, J., WORSLEY, D., 'Investigation into the Effects of Metallic Coating Thickness on the Corrosion Properties of Zn/Al Alloy Galvanising Coatings', Corrosion Science, vol. 49, 2007.
5. ELVINS, J., 'The Relationship Between Microstructure and Corrosion of Galfan Coated Steels', EngD Thesis, University of Wales, Swansea, 2005.

Chapter 6

The development of Galvanised coatings with improved corrosion performance

6.0 Introduction

The cost and competition for raw materials is always a consideration for every industrial organisation. Commercially there has been a significant drive to address the zinc content and coating thickness of the galvanised layer on strip steel products due to the fluctuations in zinc prices in recent years. Many additions have been suggested as providing benefit with regard to corrosion performance[1,2].Additions of ~4.5wt% Al to a zinc galvanizing bath are widely used in industry as they give rise to a highly durable protective metallic coating for strip steel with a distinct microstructure that has seen to have an influence on corrosion performance[3]. Research has shown that Al additions within the range of 4.5 - 10wt% give improved corrosion performance[4]. Increasing the Al level in the coating would inherently lead to less Zn being used. Is has been shown previously that increasing the Al content in galvanized coatings leads to an improved corrosion performance[4] but critically a similar microstructure to that seen in conventional Zn-Al coatings can still be achieved.

As discussed in Chapter 1, it should be noted that current commercial guarantees on external cladding for buildings are in the order of 40 years in some cases[5]. It is therefore important that any change in the system is to the benefit of the product such that the galvanised layer provides sufficient protection to the steel such that the cladding remains intact and fit for purpose.

In this chapter an investigation into the effect of microstructure and corrosion performance of Zn galvanized steels with Al levels over 4.8% Al is presented. The aims of this study are to assess how increasing the Al levels in a Zn-Al galvanised coating affect surface and edge corrosion performance and relate the finding to the microstructure observed. Optical microscopy and the Scanning Vibrating Electrode Technique (SVET) will be utilised for microstructural observation and corrosion testing respectively.

6.1 Increasing Aluminium levels in Galvalloy® Coated Steels

Test panels were produced via the Iwatani-Rhesca Hot Dip Simulator to achieve coating weights of ~265gm^{-2} giving a coating thickness of ~20μm. Batches of samples were produce with target Al levels ranging from 5% through to 6.1%. The samples to be tested in the bare state for accelerated tests and therefore no topcoat or pretreatment were necessary. Some of the samples were set aside for salt spray testing which will be discussed later. The Al levels of the samples obtained are shown in Table 6.1. In the text of the chapter the actual levels will be those referred to in terms of sample labelling.

Coating Thickness (μm)	Target Al Level (%)	Actual Al Level (%)
20	5	4.7
20	5.3	5.4
20	5.5	5.6
20	6.1	6.5

Table 6.1 Samples produced via HDS with increasing Al levels.

The microstructure will be influenced by a change in Al addition as indicated on consultation of the eutectic portion of Zn-Al binary phase diagram, shown in Figure 6.2. It is key to understand what effect this change in microstructure has on the corrosion performance of the sample group.

.

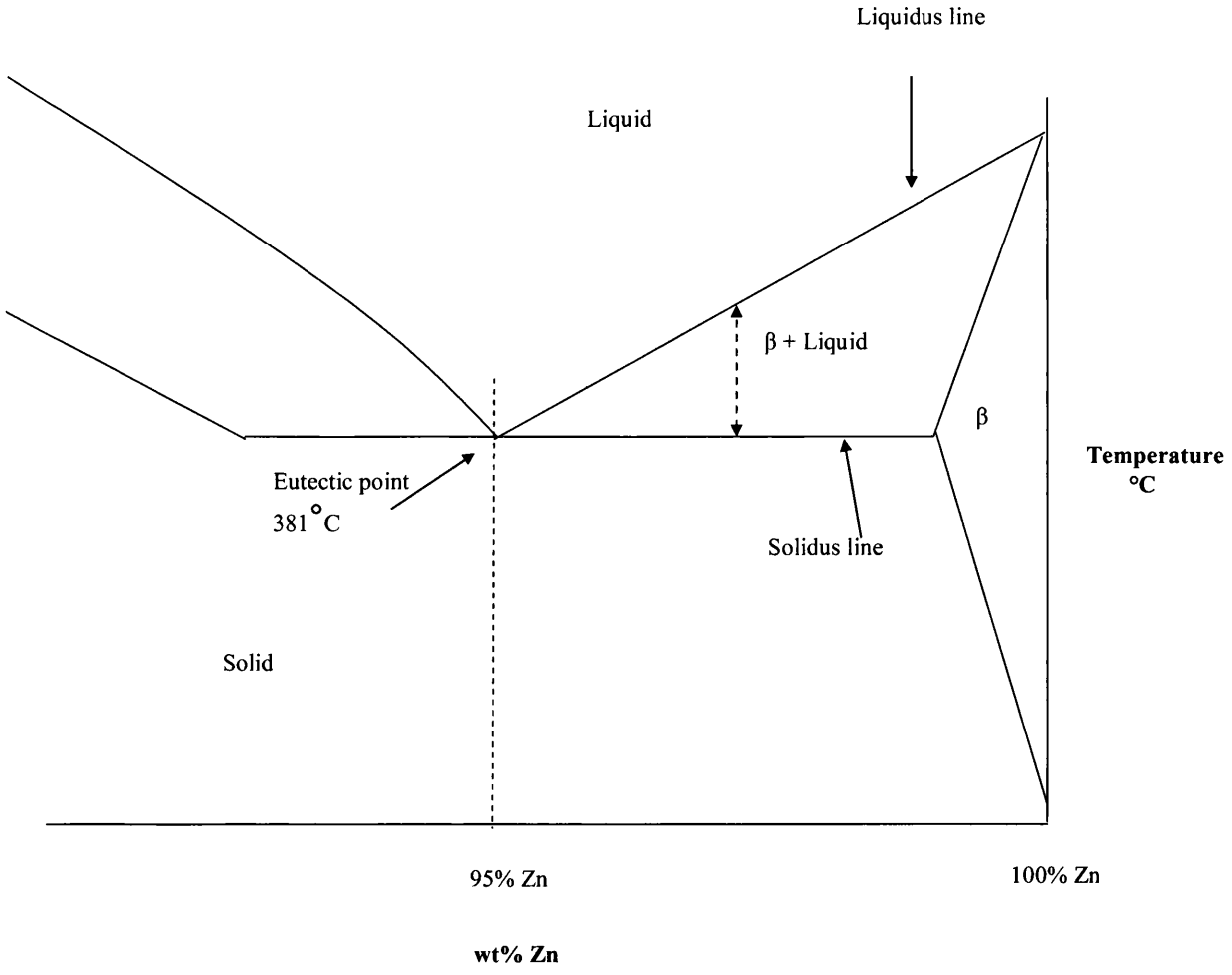

Figure 6.2 A schematic diagram of the Zn-Al binary phase diagram close to the Zn-Al eutectic point[6]

6.1.1 Effect of Al addition on microstructure

Figure 6.3 shows typical micrographs of the microstructure of a dipped coating as a function of depth. The images were obtained by systematic polishing through the coating. Following each polishing stage, the samples were etched using 1% Nital solution and observed using the Reichert MEF3 microscope as described earlier in Chapter 2 (p74). It is clear that close to the surface of the coating there is little or no primary Zn showing. The deeper into the coating the polish, the more primary zinc is exposed. The dendritic shape of the primary Zn becomes apparent, with the dendrites being surrounded

in an Al rich eutectic phase. This shows that the primary phase is the first to nucleate at or close to the substrate surface and the coating solidifies from the steel outwards.

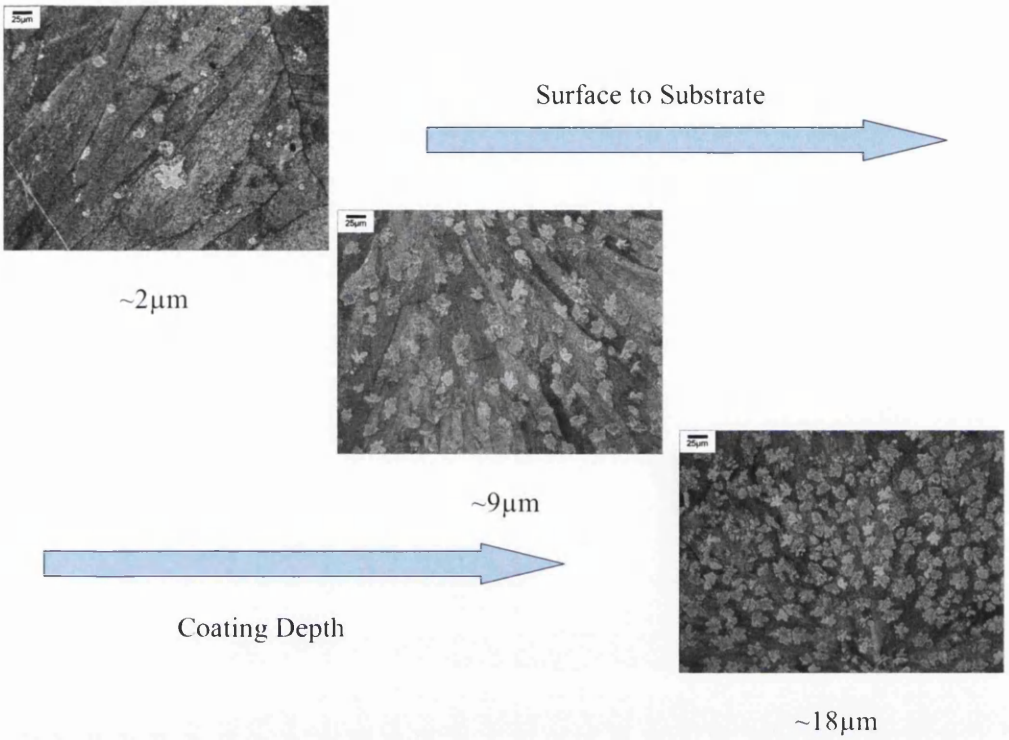

Figure 6.3 Typical microstructure as a function of depth.

Figure 6.4 shows the microstructure observed at the interface of the coating and the steel substrate for Al additions of 4.7wt%, 5.4wt% 5.6wt% and 6.5wt% respectively.

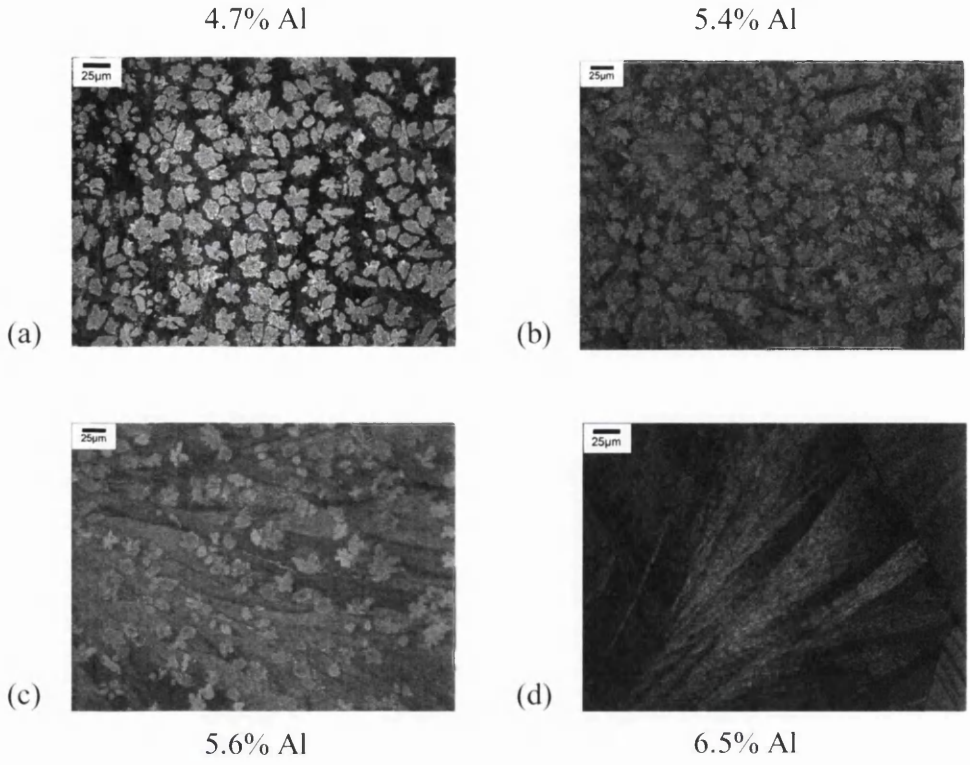

Figure 6.4 Microstructures at coating/substrate interface for hot dipped Zn alloy with increasing target Al additions.

From this it is possible to show the effect of Al addition on dendrite numbers and volume fraction. It can be seen that increasing Al content leads to a decrease in the amount of primary Zn phase in the coating to a point that at additions of 6.5% there is no primary phase present. This decrease in primary Zn phase is further shown in Figure 6.5 which shows the number of dendrites of primary Zn as a function of Al addition, where the dendrite number is taken from the substrate/coating interface. This is primarily due to the decrease in Zn in the system. However, the cooling conditions imposed by the Hot Dip Simulator are not equilibrium and these result in a shift of the eutectic composition to the left of the Zn/Al phase diagram. This also results in there being no primary Al present in the 6.5% Al coating. The correlation is again present when addressing the effect of Al addition on the total volume fraction of Primary Zn in the coating as a whole. This is illustrated graphically in Figure 6.6. Again, there is no primary Zn observed throughout

the 6.5% Al coating. This is at first sight rather strange in that one would anticipate the coating containing as close to 5% Al as being Eutectic. This effect is however related to the rapid non equilibrium cooling of the material which tends to lead to greater primary zinc formation at higher aluminium levels than expected from the phase diagram.

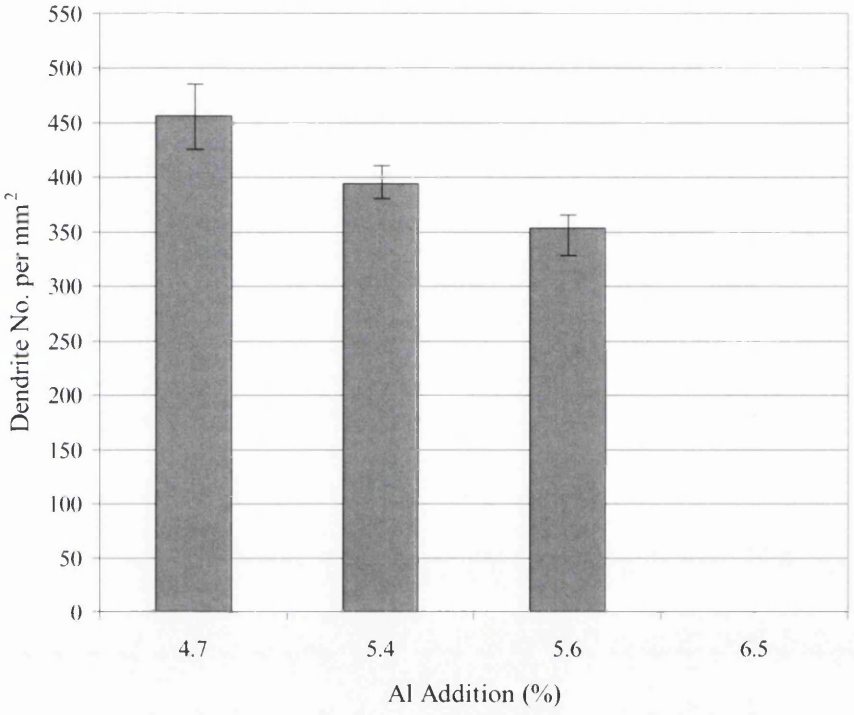

Figure 6.5 Dendrite No. at interface vs Al Addition. ERROR BARS AL Levels

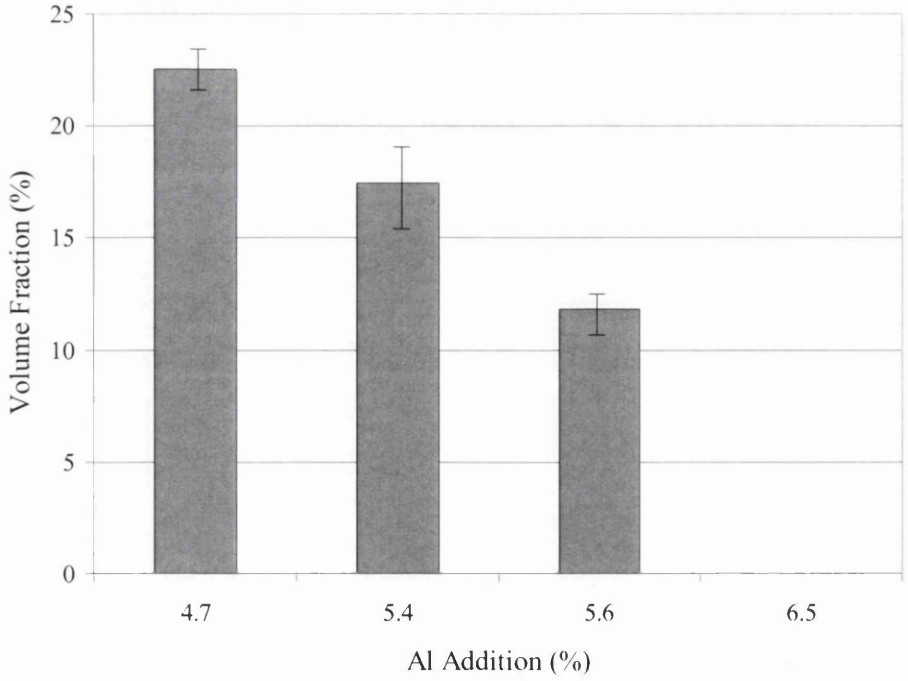

Figure 6.6 Total volume fraction of primary Zn vs Al addition ERROR BARS

6.1.2 Effect of Al addition on surface corrosion performance

Previous work has shown[7] that data gained by the SVET can be converted to give semi quantitative values for metal loss that occurs across the duration of the experiment. The results for average total Zn loss (TZL) for surface samples of each Al addition are shown in Figure 6.7.

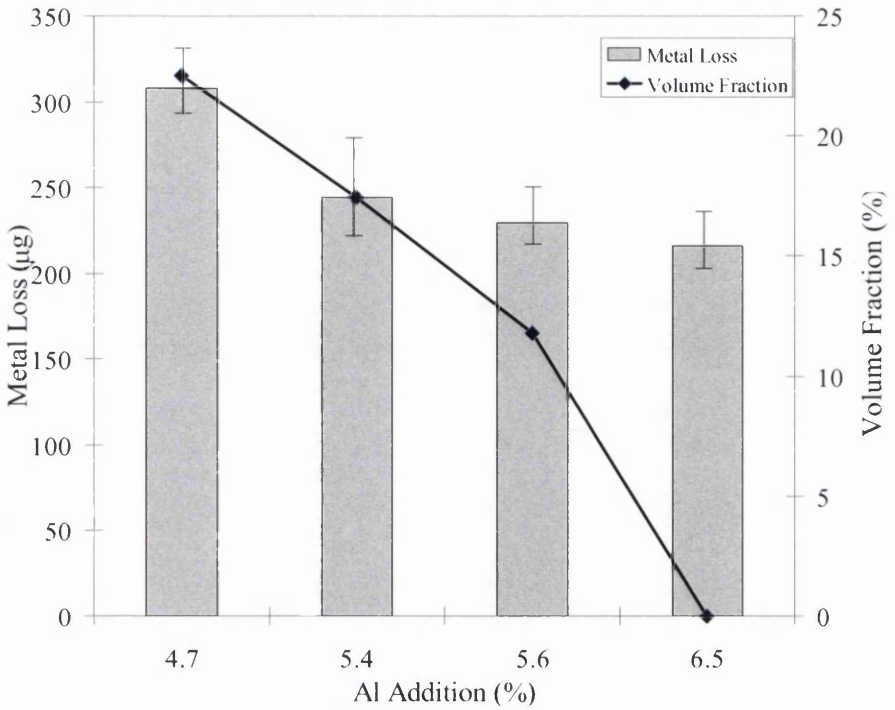

Figure 6.7 SVET total Zn loss and Volume fraction of primary Zn as a function of Al addition. Error Bars Al Levels

It is clear that on increasing Al addition Zn loss decreases in line with the volume fraction and therefore the corrosion performance is improved. If these results are related back to the microstructures observed in Figure 6.4 it appears that the corrosion rate determined for the 6.5% Al sample is the corrosion rate of the eutectic itself since there are no primary phases in these samples. This is potentially the minimum corrosion rate possible using the binary alloy at this composition. The corrosion rate clearly increases as a function of the primary zinc phase that is present. At 6.5% Al the main corrosion mechanism will be dezincification of the eutectic and this could be detriment of the integrity of any organic topcoat layer that may be applied subsequently as it would involve zinc loss from close to the organic layer whereas with primary phase present zinc loss is concentrated more closely to the steel substrate on which the primary phase nucleates.

SVET corrosion maps of surface scans from samples tested for 24 hours in 0.1% NaCl are shown in Figures 6.8-6.11, here anodic activity is shown as a function of immersion time and provides a useful visual medium to illustrate the difference in corrosion performance with regard to increasing aluminium addition.

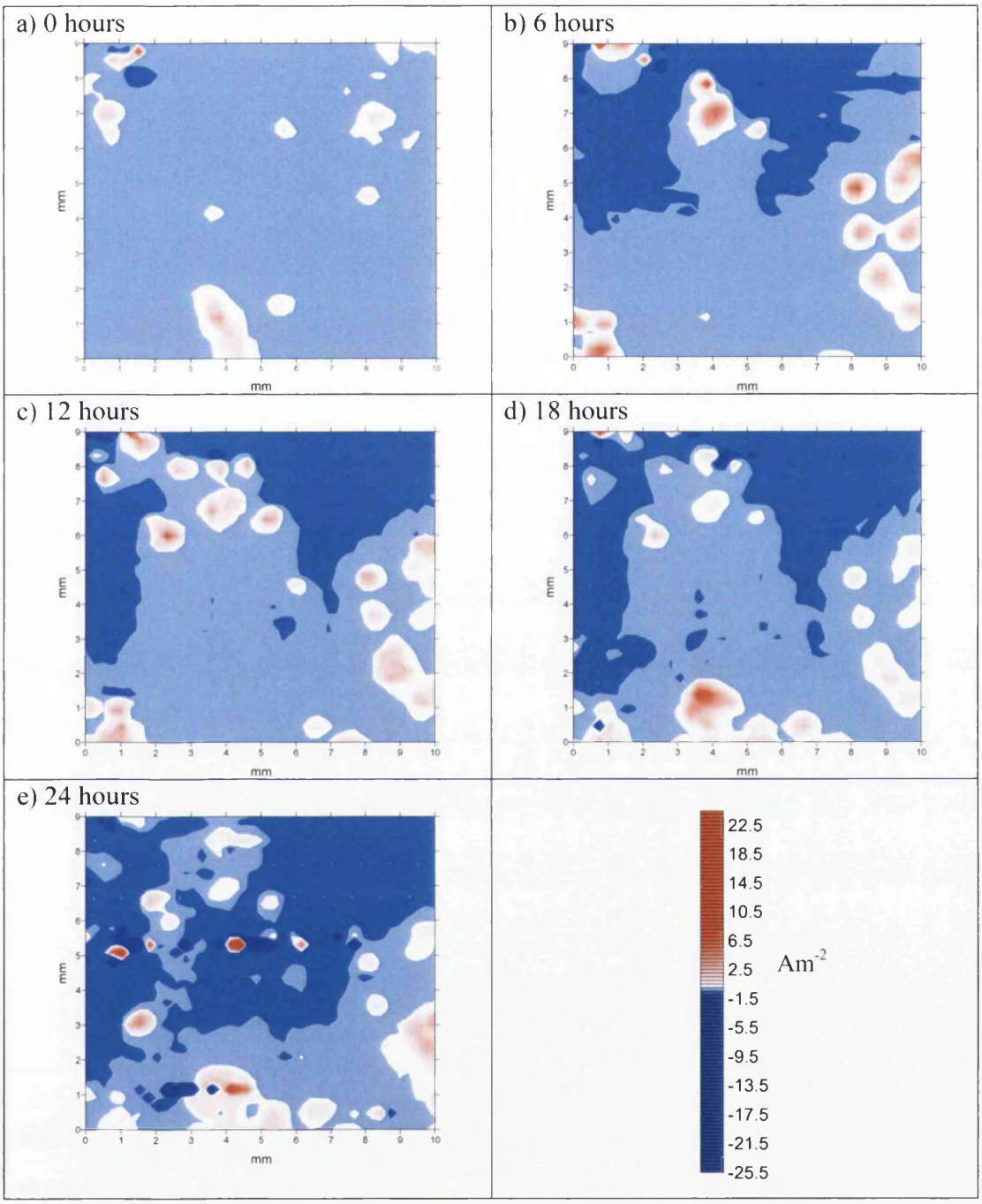

Figure 6.8 SVET corrosion maps for a 4.7% Al addition showing the anodic activity (red) as a function of immersion time. Please note scale.

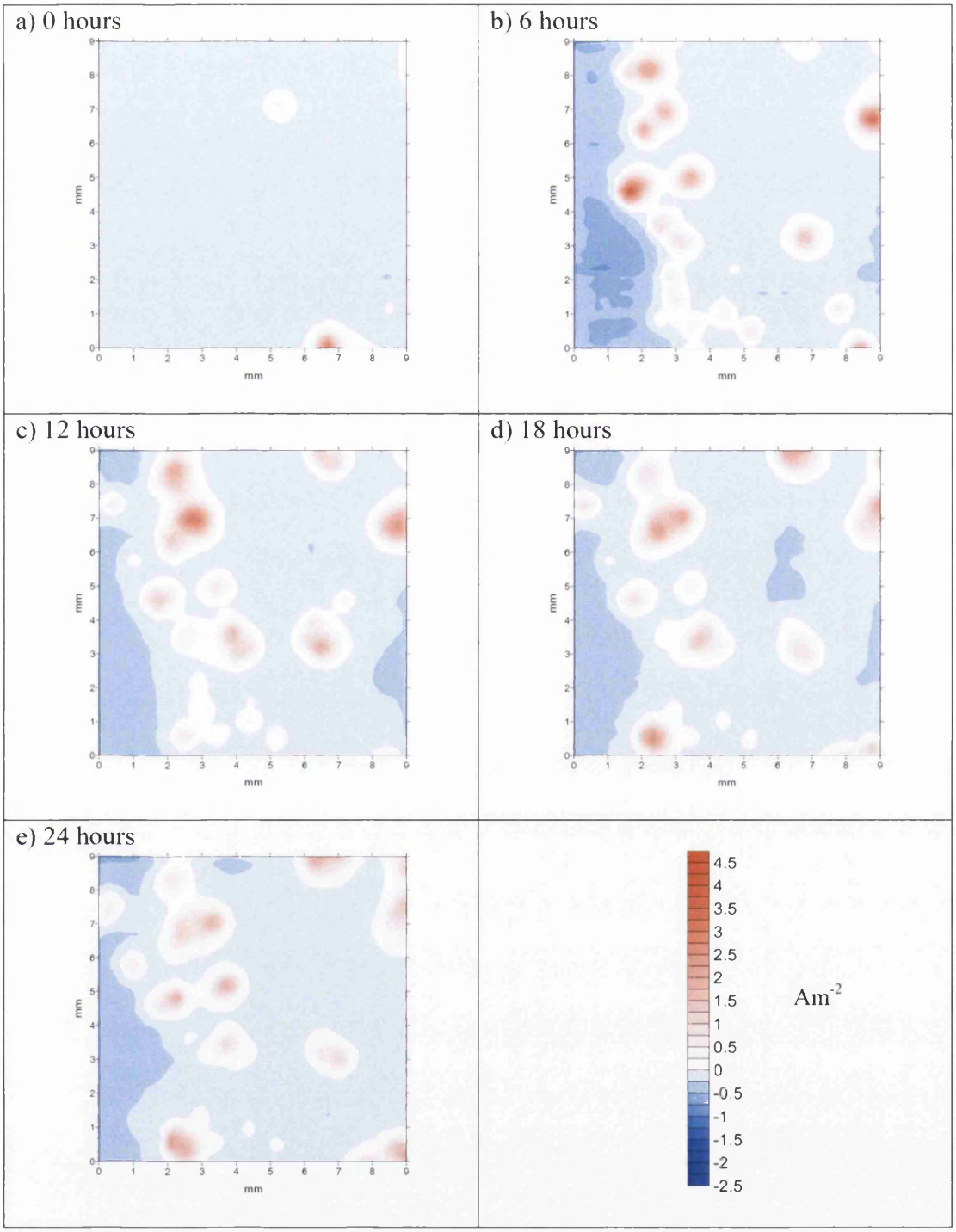

Figure 6.9 SVET corrosion maps for a 5.4% Al addition showing the anodic activity (red) as a function of immersion time. Please note scale.

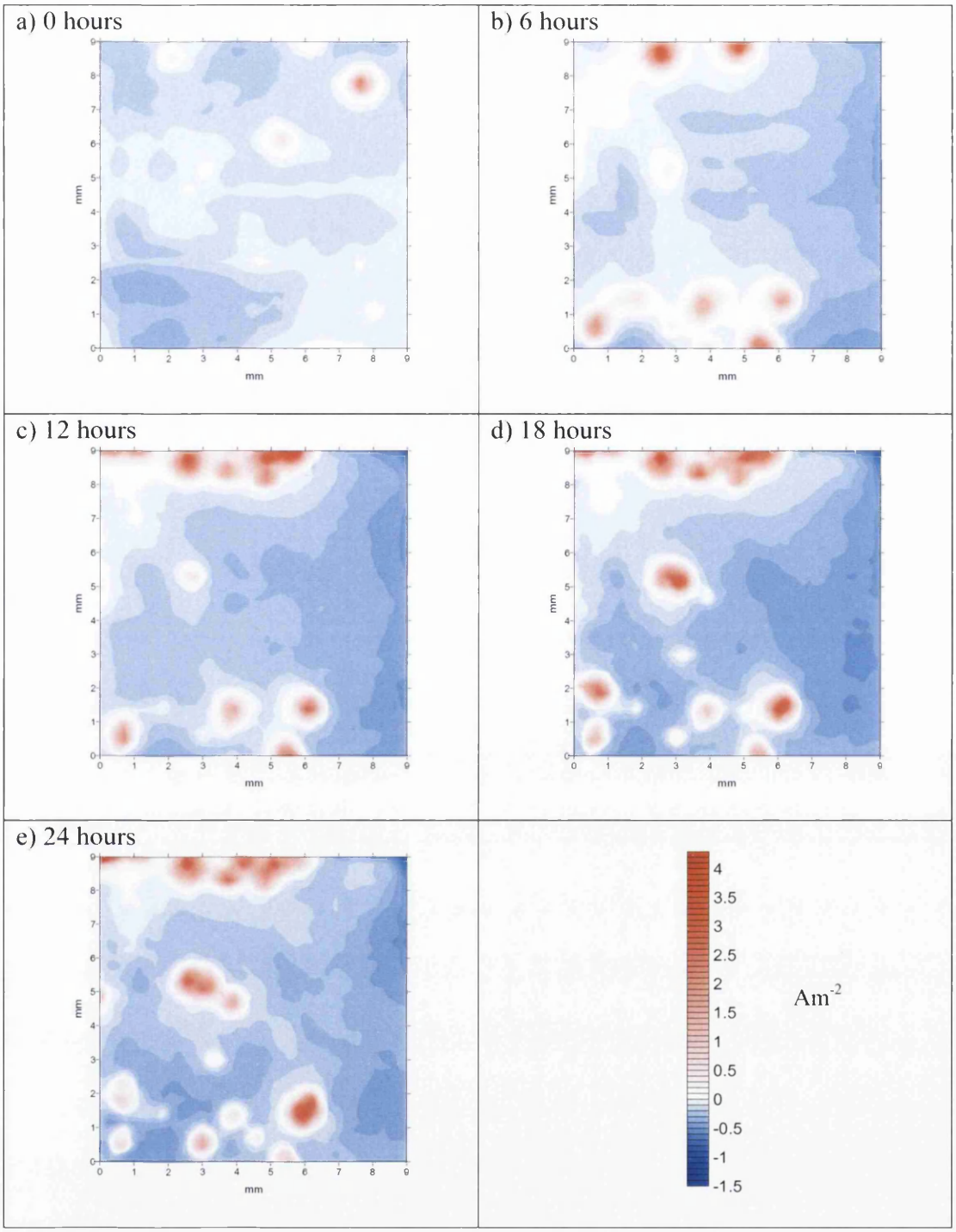

Figure 6.10 SVET corrosion maps for a 5.6% Al addition showing the anodic activity (red) as a function of immersion time. Please note scale.

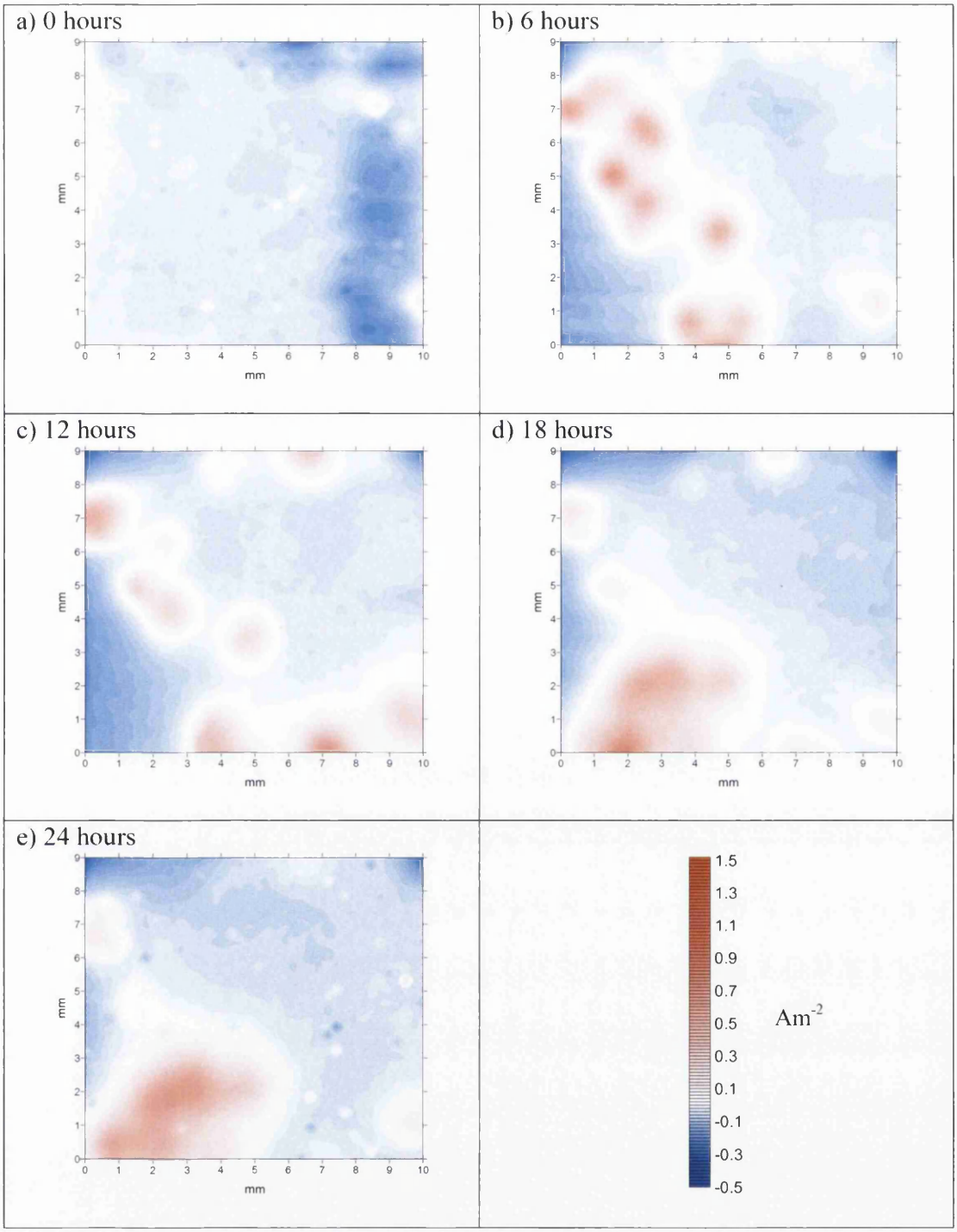

Figure 6.11 SVET corrosion maps for a 6.5% Al addition showing the anodic activity (red) as a function of immersion time. Please note scale

The SVET data has been used to quantify anodic events and group these anodic events into lifetime groups, the intensity of anodic events can also be analysed. This was achieved by analysing each individual scan and using cartography software to identify residual anodes. From this it was possible to group the anodes into four lifetime groups ranging from short lived anodic events to longer lived anodes. This data can then be used in two ways. Firstly, the intensity of each anode can be displayed as a function of immersion time, as shown in Figure 6.12 (a-d).

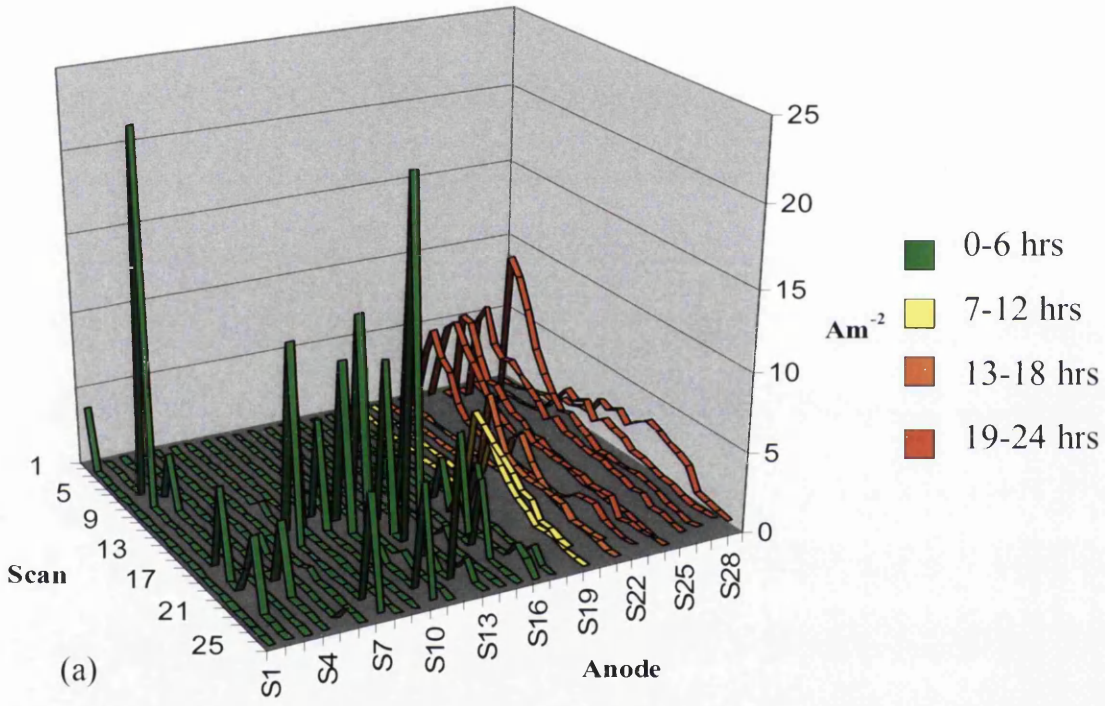

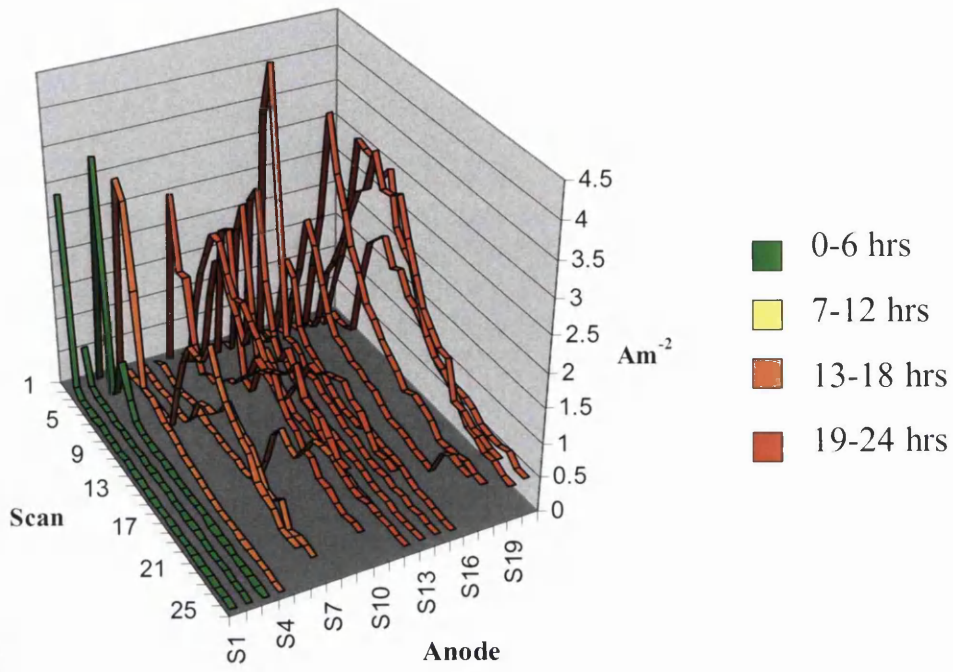
4.5
4
3.5
3
2.5
2
1.5
1
0.5
0
Am-2
0-6 hrs
7-12 hrs
13-18 hrs
19-24 hrs
1
5
9
13
17
21
25
Scan
S1
S4
S7
S10
S13
S16
S19
Anode

(b)

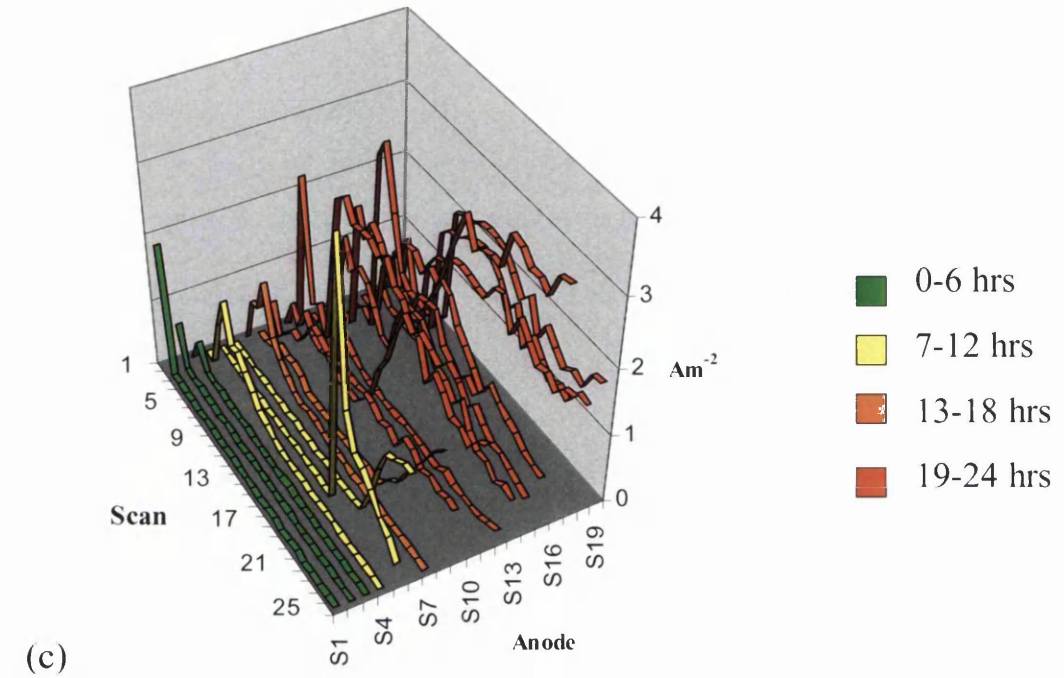

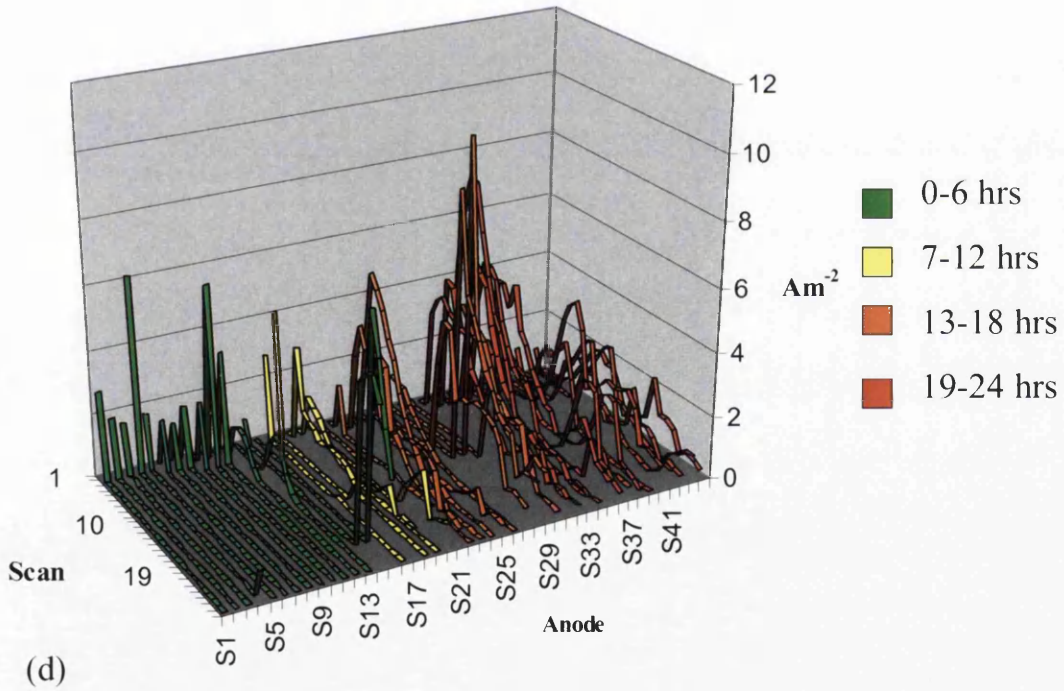

Figure 6.12 Surface anode intensity as a function of immersion time for (a) 4.7% Al, (b) 5.4% Al, (c) 5.6% Al, (d) 6.5% Al addition. Scan No. relates to immersion time.

The first thing of note from Figure 6.12 is the difference in intensity across the sample field. From the above plots it can be shown that with the exception of 6.12 (d) the addition of aluminium to the coating decreases the intensity of corrosion across the sample surface. The number of shorter lived anodes (green) also decreases with addition of aluminium to the coating. This is accompanied by an increase in the amount of longer lived anodes (red). However as these are of lower intensity and with less primary zinc available for focussed corrosion to occur, less zinc loss is observed. An addition of 6.5% provides an anomaly. Here more short lived anodes are seen, and under corrosion testing the sample exhibited least amount of zinc loss. This due to the anodic events being more generalised across the surface as is shown from the SVET maps in Figure 6.11 rather than localised as maybe occurring with the other samples.

Secondly each anode was assigned an average Zn loss calculated using the data gained from the SVET and the total number of anodes throughout the scan. This Zn loss value was then used to relate surface Zn loss to anode lifetime on a single plot. The result is shown in Figure 6.13.

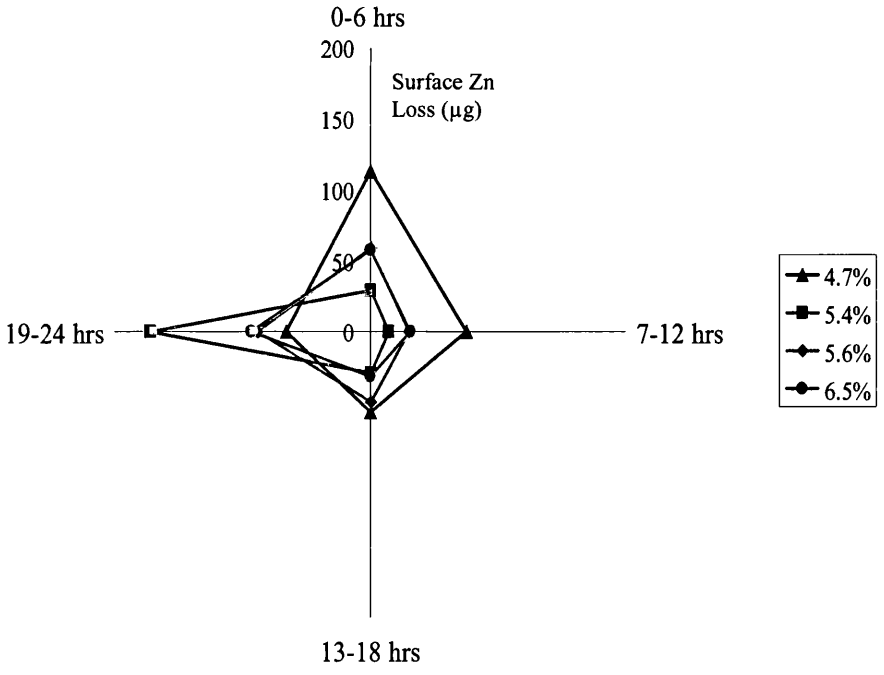

Figure 6.13 Surface Zn loss vs Anode lifetime.

From Figure 6.13 it is possible to determine which Al addition is the best with regard to corrosion performance. This is represented by the sample which achieves the smallest area around the origin. The 6.5% Al addition is the best performing however, this result should be treated with a degree of caution because as shown previously in Figure 6.4 the 6.5% Al addition no primary Zn phase present in the system. This could cause problems in the long term as it has been proposed that for maximum edge corrosion protection a certain amount of primary phase is required. The primary Zn phase corrodes preferentially while the surrounding eutectic phase stays coherent with the substrate and the organic over-layer. This is desirable from an industrial point of view as this would allow the integrity of any topcoat layer to be maintained in the longer term. For this reason the 5.6% Al addition may provide the best option for an improved galvanized coating, as it satisfies the criteria of having primary Zn present and also a reduced Zn content in the system.

From Figure 6.13 it is also easy to identify how important anode lifetime is to the corrosion performance of the galvanized layer. With the exception of the 4.7% Al addition, which shows an even spread of anode activity, it is clear that the longer the anode is active the more damaging it is to the coating.

6.1.3 Effect of Al addition on cut edge corrosion performance

From an industrial point of view, cut edge corrosion is perhaps the most important with regard to assessing the overall performance of the coating. This is due to the large usage of organic coated strip steel for external cladding in the construction industry. This will lead ultimately to the strip being cut and many metres of edge being exposed to corrosive environments.

Figure 6.14 illustrates the average total zinc loss observed over a 24 hour period from edge sections of the four test samples. Each sample was embedded in resin, polished and subjected SVET testing as described earlier in Chapter 2 section 2.5.

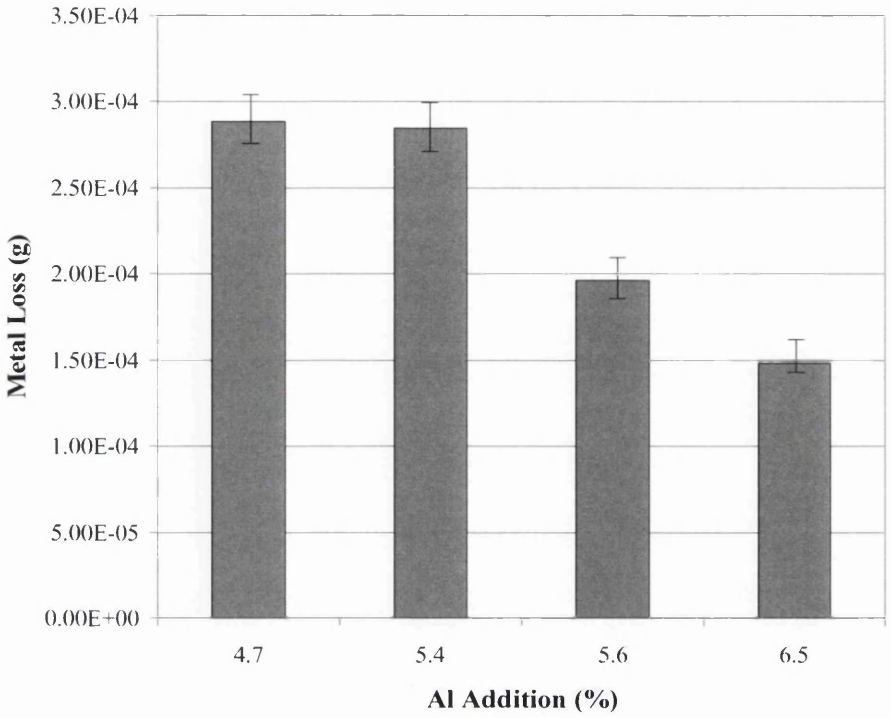

Figure 6.14 Zinc loss from cut edge as a function of Al addition.

It is clear that as well as improving the corrosion resistance of the surface, the addition of aluminium to the coating also improves the performance of the cut edge in terms of metal lost. It can be seen that on addition of aluminium, the results follow a similar trend to those obtained from the surface in that the higher the aluminium content the less zinc loss. As with the surface samples there appears to be a considerable decrease in the amount of zinc loss at an addition of 6.5% Al. This can again be attributed to the fact that there is no primary zinc present and therefore the corrosion of the zinc in the eutectic phase alone gives rise to a lower value.

Figure 6.15-6.18 show typical SVET corrosion maps gained from cut edge samples. As before, these can be used to visually identify areas of anodic activity and quantify them in number and intensity.

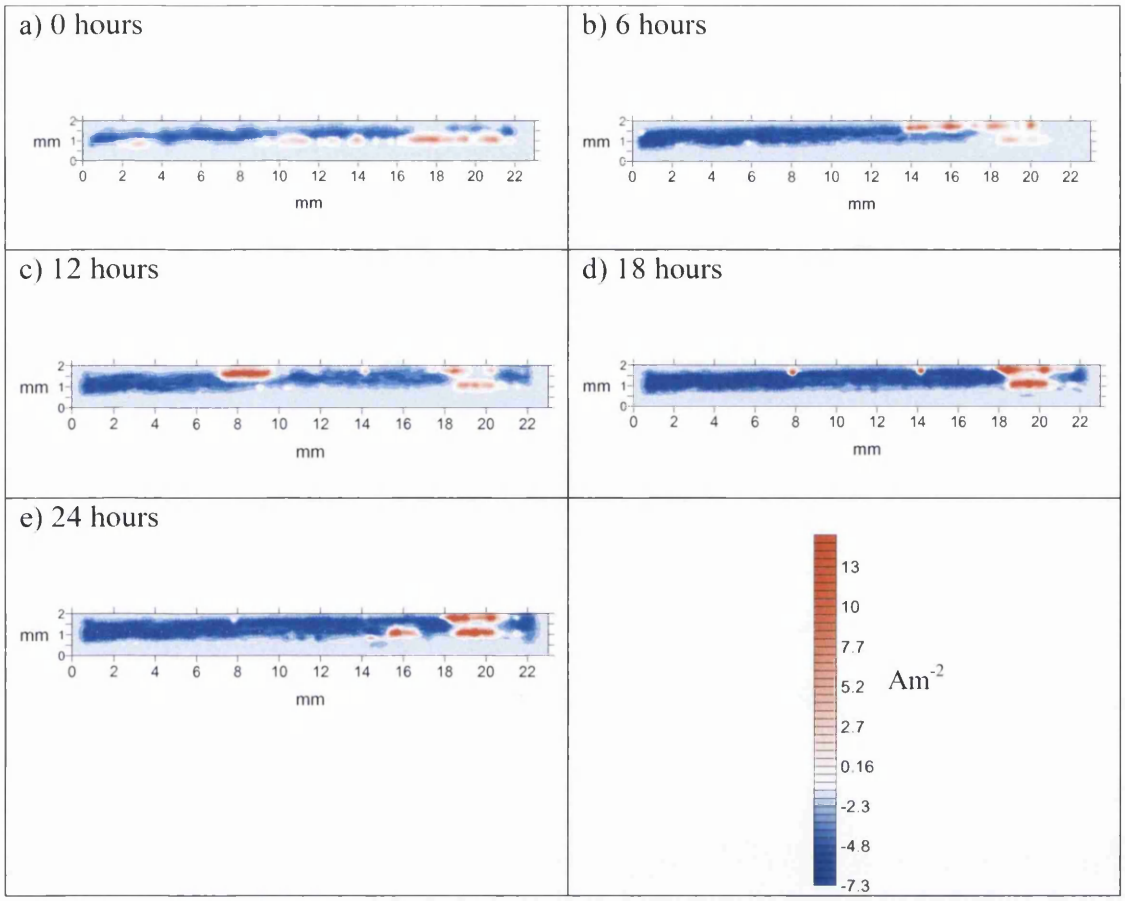

Figure 6.15 SVET cut edge corrosion maps for a 4.7% Al addition showing the anodic activity (red) as a function of immersion time. Please note scale.

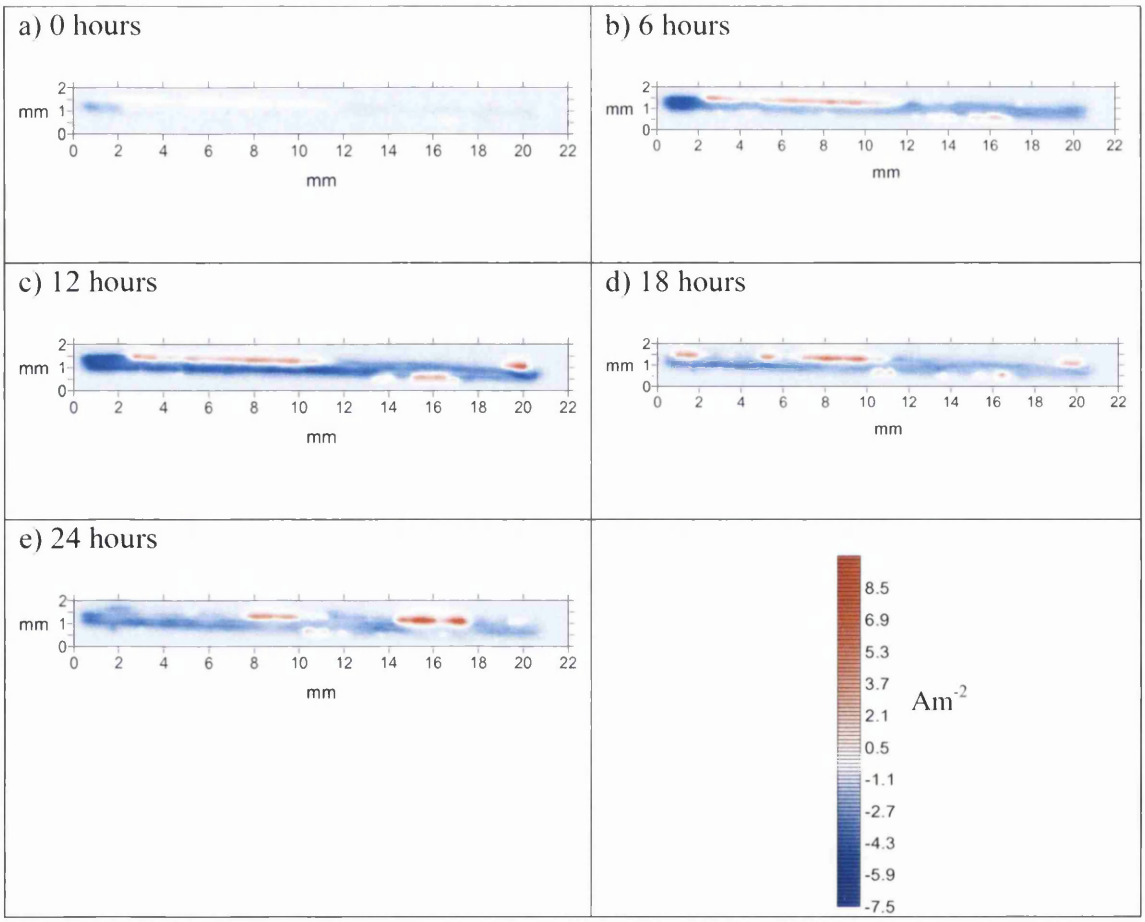

Figure 6.16 SVET cut edge corrosion maps for a 5.4% Al addition showing the anodic activity (red) as a function of immersion time. Please note scale.

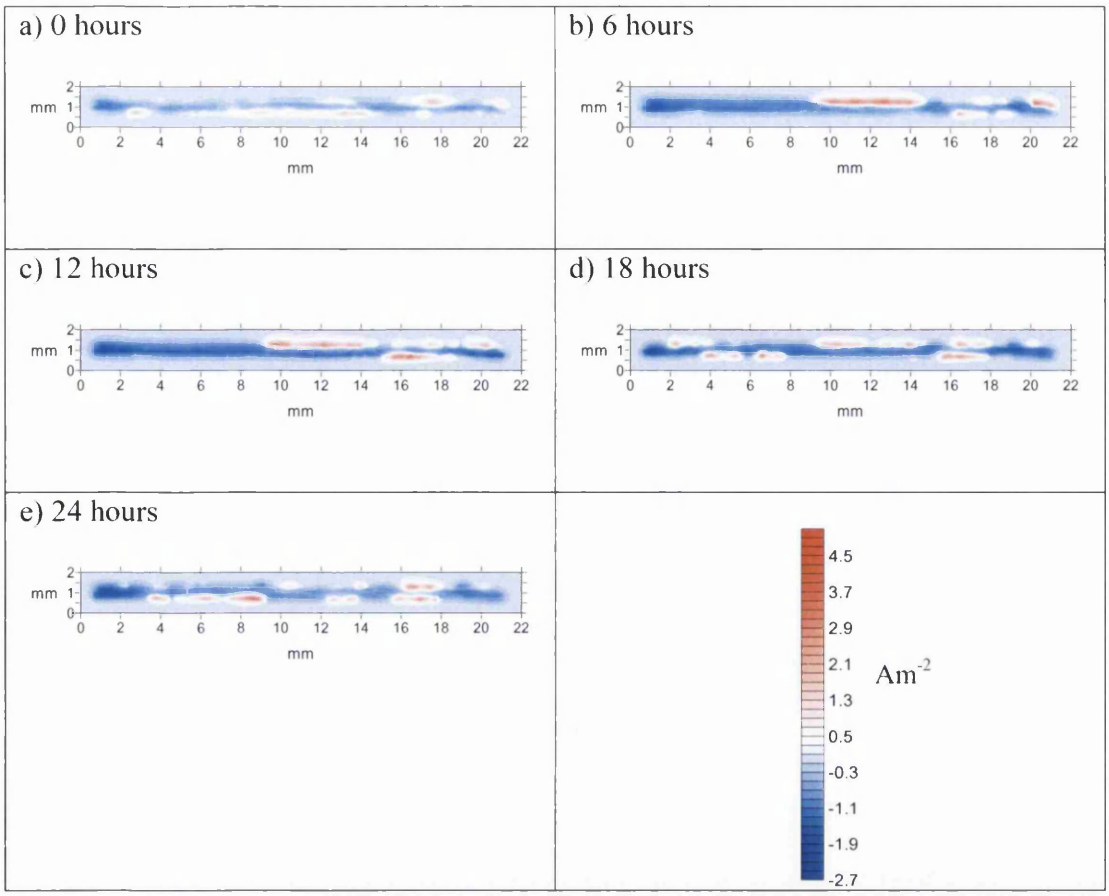

Figure 6.17 SVET cut edge corrosion maps for a 5.6% Al addition showing the anodic activity (red) as a function of immersion time. Please note scale.

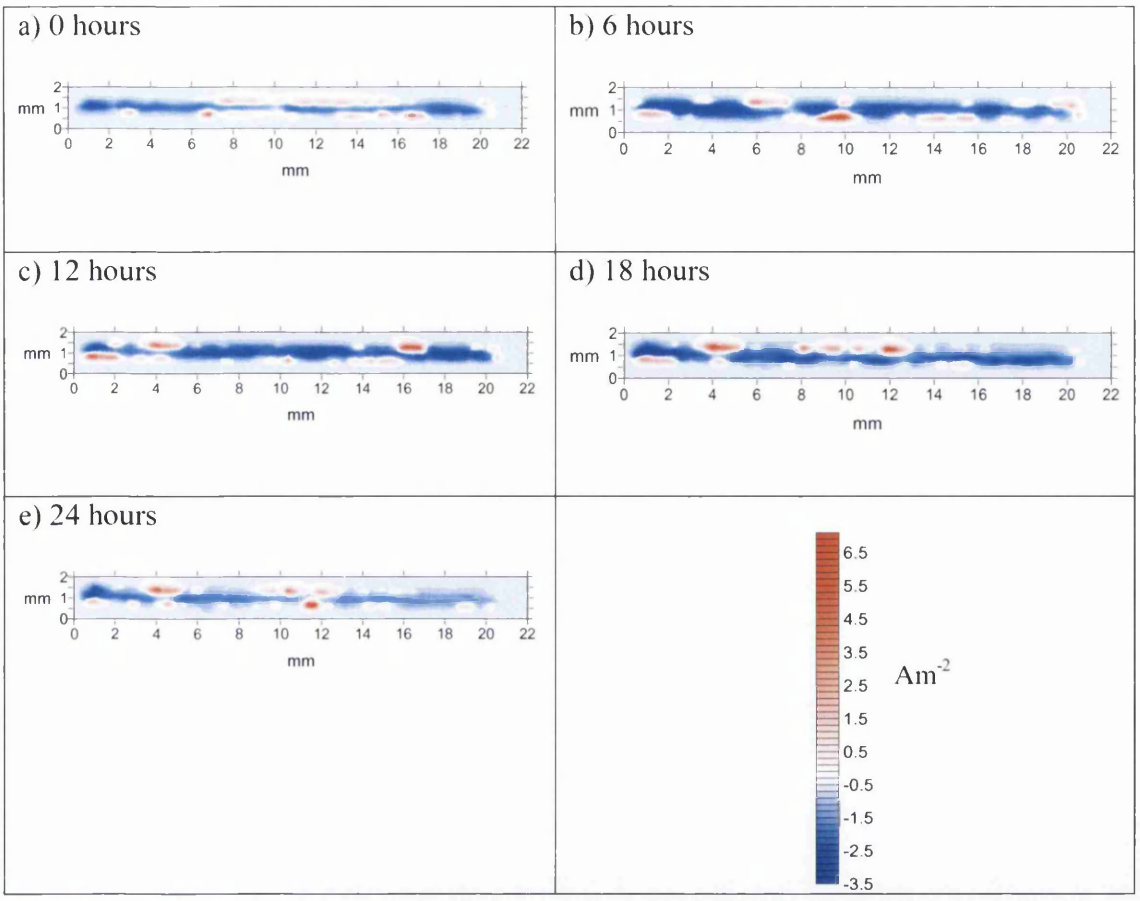

Figure 6.18 SVET cut edge corrosion maps for a 6.5% Al addition showing the anodic activity (red) as a function of immersion time. Please note scale.

It has been observed that there is still a considerable amount of primary zinc present with an addition of 5.6% Al and this sample shows significant improvement in performance relative to the 4.7% and 5.4% additions respectively. The primary zinc present in this case will be highly beneficial as the preferentially corroding phase along the edge while the surrounding eutectic phase enables any overpainted layer that may be present to hold firm to the substrate.

Figure 6.19 (a-d) shows the number and intensity of anodic events across the edge sections for the sample 4.7% through to 6.5% Al respectively.

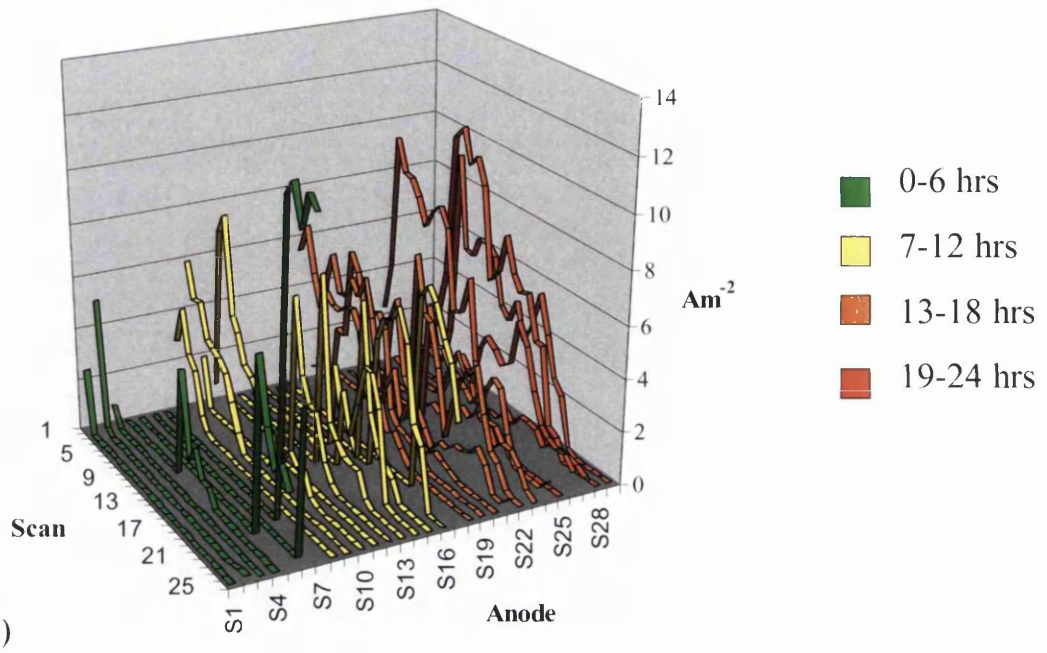
14
12
10
8
6
4
2
0
Am-2
0-6 hrs
7-12 hrs
13-18 hrs
19-24 hrs
1
5
9
13
17
21
25
Scan
S1
S4
S7
S10
S13
S16
S19
S22
S25
S28
Anode

(a)

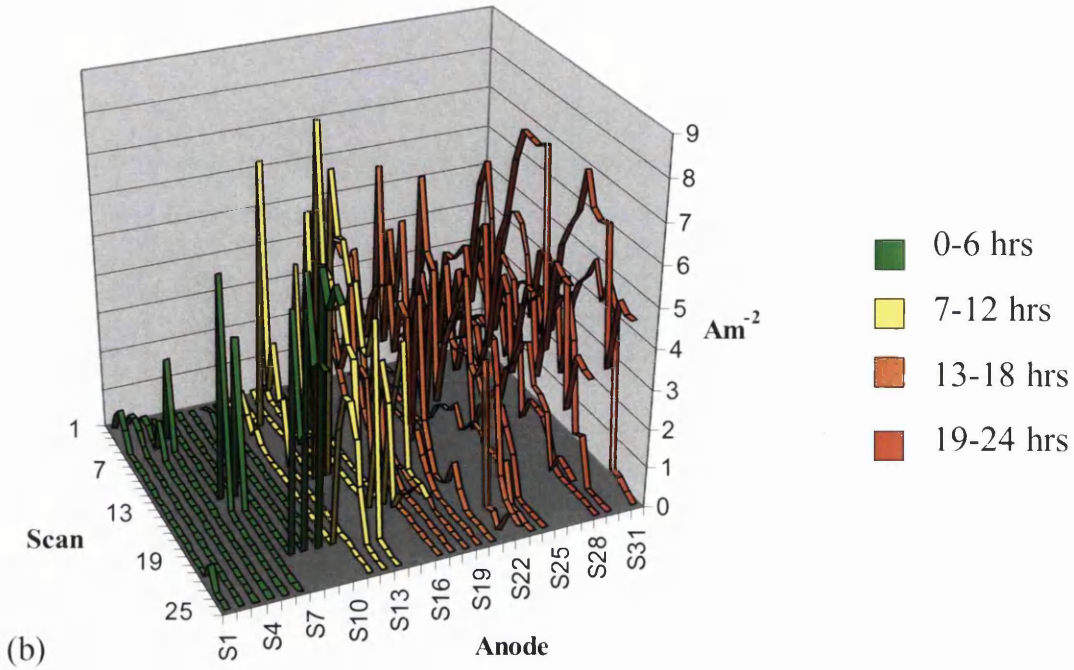
9
8
7
6
5
4
3
2
1
0
Am-2
1
7
13
19
25
Scan
S1
S4
S7
S10
S13
S16
S19
S22
S25
S28
S31
Anode
0-6 hrs
7-12 hrs
13-18 hrs
19-24 hrs

(b)

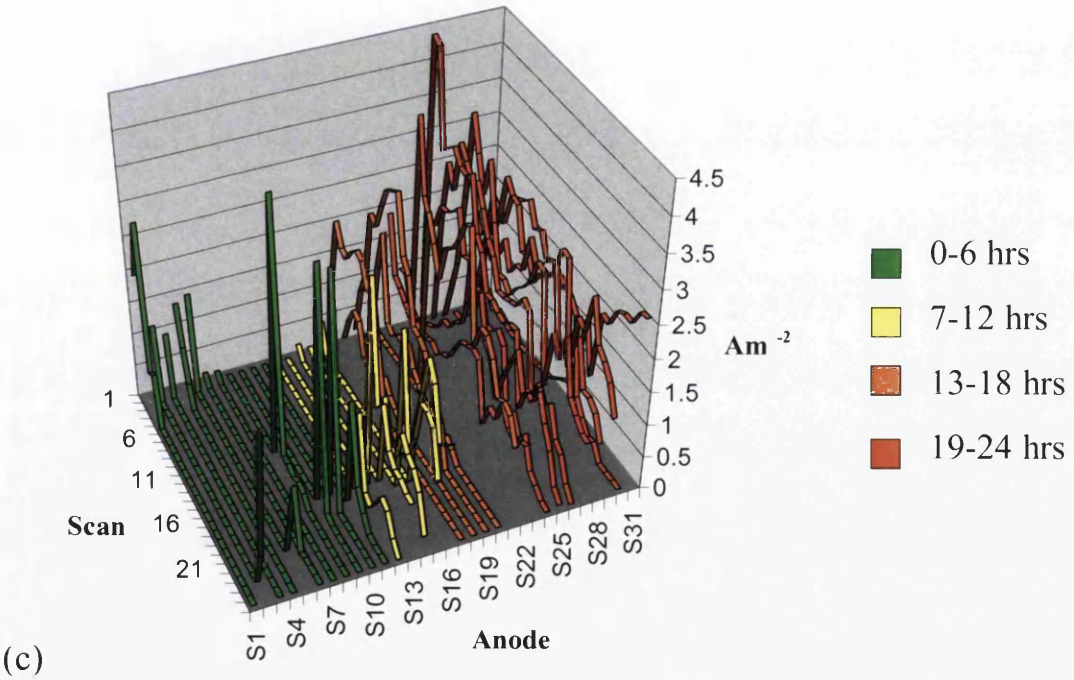
4.5
4
3.5
3
2.5
2
1.5
1
0.5
0
Am -2
1
6
11
16
21
Scan
S1
S4
S7
S10
S13
S16
S19
S22
S25
S28
S31
Anode
0-6 hrs
7-12 hrs
13-18 hrs
19-24 hrs

(c)

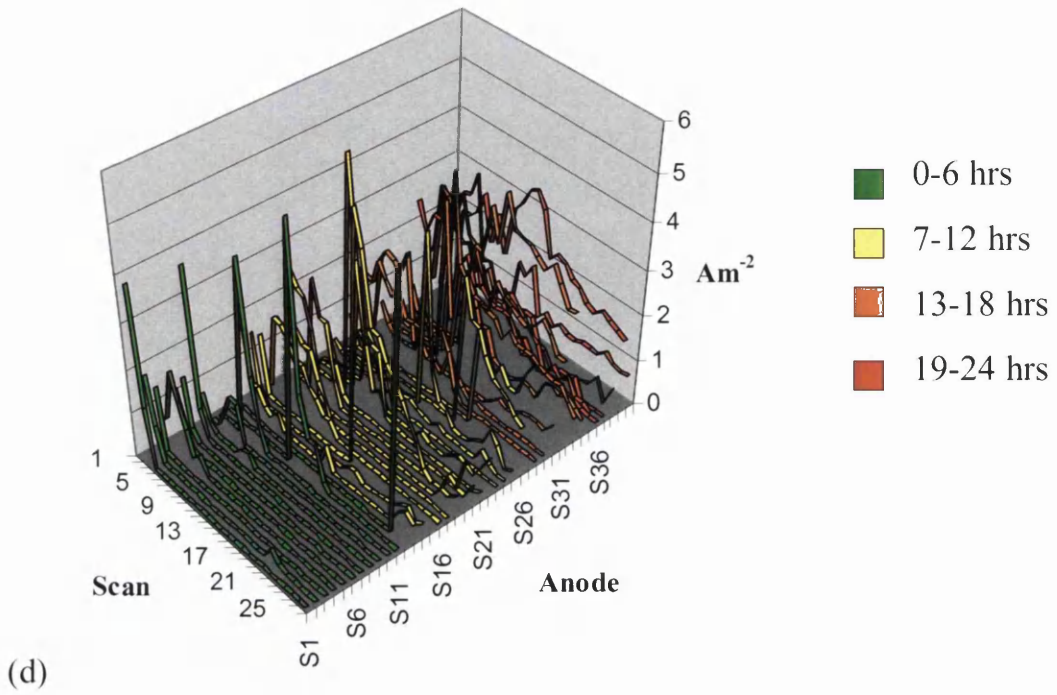

(d)

Figure 6.19 Cut edge anode intensity as a function of immersion time for (a) 4.7% Al, (b) 5.4% Al, (c) 5.6% Al, (d) 6.5% Al addition. Scan No. relates to immersion time.

Similar to the results gained from surface testing, increasing aluminium content in the coating gives rise to a lower intensity of anodic activity, this may be due to the increased passivation of the system due to additional aluminium. The number of anodes increases from 28 at 4.7% Al to maximum of 40 as shown in Figure 6.19 (d) for the 6.5% Al addition. This is because of the decrease in volume fraction of primary zinc with the increasing aluminium content. This is indicated by a general decrease in the amount of long lived anodes (red), which the primary zinc phase would provide. The 6.5% Al sample again provides a slight anomaly as with surface corrosion and could relate to the morphology and orientation of the eutectic phase that occurs in the sample.

It is clear that anode intensity is related to the zinc loss, as with the addition of aluminium to the system, a decrease in zinc loss and also intensity is observed giving rise to superior edge performance.

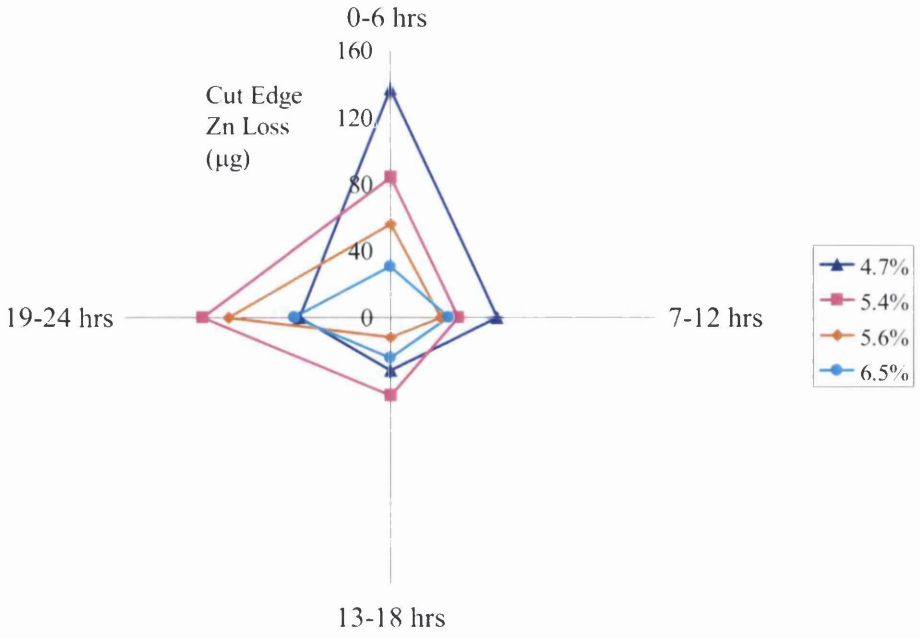

Figure 6.20 Cut edge Zn loss vs Anode lifetime.

Figure 6.20 above shows how cut edge zinc loss is related to anode lifetime. As with the surface results, the 6.1% Al sample is the best performing which reinforces all the results so far with regard to the addition of aluminium improving corrosion performance. As with the result from the surface testing, this result should be treated with a degree of caution as there is no primary zinc phase present at the edge and this could potentially lead to problems if this sample were to be coated as mentioned earlier.

The plot also shows that with the exception of the 5% Al sample longer lived anodes are the most damaging with regard to corrosion and therefore zinc loss. The 5% shows a greater spread of anode lifetime due to the increased amount of primary zinc exposed along the edge due to a greater volume fraction of primary zinc.

6.2 Conclusions

Increasing the Al level in Zn/Al galvanizing improves the corrosion performance of the coating, in both surface and cut edge testing. The SVET can be used as an effective and rapid tool not only to predict corrosion performance but to quantify number and lifetime of anodic events to further validate data. Considering the results of this investigation, the best aluminum content for a sample to be overpainted is around 5.5% Al since this coating retains enough primary zinc that this phase can preferentially be removed leaving the paint adherent to the still present eutectic. The 6.1% Al coating although displaying the least zinc loss would be more likely to suffer from anodic dissolution at the organic coating metallic coating interface and is as such both more expensive and less desirable.

6.3 References

1. ELVINS, J., SPITTLE, J. A., WORSLEY, D. A., ' Relationship Between Microstructure and Corrosion Resistance in Zn-Al Alloy Coated Galvanised Steels', Corrosion Engineering Science and Technology, vol. 38, No.3, 2003.
2. BOHM, S., CHALLIS, M., HEATLEY, T., WORSLEY D. A., 'An Investigation of the Effects of Magnesium Levels on the Kinetics and Mechanism of Cut Edge Corrosion in Organically Coated Zinc Aluminium Alloy Galvanised Steels', Trans IMF, 2001.
3. PENNEY, D., SULLIVAN, J., WORSLEY, D., 'Investigation into the Effects of Metallic Coating Thickness on the Corrosion Properties of Zn/Al Alloy Galvanising Coatings', Corrosion Science, vol. 49, 2007.
4. TANO, K., HIGUCHI, S., Nippon Steel Technical Report, No 25, 29, 1985.
5. CORUS, 'The Colorcoat Building', 2005. Commercial manual.
6. PORTER, D. A., EASTERLING, K. E., 'Phase Transformations in Metals and Alloys', Second Edition, Nelson Thornes, 2001.
7. D.A. Worsley, H.N. McMurray, J.H. Sullivan and I. M. Williams, *Corrosion*, **60**, 437 (2004).

Chapter 7

Influence of coating weight change and aluminium addition on the corrosion performance of Galvalloy® coated steels

7.0 Introduction

Further to the addition of aluminium as analysed in the previous chapter, it is proposed that a decrease in coating weight at higher aluminium content could afford a reduction in cost of raw materials as well as reducing the overall weight of the cladding itself.

Typically a coating weight of $265gm^{-2}$ is used to give a final coating thickness of ~20μm, it is thought that a reduction in coating weight to ~$132.5gm^{-2}$ would give similar corrosion performance with a cost incentive that may be commercially attractive. However it is important to note that the lower coating weight will only be beneficial if the corrosion protection is of a level that is acceptable for commercial purposes. This is due to the guarantees that are widely offered in the construction industry against product failure.

In this chapter an investigation into the effect of microstructure and corrosion performance of low coating weight Zn galvanized steels with Al levels over 4.8% Al is presented. The aims of this study are assess how increasing the Al levels in a Zn-Al galvanised coating affects surface and edge corrosion performance and relate the findings to results from larger coating weights as addressed in the previous chapter. Optical microscopy and the Scanning Vibrating Electrode Technique (SVET) will be utilised for microstructural observation and corrosion testing respectively.

7.1 Influence of coating weight change and aluminium addition on the corrosion performance of Galvalloy® coated steels

Test panels were produced via the Iwatan-Rhesca Hot Dip Simulator to achieve coating weights of ~132.5gm^{-2} giving a coating thickness of ~10μm. Batches of samples were produced with target Al levels ranging from 5% through to 6.1%. The samples to be tested in the bare state for accelerated tests and therefore no topcoat or pretreatment were necessary. Some of the samples were set aside for salt spray testing which will be discussed later. The Al levels of the samples obtained are shown in Table 7.1.

Coating Thickness (μm)	Target Al Level (%)	Actual Al Level (%)
10	5	4.7
10	5.3	5.45
10	5.5	5.58
10	6.1	6.49

Table 7.1. Samples produced via HDS with increasing Al levels.

7.2 Effect of coating thickness on microstructure

Adjusting the coating thickness the will have an effect on the microstructure of the solidified coating. Essentially the air knives that control the coating thickness by way of gas pressure, increasing the cooling rate leading to higher rate of nucleation but a decrease in growth of the primary phase. This gives rise to a higher number of smaller dendrites when compared to a longer cooling rate for thicker coatings[1]. Figure 7.1 shows the difference in microstructure close to the steel / coating interface.

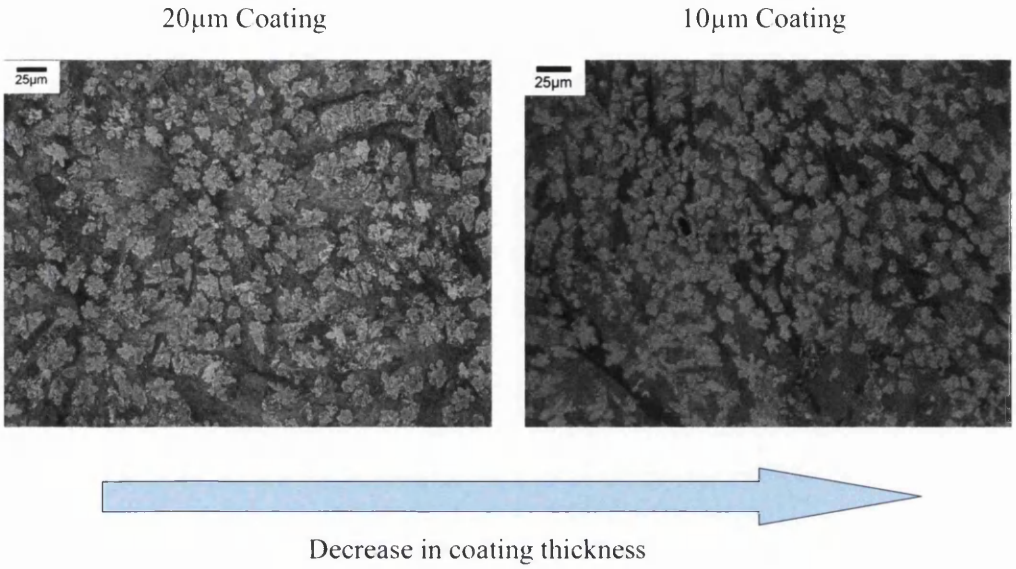

Figure 7.1. Microstructure observed at Coating/Substrate interface for 10μm and 20μm coatings produced via HDS.

Previous work has also suggested that increasing the cooling rate under continuous galvanising line conditions leads to the removal of aluminium rich liquid, exposing a variable amount of primary zinc at the surface of the coating. This will then inherently increase the volume fraction of the primary and therefore preferentially corroding phase. This has then given rise to a poor corrosion performance in relation to the thicker coatings.

The microstructure obtained from the samples generated via the HDS are comparable, however it should be noted that on analysis the volume fraction was found to be generally consistent with that of that found in the corresponding thicker coatings. This is shown graphically in 7.2. There is a slight anomaly at the 5.45% Al addition, and this may be down to the processing conditions of that particular batch of samples, which could have inadvertently altered the composition of the bath.

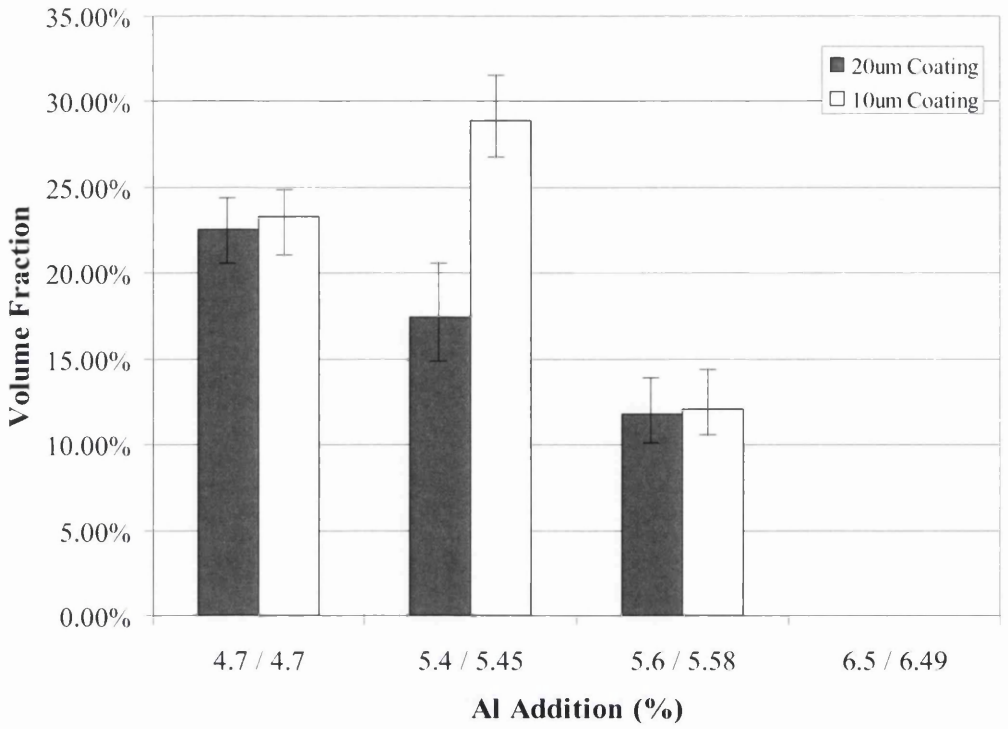

Figure 7.2 Volume fraction vs Coating thickness.

The pattern shown for the volume fraction of primary phase present in the coating is echoed when regarding the dendrite number at the interface. This is shown graphically in Figure 7.3. Again, the 5.45% proves to be the anomaly of the set. This is most likely due to a cooling effect induced by the simulated process; this would suggest that the removal of Al rich phase is occurring, thus leading to a change in composition giving rise to a higher volume fraction. However, this is conjecture at this point as the data is unavailable to confirm whether this is the case.

With regard to dendrite numbers, a general increase in number is shown through the reduction in coating thickness as expected due to the increase in nucleation at the steel surface, again bought about by the increase in cooling rate.

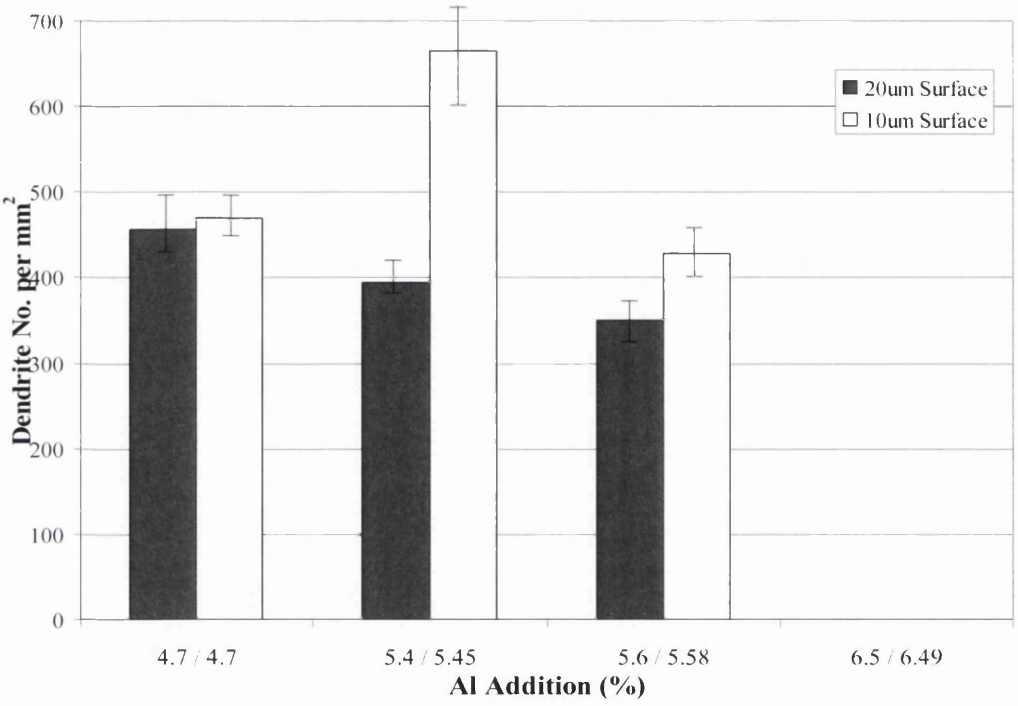

Figure 7.3. Dendrite number at interface vs Coating thickness

7.3 Effect of coating thickness on corrosion performance

It has been shown that the coating thickness has a significant effect on the microstructure of the coating and it is important to consider the impact of this change on the corrosion performance. As in Chapter 6, the samples were tested using the Scanning Vibrating Electrode Technique (SVET) while immersed in 0.1% NaCl over 24 hours. Both surface and cut edge samples were tested for each level of aluminium addition.

The volume fraction and metal loss for surface and cut edge samples are shown graphically in Figures 7.4 and 7.5 for 20μm and 10μm respectively. For both thicknesses is shown that metal loss follows the profile of volume fraction in general. The metal loss levels are generally higher from the thinner coating samples. At aluminium addition of 5.58% the thinner coating gives similar surface corrosion performance to that of the thicker 20mm sample with metal loss of 236 and 229μg respectively. It should also be noted that the volume fraction has remained consistent despite the difference in thickness.

This is likely to be a result of some cooling effect that occurred during the manufacture of the samples.

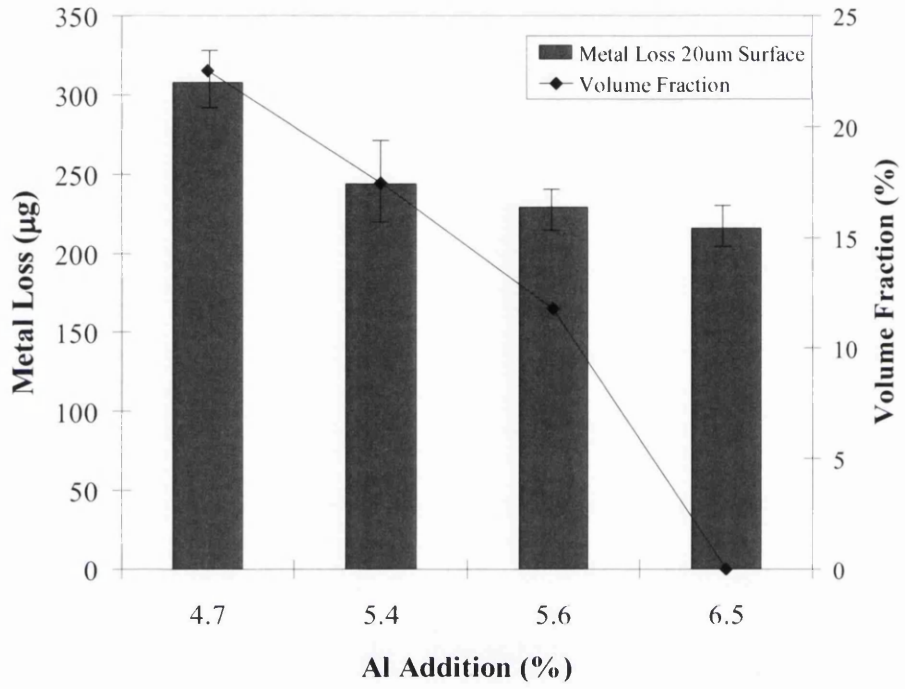

Figure 7.4 Metal loss and Volume fraction for 20µm surface samples shown as a function of aluminium addition.

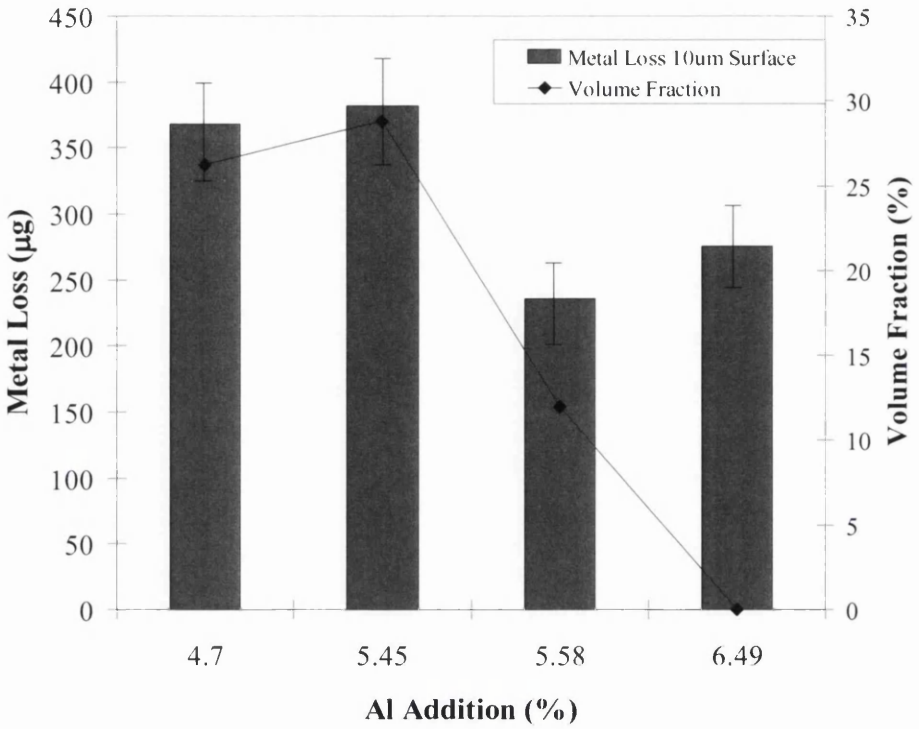

Figure 7.5 Metal loss and Volume fraction for 10µm surface samples shown as a function of aluminium addition.

While the metal loss from the 20mm surface samples falls as aluminium addition increases suggesting an improvement in corrosion resistance, the metal loss from the 10µm surface samples does not follow this pattern. It can be seen in Figure 7.5 that there is an increase in metal loss from 5.58% to 6.49% this may be due to the fact that there is no primary zinc present and as such is a result of the eutectic structure corroding. The corrosion rate clearly increases as a function of the primary zinc phase that is present. At 6.49% Al the main corrosion mechanism will be dezincification of the eutectic and this could be detriment of the integrity of any organic topcoat layer that may be applied subsequently as it would involve zinc loss from close to the organic layer whereas with primary phase present zinc loss is concentrated more closely to the steel substrate on which the primary phase nucleates[2].

As with the previous chapter (Chapter 6), the data obtained by the SVET has been used to quantify anodic events and group these anodic events into lifetime groups, the

intensity of anodic events can also be analysed. This was achieved by analysing each individual scan and using cartography software to identify residual anodes. From this it was possible to group the anodes into four lifetime groups ranging from short lived anodic events to longer lived anodes. This data can then be used in two ways. Firstly, the intensity of each anode can be displayed as a function of immersion time, secondly each anode was assigned an average Zn loss calculated using the data gained from the SVET and the total number of anodes throughout the scan. This Zn loss value was then used to relate surface Zn loss to anode lifetime on a single plot discussed later. This enables detailed analysis to be undertaken to give extra understanding as to the corrosion performance of the samples. It is perhaps easier to analyse surface and cut edge performance separately.

Figures 7.6-7.9 show the corrosion maps of surface samples of the thinner 10μm coatings as a function of Al addition and immersion time. This serves to provide a visual medium to illustrate the anodic activity and enables both the number of anodic events and intensity to be presented.

It is shown from these plots that the intensity of the anodic activity generally follows the profile of surface metal loss. The only slight anomaly is the 4.7% Al addition where there is a higher intensity shown than that of the 5.45% Al sample which exhibited the highest zinc loss. This may be because the high intensity occurred in a single scan and from one short lived anode and therefore may not have caused as much damage in terms of zinc loss as would be anticipated if the anode were consistent across the whole twenty four hour test.

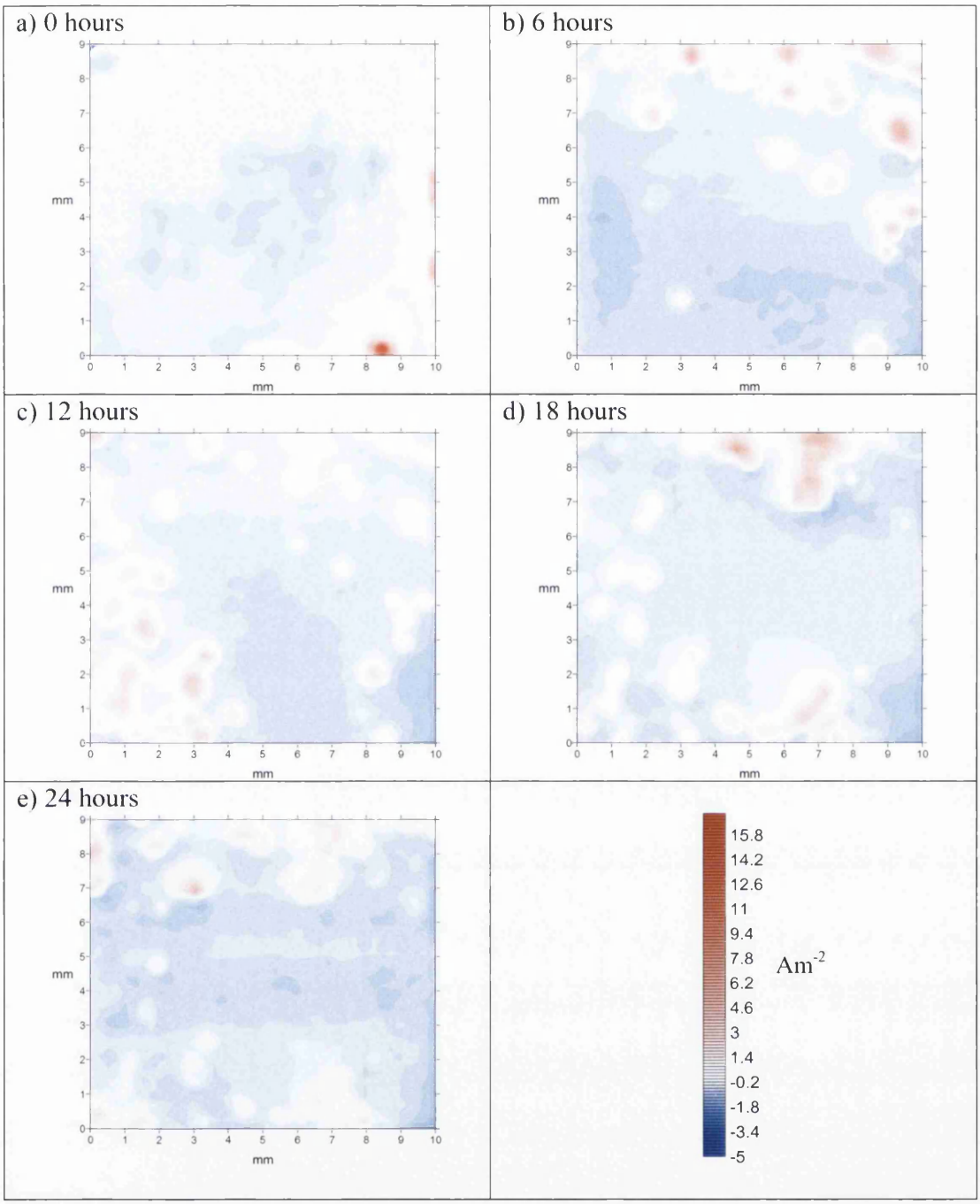

Figure 7.6 SVET corrosion maps for a 4.7% Al addition 10μm coating showing the anodic activity (red) as a function of immersion time. Please note scale

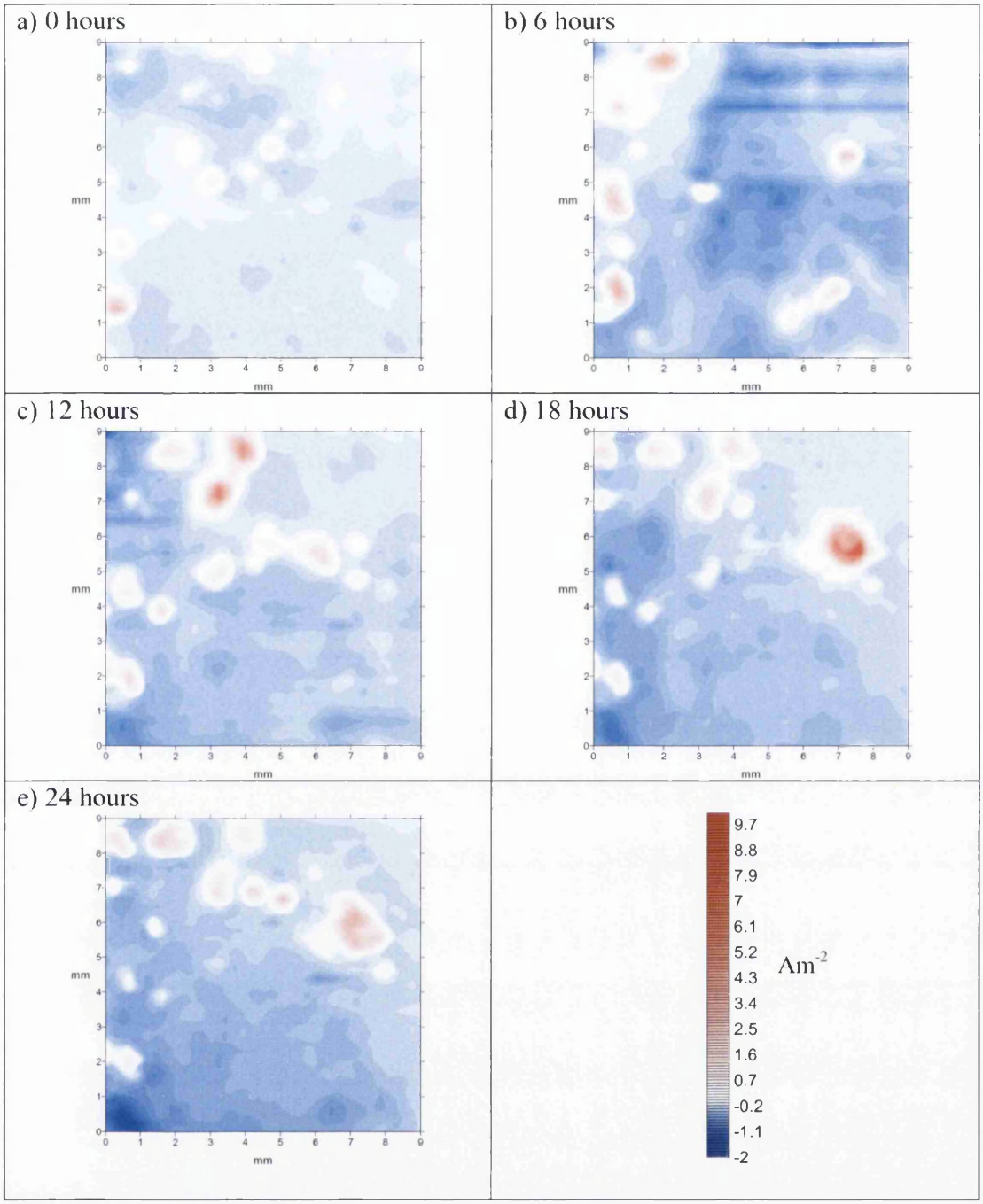

Figure 7.7 SVET corrosion maps for a 5.45% Al addition 10μm coating showing the anodic activity (red) as a function of immersion time. Please note scale.

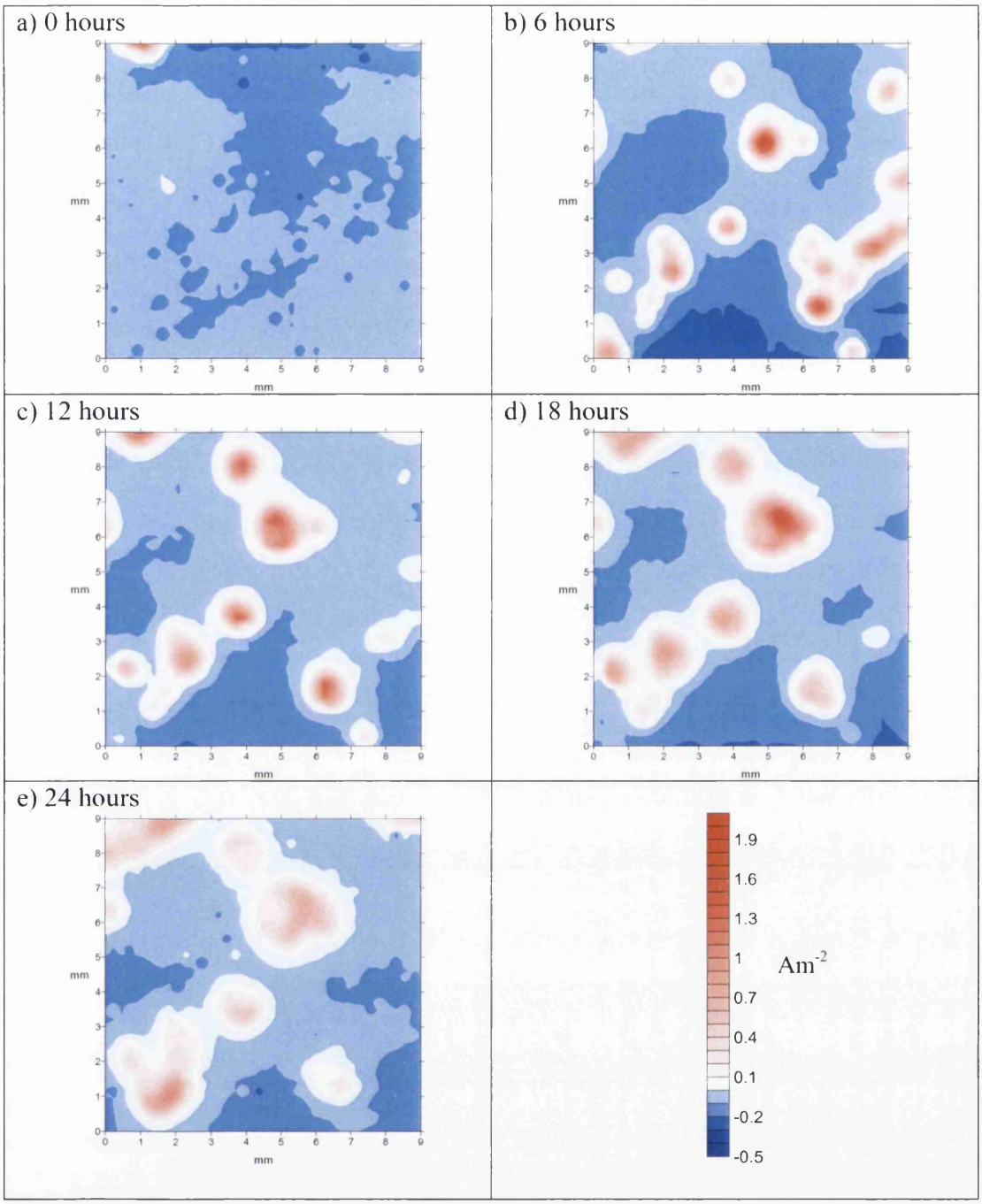

Figure 7.8 SVET corrosion maps for a 5.58% Al addition 10μm coating showing the anodic activity (red) as a function of immersion time. Please note scale.

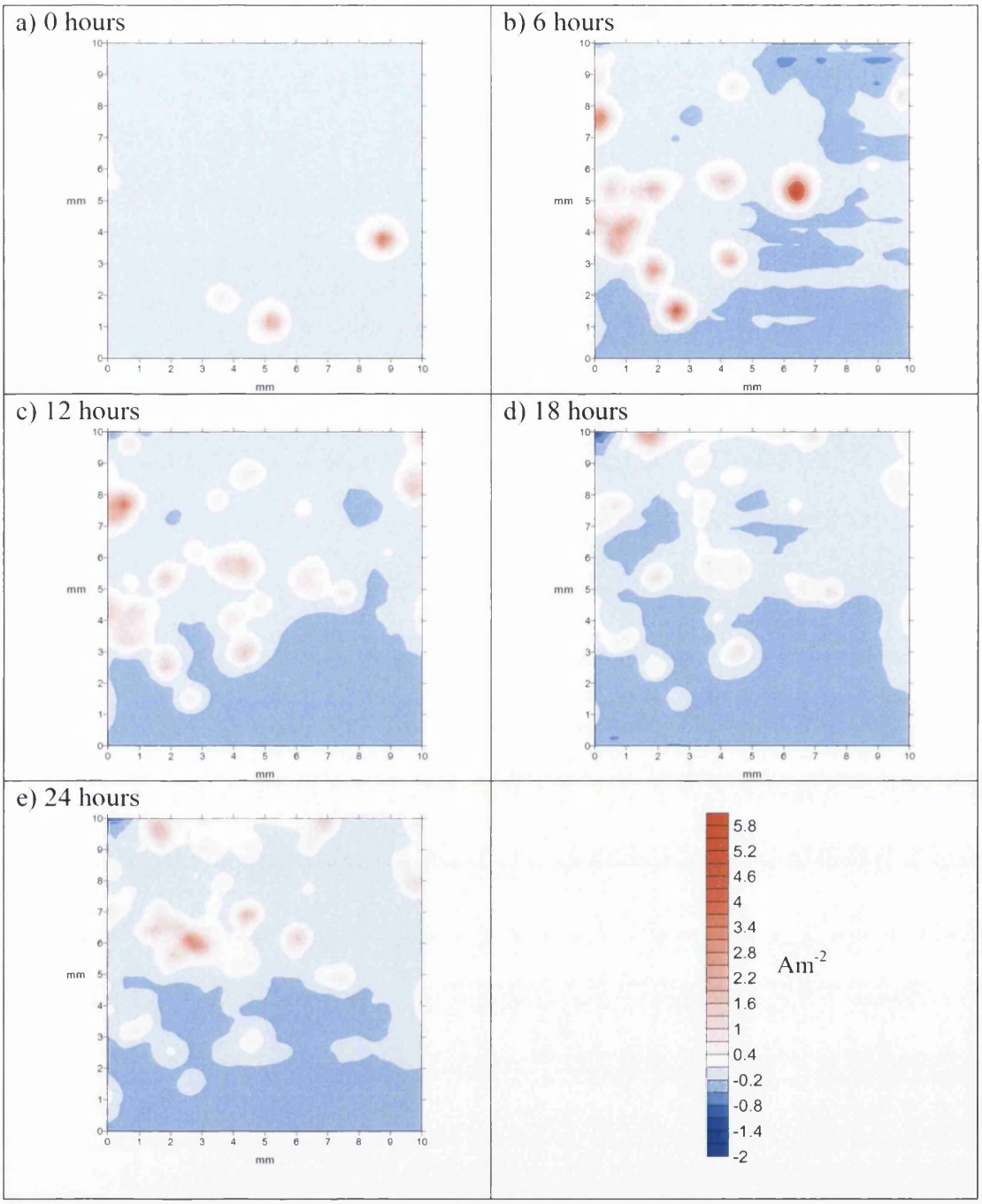

Figure 7.9 SVET corrosion maps for a 6.49% Al addition 10μm coating showing the anodic activity (red) as a function of immersion time. Please note scale.

The data obtained from the SVET has also been analysed to provide details of anode number and lifetime. This was achieved by analysing each individual scan and

using cartography software to identify residual anodes. From this it was possible to group the anodes into four lifetime groups ranging from short lived anodic events to longer lived anodes. The intensity of each anode can be displayed as a function of aluminium addition and immersion time, as shown in Figure 7.10 (a-d).

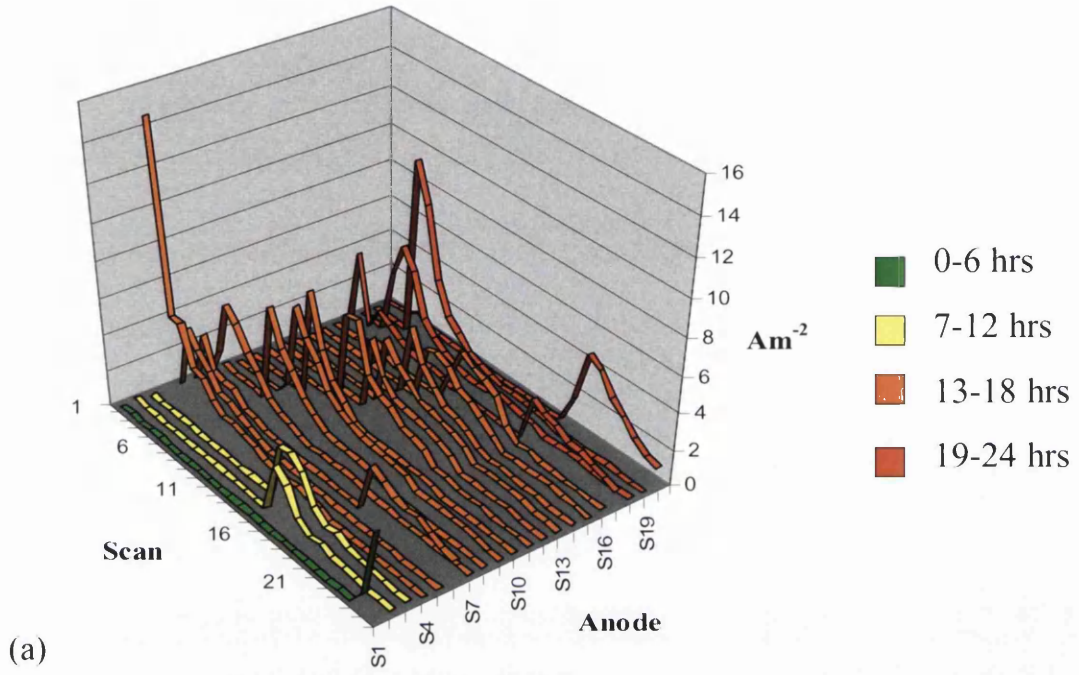

(a)

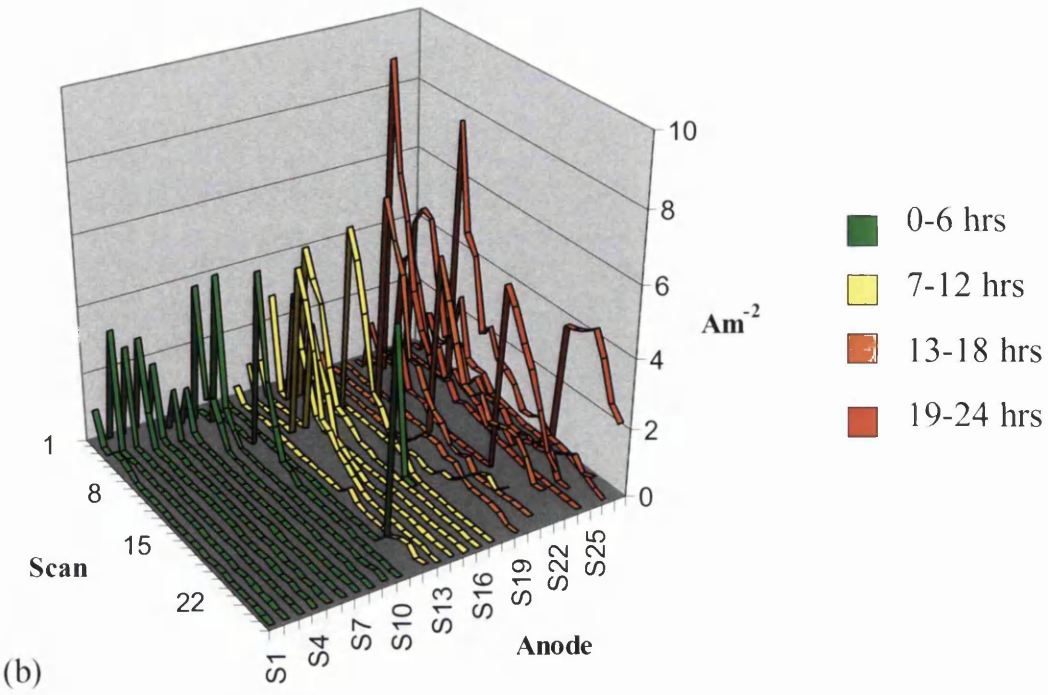
10
8
6
4
2
0
Am-2
0-6 hrs
7-12 hrs
13-18 hrs
19-24 hrs
1
8
15
22
Scan
S1
S4
S7
S10
S13
S16
S19
S22
S25
Anode

(b)

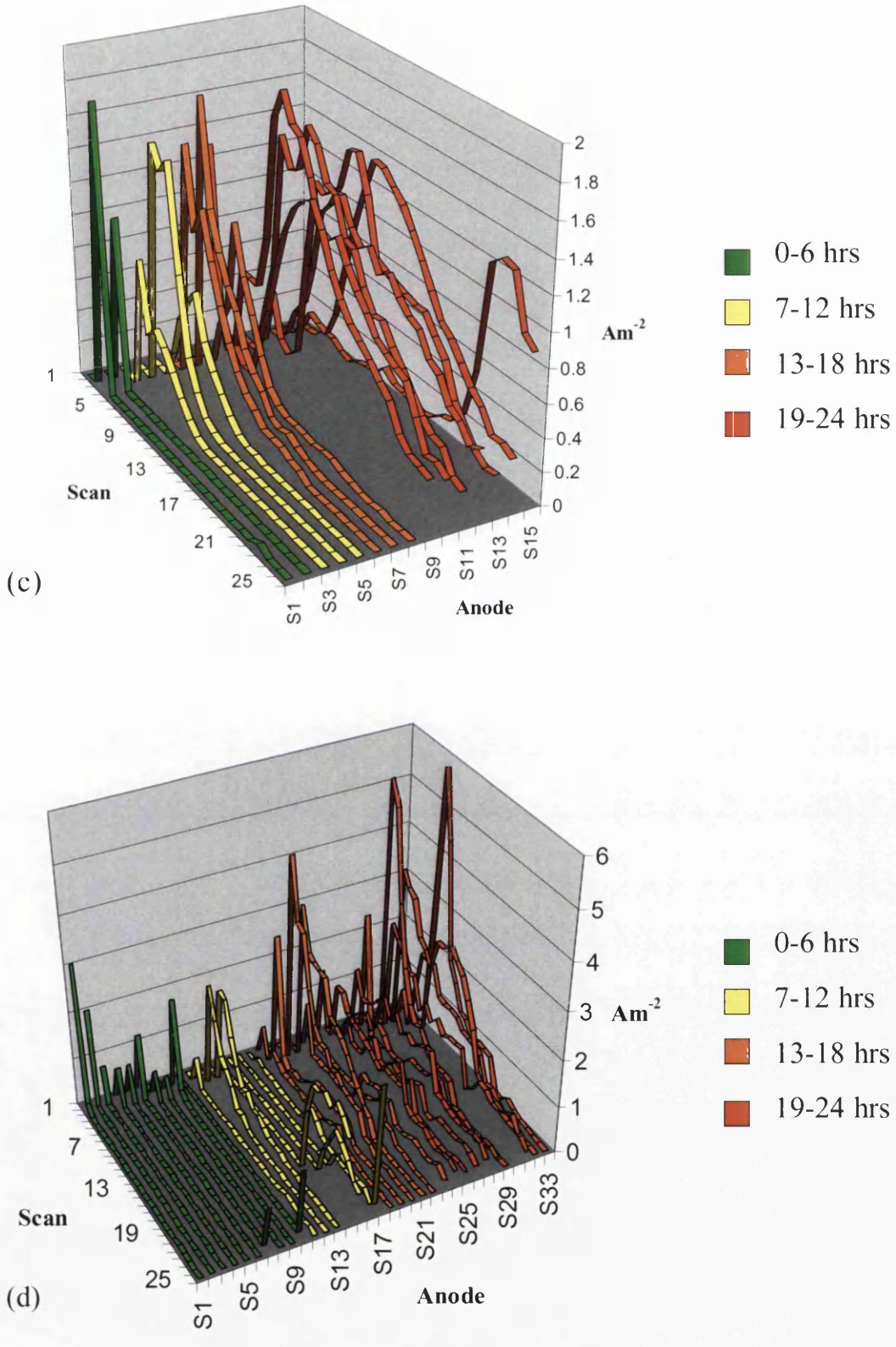

Figure 7.10 Surface anode intensity for 10μm coating as a function of immersion time for (a) 4.7% Al, (b) 5.45% Al, (c) 5.58% Al, (d) 6.49% Al addition.

In Figure 7.10 (a-d) it is shown again that the intensity of the anodic activity is related to the metal loss from the sample. As suspected previously the anomaly provided by the 5% sample (a), where the intensity of the scale was higher than expected suggesting a higher metal loss than that which occurred was indeed down to one single scan. All the rest of the anodes for this sample display consistently lower intensities, similar to those exhibited by the 5.3% sample. This is not unreasonable as although the metal loss is higher for the 5.3% sample it is not completely incomparable to that of the 5% sample.

Figures 7.11 and 7.12 show the cut edge performance of the 20μm and 10μm coatings respectively. The trend is repeated as for the surface samples. For the thicker coating set it can again be seen that on increasing aluminium addition the metal loss decreases, suggesting an improvement in corrosion performance. The metal loss for the 10μm cut edge samples again follows the same trend as the corresponding surface samples. There is again an increase in metal loss on increasing the aluminium addition from 5.5% to 6.1%. It is likely that the increase in cathode/anode ratio gives rise to more destructive corrosion. As there is no preferential phase present at this high Al content, the coating is corroded across the entire profile of the sample.

The levels of metal loss from the thinner 10μm show that a thinner coating performs better than a thicker coating when referring to cut edge performance. This is to the contrary to recent findings of other workers[3] which suggests that the reducing the coating thickness has an adverse effect on corrosion performance due to the air knives expelling Al rich liquid resulting in a greater volume fraction of primary Zn being exposed as a result. For those samples displayed in Figures 7.11 and 7.12, at an addition of 5.5% aluminium the volume fraction of primary zinc in the 10 μm coating was 12% and in the 20 μm coating 11%. This is critical in that in the previous work[3] the volume fraction of primary zinc increased during the processing due to the removal of aluminum rich liquid in the gas wiping phase. Here this has not occurred. Here the reduction in activity reflects a reduction in area of zinc exposed (i.e. self corrosion of the galvanized layer) and this is critical in lowering the zinc lost.

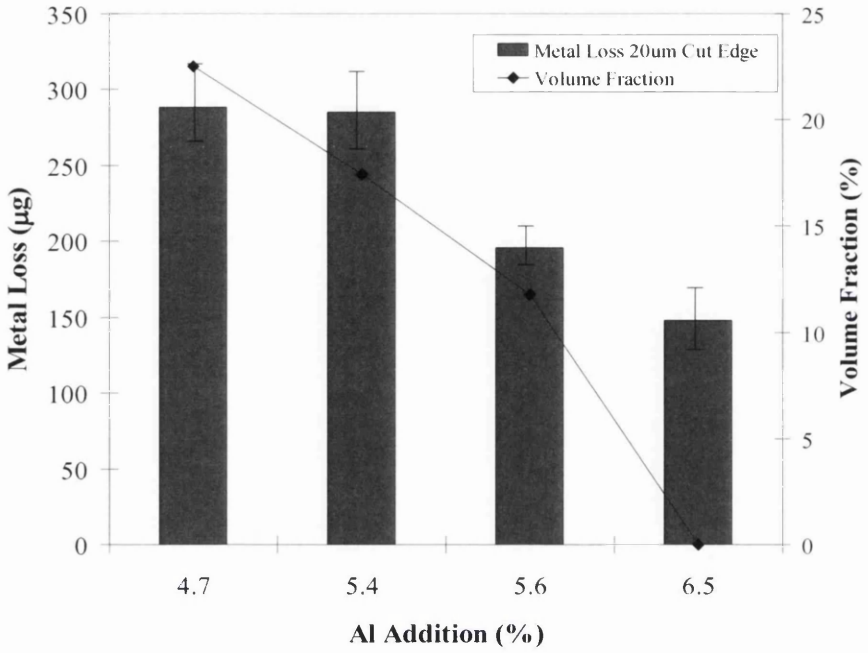

Figure 7.11 Metal loss and Volume fraction for 20µm cut edge samples shown as a function of aluminium addition.

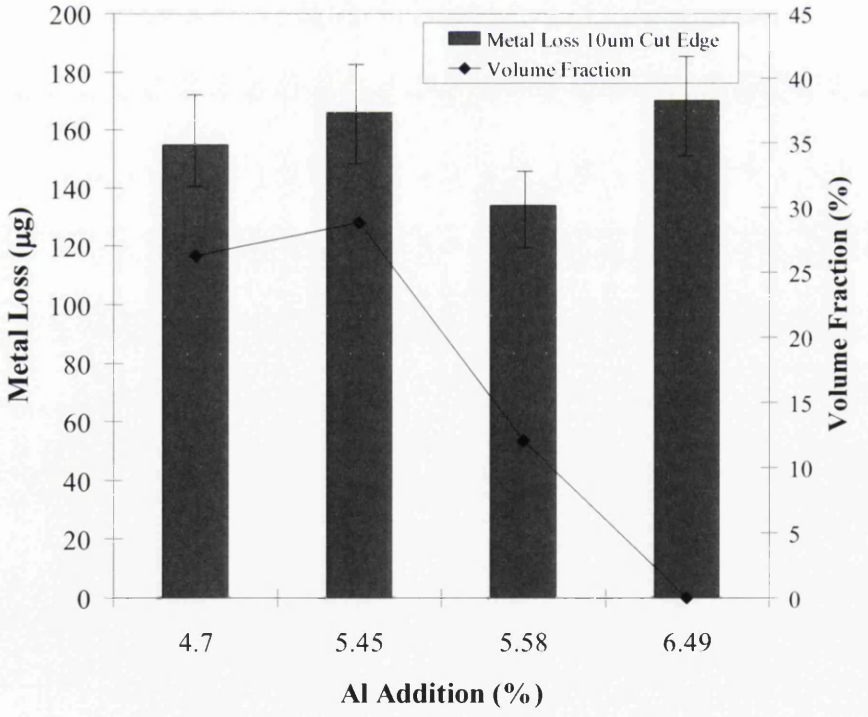

Figure 7.12 Metal loss and Volume fraction for 10µm cut edge samples shown as a function of aluminium addition.

Figures 7.13-7.16 show typical SVET corrosion maps gained from cut edge samples coated with the thinner 10μm coating. As before, these can be used to visually identify areas of anodic activity and quantify them in number and intensity.

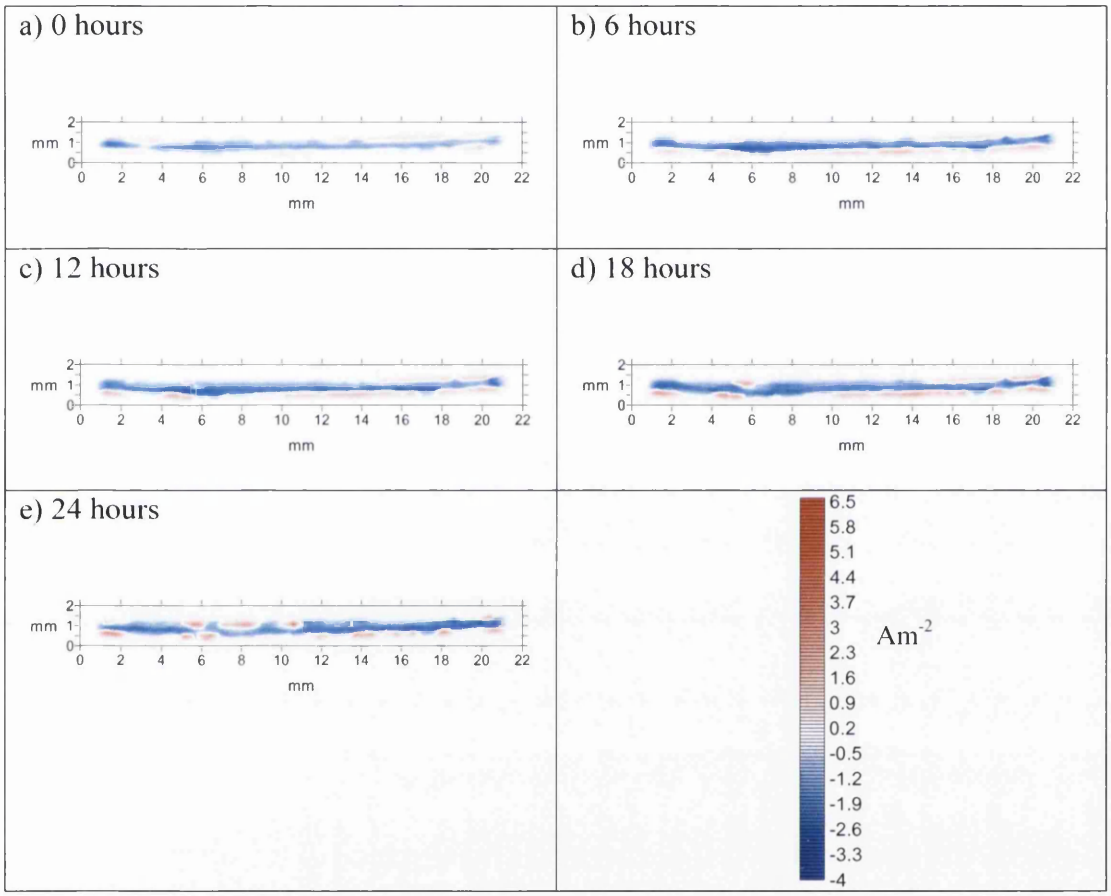

Figure 7.13 SVET cut edge corrosion maps for a 10μm 4.7% Al addition showing the anodic activity (red) as a function of immersion time. Please note scale.

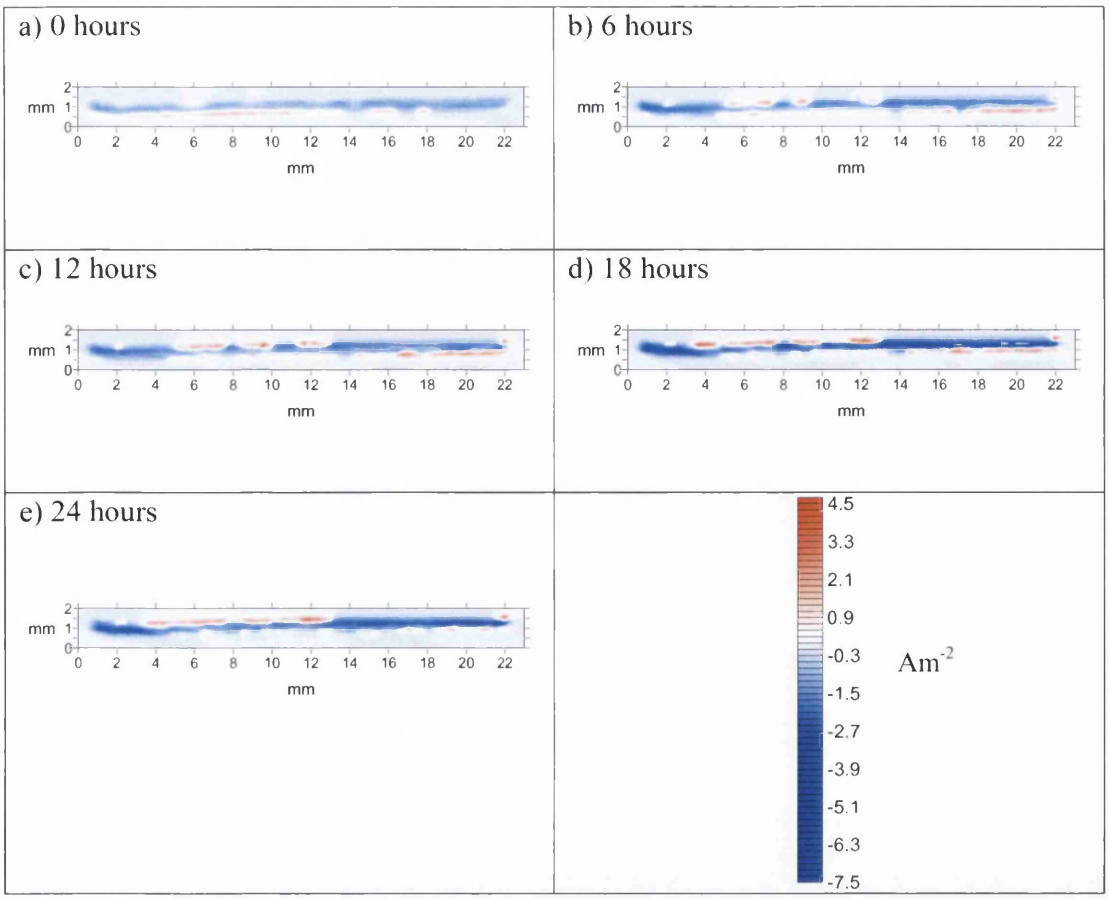

Figure 7.14 SVET cut edge corrosion maps for a 10μm 5.45% Al addition showing the anodic activity (red) as a function of immersion time. Please note scale.

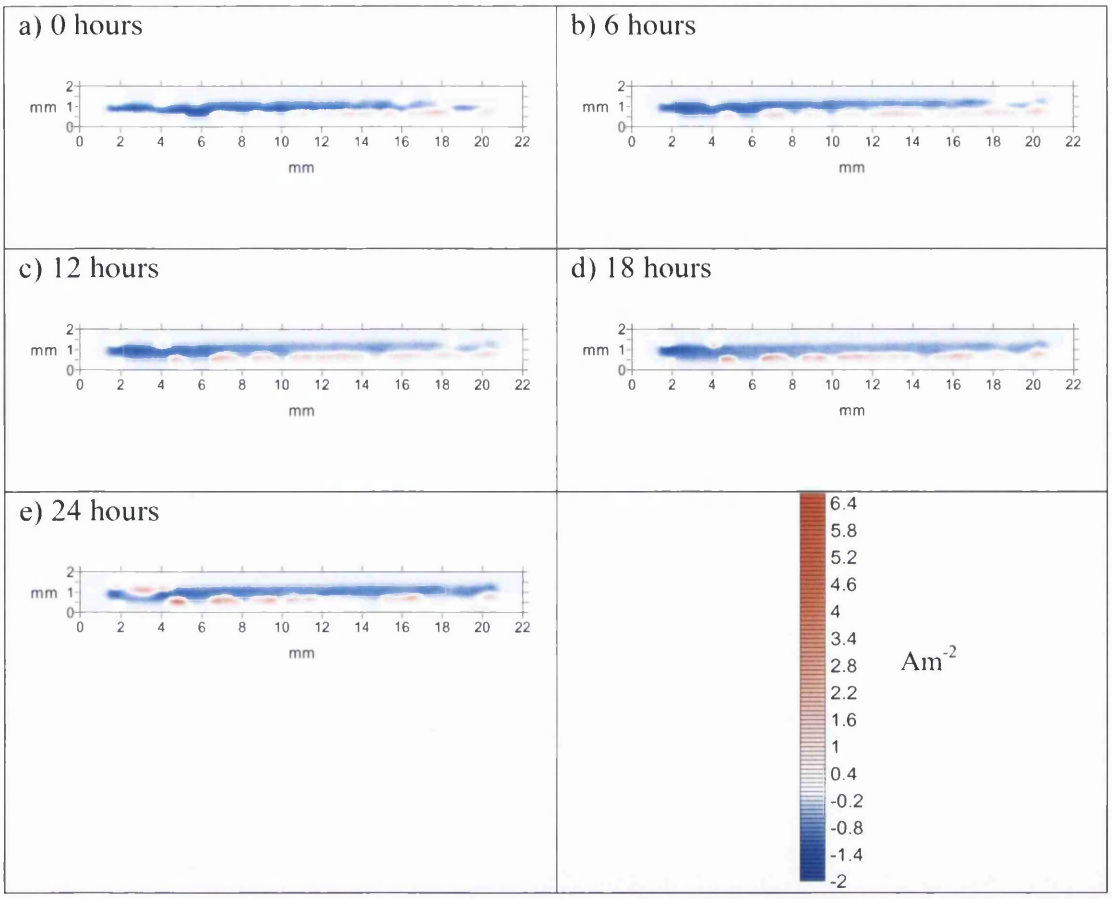

Figure 7.15 SVET cut edge corrosion maps for a 10µm 5.58% Al addition showing the anodic activity (red) as a function of immersion time. Please note scale.

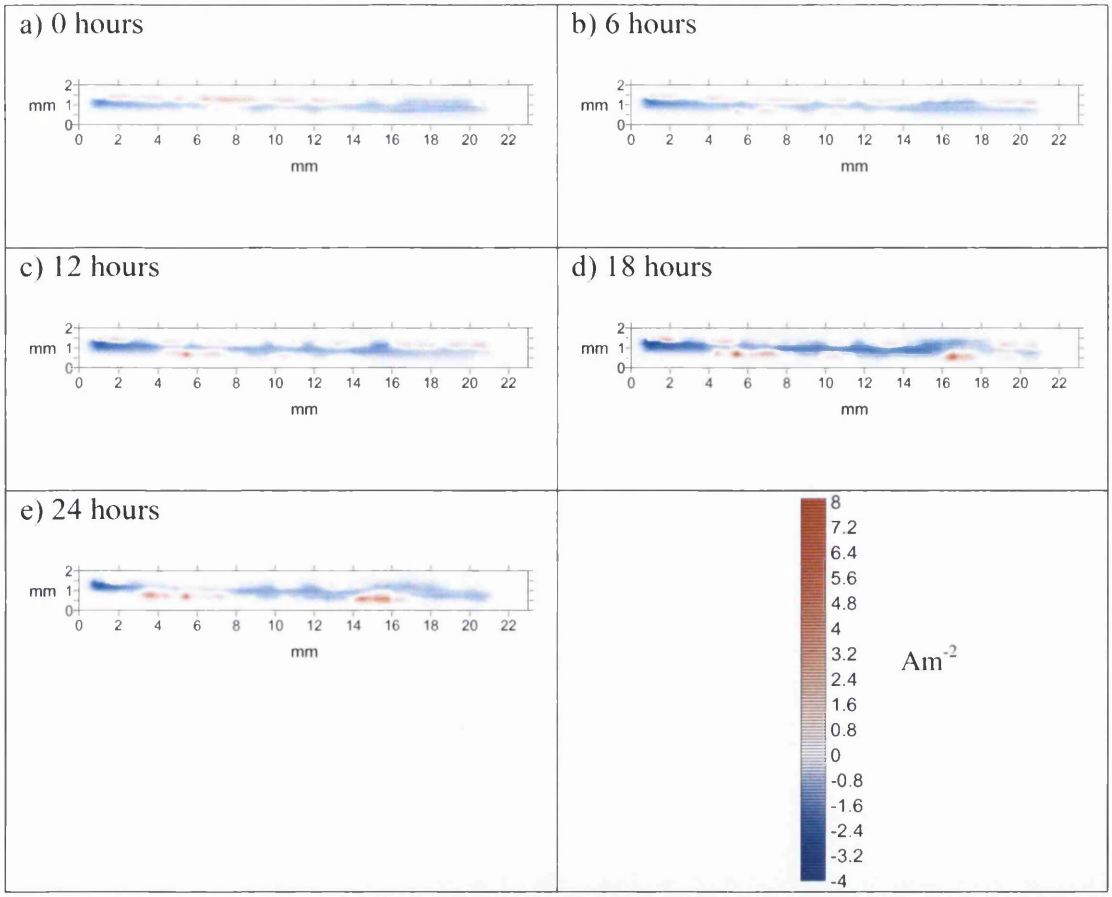

Figure 7.16 SVET cut edge corrosion maps for a 10µm 6.49% Al addition showing the anodic activity (red) as a function of immersion time. Please note scale.

The 6.49% addition gives rise to the most metal loss from the cut edge section when tested using the SVET. This is most likely due to the dezincification of the eutectic. The fact that more metal was lost from this sample is further backed up by the intensity shown from the scan as outlined in Figure 7.10 (d). This is not the case with the thicker 20µm samples and this could be contributed to the difference in anode cathode ratio when moving to the thinner coating.

The 5.45% Al sample provides an anomaly throughout the set. This is likely to be because of the high amount of primary in the sample. Even though the intensity is lower that that shown by the 5.58% sample for example, the metal loss is higher. This could be attributed to the fact that there is a larger amount of anodes able to occur throughout the scan, due to the presence of more primary phase than is expected.

As mentioned earlier, the data was analysed in such a way so that each anode could be assigned an average Zn loss calculated using the data gained from the SVET and the total number of anodes throughout the scan. This Zn loss value was then used to relate surface and cut edge Zn loss to anode lifetime on a single plot. These plots are shown in Figures 7.17 and 7.18.

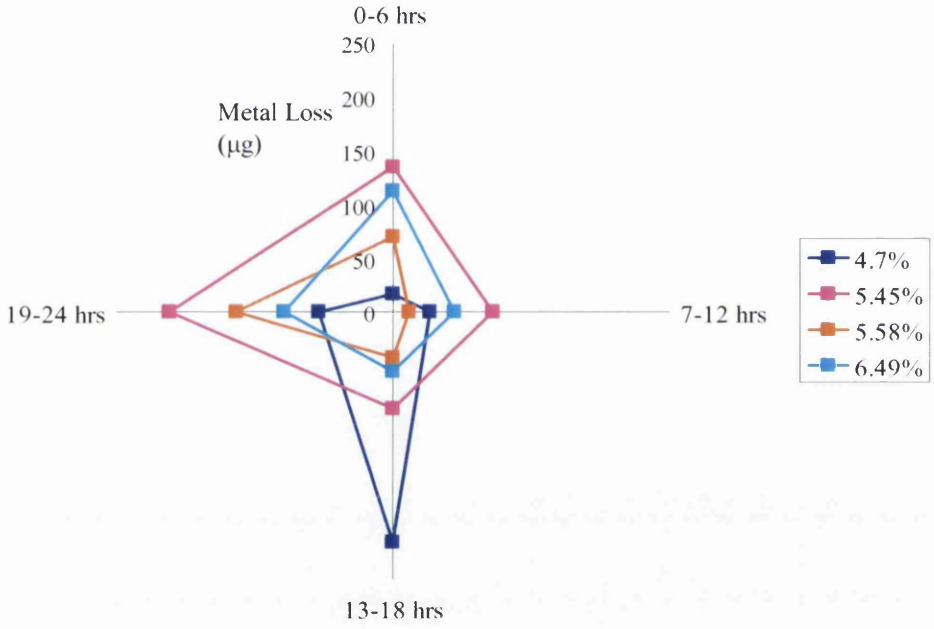

Figure 7.17 Surface Zn loss for a 10µm coating vs Anode lifetime. UNITS

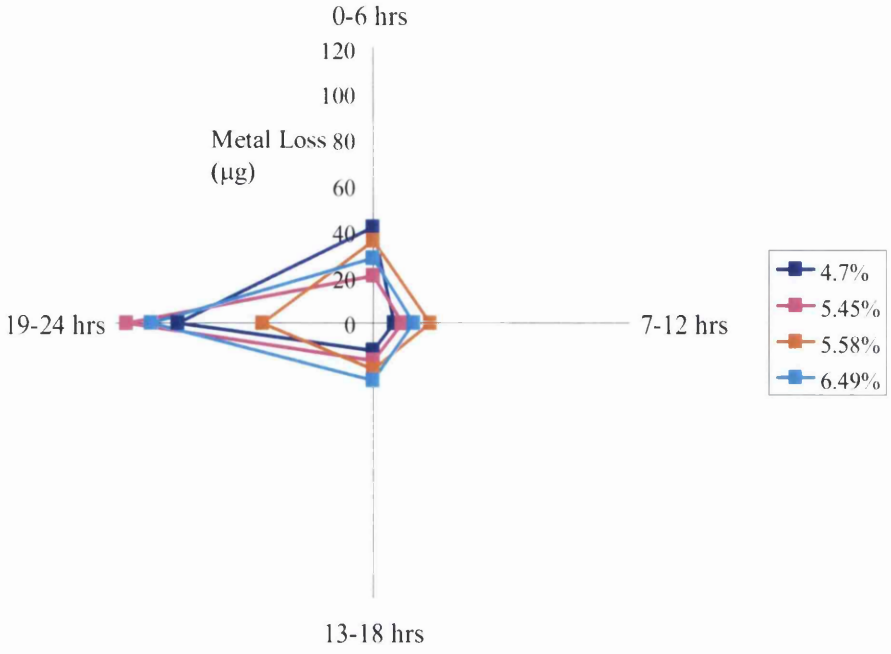

Figure 7.18 Cut edge Zn loss vs Anode lifetime. UNITS

Figures 7.17 and 7.18 show that it is longer lived anodes that cause the most damage with regard to metal loss. In each case the sample that illustrates the lowest metal loss is the 5.5% Al sample. As mentioned earlier, it has been shown that thinner coatings do not necessarily exhibit poorer corrosion performance. This has been the case with the samples tested for the purposes of this investigation.

7.4 Conclusion

The results would suggest that there is some scope for reducing the coating thickness without impacting too severely. Microstructure has a major affect on the corrosion performance of the coating. Additions of aluminium to the galvanised layer have shown to improve corrosion resistance. However, it is important in this case to maintain the two phase structure to allow the primary zinc to be the preferentially

corroding phase. It is shown that when there is no primary zinc phase present corrosion performance is reduced.

Looking at the results, if coating thickness were to be reduced, higher aluminium content than that currently used would be required. As such, an addition of 5.58% could be used to achieve an increase in corrosion performance and compensate for the reduction in thickness of the galvanised coating.

7.5 References

1. ELVINS, J., SPITTLE, J. A., WORSLEY, D. A., ' Relationship Between Microstructure and Corrosion Resistance in Zn-Al Alloy Coated Galvanised Steels', Corrosion Engineering Science and Technology, vol. 38, No.3, 2003.
2. PENNEY, D., 'The Study of Galvalloy® Coated Steels Using Metallographic and Scanning Electrochemical Techniques', EngD Thesis, University of Wales, Swansea, 2006.
3. PENNEY, D., SULLIVAN, J., WORSLEY, D., 'Investigation into the Effects of Metallic Coating Thickness on the Corrosion Properties of Zn/Al Alloy Galvanising Coatings', Corrosion Science, vol. 49, 2007.

Chapter 8

Conclusions and future work

8.1 Conclusion

The work undertaken in this thesis has firstly highlighted the importance for familiarity with the components of an organic coated system. It is important to monitor the metallic run off as this has the potential for significant environmental impact. It is clear that pigmentation has a considerable effect on the quantity and type of metallic run off from PVC based coatings. Yellow pigments have been identified as the most susceptible to photodegradation, while it has been established that some metallic elements such as barium could be used to as short term markers for photostability if coatings are subjected to natural weathering for periods as short as one month. Further to this Hydrotalcite has been identified as a cost effective, non toxic alternative to current heavy metal based stabilisers. If it is deemed that Hydrotalcite cannot perform as a stabilising role for PVC based coatings then there may be some scope for addition to the the coating system as a co-stabiliser while reducing the content of the established more environmentally sensitive compounds.

Natural weathering of commercial Zn/Al galvanised coatings with varying coating thicknesses has identified an optimum metallic coating weight of $255gm^{-2}$. This agrees with existing data from accelerated testing. A gavlanised coating of this nature far outperforms conventional hot dipped galvanised coating.

Fluctuating prices in the international metal markets, especially the zinc market in recent years has given rise to a drive for alternative galvanised coatings. Increased aluminium addition has been shown to provide increased corrosion resistance. In this thesis it has been proposed that for the use within an organic coated system, an addition of 5.6% provides the optimum corrosion performance. Higher aluminium additions were shown to give less metal loss in accelerated testing however it is proposed that a two phase microstructure is needed to prevent the possibility undercutting and delamination of the coating. It should be noted that at higher aluminium additions ~6.1% a two phase microstructure was no longer present.

Higher aluminium additions in thinner galvanised coatings have highlighted possible scope for reducing the zinc layer in an organic coating system to $\sim 132gm^{-2}$ without any significant impact on corrosion performance. Again it is still important to

maintain a two phase microstructure and therefore an aluminium addition of 5.5% is recommended. Microstruture is seen to have a considerable effect on the corrosion performance of the metallic coatings.

8.2 **Future work**

Possibilities of future work arising from this body of work include investigations into the natural weathering of commercially formulated coatings. Although the degradation may not be as prevalent as that seen in this thesis, there may be some scope for investigation into the levels of metallic run off arising from the commercially formulated coatings. Quantification could then take place to indicate the potential environmental impact with reference to the length of guarantees placed on such products.

Investigations into the addition of ternary elements on the galvanised metallic layer could provide scope for further improvement of metallic coatings. Prohesion tests, formability, expense and electrochemical performance could all be considered in future investigations.